

General Area Detector Diffraction System (GADDS)

Version 4.1.xx

USER MANUAL

M86-E01007 1/05





General Area Detector Diffraction System (GADDS) User Manual

Version 4.1.xx

This manual covers the GADDS software package. To order additional copies of this publication, request the part number shown at the bottom of the page.

© 2005, 1999 Bruker AXS Inc. All world rights reserved. Printed in the U.S.A.

Notice

The information in this publication is provided for reference only. All information contained in this publication is believed to be correct and complete. Bruker AXS Inc. shall not be liable for errors contained herein, nor for incidental or consequential damages in conjunction with the furnishing, performance, or use of this material. All product specifications, as well as the information contained in this publication, are subject to change without notice.

This publication may contain or reference information and products protected by copyrights or patents and does not convey any license under the patent rights of Bruker AXS Inc. nor the rights of others. Bruker AXS Inc. does not assume any liabilities arising out of any infringements of patents or other rights of third parties. Bruker AXS Inc. makes no warranty of any kind with regard to this material, including but not limited to the implied warranties of merchantability and fitness for a particular purpose.

No part of this publication may be stored in a retrieval system, transmitted, or reproduced in any way, including but not limited to photocopy, photography, magnetic, or other record without prior written permission of Bruker AXS Inc.

Address comments to: Technical Publications Department
 Bruker AXS Inc.
 5465 East Cheryl Parkway
 Madison, Wisconsin 53711-5373
 USA

All trademarks and registered trademarks are the sole property of their respective owners.

Revision	Date	Changes
0	10/99	Original release.
1	1/05	Added Sections 11 and 12. Revised Sections 1, 2, 3, 5, 6, 7 and 10.

Table of Contents

Notice	ii
1. Introduction and Overview	1-1
1.1 Introduction	1-1
1.2 Theory of X-ray Diffraction Using Area Detectors	1-4
1.2.1 X-ray Powder Diffraction	1-4
1.2.2 Two-Dimensional X-ray Powder Diffraction (XRD ²)	1-5
1.3 Geometry Conventions	1-8
1.3.1 Diffraction Cones and Conic Sections on 2D Detectors	1-8
1.3.2 Diffraction Cones and Laboratory Axes	1-9
1.3.3 Sample Orientation and Position in the Laboratory System	1-10
1.3.4 Detector Position in the Laboratory System	1-11
1.4 Diffraction Data Measured by an Area Detector	1-13
1.5 References	1-15
2. System Configuration	2-1
2.1 X-ray Generator	2-3
2.1.1 Radiation Energy	2-3
2.1.2 X-ray Spectrum and Characteristic Lines	2-3
2.1.3 Focal Spot and Takeoff Angle	2-4
2.1.4 Focal Spot Brightness and Profile	2-5
2.1.5 Operation of the X-ray Generator	2-6
2.2 X-ray Optics	2-8
2.2.1 Monochromator	2-9
2.2.2 Pinhole Collimator	2-10
2.2.3 Sample-to-Detector Distance and Angular Resolution	2-13
2.2.4 Single and Cross-Coupled Göbel Mirrors	2-22

2.2.5 Monocapillary	2-25
2.3 Goniometer and Stages	2-27
2.4 Sample Alignment and Monitor Systems	2-31
2.5 HI-STAR Area Detector	2-34
2.6 Small Angle X-ray Scattering (SAXS) Attachment	2-36
2.7 Standard GADDS Systems	2-37
2.8 Standard GADDS Systems for Combinatorial Screening	2-45
2.8.1 Reflection Mode Screening	2-46
2.8.2 Transmission Mode Screening	2-48
2.8.3 Sample Stage and Screening Grid	2-52
2.8.4 Retractable Knife Edge	2-54
2.8.5 Diffraction Mapping and Results Display	2-59
3. Basic System Operation	3-1
3.1 Starting the System	3-2
3.2 Selecting Optics	3-3
3.3 Choosing the Detector Position	3-3
3.4 Detector Aberration Analysis	3-5
3.4.1 Flood-Field Correction	3-8
3.4.2 Spatial Correction	3-10
3.5 System Calibration	3-14
3.6 Sample Positioning	3-18
3.6.1 XYZ Stage Sample Positioning	3-18
3.6.2 Goniometer Head Sample Positioning	3-19
3.6.3 Collision Limits for Your Sample	3-22
3.7 Data Collection	3-23
3.7.1 Scan Method	3-23
3.7.2 Add or Rotation Method	3-24
3.8 Basic Data Analysis and Preparation	3-25
4. Phase ID	4-1
4.1 Overview	4-1
4.2 Performing a phase ID analysis	4-6

5. Texture	5-1
5.1 Overview	5-1
5.2 General Data Collection Considerations for Texture Analysis	5-7
5.3 Preparation for the Texture Experiment	5-9
5.4 Data Collection Considerations for ODF Analysis	5-10
5.5 Other Texture Representations	5-11
5.6 Using POLE_FIGURE/SCHEME to Plan Strategy and Coverage	5-11
5.7 Using POLE_FIGURE/PROCESS	5-13
5.8 Polymer Orientation	5-17
5.9 Fiber Orientation	5-18
5.10 Sheet Orientation	5-20
5.11 Near Single Crystal Thin Film Orientation	5-21
5.12 Semiquantitative Analysis with CURSOR Commands	5-22
5.13 Preparation for ODF Analysis with popLA and ODF AT	5-23
5.14 Hermans and White-Spruiell Orientation Indices	5-23
5.15 Fiber Texture Plots	5-25
5.16 References	5-29
6. Residual Stress	6-1
6.1 Principle of Stress Measurement	6-1
6.1.1 Theory of Conventional Method	6-1
6.1.2 Theory and Algorithm of 2D Method	6-3
6.1.3 Relationship Between Conventional Theory and 2D Theory	6-7
6.1.4 Advantages of Using 2D Detectors	6-9
6.1.5 Parameters	6-12
6.1.6 GADDS System Requirements	6-15
6.1.7 Data Collection Strategy	6-16
6.1.8 Data Collection Procedures	6-18
6.2 Stress Evaluation Using One-Dimensional Data (Conventional Method)	6-19
6.3 Stress Evaluation Using Two-Dimensional Data (2D Method)	6-22
6.4 Application Examples	6-28
6.4.1 Example 1. (Conventional Method) Residual Stress Measurement with GADDS Microdiffraction System	6-28

6.4.2 Example 2. (2D Method) Comparison Between 2D Method and Conventional Method	6-31
6.4.3 Example 3. Stress Mapping with 2D Method	6-34
6.5 References	6-36
7. Crystal Size	7-1
7.1 Line Broadening Principles for Crystallite Size	7-1
7.2 Instrumental Broadening	7-2
7.3 Microstrain Broadening	7-6
7.4 Data Collection for the Warren-Averbach and Scherrer Methods	7-7
7.5 References	7-8
8. Percent Crystallinity	8-1
8.1 Principle of Percent Crystallinity	8-1
8.2 Data Evaluation for Two-Dimensional Data	8-4
8.2.1 Methods Supporting Percent Crystallinity	8-4
8.2.2 Application Examples	8-10
8.3 References	8-16
9. Small-Angle X-ray Scattering	9-1
9.1 Principle of Small Angle Scattering	9-1
9.1.1 General Equation and Parameters in SAXS	9-2
9.1.2 X-ray Beam Collimation	9-3
9.2 Data Collection and Analysis	9-5
9.2.1 SAXS Attachments Installation	9-5
9.2.2 SAXS System Adjustment and Calibration	9-7
9.2.3 Data Collection	9-11
9.3.14 Applications Examples	9-15
9.3.14 References	9-16
10. Script Files	10-1
10.1 SLAM Command Conventions	10-2
10.2 Executing Script Files	10-5

10.3 Creating Script Files	10-7
10.4 Using Replaceable Parameters within Script Files	10-16
10.5 Adding Script Files to the Menu Bar as User Tasks	10-21
10.6 Nesting Script Files	10-23
10.7 Flow Control Inside Script Files	10-25
11. Automation	11-1
11.1 Primitive Automation	11-2
11.2 Optimize Automation	11-4
11.3 Sample Handling	11-6
11.4 Remote Control	11-7
11.5 Audit Trails	11-8
12. Mapping	12-1
12.1 Procedure—Demo Data	12-2
12.2 Procedure—Real Data	12-4
12.2.1 Frames to Process	12-4
12.2.2 Processing Parameters	12-4
12.3 Mapping Software Features	12-7
13. Nomenclature and Glossary	13-1
13.1 Nomenclature	13-1
13.2 Glossary	13-5
13.3 Glossary of Software Terms	13-12

1. Introduction and Overview

1.1 Introduction

GADDS (General Area Detector Diffraction System), introduced by Bruker AXS Inc., is the most advanced X-ray diffraction system in the world. The core of GADDS is the high-performance two-dimensional (2D) detector—the Bruker AXS HI-STAR area detector. The HI-STAR is the most sensitive area detector, a true photon counter with a large area. The speed of data collection with an area detector can be 10^4 times faster than with a point detector and about 100 times faster than with a linear position-sensitive detector. Most importantly, the data has a large dynamic range and 2D diffraction information. Compared to 1D diffraction profiles measured with a conventional diffraction system, a 2D image collected with GADDS contains far more information for various applications. By introduction of the innovative two-dimensional X-ray diffraction (XRD²) theory, GADDS has opened a new dimension in X-ray powder diffraction.

Phase identification (Phase ID) can be done by integration over a selected range of two-theta (2θ) and chi (χ). A direct link to the ICDD database, profile fitting with conventional peak shapes and fundamental parameters, quantification of phases, and lattice parameter indexing and refinement make powder diffraction analysis easy and fast. Due to the integration along the Debye rings, the integrated data gives better intensity and statistics for phase ID and quantitative analysis, especially for those samples with texture, large grain size, or small quantity.

Texture measurement using an area detector is extremely fast compared to the measurement using a scintillation counter or a linear position-sensitive detector (PSD). The area detector collects texture data and background values simultaneously for multiple poles and multiple directions. Due to the high measurement speed, GADDS can measure pole figures at very fine steps, allowing detection of very sharp textures.

GADDs is the best tool for quantitative texture analysis.

Stress measurement using the two-dimensional area detector is based on a new 2D stress algorithm developed by Bruker AXS, which gives a direct relationship between the stress tensor and the diffraction cone distortion. Since the whole or a part of the Debye ring is used for stress calculation, GADDs can measure stress with high sensitivity, high speed, and high accuracy. It is very suitable for samples with large crystals and textures. Simultaneous measurement of stress and texture is also possible since 2D data consists of both stress and texture information.

Percent crystallinity can be measured faster and more accurately with the data analysis over the 2D frames, especially for samples with anisotropic distribution of crystalline orientation. The amorphous region can be defined externally within a user-defined region or the amorphous region can be defined with the crystalline region included when the crystalline region and the amorphous region overlap. GADDs can also calculate and display the Compton scattering so the Compton effect can be excluded from the amorphous result. The “rolling ball algorithm” calculates the percent crystallinity by extracting an amorphous background frame.

Small angle X-ray scattering (SAXS) data can be collected at high speed. Anisotropic features from specimens, such as polymers, fibrous

materials, single crystals, and bio-materials, can be analyzed and displayed in two dimensions. De-smearing correction is not necessary due to the collimated point X-ray beam. Since one exposure takes all the SAXS information, it is easy to scan over the sample to map the structure information from the small angle diffraction.

Microdiffraction data is collected with speed and accuracy. X-ray diffraction from small sample amount or small sample area has always been a slow process due to limited beam intensity, difficulty in sample positioning, and slow point detectors. In the GADDs microdiffraction system, we have solutions for all of these problems. The cross-coupled Göbel mirrors and the Mono-CapTM optics can deliver high intensity beams. The laser-video sample alignment system can accurately align the intended measurement spot of a sample to the instrument center where the X-ray beam hits. The motorized XYZ stage can move the measurement spot to the instrument center and map many sample spots automatically. The 2D detector captures the whole or a large portion of the diffraction rings, so that spotty, textured, or weak diffraction data can be integrated over the selected diffraction rings.

Thin film samples with a mixture of single crystal, random polycrystalline layers and highly textured layers can be measured with all the features appearing simultaneously in diffraction frames. Stress and texture can be measured quickly, or even simultaneously, with the new stress and texture approach developed for

XRD². The texture can be displayed as a pole figure or fiber plot. The weak and spotty diffraction pattern can be compensated by integration over the 2D diffraction pattern.

1.2 Theory of X-ray Diffraction Using Area Detectors

1.2.1 X-ray Powder Diffraction

X-ray diffraction (XRD) is a technique used to measure the atomic arrangement of materials. When a monochromatic X-ray beam hits a sample, in addition to absorption and other phenomena, we observe X-ray scattering with the same wavelength as the incident beam, called coherent X-ray scattering. The coherent scattering of X-rays from a sample is not evenly distributed in space but is a function of the electron distribution in the sample. The atomic arrangement in materials can be ordered like a single crystal or disordered like glass or liquid. As such, the intensity and spatial distributions of the scattered X-rays form a specific diffraction pattern which is the “fingerprint” of the sample.

There are many theories and equations about the relationship between the diffraction pattern and the material structure. Bragg’s law is a simple way to describe the diffraction of X-rays by a crystal. In Figure 1.1, the incident X-rays hit the crystal planes in an angle θ , and the reflection angle is also θ . The diffraction pattern is a delta function when the Bragg condition is satisfied:

$$\lambda = 2d \sin\theta$$

where λ is the wavelength, d is the distance between each adjacent crystal plane (d -spacing), and θ is the Bragg angle at which one observes a diffraction peak.

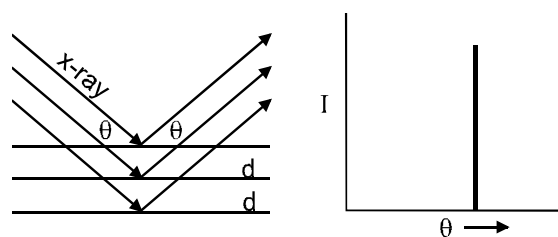


Figure 1.1 - The incident X-rays and reflected X-rays make an angle of θ symmetric to the normal of the crystal plane. The diffraction peak is observed at the Bragg angle θ

Figure 1.1 is an oversimplified model. For real materials, the diffraction patterns vary from theoretical delta functions with discrete relationships between points to continuous distributions with spherical symmetry. Figure 1.2 shows the diffraction from a single crystal and from a polycrystalline sample. The diffracted beams from a single crystal point to discrete directions each corresponding to a family of diffraction planes. The diffraction pattern from a polycrystalline (powder) sample forms a series of diffraction cones if a large number of crystals oriented randomly in the space are covered by the incident X-ray beam. Each diffraction cone corresponds to the diffraction from the same family of crystal-line planes in all of the participating grains. The diffraction patterns from polycrystalline materials will be considered later in the discussion of the theory and configuration of X-ray diffraction using area detectors. The theory also applies to any system with a two-dimensional detector.

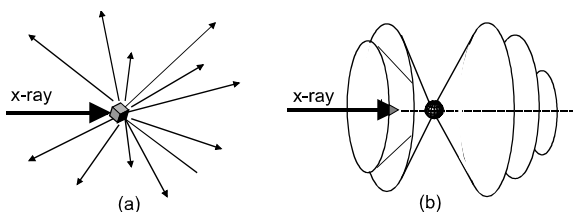


Figure 1.2 - The patterns of diffracted X-rays: (a) from a single crystal and (b) from a polycrystalline sample

Polycrystalline materials consist of many crystalline domains, numbering from two to more than a million in the incident beam. In single-phase polycrystalline materials, all of these domains have the same crystal structure with multiple orientations. Polycrystalline materials could also be multiphase materials with more than one kind of crystal blended together. Polycrystalline materials can also be bonded to different materials such as semiconductor thin films on single crystal substrates. The crystalline domains could be embedded in an amorphous matrix or stressed from a forming operation. Usually, the sample undergoing X-ray analysis has a combination of these effects. Polycrystalline diffraction deals with this range of scattering to determine the constituent phases in a material or the effect of processing conditions on the crystallite structure and distribution. The myriad properties that can be measured with X-rays are related to material purity, strength, durability,

electrical conductivity, coefficient of expansion, and so forth.

Analyses commonly performed on polycrystalline materials with X-rays include:

- Phase identification
- Quantitative phase analysis
- Texture (orientation)
- Residual stress
- Crystallite size
- Percent crystallinity
- Lattice dimensions
- Structure refinement (Rietveld)

1.2.2 Two-Dimensional X-ray Powder Diffraction (XRD²)

Two-dimensional X-ray diffraction (2DXRD or XRD²) is a new technique in the field of X-ray diffraction (XRD). XRD² is not simply a diffractometer with a two-dimensional (2D) detector. In addition to 2D detector technology, XRD² involves 2D image processing and 2D diffraction pattern manipulation and interpretation. Because of the unique nature of the data collected with a 2D detector, a completely new concept and new approach are necessary to configure the XRD² system and to understand and analyze the 2D diffraction data. In addition, the new theory should also be consistent with

the conventional theory so that the 2D data can be used for conventional applications.

First, we compare conventional X-ray diffraction (XRD) and two-dimensional X-ray diffraction (XRD²). Figure 1.3 is a schematic of X-ray diffraction from a powder (polycrystalline) sample. For simplicity, it shows only two diffraction cones, one represents forward diffraction ($2\theta < 90^\circ$) and one backward diffraction ($2\theta > 90^\circ$). The diffraction measurement in the conventional diffractometer is confined within a plane, here referred to as the diffractometer plane. A point detector makes a 2θ scan along a detection circle. If a one-dimensional position-sensitive detector (PSD) is used in the diffractometer, it is mounted along the detection circle (i.e., diffraction plane). Since the variation of the diffraction pattern in the direction (Z) perpendicular to the diffractometer plane is not considered in the conventional diffractometer, the X-ray beam is normally extended in the Z direction (line focus). The actual diffraction pattern measured by a conventional diffractometer is an average over a range defined by beam size in the Z direction. Since the diffraction data outside of the diffractometer plane is not detected, the material structure represented by the missing diffraction data will either be ignored, or extra sample rotation and time are needed to complete the measurement.

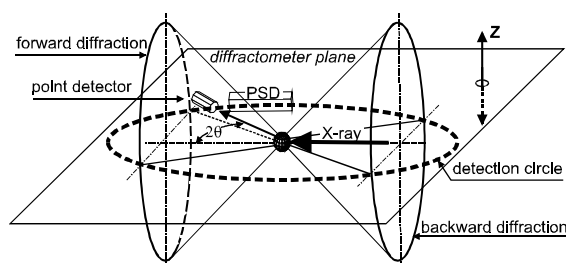


Figure 1.3 - Diffraction patterns in 3D space from a powder sample and the diffractometer plane

With a two-dimensional detector, the diffraction is no longer limited to the diffractometer plane. Depending on the detector size, distance to the sample and detector position, the whole or a large portion of the diffraction rings can be measured simultaneously. Figure 1.4 shows the diffraction pattern on a two-dimensional detector compared with the diffraction measurement range of a scintillation detector and PSD. Since the diffraction rings are measured, the variations of diffraction intensity in all directions are equally important, and the ideal shape of the X-ray beam cross-section for XRD² is a point (point focus). In practice, the beam cross-section can be either round or square in limited size.

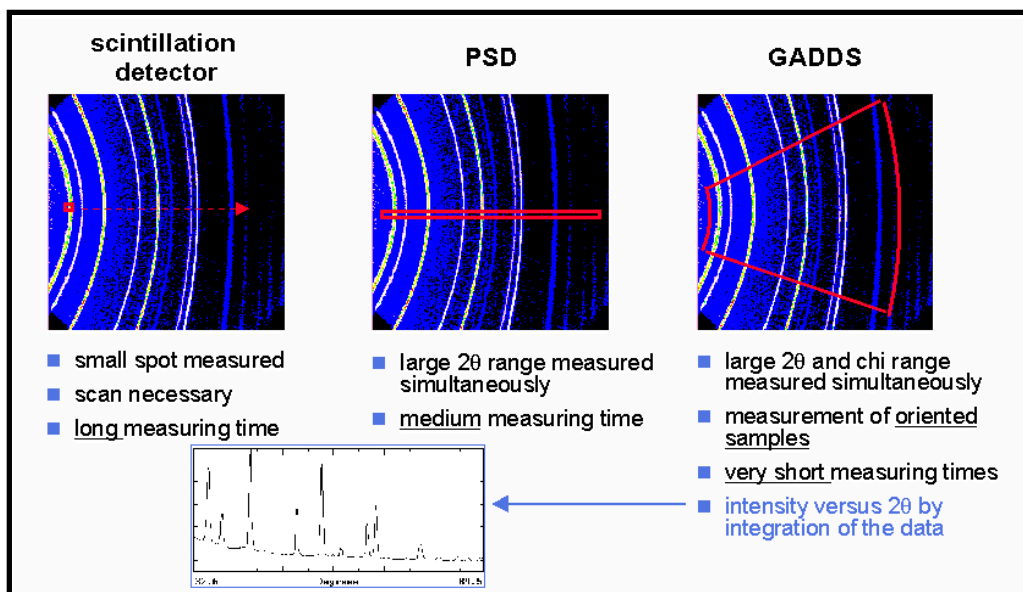


Figure 1.4 - Coverage comparison: point, line, and area detectors

1.3 Geometry Conventions

1.3.1 Diffraction Cones and Conic Sections on 2D Detectors

Figure 1.5 shows the geometry of a diffraction cone. The incident X-ray beam always lies along the rotation axis of the diffraction cone. The whole apex angle of the cone is twice the 2θ value given by the Bragg relation. The surface of the 2D detector can be considered as a plane, which intersects the diffraction cone to form a conic section. D is the distance between the sample and the detector, and α is the detector swing angle, also referred to as the detector 2θ angle. The conic section takes different shapes for different α angles. When imaged on-axis ($\alpha = 0^\circ$), the conic sections appear as circles, producing the Debye rings familiar to most diffractionists. When the detector is at off-axis position ($\alpha \neq 0^\circ$), the conic section may be an ellipse, parabola, or hyperbola. For convenience, all kinds of conic sections will be referred to as diffraction rings or Debye rings alternatively hereafter in this manual. All diffraction rings collected in a single exposure will be referred to as a frame. The area detector image (frame) is normally stored as intensity values on a 1024x1024-pixel grid or a 512x512-pixel grid.

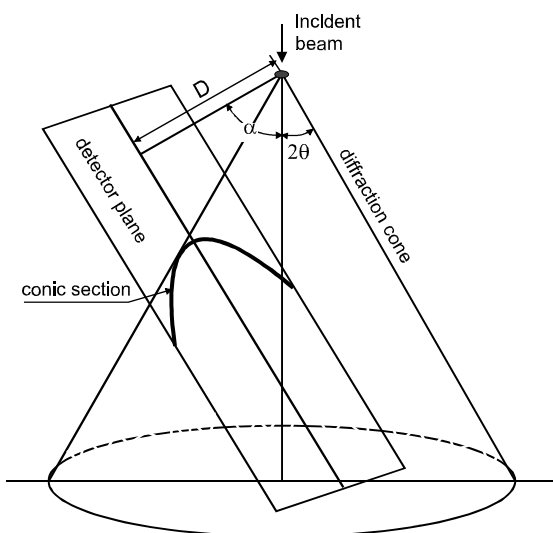


Figure 1.5 - A diffraction cone and the conic section with a 2D detector plane

1.3.2 Diffraction Cones and Laboratory Axes

Figure 1.6 describes the geometric definition of diffraction cones in the laboratory coordinates system, $X_L Y_L Z_L$.

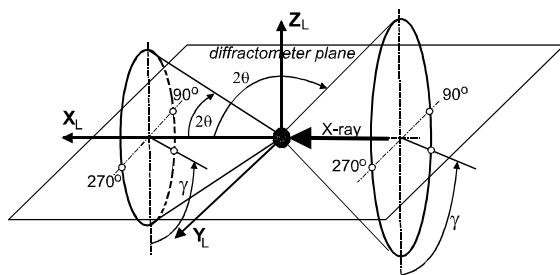


Figure 1.6 - The geometric definition of diffraction rings in laboratory axes

GADDS uses the same diffraction geometry conventions as the conventional 3-circle goniometer, which is consistent with the Bruker AXS P3 and P4 diffractometers. In these conventions, the direct X-ray beam propagates along the X_L axis, Z_L is up, and Y_L makes up a right-handed rectangular coordinate system. The axis X_L is also the rotation axis of the cones. The apex angles of the cones are determined by the 2θ values given by the Bragg equation. The apex angles are twice the 2θ values for forward reflection ($2\theta < 90^\circ$) and twice the values of $180^\circ - 2\theta$ for backward reflection ($2\theta > 90^\circ$). The γ angle is the azimuthal angle from the origin at the 6 o'clock direction ($-Z_L$ direction) with a right-

handed rotation axis along the opposite direction of the incident beam ($-X_L$ direction). The γ angle here is used to define the direction of the diffracted beam on the cone. In the past, " χ " was used to denote this angle, it was changed to γ to avoid confusion with the goniometer angle χ . The γ angle actually defines a half plane with the X_L axis as the edge, referred to as γ -plane hereafter. Intersections of any diffraction cones with a γ -plane have the same γ value. The conventional diffractometer plane consists of two γ -planes with one $\gamma = 90^\circ$ plane in the negative Y_L side and $\gamma = 270^\circ$ plane in the positive Y_L side. γ and 2θ angles form a kind of spherical coordinate system which covers all the directions from the origin of sample (goniometer center). The γ - 2θ system is fixed in the laboratory systems $X_L Y_L Z_L$, which is independent of the sample orientation in the goniometer. This is a very important concept when we deal with the 2D diffraction data.

As mentioned previously, the diffraction rings on a 2D detector can be any one of the four conic sections: circle, ellipse, parabola, or hyperbola. The determination of the diffracted beam direction involves the conversion of pixel information into the γ - 2θ coordinates. In the GADDS system, the γ and 2θ values for each pixel are given and displayed on the frame. Users can observe all the diffraction rings in terms of γ and 2θ coordinates with a conic cursor, disregarding the actual shape of each diffraction ring.

1.3.3 Sample Orientation and Position in the Laboratory System

In the GADDS geometric convention, we use three rotation angles to describe the orientation of a sample in the diffractometer. The three angles are ω (omega), χ_g (goniometer chi) and ϕ (phi). Since the χ symbol has been used for the azimuthal angle on the diffraction cones in this manual, we use χ_g to represent the χ rotation in the 3- and 4-circle goniometer. Figure 1.7(a) shows the relationship between rotation axes (ω , χ_g , ϕ) and the laboratory system $X_L Y_L Z_L$. ω is defined as a right-handed rotation about Z_L axis. The ω axis is fixed on the laboratory coordinates. χ_g is a left-handed rotation about a horizontal axis. The χ_g axis makes an angle of ω with X_L axis in the $X_L Y_L$ plane when $\omega \neq 0$. The χ_g axis lies on X_L when ω is set at zero. ϕ is a left-handed rotation. The ϕ axis overlaps with the Z_L axis when $\chi_g = 0$. The ϕ axis is away from the Z_L axis by χ_g rotation for any nonzero χ_g angle.

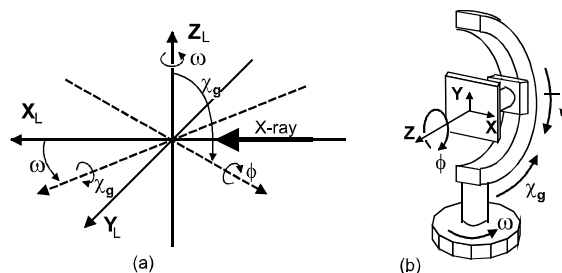


Figure 1.7 - Sample rotation and translation in the laboratory system. (a) Relationship between rotation axes and $X_L Y_L Z_L$ coordinates; (b) Relationship among rotation axes (ω , χ_g , ψ , ϕ) and translation axes XYZ

Figure 1.7(b) shows the relationship among all rotation axes (ω , χ_g , ψ , ϕ) and translation axes XYZ . ω is the base rotation, all other rotations and translations are on top of this rotation. The next rotation above ω is the χ_g rotation. ψ is also a rotation above a horizontal axis. ψ and χ_g have the same axis but different starting positions and rotation directions, and $\chi_g = 90^\circ - \psi$. In order to make the GADDS geometry definition consistent with other Bruker XRD systems, the ψ angle will be used in the later version of GADDS system. The next rotation above ω and (ψ) is ϕ rotation. The sample translation coordinates XYZ are so defined that, when $\omega = \chi_g = \phi = 0$, X is in the opposite direction of the incident X-ray beam ($X = -X_L$), Y is in the opposite direction of Y_L ($Y = -Y_L$), and Z overlaps with ($Z = Z_L$). In GADDS, it is very common to set the $\chi_g = 90^\circ$ ($\psi = 0$) for a reflection mode diffraction as is

shown in Figure 1.7(b). In this case, the relationship becomes $X = -X_L$, $Y = Z_L$, and $Z = Y_L$ when $\omega = \psi = \phi = 0$. The ϕ rotation axis is always the same as the Z -axis at any sample orientation.

In an aligned diffraction system, all three rotation axes and the primary X-ray beam cross at the origin of $X_L Y_L Z_L$ coordinates. This cross point is also known as goniometer center or instrument center. The X - Y plane is normally the sample surface and Z is the sample surface normal. In a preferred embodiment, XYZ translations are above all the rotations so that the translations will not move any rotation axis away from the goniometer center. Instead, the XYZ translations bring a different part of the sample into the goniometer center. Due to this nature, if a sample is moved for the distances of x and y away from the origin in the X - Y plane, the new spot on the sample exposed to the X-ray beam will be $-x$ and $-y$ away from the original spot.

In the past, GADDS documents and software have used the symbol χ (or chi) for both diffraction cone and sample orientation. In this manual, we will adopt the two new symbols. γ (gamma) represents the direction of diffracted beam on the diffraction cone, and ψ (psi) represents a sample rotation angle. Users may see either the old or new symbol definition depending on the version of hardware or software, but can normally distinguish the two parameters from the definition if they are aware of the difference.

1.3.4 Detector Position in the Laboratory System

As previously mentioned, the detector position is defined by the sample-to-detector distance D and the detector swing angle α . In the laboratory coordinates $X_L Y_L Z_L$, detectors at different positions are shown in Figure 1.8.

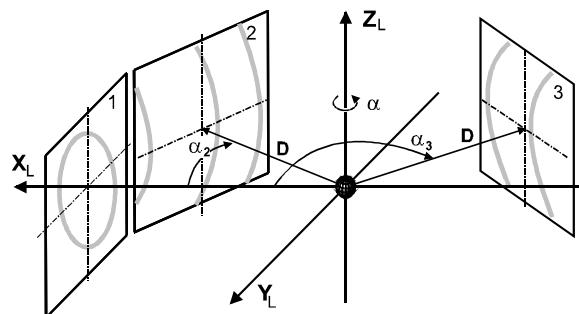


Figure 1.8 - Detector position in the laboratory system $X_L Y_L Z_L$: D is the sample-to-detector distance; α is the swing angle of the detector

Three planes (1-3) represent the detection planes of three 2D detectors. The detector distance D is defined as the perpendicular distance from the goniometer center to the detection plane. The swing angle α is a right-handed rotation angle above Z_L axis. Detector 1 is exactly centered on the positive side of X_L axis, and its swing angle is zero (on-axis). Detectors 2 and 3 are rotated away from X_L axis with negative swing angles ($\alpha_2 < 0$ and $\alpha_3 < 0$). The swing angle is sometimes called detector two-theta in

GADDS documents and software. We will use $2\theta_D$ to represent the detector swing angle hereafter in this manual. It is very important to distinguish between the Bragg angle 2θ and detector angle $2\theta_D$. 2θ is the measured diffraction angle on the data frame. At a given detector angle $2\theta_D$, a range of 2θ values can be measured. The 2θ value corresponding to the center pixel is equal to $2\theta_D$. Users should be able to tell the difference between two parameters although the same symbol may be used for both variables in GADDS software or documents.

1.4 Diffraction Data Measured by an Area Detector

Without any analysis, an area detector frame can provide a quick overview of the crystallinity, composition, and orientation of a material. If the observed Debye rings are smooth and continuous, the sample is polycrystalline and fine grained. If the rings are continuous but spotty, the material is polycrystalline and large grained (Figure 1.11). Incomplete Debye rings indicate orientation or texture (Figure 1.10). If only individual spots are observed, the material is single crystal, which can be considered the extreme case of crystallographic texture (Figure 1.9). Often, you can visually determine the number of phases when the phases have different degrees of orientation (texture).

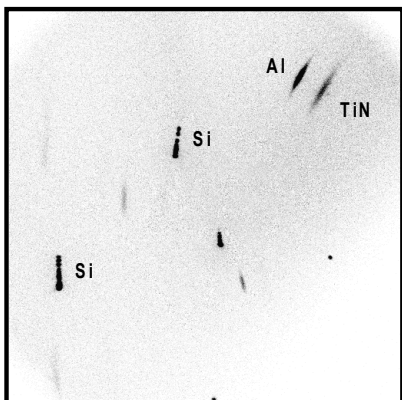


Figure 1.9 - Al TiN film on Si Specimen was rotated in ϕ . Note that the Al and TiN have the same (111) orientation,

and both have fiber texture. The Al and TiN are highly oriented polycrystalline materials, while the Si substrate is single crystal. The stack is roughly 0.5 μm thick

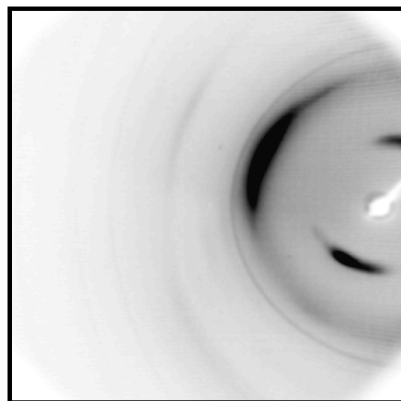


Figure 1.10 - Nylon 6 fiber with an inorganic filler. Two distinct, orthogonal orientations are visible. The faint, continuous rings are from the polycrystalline, inorganic filler

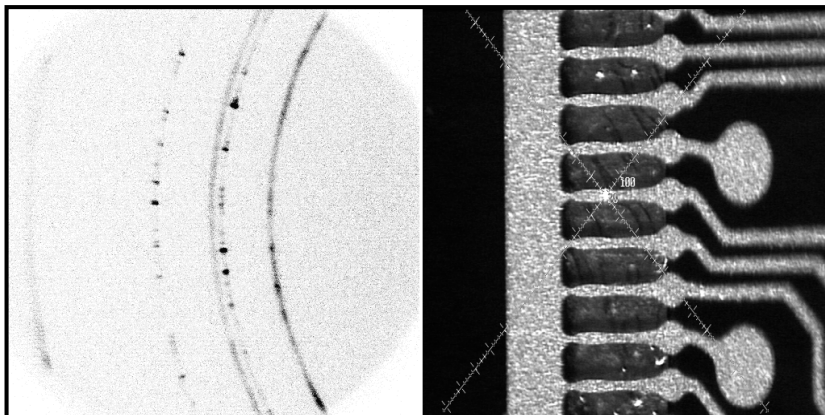


Figure 1.11 - Flexible TAB (Tape Automated Bonding) material. The two phases are gold and copper. The smooth and continuous rings are the fine-grained gold. The spotty rings belong to large-grained copper. The small divisions on the crosshair are 20 μm

When integrating an area detector frame in the χ direction, a standard “powder pattern” (intensity versus 2θ diagram) is obtained. The added benefit of the area detector is that the intensities so obtained take preferred orientation into account. This is a tremendous advantage when performing phase analysis on oriented materials such as clay minerals. Area detector frames may also be processed to obtain texture information in the form of pole figures, fiber texture plots, and orientation indices. The coverage of the area detector frequently enables multiple poles with backgrounds to be collected simultaneously, in a small fraction of the time it takes a

conventional texture diffractometer with a scintillation detector to collect a single pole.

The HI-STAR detector is a gas-filled multiwire proportional counter. It is a true photon counter, which makes it extremely sensitive for weakly diffracting materials. The extremely low background of the HI-STAR makes it ideal for applications requiring “long” measurement times (tens of minutes to hours), such as small-angle X-ray scattering and microdiffraction.

1.5 References

1. B. D. Cullity, *Elements of X-Ray Diffraction*, 2nd ed., Addison-Wesley, Reading, MA, 1978.
2. R. Jenkins and R. L. Snyder, *Introduction to X-Ray Powder Diffractometry*, John Wiley, New York, 1996.
3. A. J. C. Wilson, *International Tables for Crystallography*, Kluwer Academic, Boston, 1995.
4. Philip R. Rudolf and Brian G. Landes, Two-dimensional X-ray Diffraction and Scattering of Microcrystalline and Polymeric Materials, *Spectroscopy*, 9(6), pp 22-33, July/August 1994.
5. J. Formica, "X-Ray Diffraction," In *Handbook of Instrumental Techniques for Analytical Chemistry*, edited by F. Settle (Prentice-Hall, New Jersey, 1997).
6. N. F. M. Henry, H. Lipson, and W. A. Wooster, *The Interpretation of X-Ray Diffraction Photographs* (St. Martin's Press, New York, 1960).
7. H. Lipson and H. Steeple, *Interpretation of X-Ray Powder Diffraction Patterns* (St. Martin's Press, New York, 1970).
8. S. N. Sulyanov, A. N. Popov and D. M. Kheiker, Using a Two-Dimensional Detector for X-ray Powder Diffractometry, *J. Appl. Cryst.* **27**, pp 934-942, 1994.
9. Hans J. Bunge and Helmut Klein, Determination of Quantitative, High-Resolution Pole-Figures with the Area Detector, *Z. Metallkd.* **87**(6), pp 465-475, 1996.
10. Kingsley L. Smith and Richard B. Ortega, Use of a Two-Dimensional, Position Sensitive Detector for Collecting Pole Figures, *Advances in X-ray Analysis, Vol. 36*, pp 641-647, Plenum, New York, 1993.
11. Bob B. He and Kingsley L. Smith, Strain and Stress Measurement with Two-Dimensional Detector, *Advances in X-ray Analysis, Vol. 41, Proceedings of the 46th Annual Denver X-ray Conference*, Steamboat Springs, Colorado, USA, 1997.
12. Bob B. He and Kingsley L. Smith, Fundamental Equation of Strain and Stress Measurement Using 2D Detectors, *Proceedings of 1998 SEM Spring Conference on Experimental and Applied Mechanics*, Houston, Texas, USA, 1998.
13. Bob B. He, Uwe Preckwinkel and Kingsley L. Smith, Advantages of Using 2D Detectors for Residual Stress Measurements, *Advances in X-ray Analysis, Vol. 42, Proceedings of the 47th Annual Denver X-ray Conference*, Colorado Springs, Colorado, USA, 1998.
14. Roger D. Durst *et. al.*, The Use of CCD Detectors for X-ray Diffraction, invited paper to: 1998 Denver X-ray Conference.

2. System Configuration

GADDS systems are available in a variety of configurations to fulfill requirements of different applications and samples. A system normally consists of the following five major units (each of which may have several options):

- an X-ray generator to produce X-rays,
- X-ray optics to condition the primary X-ray beam,
- a goniometer and sample stage to establish and manipulate the geometric relationship between primary beam, sample, and detector,
- a sample alignment and monitor to assist users in positioning the sample into the instrument center and in monitoring the sample state and position,
- a detector (HI-STAR Area Detector System) to intercept and record the scattering X-rays from a sample and to save and display the

diffraction pattern into a two-dimensional image frame.

Figure 2.1 shows a typical system.

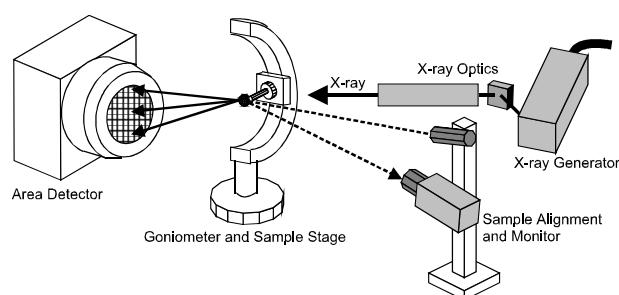


Figure 2.1 - Five major units in a GADDS system: X-ray generator (sealed tube); X-ray optics (monochromator and collimator); goniometer and sample stage; sample alignment and monitor (laser-video); and area detector

In addition to the five major units there are other accessories, such as a low temperature stage, a high temperature stage, a Helium (or vacuum) beam path for SAXS, a beam stop, and alignment and calibration fixtures. The whole system is controlled by a computer that uses GADDS software.

D8 DISCOVER with GADDS (designed for speed, precision, flexibility, versatility, and reliability) is the new generation of our GADDS products. The following sections will introduce the five major units, several standard systems, and some accessories based on the D8 series. Due to the large variety of customer needs and the availability of new technologies and new components that make for numerous system combinations, this section introduces only the most commonly used GADDS components. Refer to other documents, the GADDS Administrator Manual, or consult our service personnel for components not covered.

2.1 X-ray Generator

The X-ray generator produces X-rays with the required radiation energy, focal spot, and intensity.

2.1.1 Radiation Energy

GADDS can use a variety of X-ray sources, from a sealed tube generator to a rotating anode generator (RAG) to synchrotron radiation (with CCD detector). The sealed tube generator is the most commonly used X-ray source in the GADDS system.

2.1.2 X-ray Spectrum and Characteristic Lines

X-rays generated by sealed tubes or rotating anode generator have an X-ray spectrum, which presents intensity vs. wavelength (Figure 2.2).

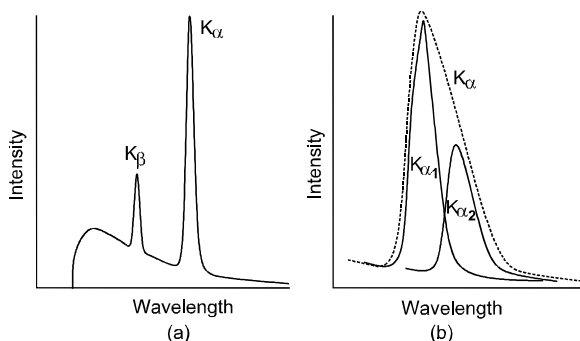


Figure 2.2 - X-ray spectrum generated by a sealed X-ray tube or rotating anode generator showing (a) continuous

(white) radiation and characteristic radiation lines K_{α} and K_{β} and (b) K_{α} line, a combination of two lines $K_{\alpha1}$ and $K_{\alpha2}$

The spectrum consists of continuous radiation (also called white radiation, or *Bremsstrahlung*) and a number of discrete characteristic lines. For X-ray diffraction, the three most important characteristic lines are $K_{\alpha1}$ and $K_{\alpha2}$ and K_{β} . The $K_{\alpha1}$ and $K_{\alpha2}$ lines are so close in their wavelengths that they are also called K_{α} doublet. The $K_{\alpha1}$ line is about twice the intensity of $K_{\alpha2}$. If the two K_{α} lines cannot be resolved, they are simply referred to as K_{α} line. The wavelengths of characteristic lines are determined by the target (anode) materials of the X-ray generator. Table 2.1 gives a list of common target materials and their wavelengths. Table 2.2 lists typical applications for each target material.

Table 2.1 – Wavelengths of characteristic lines of common target elements

Target	Energy (Ka) keV	Wavelength (\AA =10 ⁻¹ nm)			
		Ka	Ka1	Ka2	Kb
Ag	22.11	0.560868	0.5594075	0.563789	0.497069
Mo	17.44	0.710730	0.709300	0.713590	0.632288
Cu	8.04	1.541838	1.540562	1.544390	1.392218
Co	6.93	1.790260	1.788965	1.792850	1.62079
Fe	6.40	1.937355	1.936042	1.939980	1.75661
Cr	5.41	2.29100	2.28970	2.293606	2.08487

Table 2.2 – Selection of target material with respect to the applications

Target	Typical Applications
Ag	Low absorption; single crystal, transmission diffraction, (with CCD detector).
Mo	Low absorption; single crystal, transmission diffraction, (with CCD detector).
Cu	Most powder diffraction, stress, texture, thin films, polymer, SAXS, single crystal
Co	Used for ferrous alloys (steels) to reduce Fe fluorescence, ideal for residual stress.
Fe	Used for ferrous alloys (steels) to reduce Fe fluorescence, ideal for residual stress.
Cr	Ideal for materials with large unit cell, ideal for residual stress with high resolution.

2.1.3 Focal Spot and Takeoff Angle

The focal spot (also called focal spot on target) and takeoff angle are critical features in the production of X-rays by sealed tube and rotating anode generators. Sealed tube and rotating anode generators produce X-rays (Figure 2.3) by bombarding the target sample with electrons generated from the filament (cathode). The area bombarded by electrons is called focal spot on target, or simply focal spot, and the angle between the primary X-ray beam and the anode surface is called takeoff angle.

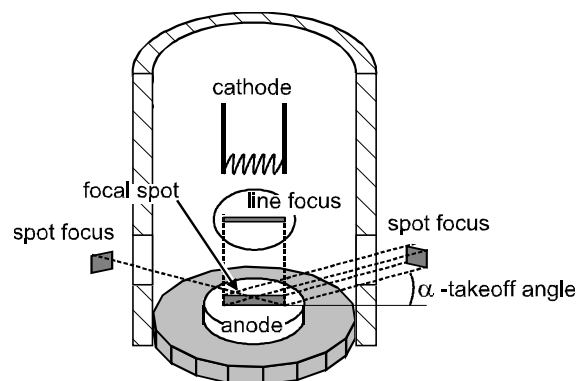


Figure 2.3 - Schematic of a sealed X-ray tube showing filament (cathode), anode, focal spot on anode, takeoff angle, projected line focus beam, and point focus beam

The size and shape of the focal spot is one of the most important features for an X-ray generator. Sealed X-ray tubes normally have 2 to 4 beryllium windows through which X-rays may exit. The focal spot is typically rectangular with a

length-to-width ratio of 10 to 1. The projection along the length of the focal spot at a takeoff angle from the anode surface is called spot focus (or square focus, or point focus). The projection of the focal spot perpendicular to its length is called line focus. Thus, line focus and spot focus are separated by an angle of 90° around the tube cylinder. The line focus is commonly used for the conventional diffractometer with point detector or PSD. A standard GADDS system uses the spot focus.

The takeoff angle can be set from 3° to 7° (6° for most systems). Table 2.3 lists focal spot size, line focus size, and spot focus size at a 6° takeoff angle for typical X-ray tubes used with GADDS systems.

Table 2.3 – Focal spot size, line focus size, and spot focus size of some typical X-ray tubes

Tube Type	Focal Spot Size at Anode (mm x mm)	Line Focus Size (mm x mm)	Spot Focus Size (mm x mm)
Normal focus	1 x 10	0.1 x 10	1 x 1
Fine focus	0.4 x 8	0.04 x 8	0.4 x 0.8
Long fine focus	0.4 x 12	0.04 x 12	0.4 x 1.2
Micro focus	0.15 x 8	0.015 x 8	0.15 x 0.8

2.1.4 Focal Spot Brightness and Profile

Focal spot brightness, focal spot profile, and X-ray optics (discussed in the next section) influence X-ray beam intensity. The focal spot brightness is determined by the maximum target loading, more specifically by power per unit area. Table 2.4 gives the maximum target loading and brightness (power per unit area) for some typical sealed tubes as well as some rotating anode sources equipped with a Cu target.

Table 2.4 – Focal spot brightness for sealed tubes and rotating anode sources with Cu target

Source	Focal Spot Size (mm x mm)	Maximum Load (kW)	Maximum Brightness (kW/mm ²)
Normal focus	1 x 10	2.0	0.2
Fine focus	0.4 x 8	1.5	0.5
Long fine focus	0.4 x 12	2.2	0.5
Micro focus	0.15 x 8	0.8	0.7
Rotating Anode Generator	0.5 x 10	18.0	3.6
	0.3 x 3	5.4	6.0
	0.2 x 2	3.0	7.5
	0.1 x 1	1.2	12.0

As shown, the micro focus sealed tubes have the brightest focal spot of all sealed tubes. Rotating anode generators have very high brilliance compared with sealed tubes. The intensity over the focal spot is not evenly distributed.

The focal spot profile is the intensity distribution over the area of the beam cross section and is eventually translated to the beam profile. The beam profile is sometimes very important to the diffraction result. The focal spot profile across the beam from fine focus and long fine focus sealed tube are typically saddled in the center with the maximum near the edge. The intensity at the center can be as low as 50% of the maximum. The focal spot profile for RAG is normally more evenly distributed, like a flat-topped Gaussian distribution. The focal profile from a fine focus or long fine focus sealed tube can satisfy most GADDS applications. The micro focus sealed tube and RAG may be necessary for some applications.

2.1.5 Operation of the X-ray Generator

Correct and careful operation of an X-ray generator is critical for satisfactory performance and useful lifetime. All X-ray tubes have a maximum power rating, which defines the highest power input to the tube. A cathode current vs. anode voltage chart (or table) is normally supplied for a sealed tube. The tube's filament current is also provided by the tube vendors. D8 DISCOVER with GADDS uses the K760 or K780 X-ray Generator (C79249-A3054-A3, -A4). The following information is for the K760. The K780 is only controlled by the software.

Detailed information for installation and operation is available in the vendor's Operating Instructions (C79000-B3476-C182-06). Refer to the manufacturer's manuals if your system has a rotating anode generator (RAG). Generally, you should adapt the following precautions when operating an X-ray generator:

1. Before starting the generator.
 - 1.1 Make sure the cooling water supply is available and running properly (temperature, pressure, flow rate, clean water and filter).
 - 1.2 Make sure all the safety interlocks work properly and are set correctly.
 - 1.3 Set the key switch to position "I". Position "II" is reserved for qualified service personnel, so you should not operate the generator on this setting.

2. Start the generator.
 - 2.1 Press the Heater key for approximately 2 seconds, and wait until the LED in the Heater key lights continuously.
 - 2.2 Then press the ON key. The X-RAYS ON signal lamp and radiation warning lamps light, the LED in the Heater key goes off, the LED in the ON key lights. And the display values read "kV=20 mA=5". (See the Operating Instructions if the generator responds differently).
3. Adjust the voltage and current.
 - 3.1 You can adjust the voltage and current manually (for PLATFORM GADDS) or through GADDS software (Collect > Goniometer > Generator, or press the Ctrl+Shft+G keys).
 - 3.2 When increasing the generator power manually, always increase voltage first and then current. When reducing the generator power, always reduce the current first and then voltage.
 - 3.3 When using a new X-ray tube or when the generator has been shut down for more than 12 hours, observe the following start-up procedures (Table 2.5), unless suggested otherwise by the manufacturer. An automatic start-up routine can be selected for new tubes (see Operating Instructions).
 - 3.4 To increase the lifetime of X-ray tubes, set the generator to standby mode (20kV, 5mA for sealed tube) if the generator is not in use for extended time (hours to days).

Table 2.5 – Start-up procedures for "cold generator" or new tube

Pause in Operation (days)	High Voltage/Duration								Total time for 55 kV
	20 kV	25 kV	30 kV	35 kV	40 kV	45 kV	50 kV	55 kV	
0.5 to 3	30 s	30 s	30 s	30 s	30 s	30 s	1 min	2 min	6 min
3 to 30	30 s	30 s	2 min	2 min	5 min	5 min	10 min	10 min	35 min
> 30 or new tube	30 s	30 s	2 min	2 min	5 min	10 min	15 min	15 min	50 min

2.2 X-ray Optics

The function of X-ray optics is to condition the primary X-ray beam into the required wavelength, beam focus size, beam profile, and divergence. The X-ray optics components commonly used for GADDS systems (and discussed in this section) are a monochromator, a pinhole collimator, cross-coupled Göbel mirrors, and a monocapillary.

Figure 2.4 shows an X-ray tube, a monochromator, a collimator, and a beam stop in a standard GADDS system. It also shows the instrument center and the shadow of a fixed chi stage.

Using a point X-ray source with pinhole collimation enables you to examine small samples (microdiffraction) or small regions on larger samples (selected-area diffraction). This configuration enables you to measure crystallographic phase, texture, and residual stress from precise locations on irregularly shaped parts, including curved surfaces.

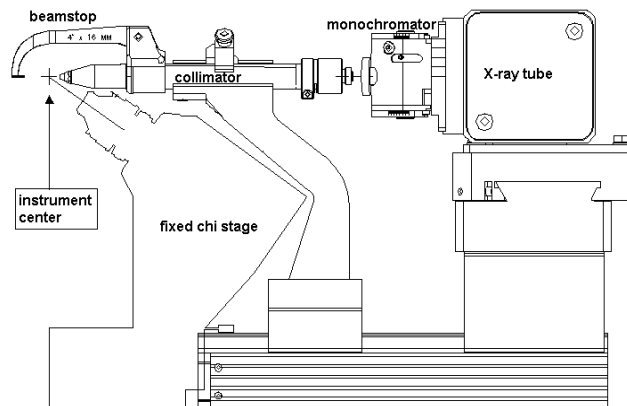


Figure 2.4 - Typical X-ray optics in standard GADDS includes X-ray tube, monochromator, collimator, and beam stop. Also shown are the instrument center and the shadow of a fixed chi stage

2.2.1 Monochromator

An important consideration for your system is that you will want to have an appropriate monochromator for the characteristics of the source, specimen, and instrument geometry. A crystal monochromator is typically used with a sealed tube or rotating anode generator to allow only a selected characteristic line (K_α or $K_{\alpha 1}$) to pass through the optics. While X-rays generated from a sealed X-ray tube or rotating anode generator consist of white radiation and other characteristic radiation lines, most X-ray diffraction applications need only the K_α (or $K_{\alpha 1}$) line. They need only this line because the white radiation produces an unwanted high background in the diffraction pattern, and the other characteristic lines produce extra and unwanted diffraction peaks (rings) in the diffraction pattern.

A crystal monochromator is illustrated in Figure 2.5. The single crystal has a d-spacing: d . The wavelength of the X-rays diffracted by the crystal is given by the Bragg law, $\lambda = 2d \sin \theta_M$. We can set the monochromator crystal to a diffraction condition such that only the wavelength of $K_{\alpha 1}$ satisfies the Bragg law. X-rays of other wavelengths are filtered out by the monochromator. As shown, the X-rays must also be in the correct direction to satisfy the diffraction condition. Thus, the reflected beam from a monochromator with a perfect crystal will be a parallel X-ray beam.

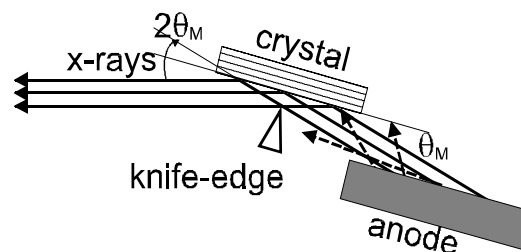


Figure 2.5 - Illustration of a crystal monochromator. Monochromatic X-rays are obtained by diffraction from a single crystal plate

In practice, the reflected beam from a monochromator is not strictly monochromatic due to the mosaic of the crystal (measured by rocking angle).

The crystal type in a monochromator must be chosen based on the performance you require in terms of intensity and resolution. Crystals such as Si, Ge, and quartz have small rocking angles, accompanied by high resolution and low intensity, while graphite and LiF crystals have high intensity and low resolution due to large mosaic spreads. The monochromator crystal shape also varies from flat to bent to cut-to-curve. A flat crystal is used for parallel beams and a curved crystal is used for focus geometry.

The standard GADDS system uses the flat graphite monochromator, which gives the strongest beam intensity. The monochromator is designed to accept a limited angular range of X-rays about the takeoff angle. The monochroma-

tor can be used for takeoff angles from 3° to 6° (typically set to 6°). The graphite crystal cannot resolve $K_{\alpha 1}$ and $K_{\alpha 2}$ lines, so it is aligned to the K_α line. The monochromator is designed to use various anode materials. Their $2\theta_M$ angles are listed in Table 2.6. You may need to input the $2\theta_M$ value if you choose to process data with polarization correction. See the service manual (269-005502 for P4 monochromator) for monochromator alignment.

Table 2.6 – Bragg angles of graphite crystal (002) plane for various target materials

Target Materials	K_α Wavelength	Bragg angle $2\theta_M$
Ag	0.560868	9.58
Mo	0.710730	12.14
Cu	1.541838	26.53
Co	1.790260	30.90
Fe	1.937355	33.51
Cr	2.29100	39.87

2.2.2 Pinhole Collimator

The pinhole collimator is normally used to control the beam size and divergence. In GADDS systems, the pinhole collimator is normally used with a monochromator or a set of cross-coupled Göbel mirrors. Figure 2.6 shows the X-ray beam path in a pinhole collimator achieved with two pinholes apertures of the same diameter d separated by a distance h . F is the dimension of the projection of focal spot or beam focus projection from the monochromator or Göbel mirrors. The distance between the focus and the second pinhole is H . The distance from the second pinhole to the sample surface is g .

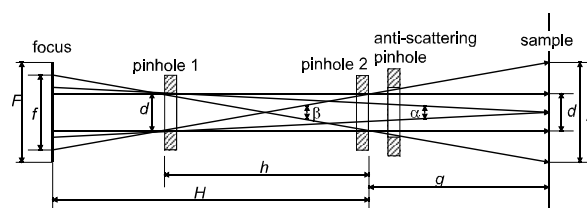


Figure 2.6 - Schematic of the beam path in a pinhole collimator showing the parallel, divergent, and convergent X-rays and beam spot on sample surface

The beam consists of three components: parallel, divergent, and convergent X-rays. The parallel part of the beam has a size of d all the way from focus to sample. The anti-scattering pinhole is used to block the X-ray scattering from the second pinhole. The size of the anti-scattering pinhole must be such that it allows no exposure to direct rays from the focus.

The maximum divergence angle β is given by

$$\beta = \frac{2d}{h} \quad (2-1)$$

The maximum angle of convergence α is given by

$$\alpha = \frac{d}{h+g} \quad (2-2)$$

The maximum beam spot D on a flat sample facing the X-ray source is given by

$$D = d \left(1 + \frac{2g}{h} \right) \quad (2-3)$$

As shown in the equation, the shorter the distance between the second pinhole and the sample (or the longer the distance between two pinholes), the smaller the beam spot on the sample. The effective beam focus size f is determined by the pinhole distance h and the distance between the X-ray source and the pinholes.

$$f = d \left(\frac{2H}{h} - 1 \right) \quad (2-4)$$

If the actual X-ray source F is larger than the effective focus size f , the difference between F and f represents the wasted X-ray energy. Sometimes, a micro-focus tube is required when a small beam size is used. The actual beam divergence is also determined by the monochromator and mirrors advancing the collimator in

the beam path. For example, when cross-coupled Göbel mirrors are used, the X-ray beam is almost a parallel beam, and the divergence of the beam is smaller than the value calculated from equation (2-1). When the actual beam focus on the source f is smaller than f , we have the following equations to calculate the maximum divergence (β'), convergence (α'), and beam spot size on sample (D'):

$$\beta' = \left(\frac{d+f'}{H} \right) \quad (2-5)$$

$$\alpha' = \frac{f'}{H+g} \quad (2-6)$$

$$D' = (\beta'(H+g) - f') \quad (2-7)$$

Table 2.7 lists the values of beam divergence, convergence, and beam spot on sample for a system with a 0.4 mm x 0.8 mm fine focus tube. The graphite monochromator has a rocking curve of 0.4° and cross-coupled Göbel mirrors of 0.06°. The beam divergence and convergence angles should not be above these values.

Table 2.7 – X-ray beam divergence angle (β), convergence angle (α), and beam spot size on sample (**D**) for a 0.4 mm point focus tube with graphite monochromator or cross-coupled Göbel Mirrors

Collimator Size	Graphite Monochromator				Göbel Mirrors		
d (mm)	β (°)	α (°)	D (mm)	f (mm)	β (°)	α (°)	D (mm)
0.05	0.041	0.017	0.07	0.15	0.041	0.017	0.07
0.10	0.082	0.034	0.14	0.30	0.060	0.034	0.13
0.20	0.164	0.067	0.29	0.60	0.060	0.060	0.23
0.30	0.246	0.101	0.42	0.80	0.060	0.060	0.33
0.50	0.266	0.148	0.64	0.80	0.060	0.060	0.53
0.80	0.327	0.148	0.97	0.80	0.060	0.060	0.83

The table also shows that the beam divergency decreases continuously with decreasing pinhole size for the combination of double pinhole collimator and monochromator. In some cases, the application requires small beam size but not necessarily the small divergence. We recommend that you remove the pinhole 1 from the collimator tube to achieve higher beam intensity.

Table 2.8 gives the comparison between double pinhole collimators and single pinhole collimators in terms of intensity gain (the approximate ratio of single-to-double pinhole), beam divergency, and beam spot size on sample.

Table 2.8 – Comparison between single pinhole collimator and double pinhole collimator in terms of intensity gain, beam divergency angle (β), and beam spot size on sample (D)

Collimator size	Intensity gain	Single pinhole		Double pinhole	
		b (x)	D (mm)	b (x)	D (mm)
d (mm)	Single/ double				
0.05	>20	0.174	0.14	0.041	0.07
0.10	16	0.184	0.20	0.082	0.14
0.20	4	0.205	0.31	0.164	0.29
0.30	2.4	0.225	0.42	0.225	0.42
0.50	1.2	0.266	0.64	0.266	0.64
0.80	1.0	0.327	0.97	0.327	0.97

The microdiffraction collimators are 50 μm and 100 μm in diameter. For quantitative analysis, texture, or percent crystallinity measurements, 0.5 mm or 0.8 mm collimators are typically used. In the case of quantitative analysis and texture measurements, using too small a collimator can actually be a detriment, causing poor statistical grain sampling. In such cases, you can improve statistics by oscillating the sample. Crystallite size measurements are usually measured with a 0.2 mm collimator at 30 cm sample-to-detector distance. The choice of collimator size is often a trade-off between intensity and the ability to illuminate small regions or to resolve closely spaced lines. The smaller the collimator, the lower the photon flux that strikes the sample, and the longer the count time to acquire statistically significant data.

2.2.3 Sample-to-Detector Distance and Angular Resolution

The divergence of the X-ray beam is a function of collimator size, sample-to-detector distance, ω and 2θ . The tables that follow can be used to determine a suitable collimator size and sample-to-detector distance to resolve closely spaced peaks. In all cases, the standard two-pinhole collimators are assumed, which have a sample-to-front pinhole distance of 8 mm. Only the more common combinations of collimator sizes and sample-to-detector distances are tabulated. These tables are for reflection mode. Transmission mode values for the apparent beam size can be located by translating ω by 90° , $\omega - 90^\circ$.

Table 2.9 – Beam divergence (2θ spread in $^{\circ}$) as a function of ω and 2θ with a 0.05 mm collimator, 30 cm sample-to-detector distance, and 1024x1024 frames

ω	Apparent Size [mm]	2θ									
		4 $^{\circ}$	10 $^{\circ}$	20 $^{\circ}$	40 $^{\circ}$	60 $^{\circ}$	80 $^{\circ}$	100 $^{\circ}$	120 $^{\circ}$	140 $^{\circ}$	160 $^{\circ}$
1 $^{\circ}$	3.21	—	0.01	0.02	0.04	0.06	0.07	0.07	0.06	0.04	0.02
2 $^{\circ}$	1.60	—	—	0.01	0.02	0.03	0.03	0.03	0.03	0.02	0.01
5 $^{\circ}$	0.64	—	—	—	0.01	0.01	0.01	0.01	0.01	0.01	0.01
10 $^{\circ}$	0.32	—	—	—	—	0.01	0.01	0.01	0.01	0.01	—
20 $^{\circ}$	0.16	—	—	—	—	—	—	—	—	—	—
30 $^{\circ}$	0.11	—	—	—	—	—	—	—	—	—	—
40 $^{\circ}$	0.09	—	—	—	—	—	—	—	—	—	—
50 $^{\circ}$	0.07	—	—	—	—	—	—	—	—	—	—
90 $^{\circ}$	0.06	—	—	—	—	—	—	—	—	—	—

Table 2.10 – Beam divergence (2θ spread in $^{\circ}$) as a function of ω and 2θ with a 0.1 mm collimator, 30 cm sample-to-detector distance, and 1024x1024 frames

ω	Apparent Size [mm]	2θ									
		4 $^{\circ}$	10 $^{\circ}$	20 $^{\circ}$	40 $^{\circ}$	60 $^{\circ}$	80 $^{\circ}$	100 $^{\circ}$	120 $^{\circ}$	140 $^{\circ}$	160 $^{\circ}$
1 $^{\circ}$	6.42	0.01	0.02	0.04	0.09	0.12	0.13	0.13	0.12	0.09	0.05
2 $^{\circ}$	3.21	—	0.01	0.02	0.04	0.06	0.07	0.07	0.06	0.05	0.03
5 $^{\circ}$	1.28	—	—	0.01	0.02	0.02	0.03	0.03	0.02	0.02	0.01
10 $^{\circ}$	0.64	—	—	—	0.01	0.01	0.01	0.01	0.01	0.01	0.01
20 $^{\circ}$	0.33	—	—	—	—	—	0.01	0.01	0.01	0.01	—
30 $^{\circ}$	0.22	—	—	—	—	—	—	—	—	—	—
40 $^{\circ}$	0.17	—	—	—	—	—	—	—	—	—	—
50 $^{\circ}$	0.15	—	—	—	—	—	—	—	—	—	—
90 $^{\circ}$	0.11	—	—	—	—	—	—	—	—	—	—

Table 2.11 – Beam divergence (2θ spread in $^{\circ}$) as a function of ω and 2θ with a 0.2 mm collimator, 30 cm sample-to-detector distance, and 1024x1024 frames

ω	Apparent Size [mm]	2θ									
		4°	10°	20°	40°	60°	80°	100°	120°	140°	160°
1°	12.83	0.01	0.04	0.09	0.17	0.23	0.27	0.27	0.24	0.18	0.10
2°	6.42	—	0.02	0.04	0.08	0.12	0.13	0.13	0.12	0.09	0.05
5°	2.57		—	0.01	0.03	0.04	0.05	0.05	0.05	0.04	0.02
10°	1.29			—	0.01	0.02	0.03	0.03	0.03	0.02	0.01
20°	0.65				—	0.01	0.01	0.01	0.01	0.01	0.01
30°	0.45				—	—	0.01	0.01	0.01	0.01	0.01
40°	0.35					—	—	0.01	0.01	0.01	0.01
50°	0.29					—	—	—	0.01	0.01	0.01
90°	0.22							—	—	—	—

Table 2.12 – Beam divergence (2θ spread in $^{\circ}$) as a function of ω and 2θ with a 0.3 mm collimator, 30 cm sample-to-detector distance, and 1024x1024 frames

ω	Apparent Size [mm]	2θ									
		4°	10°	20°	40°	60°	80°	100°	120°	140°	160°
1°	19.25	0.02	0.06	0.13	0.26	0.35	0.40	0.40	0.36	0.27	0.15
2°	9.63	0.01	0.03	0.06	0.13	0.17	0.20	0.20	0.18	0.14	0.08
5°	3.85		0.01	0.02	0.05	0.07	0.08	0.08	0.07	0.06	0.03
10°	1.93			0.01	0.02	0.03	0.04	0.04	0.04	0.03	0.02
20°	0.98				0.01	0.01	0.02	0.02	0.02	0.02	0.01
30°	0.67				—	0.01	0.01	0.01	0.01	0.01	0.01
40°	0.52					—	0.01	0.01	0.01	0.01	0.01
50°	0.44					—	—	0.01	0.01	0.01	0.01
90°	0.34							—	—	0.01	0.01

Table 2.13 – Beam divergence (2θ spread in $^{\circ}$) as a function of ω and 2θ with a 0.5 mm collimator, 30 cm sample-to-detector distance, and 1024x1024 frames

ω	Apparent Size [mm]	2θ									
		4 $^{\circ}$	10 $^{\circ}$	20 $^{\circ}$	40 $^{\circ}$	60 $^{\circ}$	80 $^{\circ}$	100 $^{\circ}$	120 $^{\circ}$	140 $^{\circ}$	160 $^{\circ}$
1 $^{\circ}$	32.08	0.04	0.11	0.22	0.43	0.58	0.67	0.67	0.59	0.45	0.24
2 $^{\circ}$	16.04	0.01	0.05	0.11	0.21	0.29	0.33	0.34	0.30	0.23	0.13
5 $^{\circ}$	6.42		0.01	0.04	0.08	0.11	0.13	0.14	0.12	0.10	0.06
10 $^{\circ}$	3.22			0.01	0.03	0.05	0.06	0.07	0.06	0.05	0.03
20 $^{\circ}$	1.64				0.01	0.02	0.03	0.03	0.03	0.03	0.02
30 $^{\circ}$	1.12				—	0.01	0.02	0.02	0.02	0.02	0.02
40 $^{\circ}$	0.87					0.01	0.01	0.02	0.02	0.02	0.02
50 $^{\circ}$	0.73					—	0.01	0.01	0.01	0.02	0.01
90 $^{\circ}$	0.56							—	0.01	0.01	0.01

Table 2.14 – Beam divergence (2θ spread in $^{\circ}$) as a function of ω and 2θ with a 0.05 mm collimator, 15 cm sample-to-detector distance, and 1024x1024 frames

ω	Apparent Size [mm]	2θ									
		4 $^{\circ}$	10 $^{\circ}$	20 $^{\circ}$	40 $^{\circ}$	60 $^{\circ}$	80 $^{\circ}$	100 $^{\circ}$	120 $^{\circ}$	140 $^{\circ}$	160 $^{\circ}$
1 $^{\circ}$	3.21	0.01	0.02	0.04	0.08	0.11	0.13	0.13	0.11	0.09	0.05
2 $^{\circ}$	1.60	—	0.01	0.02	0.04	0.06	0.06	0.07	0.06	0.04	0.02
5 $^{\circ}$	0.64		—	0.01	0.02	0.02	0.03	0.03	0.02	0.02	0.01
10 $^{\circ}$	0.32			—	0.01	0.01	0.01	0.01	0.01	0.01	0.01
20 $^{\circ}$	0.16				—	—	0.01	0.01	0.01	0.01	—
30 $^{\circ}$	0.11				—	—	—	—	—	—	—
40 $^{\circ}$	0.09					—	—	—	—	—	—
50 $^{\circ}$	0.07					—	—	—	—	—	—
90 $^{\circ}$	0.06							—	—	—	—

Table 2.15 – Beam divergence (2θ spread in $^{\circ}$) as a function of ω and 2θ with a 0.1 mm collimator, 15 cm sample-to-detector distance, and 1024x1024 frames

ω	Apparent Size [mm]	2θ									
		4 $^{\circ}$	10 $^{\circ}$	20 $^{\circ}$	40 $^{\circ}$	60 $^{\circ}$	80 $^{\circ}$	100 $^{\circ}$	120 $^{\circ}$	140 $^{\circ}$	160 $^{\circ}$
1 $^{\circ}$	6.42	0.01	0.04	0.09	0.17	0.23	0.26	0.26	0.23	0.17	0.09
2 $^{\circ}$	3.21	—	0.02	0.04	0.08	0.11	0.13	0.13	0.12	0.09	0.05
5 $^{\circ}$	1.28		—	0.01	0.03	0.04	0.05	0.05	0.05	0.04	0.02
10 $^{\circ}$	0.64			—	0.01	0.02	0.02	0.03	0.02	0.02	0.01
20 $^{\circ}$	0.33				—	0.01	0.01	0.01	0.01	0.01	0.01
30 $^{\circ}$	0.22				—	—	0.01	0.01	0.01	0.01	0.01
40 $^{\circ}$	0.17					—	—	0.01	0.01	0.01	0.01
50 $^{\circ}$	0.15					—	—	—	0.01	0.01	0.01
90 $^{\circ}$	0.11							—	—	—	—

Table 2.16 – Beam divergence (2θ spread in $^{\circ}$) as a function of ω and 2θ with a 0.2 mm collimator, 15 cm sample-to-detector distance, and 1024x1024 frames

ω	Apparent Size [mm]	2θ									
		4 $^{\circ}$	10 $^{\circ}$	20 $^{\circ}$	40 $^{\circ}$	60 $^{\circ}$	80 $^{\circ}$	100 $^{\circ}$	120 $^{\circ}$	140 $^{\circ}$	160 $^{\circ}$
1 $^{\circ}$	12.83	0.03	0.08	0.17	0.33	0.45	0.52	0.52	0.46	0.34	0.19
2 $^{\circ}$	6.42	0.01	0.04	0.08	0.16	0.22	0.26	0.26	0.23	0.18	0.10
5 $^{\circ}$	2.57		0.01	0.03	0.06	0.09	0.10	0.10	0.10	0.07	0.04
10 $^{\circ}$	1.29			0.01	0.03	0.04	0.05	0.05	0.05	0.04	0.03
20 $^{\circ}$	0.65				0.01	0.02	0.02	0.03	0.03	0.02	0.02
30 $^{\circ}$	0.45				—	0.01	0.01	0.02	0.02	0.02	0.01
40 $^{\circ}$	0.35					—	0.01	0.01	0.01	0.01	0.01
50 $^{\circ}$	0.29					—	0.01	0.01	0.01	0.01	0.01
90 $^{\circ}$	0.22							—	—	0.01	0.01

Table 2.17 – Beam divergence (2θ spread in $^{\circ}$) as a function of ω and 2θ with a 0.3 mm collimator, 15 cm sample-to-detector distance, and 1024x1024 frames

ω	Apparent Size [mm]	2θ									
		4 $^{\circ}$	10 $^{\circ}$	20 $^{\circ}$	40 $^{\circ}$	60 $^{\circ}$	80 $^{\circ}$	100 $^{\circ}$	120 $^{\circ}$	140 $^{\circ}$	160 $^{\circ}$
1 $^{\circ}$	19.25	0.04	0.12	0.26	0.50	0.68	0.78	0.79	0.69	0.52	0.28
2 $^{\circ}$	9.63	0.01	0.05	0.12	0.24	0.33	0.39	0.39	0.35	0.26	0.15
5 $^{\circ}$	3.85		0.01	0.04	0.09	0.13	0.15	0.16	0.14	0.11	0.07
10 $^{\circ}$	1.93			0.01	0.04	0.06	0.07	0.08	0.07	0.06	0.04
20 $^{\circ}$	0.98				0.01	0.03	0.03	0.04	0.04	0.03	0.03
30 $^{\circ}$	0.67				—	0.01	0.02	0.03	0.03	0.03	0.02
40 $^{\circ}$	0.52					0.01	0.01	0.02	0.02	0.02	0.02
50 $^{\circ}$	0.44					—	0.01	0.01	0.02	0.02	0.02
90 $^{\circ}$	0.34							—	0.01	0.01	0.01

Table 2.18 – Beam divergence (2θ spread in $^{\circ}$) as a function of ω and 2θ with a 0.5 mm collimator, 15 cm sample-to-detector distance, and 1024x1024 frames

ω	Apparent Size [mm]	2θ									
		4 $^{\circ}$	10 $^{\circ}$	20 $^{\circ}$	40 $^{\circ}$	60 $^{\circ}$	80 $^{\circ}$	100 $^{\circ}$	120 $^{\circ}$	140 $^{\circ}$	160 $^{\circ}$
1 $^{\circ}$	32.08	0.07	0.21	0.43	0.83	1.13	1.29	1.30	1.15	0.86	0.47
2 $^{\circ}$	16.04	0.02	0.09	0.20	0.40	0.56	0.64	0.65	0.58	0.44	0.25
5 $^{\circ}$	6.42		0.02	0.07	0.15	0.22	0.25	0.26	0.24	0.19	0.11
10 $^{\circ}$	3.22			0.02	0.07	0.10	0.12	0.13	0.12	0.10	0.07
20 $^{\circ}$	1.64				0.02	0.04	0.06	0.07	0.07	0.06	0.04
30 $^{\circ}$	1.12				0.01	0.02	0.04	0.04	0.05	0.04	0.04
40 $^{\circ}$	0.87					0.01	0.02	0.03	0.04	0.04	0.03
50 $^{\circ}$	0.73					0.01	0.02	0.02	0.03	0.03	0.03
90 $^{\circ}$	0.56							—	0.01	0.02	0.02

Table 2.19 – Beam divergence (2θ spread in $^{\circ}$) as a function of ω and 2θ with a 0.8 mm collimator, 15 cm sample-to-detector distance, and 1024x1024 frames

ω	Apparent Size [mm]	2θ									
		4 $^{\circ}$	10 $^{\circ}$	20 $^{\circ}$	40 $^{\circ}$	60 $^{\circ}$	80 $^{\circ}$	100 $^{\circ}$	120 $^{\circ}$	140 $^{\circ}$	160 $^{\circ}$
1 $^{\circ}$	51.33	0.11	0.33	0.68	1.32	1.80	2.06	2.08	1.84	1.38	0.75
2 $^{\circ}$	25.67	0.04	0.15	0.32	0.65	0.89	1.03	1.04	0.93	0.70	0.39
5 $^{\circ}$	10.28		0.04	0.11	0.24	0.34	0.41	0.42	0.38	0.30	0.18
10 $^{\circ}$	5.16			0.04	0.11	0.16	0.20	0.21	0.20	0.16	0.11
20 $^{\circ}$	2.62				0.04	0.07	0.09	0.11	0.11	0.09	0.07
30 $^{\circ}$	1.79				0.01	0.04	0.06	0.07	0.07	0.07	0.06
40 $^{\circ}$	1.39					0.02	0.04	0.05	0.06	0.06	0.05
50 $^{\circ}$	1.17					0.01	0.02	0.04	0.05	0.05	0.05
90 $^{\circ}$	0.90							0.01	0.02	0.03	0.03

Table 2.20 – Beam divergence (2θ spread in $^{\circ}$) as a function of ω and 2θ with a 0.2 mm collimator, 6 cm sample-to-detector distance, and 1024x1024 frames

ω	Apparent Size [mm]	2θ									
		4 $^{\circ}$	10 $^{\circ}$	20 $^{\circ}$	40 $^{\circ}$	60 $^{\circ}$	80 $^{\circ}$	100 $^{\circ}$	120 $^{\circ}$	140 $^{\circ}$	160 $^{\circ}$
1 $^{\circ}$	12.83	0.06	0.17	0.36	0.69	0.94	1.08	1.08	0.96	0.72	0.39
2 $^{\circ}$	6.42	0.02	0.08	0.17	0.34	0.47	0.54	0.54	0.48	0.37	0.21
5 $^{\circ}$	2.57		0.02	0.06	0.13	0.18	0.21	0.22	0.20	0.16	0.09
10 $^{\circ}$	1.29			0.02	0.06	0.08	0.10	0.11	0.10	0.08	0.06
20 $^{\circ}$	0.65				0.02	0.04	0.05	0.06	0.06	0.05	0.04
30 $^{\circ}$	0.45				0.01	0.02	0.03	0.04	0.04	0.04	0.03
40 $^{\circ}$	0.35					0.01	0.02	0.03	0.03	0.03	0.03
50 $^{\circ}$	0.29					—	0.01	0.02	0.02	0.03	0.02
90 $^{\circ}$	0.22							—	0.01	0.01	0.02

Table 2.21 – Beam divergence (2θ spread in $^{\circ}$) as a function of ω and 2θ with a 0.3 mm collimator, 6 cm sample-to-detector distance, and 1024x1024 frames

ω	Apparent Size [mm]	2θ									
		4 $^{\circ}$	10 $^{\circ}$	20 $^{\circ}$	40 $^{\circ}$	60 $^{\circ}$	80 $^{\circ}$	100 $^{\circ}$	120 $^{\circ}$	140 $^{\circ}$	160 $^{\circ}$
1 $^{\circ}$	19.25	0.09	0.26	0.54	1.04	1.41	1.62	1.63	1.44	1.08	0.59
2 $^{\circ}$	9.63	0.03	0.11	0.25	0.51	0.70	0.81	0.82	0.73	0.55	0.31
5 $^{\circ}$	3.85		0.03	0.09	0.19	0.27	0.32	0.33	0.30	0.23	0.14
10 $^{\circ}$	1.93			0.03	0.08	0.13	0.16	0.17	0.16	0.13	0.08
20 $^{\circ}$	0.98				0.03	0.05	0.07	0.08	0.08	0.07	0.05
30 $^{\circ}$	0.67				0.01	0.03	0.04	0.05	0.06	0.05	0.04
40 $^{\circ}$	0.52					0.02	0.03	0.04	0.04	0.04	0.04
50 $^{\circ}$	0.44					0.01	0.02	0.03	0.04	0.04	0.04
90 $^{\circ}$	0.34							0.01	0.01	0.02	0.03

Table 2.22 – Beam divergence (2θ spread in $^{\circ}$) as a function of ω and 2θ with a 0.5 mm collimator, 6 cm sample-to-detector distance, and 1024x1024 frames

ω	Apparent Size [mm]	2θ									
		4 $^{\circ}$	10 $^{\circ}$	20 $^{\circ}$	40 $^{\circ}$	60 $^{\circ}$	80 $^{\circ}$	100 $^{\circ}$	120 $^{\circ}$	140 $^{\circ}$	160 $^{\circ}$
1 $^{\circ}$	32.08	0.14	0.43	0.89	1.73	2.35	2.69	2.71	2.40	1.80	0.98
2 $^{\circ}$	16.04	0.05	0.19	0.42	0.84	1.16	1.34	1.36	1.21	0.92	0.51
5 $^{\circ}$	6.42		0.05	0.14	0.32	0.45	0.53	0.55	0.50	0.39	0.23
10 $^{\circ}$	3.22			0.05	0.14	0.21	0.26	0.28	0.26	0.21	0.14
20 $^{\circ}$	1.64				0.05	0.09	0.12	0.14	0.14	0.12	0.09
30 $^{\circ}$	1.12				0.02	0.05	0.07	0.09	0.10	0.09	0.07
40 $^{\circ}$	0.87					0.03	0.05	0.06	0.07	0.07	0.06
50 $^{\circ}$	0.73					0.01	0.03	0.05	0.06	0.06	0.06
90 $^{\circ}$	0.56							0.01	0.02	0.04	0.05

Table 2.23 – Beam divergence (2θ spread in $^{\circ}$) as a function of ω and 2θ with a 0.8 mm collimator, 6 cm sample-to-detector distance, and 1024x1024 frames

ω	Apparent Size [mm]	2θ									
		4°	10°	20°	40°	60°	80°	100°	120°	140°	160°
1°	51.33	0.23	0.69	1.43	2.76	3.76	4.31	4.34	3.84	2.88	1.57
2°	25.67	0.08	0.31	0.68	1.35	1.86	2.15	2.17	1.94	1.47	0.82
5°	10.28		0.08	0.23	0.50	0.72	0.85	0.88	0.80	0.62	0.37
10°	5.16			0.08	0.22	0.34	0.41	0.44	0.41	0.34	0.22
20°	2.62				0.08	0.14	0.19	0.22	0.22	0.19	0.14
30°	1.79				0.03	0.08	0.12	0.14	0.15	0.14	0.12
40°	1.39					0.04	0.08	0.10	0.12	0.12	0.10
50°	1.17					0.02	0.05	0.08	0.09	0.10	0.09
90°	0.90							0.01	0.04	0.06	0.07

2.2.4 Single and Cross-Coupled Göbel Mirrors

Recent developments in X-ray optics include graded multilayer X-ray mirrors, known as Göbel mirrors. A cross-coupled arrangement of these optics for the GADDS system provides a highly parallel beam which is much more intense than can be obtained with standard pinhole collimation and a graphite monochromator. For applications such as microdiffraction, where a small spot size is desired, Göbel mirrors can offer greater intensity than conventional optics. The low divergence of the beam incident on the sample from Göbel mirrors also decreases the width of crystalline peaks, improving the resolution of a GADDS system.

The Göbel mirror is a parabolic-shaped multilayer mirror. Multilayer mirrors reflect X-rays in the same way as Bragg diffraction from crystals, so multilayer mirrors can be used as a monochromator. In contrast to a conventional crystal monochromator, Göbel mirrors are manufactured so that the d-spacing between the layers varies in a controlled manner. The appropriate gradient in the d-spacing depends on factors which include wavelength, the location of the mirror with respect to the source, and the application for which the mirror is designed.

Figure 2.7(a) illustrates a single Göbel mirror. The Göbel mirror is parabolically bent, which causes a divergent beam striking the mirror at different locations and angles to yield an intense

and highly parallel beam. With Bragg diffraction, the radiation is monochromatized to K_{α} , while K_{β} and Bremsstrahlung are suppressed. The single mirror can be used with either a point focus or line focus tube. In Bruker UBC (universal beam concept) optics, a single mirror is coupled with a line focus tube. The combination allows an easy switch between line focus geometry and point focus geometry without changing the X-ray tube. When these optics are on a GADDS system, a set of pinhole collimators and pinhole slits convert the line focus beam into a point focus beam. Figure 2.7(b) shows the cross-coupled Göbel mirrors used for an X-ray source with point focus, where a second Göbel mirror turned 90° collimates the beam in the direction perpendicular to the first mirror.

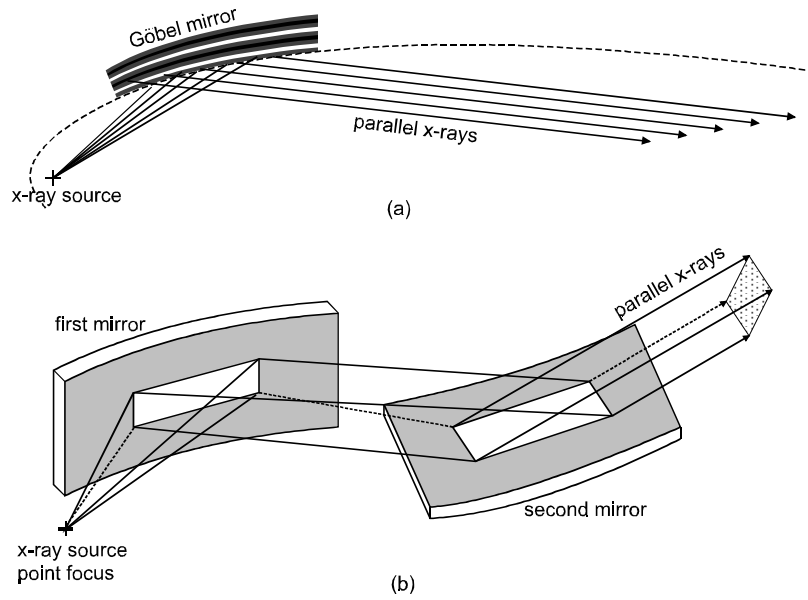


Figure 2.7 - (a) A single parabolically bent Göbel mirror transforms the divergent primary beam from source into a parallel beam. (b) In the cross-coupled Göbel mirrors, the second Göbel mirror turned 90° collimates the beam in the direction perpendicular to the first mirror.

For all applications requiring strong collimation of the beam, Göbel mirrors provide considerable intensity gains. Experimental results show that the smaller the beam size, the stronger the intensity gains from cross-coupled Göbel mirrors compared with a monochromator (Figure 2.8). Therefore, the cross-coupled Göbel mirrors are especially suitable for microdiffraction and small angle X-ray scattering. The specifications of Göbel mirrors for various applications are listed in Table 2.24.

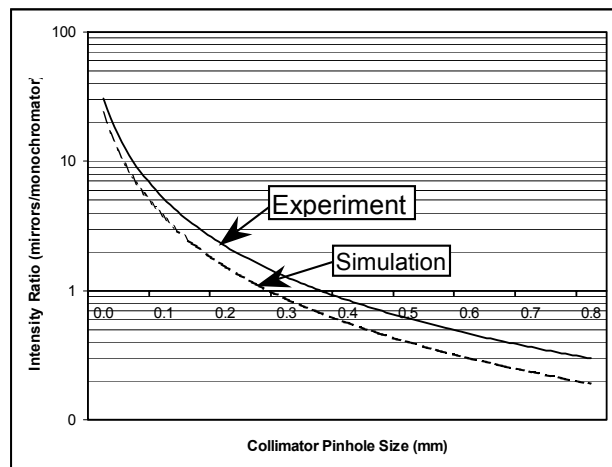


Figure 2.8 - Comparison of X-ray intensity between cross-coupled Göbel mirrors and monochromator for various collimator pinhole size. The solid line represents experimental value, and the broken line is the computer-simulated values.

The intensity break-even point for Göbel mirrors versus standard pinhole collimation is about 0.3 to 0.4 mm. Thus, for applications such as texture or phase identification from a bulk powdered specimen, which ordinarily employ collimators larger than 0.4 mm, there is no benefit to using Göbel mirrors. In fact, the low divergence of the resulting beam can cause poor statistical grain sampling in such cases.

Table 2.24 – Specifications of the single Göbel mirror and the cross-coupled Göbel mirrors.

Goniometer	D500X	D8	GADDS/SMART	
Beam	parallel	parallel	parallel	
Focus	line focus	line focus	point focus	
Dimension (mm)	40x20	40x20 or 60x20	40x20	60x20
d-spacing Range (Å)	31–38	31–38	31–38	40–50
Radiation	Cu/Co/Cr	Cu/Co/Cr	Cu	Cu
Approximate $2\theta_M(\text{Cu})$	2.5×	2.5×	2.5×	2.0×
Angle of Acceptance	0.6×	0.6×	0.6×	1×
Beam Divergence	0.05–0.07×	0.05–0.07×	0.05–0.07×	0.05–0.07×
Max. Beam Size (mm)	>0.5	>0.5	>0.5	>0.5
Monochromatization	K_α	K_α	K_α	K_α

2.2.5 Monocapillary

The monocapillary is a cylindrical tube with a smooth inner surface that may be used in place of a pinhole collimator. The monocapillary is a product of capillary X-ray optics, which is based on the concept of total external reflection. That is, X-rays can be reflected by a smooth surface when the angle of incidence is smaller than the critical angle θ_c . The critical angle is a function of the wavelength and materials. The shorter the wavelength, the lower the critical angle. When X-rays are reflected by the inner surface of a capillary at a grazing angle smaller than the critical angle of the capillary materials, X-rays are reflected with little energy loss. The transmission efficiency depends upon the X-ray energy, the capillary materials, reflection surface smoothness, the capillary inner diameter, and incident beam divergence. The K_β radiation, having higher energy than K_α , has less transmission efficiency. For typical capillary materials, the critical angle is about 0.2° for Cu- K_α radiation.

For GADDS systems, the monocapillary (trade name MonoCap™) is mounted inside a steel tube. The tube is of the same design as the one used for the pinhole collimator. Therefore, it is easy to switch between pinhole collimator and monocapillary. The monocapillary performs the following main functions:

- It collimates the beam spatially to a variety of beam sizes for different applications. You have a choice of monocapillary sizes from 1.0 mm down to 0.01 mm.
- It collimates the beam divergency. The exit beam divergency is controlled by the capillary dimensions (diameter and length) and the critical angle of total reflection.
- It can produce significant intensity gain on the sample relative to pinhole collimators.

Table 2.25 shows that 0.1 to 1.0 mm capillaries give practically the same spot sizes on the sample as the corresponding double-pinhole collimators. The capillaries produce large intensity gain relative to the corresponding double-pinhole collimators. In the case of small beam size, a special combination of capillary and pinhole may be favorable. A capillary of large diameter captures more radiation near the source and transports it with less intensity loss. The pinhole with smaller diameter defines the final beam size. The combination can obtain more uniformly distributed radiation energy on the sample.

Table 2.25 – Intensity gain (calculated and experimental) and beam spot size including 90% energy on sample for monocapillaries compared with double pinhole collimator

Capillary/ Pinhole size: d (mm)	Cu-Ka-radiation (8.0 keV)			Mo-Ka-radiation (17.4 keV)			Collimator
	Gain calc.	Gain exp.	Spot 90%	Gain calc.	Gain exp.	Spot 90%	Spot 90%
0.10	110	66	0.18	39	40	0.14	0.10
0.30	15	10	0.34	5.6	5.9	0.31	0.31
0.50	7.4	6.0	0.50	2.6	3.0	0.49	0.50
1.00	3.4	4.2	0.89	1.2	1.5	0.97	0.98

2.3 Goniometer and Stages

The purpose of a goniometer and sample stages is to establish and control the geometric relationship between primary beam, sample, and detector. All GADDS configurations are based on a D8 (or PLATFORM for earlier versions) goniometer. The D8 goniometer is a high-precision, two-circle goniometer with independent stepper motors and optical encoders for θ

and 2θ circles. The selectable driving step size can be as small as 0.0001° . The goniometer reproducibility is $\pm 0.0001^\circ$. The D8 goniometer can be used in horizontal θ - 2θ , vertical θ - 2θ , and vertical θ - θ geometry. Typical GADDS systems are built on the D8 goniometers in horizontal θ - 2θ geometry (Figure 2.9). A vertical θ - θ configuration is also available.

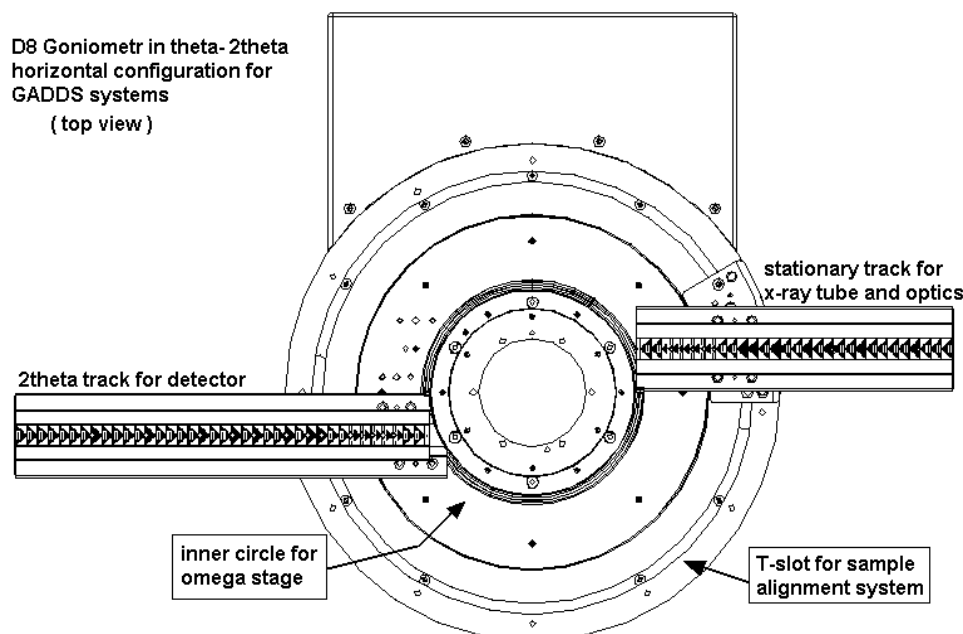
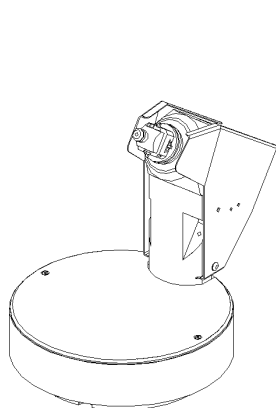


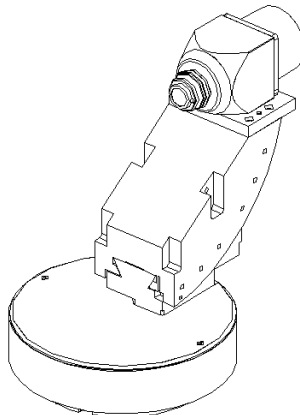
Figure 2.9 - D8 goniometer and two tracks for X-ray tube and optics and detector

The central opening in the θ ring provides the maximum possible flexibility for different samples and sample stages. The offset track mount mechanism allows the maximum θ , 2θ , and ω ranges for different configurations. Two tracks are typically mounted on the D8 goniometer, one for the X-ray source and optics, and one for the detector. The T-slot is available for mounting the sample alignment system or other attachments.

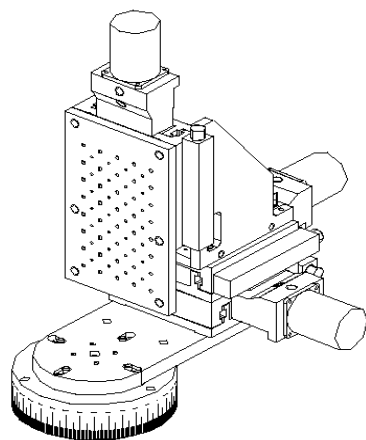
A variety of sample stages are used in GADDS systems. The sample stages are usually mounted on the inner θ circle of the goniometer. In θ - 2θ mode, the sample rotation is defined as ω rotation, so a sample stage directly mounted on the goniometer inner circle is also called ω -stage. The most commonly used sample stages are fixed-chi, two-position, XYZ, and $\frac{1}{4}$ -cradle (Figure 2.10.).



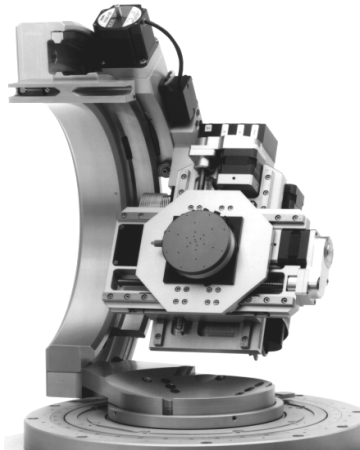
(a) Fixed-chi stage



(b) 2-position chi stage



(c) XYZ stage



(d) 1/4-circle Eulerian Cradle

Figure 2.10 - Four typical sample stages used in the GADDS system

Table 2.26 lists the specifications and typical applications for these stages.

Table 2.26 – Specifications and Applications of Sample Stages

Stages	Specification	Application
Fixed-Chi	Motorized ϕ axis, $\chi_g = 54.74^\circ$ ($\psi = 35.26^\circ$), $-\infty < \phi < \infty$ (usually used with a goniometer head with XYZ translation)	Phase ID with powder sample in capillary. Polymer applications. Texture and stress for small samples.
2-Position	Motorized ϕ axis, $\chi_g = 54.74^\circ$ and 90° ($\psi = 35.26^\circ$ and 0°), $-\infty < \phi < \infty$ (usually used with a goniometer head with XYZ translation)	The same as fixed-chi stage at $\chi_g = 54.74^\circ$. $\chi_g = 90^\circ$ is suitable for reflection mode diffraction, stress (tensor), and microdiffraction.
XYZ	Motorized X, Y and Z axes, Fixed $\chi_g = 90^\circ$ ($\psi = 0^\circ$), Fixed $\phi = 0^\circ$ (no ϕ rotation), X, Y, and Z travels: ± 50 mm, Max sample load: 10 kg, Position accuracy: 12.5 μm , Repeatability: 5 μm	Microdiffraction. Phase ID. Stress analysis. X-Y mapping. Multi-target screening.

Centric ¼-Circle Eulerian Cradle	Motorized ψ , ϕ , X, Y and Z axes, $-11 \leq \chi_g \leq 98^\circ$, $(-8 \leq \psi \leq 101^\circ)$, $-\infty < \phi < \infty$, $-40 \text{ mm} \leq X \leq 40 \text{ mm}$, $-40 \text{ mm} \leq Y \leq 40 \text{ mm}$, $-1 \text{ mm} \leq Z \leq 2 \text{ mm}$ Max sample load: 1 kg, Sphere of confusion: $\leq 50 \mu\text{m}$	Microdiffraction. Phase ID. Stress analysis. Texture analysis. X-Y mapping. High-resolution diffraction.
Huber ¼-Circle Eulerian Cradle	Motorized ψ , ϕ , X, Y and Z axes, $-3 \leq \chi_g \leq 94^\circ$, $-\infty < \phi < \infty$, $-75 \text{ mm} \leq X \leq 75 \text{ mm}$, $-75 \text{ mm} \leq Y \leq 75 \text{ mm}$, $-1 \text{ mm} \leq Z \leq 12 \text{ mm}$ Max sample load: 5 kg, Sphere of confusion: $\leq 50 \mu\text{m}$	Microdiffraction. Phase ID. Stress analysis. Texture analysis. X-Y mapping. High-resolution diffraction.

2.4 Sample Alignment and Monitor Systems

Sample alignment systems assist you in positioning the sample into the instrument center and in monitoring the sample's state and position before and during data collection. GADDs uses three types of sample alignment systems: optical microscope, video microscope, and laser/video microscope systems.

The optical microscope allows you to directly observe the sample in a magnified image with a crosshair to determine the sample position (Figure 2.11a).

The video microscope system includes a microscope head with manual zoom, a color CCD camera, and a frame grabber to capture and display the image of the sample (Figure 2.11b). User-selectable reticles are available in the video software. You can set the crosshair position and calibrate the image to determine the sample position and size. Since the video image can be captured with the safety enclosure closed, the video microscope can monitor the sample's state and position during the data collection. You can also save the image as a computer image file.

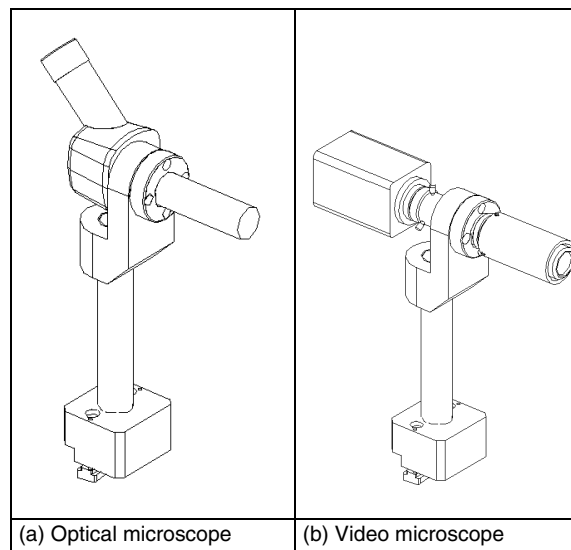


Figure 2.11 - Sample alignment systems: (a) optical microscope and (b) video microscope

The laser-video sample alignment system is based on a patent owned by Bruker AXS Inc. The cross-point of the laser beam and the optical axis of the zoom video are pre-aligned to the instrument center (Figure 2.12a). The laser image spot falls on the center of the crosshair when the sample surface is positioned at the instrument center (Figure 2.12b). The 3D view of the laser-video sample alignment system is illustrated in Figure 2.12c.

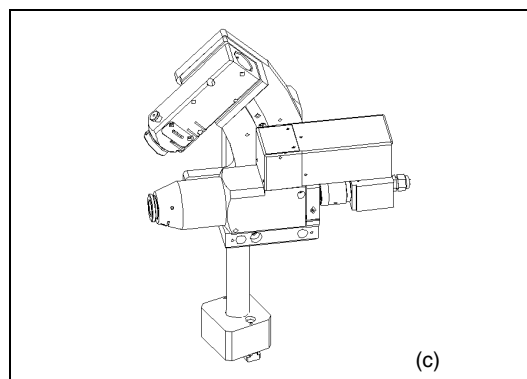
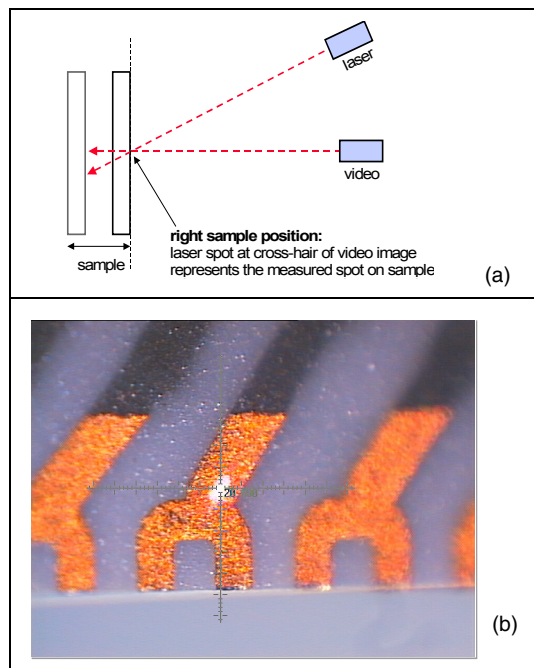


Figure 2.12 - Laser video sample alignment system with (a) principle of laser-video alignment system, (b) image of laser spot and crosshair, and (c) illustration of the laser video system

The specifications and applications of the three sample alignment systems are listed in Table 2.27.

Table 2.27 – Specifications and Applications of Three Sample Alignment Systems

System	Specification	Application
Optical Microscope	Magnification: 40x. Working distance: 73 mm. Field of view: 6.1 mm. Reticle: crosshair / 20mm division.	Sample alignment, suitable for capillary, single crystal and small samples. System alignment.
Video Microscope	Magnification: 30-114x (1/2 ϕ CCD /13 ϕ display), 45-171x (1/3 ϕ CCD /13 ϕ display). Primary zoom magnification: 0.75-3x. Working distance: 61 mm. Field of view: 8-2 mm. Color video camera (NTSC). Picture element: 768H x 494V. Horizontal resolution: > 480 TV lines. Frame grabber and image software. User selectable video reticles.	Sample alignment, suitable for capillary, single crystal and small samples. Monitor the sample during data collection. Save the video image into files. System alignment.
Laser/video Microscope	Video features Magnification: 40-280x (1/2 ϕ CCD /13 ϕ display). Computer controlled zoom lens: 1-7x. Working distance: 78 mm. Field of view: 6-0.9 mm. Color video camera (NTSC). Picture element: 768H x 494V. Horizontal resolution: > 460 TV lines. Frame grabber and image software. User selectable video reticles. Laser features Beam size: < 20 mm. Variable neutral density filter: manually adjustable from 10% to 80% transmission.	Laser pointer for accurate sample positioning, suitable for reflection samples. Micro-sample and micro-area alignment. Monitor the sample during data collection. Save the video image into files. System alignment.

2.5 HI-STAR Area Detector

The HI-STAR Area Detector is a two-dimensional multiwire proportional counter (MWPC) and is the core of a GADDS system (Figure 2.13).

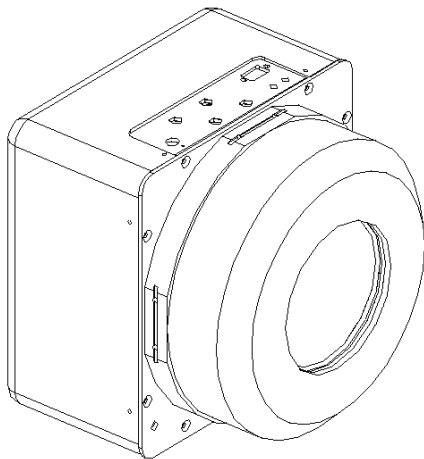


Figure 2.13 - HI-STAR Area Detector

The area detector has a large imaging area (11.5 cm diameter) for X-ray detection. It is sensitive to X-ray wavelengths corresponding to the 3-15keV energy range and is a true photon-counting device, with an absolute detection efficiency of 80 percent. It can collect a data frame of 1024x1024 (or 512x512) pixels with the pixel size of 105 μm (210 μm for 512x512 frames). For most X-ray diffraction applications, the HI-STAR system can be 104 times faster than a scintillation counter and 100 times faster than a linear position sensitive detector (PSD). Table

2.28 lists the specifications of the HI-STAR area detector compared with a typical scintillation detector and PSD. Table 2.29 lists the angular resolution for various detector distances.

Table 2.28 – Specifications of HI-STAR area detector, some properties are compared with typical PSD and scintillation detector

Specifications	HI-STAR	PSD	Scintillation
Data format	2D image	1D profile	0-D point
Field of view	11.5 cm diameter area	10-15 cm linear	point
Pixel format	1024x1024 (512x512)	1x(1000~2000)	1
Pixel size	105 μm (210 mm)	~100 μm	N/A
Point spread function	200 μm		
Quantum efficiency (8 keV)	80%	80%	70-90%
Sensitivity	1 photon / pixel	1 photon/pixel	
Dynamic range	$>10^6$	$>10^6$	10^7
Overall count rate	$10 \times 10^5 \text{ s}^{-1}$	$5 \times 10^4 \text{ s}^{-1}$	10^5 s^{-1}
Local count rate/pixel	200 cps/pixel with 512x512 frame		N/A
Noise rate	$\sim 10^{-5} \text{ pixel}^{-1} \text{ s}^{-1}$		$2-10 \text{ s}^{-1}$
Energy range	3-15 keV		5-50 keV
Energy resolution $\Delta E/E$	18%	18%	45%

The HI-STAR consists of an X-ray proportional chamber with a precision, two-dimensional multiwire grid; an integral pre-amplifier; high-resolution, high-speed decoding electronics; and a frame buffer computer for data collection, storage and detector control.

Table 2.29 – HI-STAR detector resolution.

Mode	Sample-to-Detector Distance	Pixel Size (Microns)	Resolution
1024x1024	30 cm	105	0.02°
1024x1024	15 cm	105	0.04°
1024x1024	6 cm	105	0.09°
512x512	30 cm	210	0.04°
512x512	15 cm	210	0.08°
512x512	6 cm	210	0.17°

Figure 2.14 illustrates the cross-section of the proportional chamber.

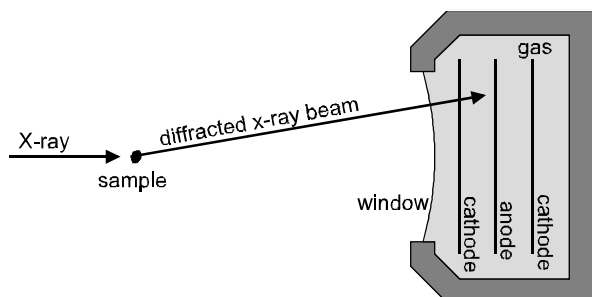


Figure 2.14 - Cross-section and work principle of area detector

The chamber is filled with a Xe/methane gas mixture pressurized to approximately 4 atmospheres. The window is 80% transparent to 8 keV radiation and permits pressurized operation. When an X-ray photon enters the detector, it interacts with the Xenon near the front window, ionizing the gas and creating a cloud of electrons. An electric field accelerates these electrons from the near-window region through a drift region. The detection grid consists of plane of fine anode wires located between two cathode planes of very fine-pitched wires. The electron cloud passes through the first cathode and is amplified by a factor of 2000 as it is collected at the anode wire surface.

Analog signal processing electronics, located directly behind the detector, produce very low noise signals, permitting high spatial resolution (200 μm) to be achieved at low charge gains of 2000. The position decoding circuit (PDC) converts the analog signals from the detector into digital values representing the X-Y position of each X-ray photon. Data from the PDC transfers to the frame buffer computer over a 32-bit wide parallel data link, allowing the frame to be displayed in real time as a 512x512 or a 1024x1024 pixel frame (with 32-bit data for each pixel) or to be stored in 8-, 16-, or 32-bit frames.

Because the detector is sealed, the xenon tube remains stable for years and adjustments to its circuitry are not usually necessary. Adjustment of the detector bias is, however, required for use

with different X-ray sources. Two preset bias settings are available, normally one for the given X-ray source and one for the calibration source. Two settings can be selected automatically or manually.

2.6 Small Angle X-ray Scattering (SAXS) Attachment

The small angle X-ray scattering (SAXS) attachment is designed for GADDs users to perform small angle X-ray scattering measurements (Figure 2.15). The beam stop assembly shown is mounted directly to the face of the HI-STAR detector. You align the beam stop using a pair of micrometers. The helium beam path can be adjusted over a range of sample-to-detector distances. The vacuum beam path, designed for a long sample-to-detector distance of 60 cm, is also available to achieve higher resolution.

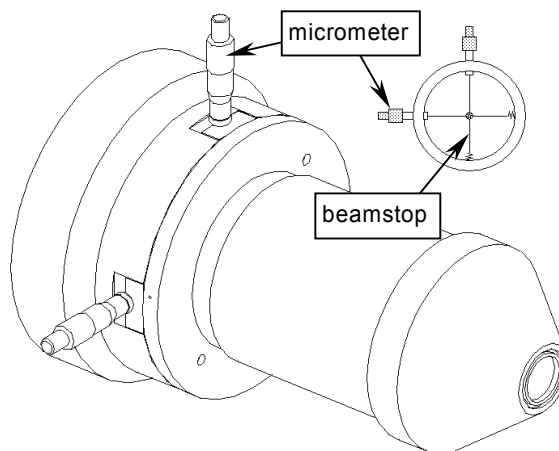


Figure 2.15 - Helium beam path for small angle X-ray scattering measurement. The cross-section shows the beam stop and adjustment micrometer

2.7 Standard GADDS Systems

A GADDS system can be built with the typical components introduced in the previous sections and many special components in various configurations for different applications. Due to the modular design concept of the D8 DISCOVER, GADDS systems have the compatibility and the flexibility to switch quickly and easily between different configurations and options. Based on the majority of application requirements, we have five standard GADDS systems in horizontal configuration: Standard Basic (Fixed-Chi) System (Figure 2.16), Standard Microdiffraction System (Figure 2.17), Standard Stress/Texture System (Figure 2.18), Standard Huber Eulerian $\frac{1}{4}$ -Cradle System (Figure 2.19), and Standard Centric Eulerian $\frac{1}{4}$ -Cradle System (Figure 2.20).

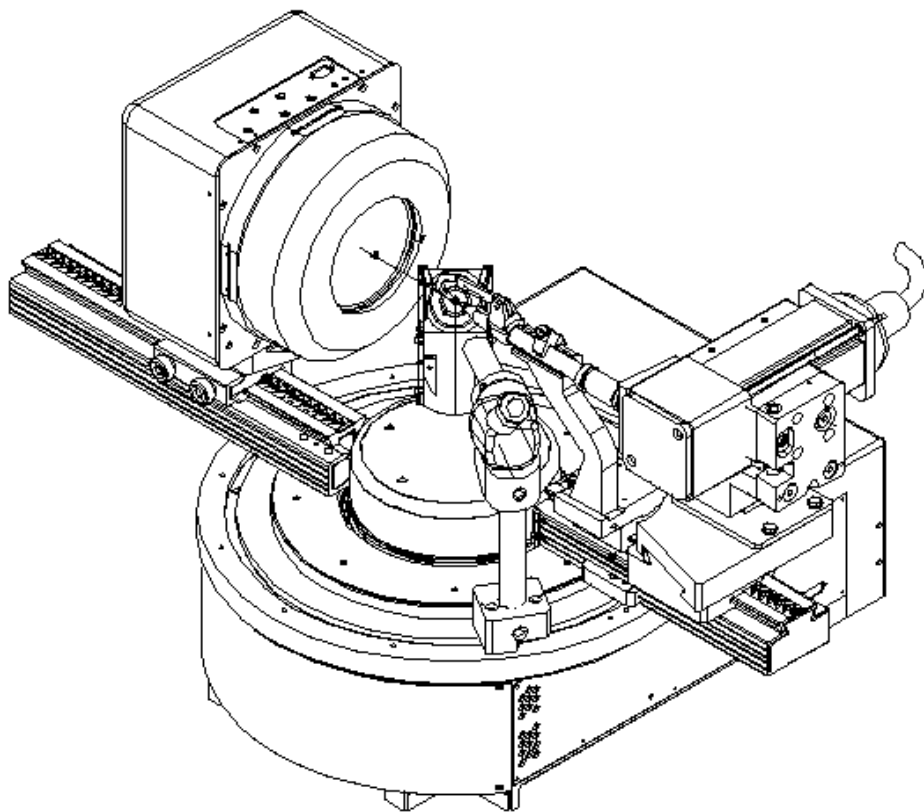


Figure 2.16 - Standard Basic (Fixed Chi) System

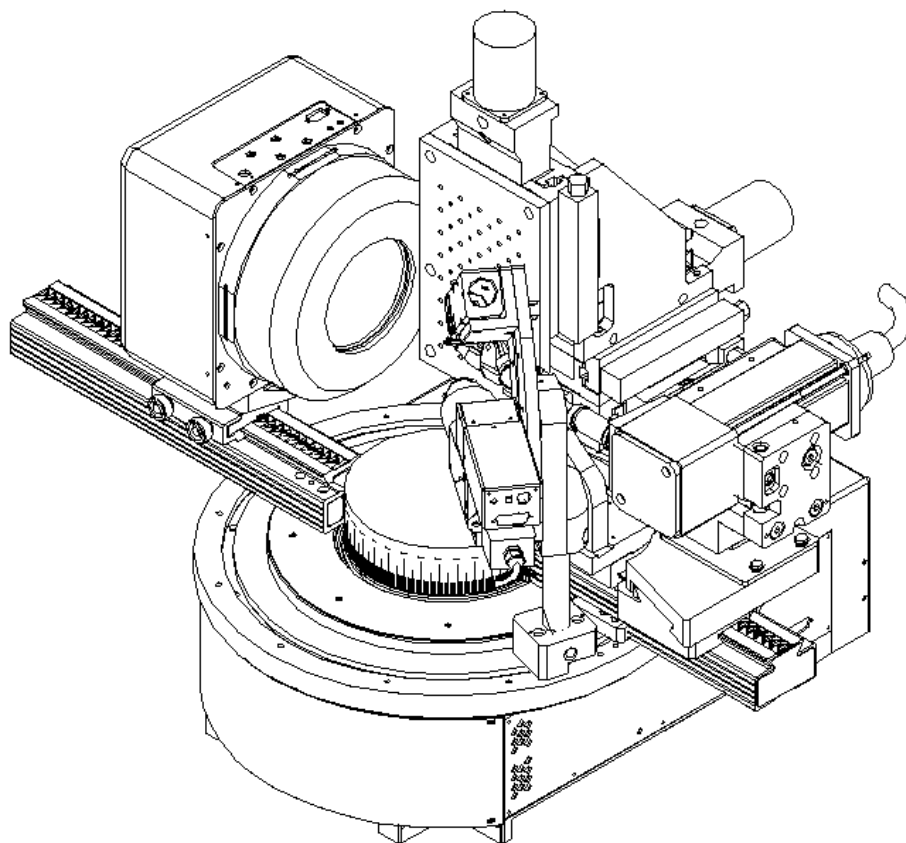


Figure 2.17 - Standard Microdiffraction System

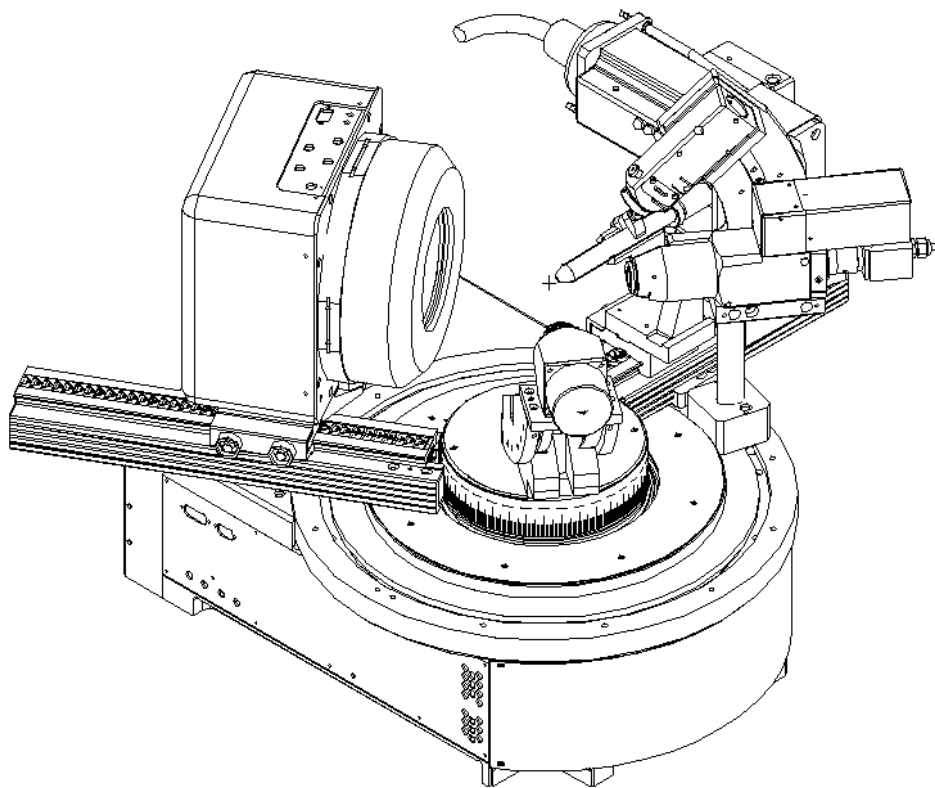


Figure 2.18 - Standard Stress/Texture System

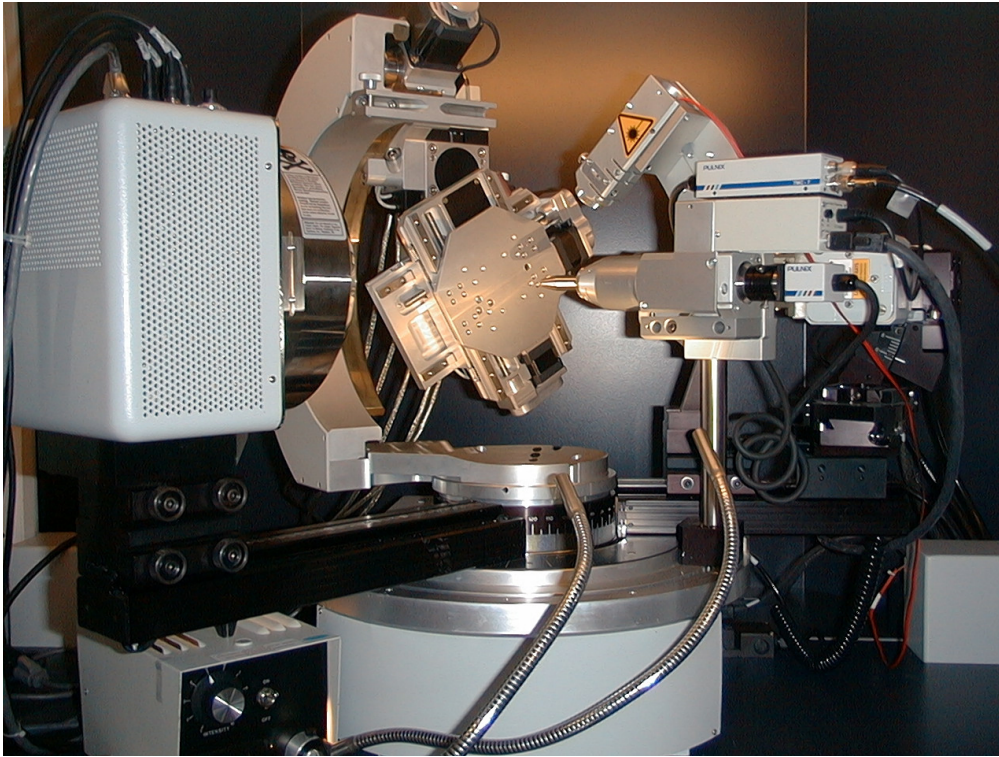


Figure 2.19 - Standard Huber Eulerian 1/4-Cradle System

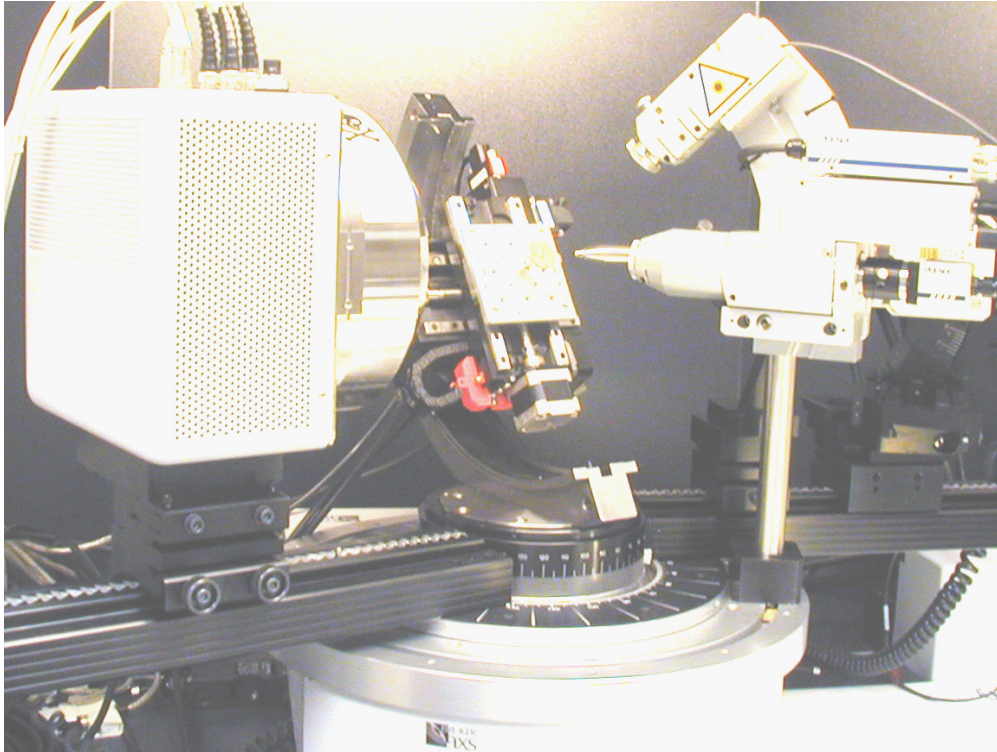


Figure 2.20 - Standard Centric Eulerian $\frac{1}{4}$ -Cradle System

The specifications and application features of the five standard systems are listed in Tables 2.30 and 2.31. A custom system can be built by modifying one of the five standard systems.

Table 2.30 – Specifications and major components of the five standard GADDS systems in horizontal configuration

Specifications	Basic (Fixed-Chi)	Microdiffraction	Stress/Texture	Eulerian 1/4-Cradle (Large or Small)
Major Components: (same for all five)	Horizontal D8 θ -2 θ goniometer and microprocessor control unit; D8 radiation safety enclosure; Base cabinet; Kristalloflex 760 X-ray generator; Outer circle track for detector; Stationary track for X-ray tube and optics; 3DOF tube mount; HI-STAR area detector system and frame buffer computer; Graphite monochromator and pinhole collimator support; GADDS software.			
Major Components:	Fixed-chi stage and goniometer head; optical microscope; 0.5 mm pinhole collimator.	XYZ stage; Laser/video sample alignment system; 0.05, 0.1, 0.3, and 0.5 mm pinhole collimators.	Two-position chi stage; Laser/video sample alignment system; 0.5 and 0.8 mm pinhole collimators.	Huber or Centric Eulerian 1/4- cradle Laser/video sample alignment system; 0.05, 0.1, 0.3, 0.5 and 0.8 mm pinhole collimators.
X-ray Target Material	Cu (optional Co, Cr)	Cu (optional Co, Cr)	Cr (optional Co, Cu)	Cu (optional Co, Cr)
Detector-to-Sample Distance	6 cm to 30 cm	6 cm to 30 cm	6 cm to 30 cm	6 cm to 30 cm
Measuring Range (2θ)	65° at 6 cm detector distance; 18° at 30 cm detector distance			
Resolution (2θ)	0.10° at 6 cm (1024x1024); 0.20° at 6 cm (512x512) 0.02° at 30 cm (1024x1024); 0.04° at 30 cm (512x512)			
Max. Measurable 2θ	161° depending on the detector distance			
Smallest Step Size	0.0001°			
Reproducibility	±0.0001°			

Table 2.31 – Application Features of the five standard GADDS systems

Applications	Basic (Fixed-Chi)	Microdiffraction	Stress/Texture	Eulerian $\frac{1}{4}$ -Cradle (Large or Small)
Sample Type and Handling	Powder in glass capillary without preferred orientation; small or medium samples (flat plate or curved surface); films, foils or fibers; mount in transmission or reflection mode	Small or large samples; thin films; large wafer plate; multiple samples; accurate sample area selection, alignment, and video monitoring; automatic mapping grid for flat samples; transmission or reflection mode	Powder in glass capillary without preferred orientation; small or medium samples (flat plate or curved surface); films, foils or fibers; accurate sample alignment and video monitoring; transmission or reflection mode	Small or large samples; thin films; large wafer plate; multiple samples; accurate sample area selection, alignment, and video monitoring; automatic mapping grid for flat samples; transmission or reflection mode
Phase ID	Yes, powder and small sample preferred	Yes, especially for phase ID mapping	Yes, powder and small sample preferred	Yes, especially for phase ID mapping
Texture	Pole-figure or fiber plot; ω and/or ϕ scan for orientation coverage	Pole-figure or fiber plot; ω scan only; mapping ability	Pole-figure or fiber plot; ω and/or ϕ scan for orientation coverage	Pole-figure or fiber plot; choice of ω , ψ and ϕ scan for orientation coverage
Stress	Stress or stress tensor; ω and ϕ scans for stress tensor	Stress or stress mapping; ω scan only	Stress or stress tensor; ω and ϕ scans for stress tensor	Stress or stress tensor; ω , ψ and ϕ scans for stress tensor
Percent Crystallinity	Yes	Yes, mapping capability	Yes	Yes, mapping capability
Micro-Diffraction	Yes, optional microdiffraction collimators are required	Yes, mapping capability	Yes, optional microdiffraction collimators are required	Yes, mapping capability
Thin Film	Yes	Yes, mapping capability	Yes	Yes, mapping capability
Small Angle Scattering	Optional helium beam path or vacuum beam path is required; Göbel optics is preferred for high resolution			
High Temperature	Optional high temperature attachment is required			

2.8 Standard GADDS Systems for Combinatorial Screening

Combinatorial chemistry refers to techniques to fabricate, test, and store the resulting data for a material library containing tens, hundreds or even thousands of different materials or compounds. Combinatorial investigations require rapid screening techniques to test and evaluate variations of composition, structure and property within a material library. X-ray diffraction is one of the most suitable screening techniques because abundant information can be revealed from the diffraction pattern, and X-ray diffraction is fast and non-destructive.

The concept of combinatorial chemistry was introduced about 30 years ago. Instead of the traditional way of making and testing a few new materials one at a time, the combinatorial technology allows scientists to fabricate, test, evaluate and store the resulting data for a material library containing tens, hundreds or even thousands of different materials or compounds. Combinatorial chemistry has become increasingly accepted by academia, government and industry in the past few years. Excellent results have been achieved in the discovery and synthesis of new phosphors, catalysts, zeolites and new drugs. Combinatorial chemistry requires rapid screening techniques to test and evaluate the variation of composition, structure and property of the entire material library. X-ray diffraction is one of the most suitable rapid screening

techniques because of the penetrating power of the X-ray beam, it is nondestructive to samples, data collection is rapid, and there is a lot of useful information about the materials contained in the diffraction pattern. X-ray diffraction, especially two-dimensional X-ray diffraction, can be used to measure the structural information of a material library with high speed and high accuracy.

The D8 DISCOVER with GADDS for Combinatorial Chemistry is designed for the rapid screening of combinatorial libraries. The system design is based on two-dimensional X-ray diffraction (XRD²) theory. A two-dimensional multi-wire area detector can collect a large area of a diffraction pattern with high speed, high sensitivity, low noise, and in a real-time mode. A 2D diffraction pattern contains information about the structure, quantitative phase contents, crystal orientation and deformation. The laser/video system ensures that each sample is aligned accurately on the instrument center. The X-ray beam is collimated to various sizes from 1000 to 50 μm . The vertical theta-theta geometry and horizontally mounted XYZ stage allow one to load the combinatorial library with ease, even for loose powders or liquids. The GADDS software helps to select and save a record of the screening area and steps. The diffraction results are processed and mapped to the screening grid based on the user-selected parameters.

2.8.1 Reflection Mode Screening

An XRD² combinatorial screening system mainly for reflection mode screening is shown in Figure 2.21 (drawing) and Figure 2.22 (photo). All components are mounted on a vertical θ - θ goniometer. The X-ray tube and optics are mounted on a dovetail track, referred to as the

θ_1 track. A 2D detector is mounted on a dovetail track, the θ_2 track. The XYZ stage is located with X-Y in the horizontal surface and Z vertical. A laser/video system is used to align and monitor the sample.

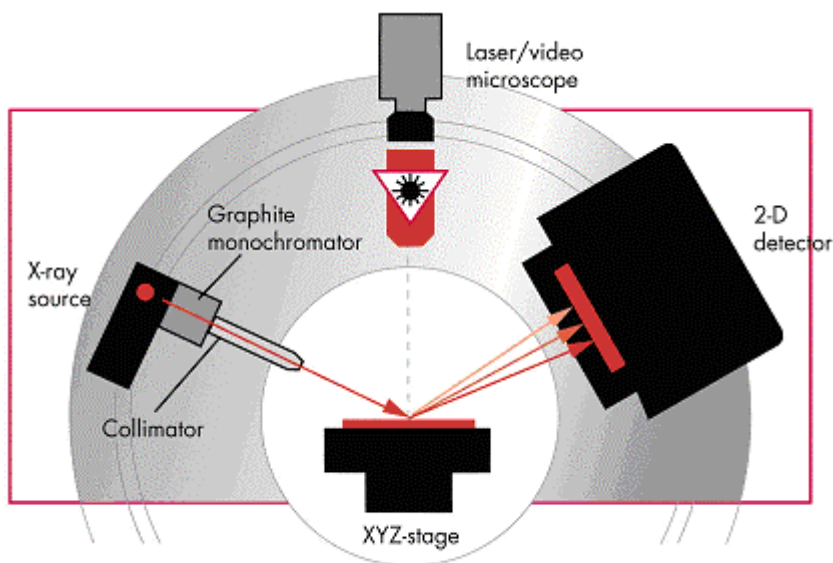


Figure 2.21 - Drawing of an XRD² combinatorial screening system; including a 2D detector, X-ray generator, X-ray optics (monochromator and collimator), theta-theta goniometer, XYZ sample stage, and a laser/video sample alignment and monitoring system

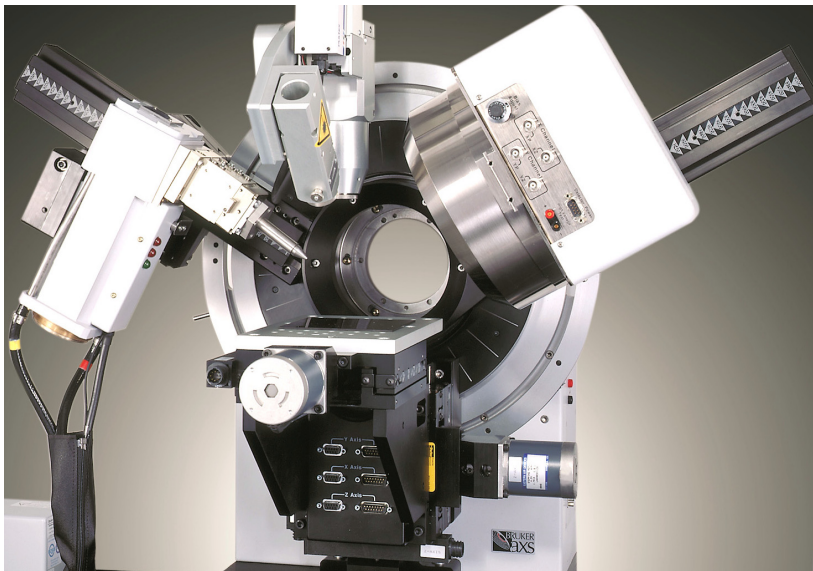


Figure 2.22 - Photo of an XRD² combinatorial screening system; including a 2D detector, X-ray generator, X-ray optics (monochromator and collimator), theta-theta goniometer, XYZ sample stage, and a laser/video sample alignment and monitoring system

short distance (65° measuring range at 6 cm) or high angular resolution at a long distance (0.02° resolution at 30 cm).

The X-ray beam is monochromatized with either a graphite monochromator or a multi-layer mirror. The X-ray beam can be collimated to various sizes by using a pinhole collimator or monocapillary. The multiwire detector has a pixel resolution of 100 μm or 200 μm with a frame size of 1024x1024 or 512x512. The detector can be set at a sample-to-detector distance between 6 cm to 30 cm depending on the application: For larger angular coverage at a

2.8.2 Transmission Mode Screening

In an XRD² system, the diffracted X-rays are measured simultaneously in a 2D range so no slit or scanning step can be used to control the instrument broadening. The beam-spread over the sample surface can not be focused back to the detector. Figure 2.23 shows geometry of 2D diffraction in reflection mode (a) and transmission mode (b). Defocusing effect is observed with low incident angle over a flat sample surface in reflection mode diffraction. In reflection mode, the diffracted beam in low 2θ angle is narrower than the diffracted beam in high 2θ angle. In transmission mode with the incident beam perpendicular to the sample surface, no such defocusing effect is observed.

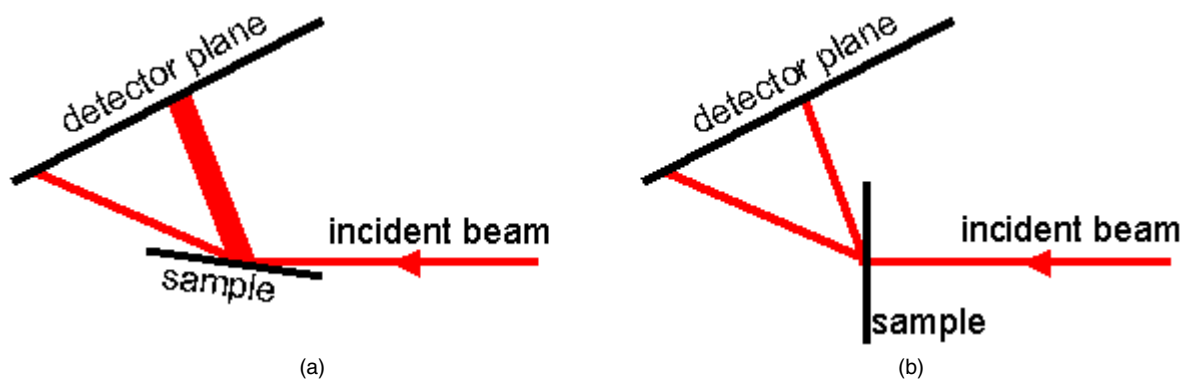


Figure 2.23 - Geometry of XRD²: (a) reflection mode;
(b) transmission mode

If one looks at the cross-section on the diffractometer plane and forward diffraction ($2\theta < 90^\circ$) only, the defocusing effect with reflection mode diffraction can be expressed as:

$$\frac{B}{b} = \frac{\sin(2\theta - \omega)}{\sin \omega} \quad (2-8)$$

where ω is the incident angle, b is the incident beam size and B is diffracted beam size.

The defocusing with transmission mode with a perpendicular incident beam can be given as:

$$\frac{B}{b} = \cos 2\theta + \left(\frac{t}{b}\right) \sin 2\theta \quad (2-9)$$

where t is the sample thickness.

If the sample thickness t is negligible compared to the incident beam size b , we have:

$$\frac{B}{b} = \cos 2\theta \leq 1 \quad (2-10)$$

There should be no defocusing effect at all.

Figure 2.24 is a comparison between reflection mode and transmission mode diffraction with data frames collected from corundum powder. With 5° incident angle (a), the reflection pattern shows severe peak broadening compared with no defocusing in transmission mode pattern (b).

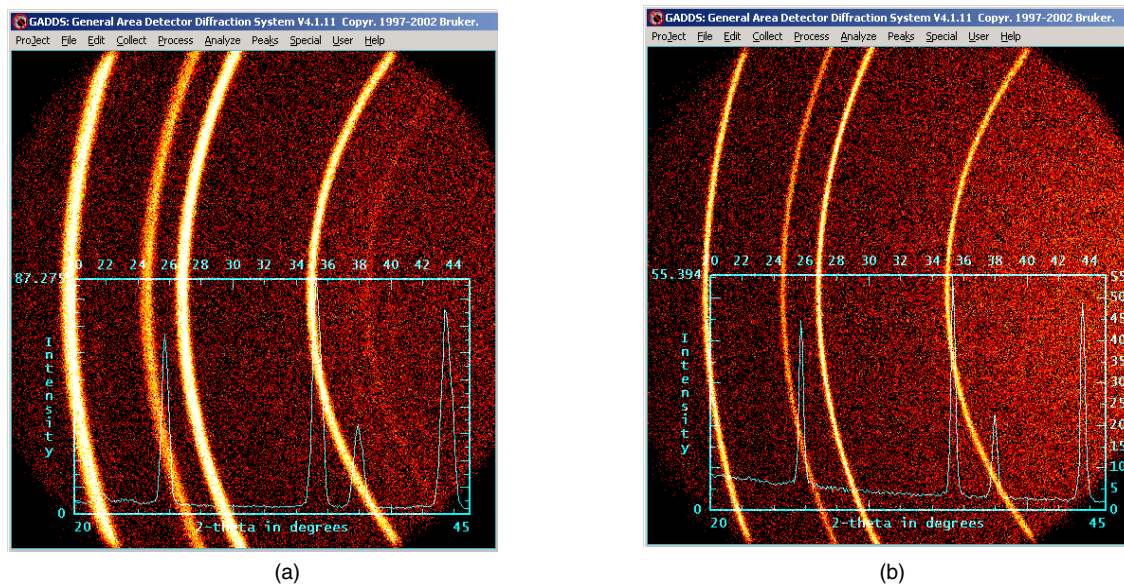


Figure 2.24 - Diffraction pattern from corundum:
(a) reflection mode diffraction 5° incident angle,
(b) transmission mode diffraction with perpendicular incident beam

In many combinatorial screening applications, such as polymorphism study in pharmaceutical chemistry and catalysis development in the oil industry, a typical 2θ measuring range is $2\text{--}60^\circ$. It is necessary to run combinatorial XRD screening in transmission mode in order to avoid the defocusing effect. A 2D diffraction system is designed for XRD screening in transmission mode for various applications, including screening of material libraries for combinatorial chemistry. As shown in Figure 2.25, the system is built on a vertical two-circle goniometer. An offset-mounted XYZ translation stage yields space for an X-ray source, optics, and X-ray detector, while it provides translations in X, Y and Z directions for material library scanning and sample alignment. A laser/video sample alignment system is mounted on the outer circle of the goniometer so it can be driven away after alignment. An optional motorized beam stop has two positions: retracted position for loading, unloading and aligning the sample; and extended position during diffraction and scattering measurement. In a transmission mode X-ray diffraction measurement, the incident beam is typically perpendicular to the sample so the irradiated area on the specimen is limited to a size comparable to the X-ray beam size, allowing the X-ray beam concentrated to the intended measuring area. In combinatorial screening applications, sample cells are located close to each other. Therefore, transmission mode diffraction can also avoid cross-contamination between adjacent samples.

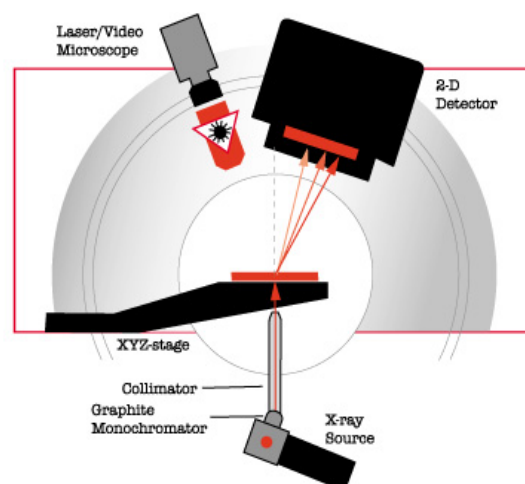


Figure 2.25 - Transmission diffraction system for combinatorial screening

2.8.3 Sample Stage and Screening Grid

The XYZ stage has a travel range of 100 mm (150 for transmission) x 100 (or 150) mm x 100 mm, and a maximum loading capacity of 10 kg (5 kg for transmission) with a 12.5 μm position accuracy and a 5 μm repeatability. The instrument center is defined by the cross-point of the incident X-ray beam and the center line of the detector. The system automatically and sequentially puts each cell in the material library into the instrument center based on the predetermined XYZ grid points. The system can also generate an XYZ grid file by inputting the X-Y coordinates of the starting point and end point, and the separation (step) between each grid point (see Figure 2.26).

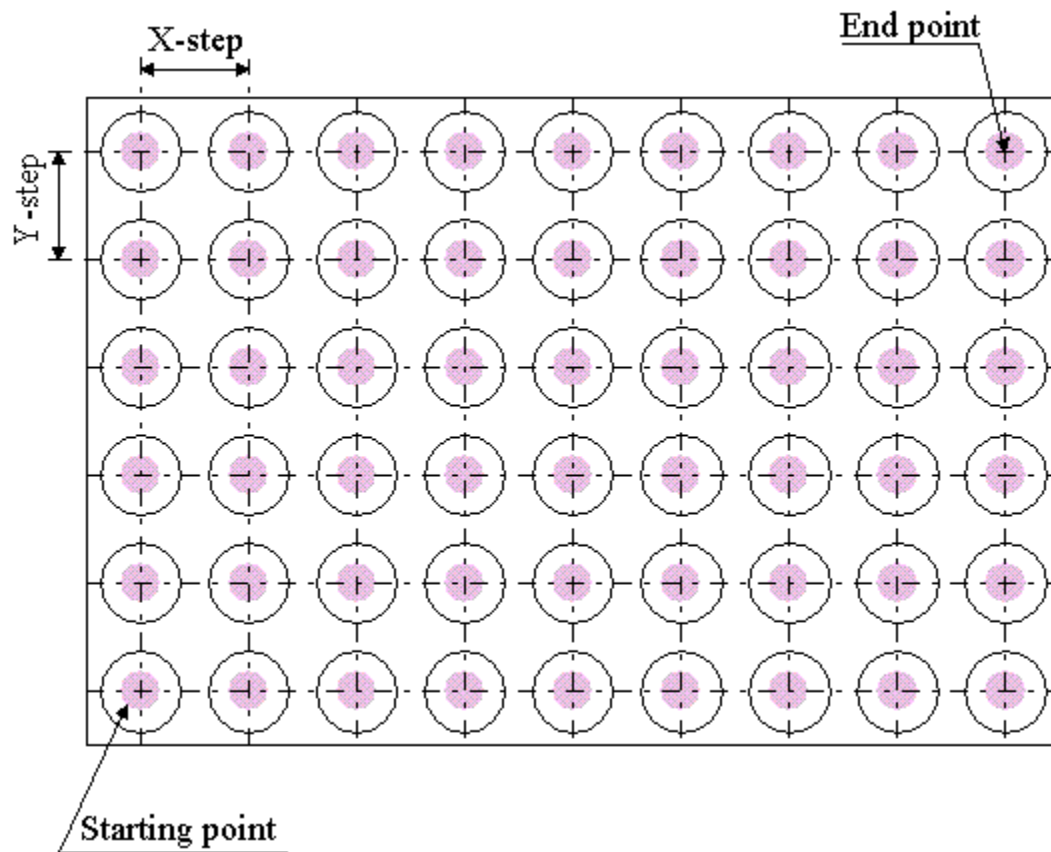


Figure 2.26 - The grid points are determined by the starting and ending points and steps

2.8.4 Retractable Knife Edge

A motorized retractable knife can be used for reflection mode screening at low Bragg angle range to improve the resolution, reduce the air scattering and cross-contamination. The retractable knife edge is mounted on the stationary base independent of the sample translation stage so the knife edge stays at the same aligned position while each cell of the combinatorial library moves into the X-ray diffraction measurement position. The retractable knife edge can be driven to two positions: retracted position and extended position. In retracted position, a laser-video alignment system aligns each cell to the instrument center. In extended position, the knife edge collimates the X-ray beam for low angle diffraction. The motorized retractable knife edge makes it possible to scan over the whole combinatorial library with automatic sample alignment.

In the low angle diffraction measurement, the incident X-ray beam is spread over the sample surface into an area much larger than the size of the original X-ray beam. In combinatorial screening applications, sample cells are located close to each other so the spread beam may cause cross contamination in the collected diffraction data. Therefore it is necessary to use a knife edge to limit the diffracted area.

Figure 2.27 shows the front view of the retractable knife edge in a 2D X-ray diffraction system.

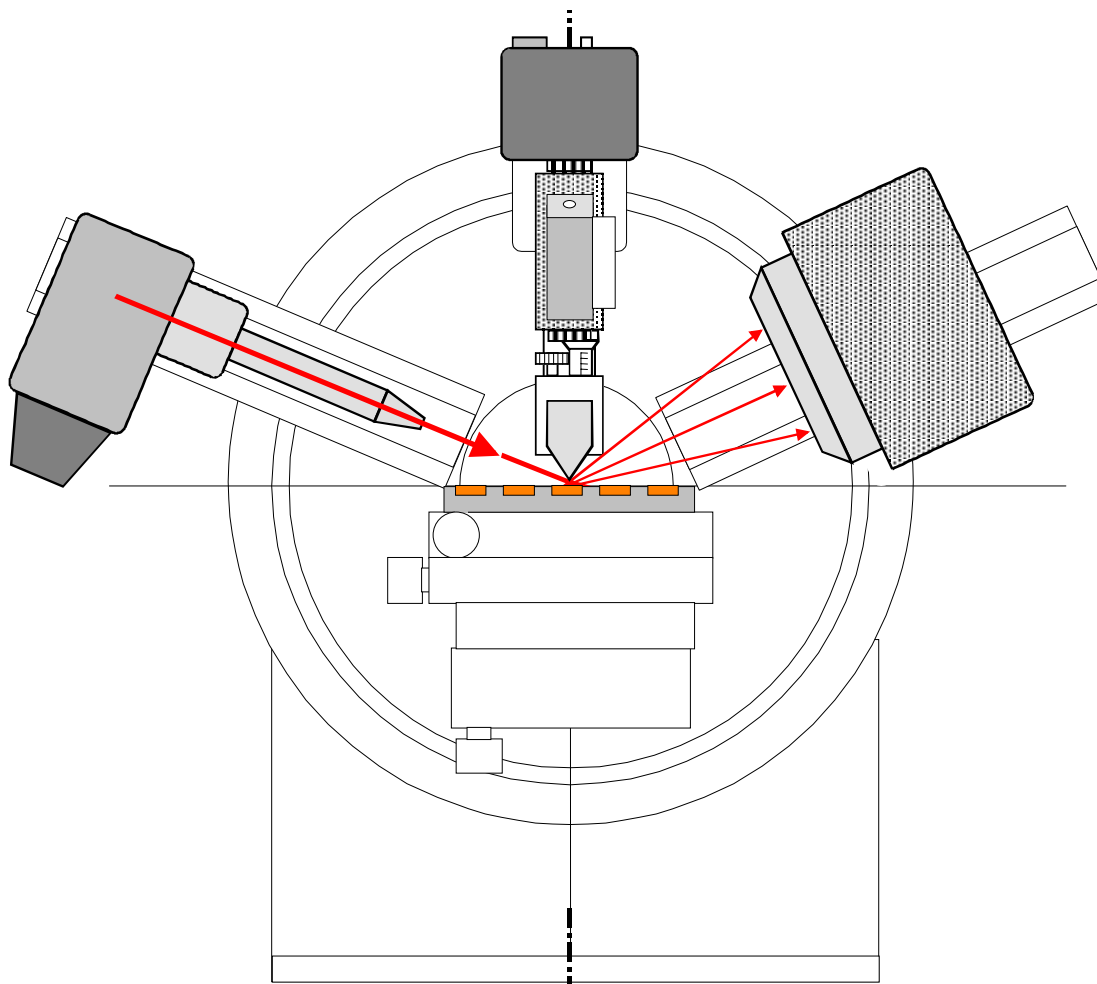


Figure 2.27 - Front view of the retractable knife edge on a 2D X-ray diffraction system for combinatorial screening

Figure 2.28 shows the retractable knife edge. The knife edge tilt angle is adjusted with the adjusting knob to form a parallel gap between the knife edge and the sample surface. The size of the gap is adjusted through the micrometer.

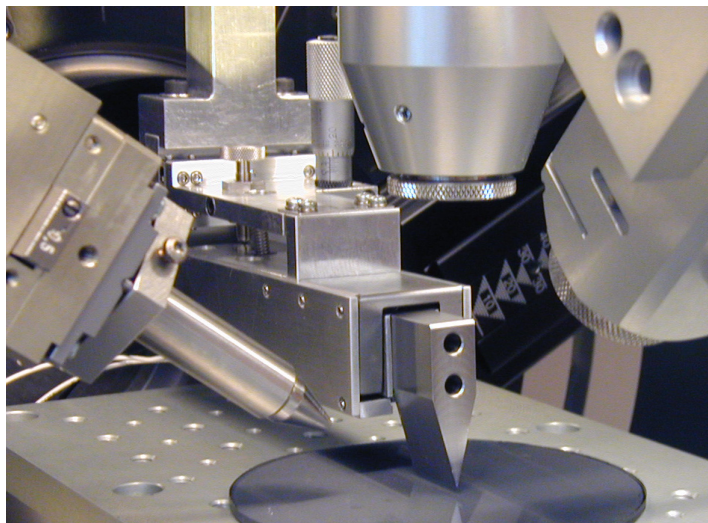


Figure 2.28 - The retractable knife edge and the tilt and gap adjustments

The function of the knife edge in the extended position is shown in Figure 2.29. θ_1 and θ_2 are the incident and diffracting angles, respectively, and δ is the gap between the knife edge and the sample surface. The knife edge collimates the X-ray beam for low angle diffraction. Parts of the primary X-rays are blocked by the knife edge so they will not reach the adjacent cells on the other side of the knife edge (right). The dif-

fracted X-rays from the adjacent cells before the knife edge (left) are also blocked by the knife edge. Therefore, only the diffraction from the defined area S can reach the detector. The knife edge can also prevent the direct beam from hitting the detector.

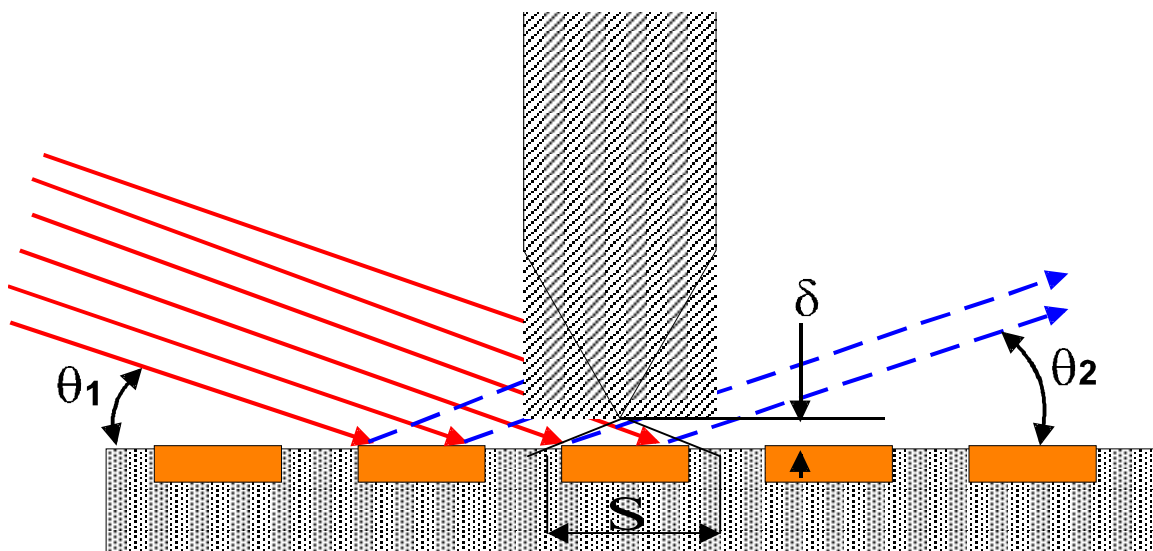


Figure 2.29 - The knife edge defines the area of diffraction

The relationship between the size of the diffracted area S and the incident angle θ_1 , diffracting angle θ_2 and the gap δ is:

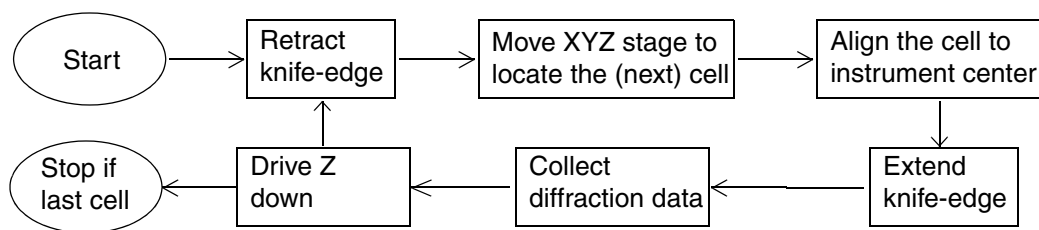
$$S = \delta(\cot\theta_1 + \cot\theta_2) \quad (2-11)$$

for a given cell size or distance between the center of adjacent cells.

The required knife edge gap δ is given as:

$$\delta = \frac{S}{\cot\theta_1 + \cot\theta_2} \quad (2-12)$$

If a range of θ_1 and θ_2 angles are used for the data collection, use the lowest possible angles for this calculation.



2.8.5 Diffraction Mapping and Results Display

The multiwire area detector can capture a large area of diffraction data containing information for various applications such as: Phase ID (qualitative or quantitative); Percent Crystallinity; Particle Size and Shape; Texture; and Stress.

Figure 2.30 shows two examples of the diffraction frame and integrated diffraction profile, each from a single library point. Almost all of the parameters measured by X-ray diffraction can be used for the screening of material libraries. The data collection grid, including XYZ coordinates of all the cells, is determined by GADDS software based on the coordinates of the two cells at extreme positions (lower left and upper right) and step size between cells. The data collection is automatically scanned over all of the cells in the material library. Selection of screening parameters includes integrated intensity, maximum intensity, peak width (FWHM), peak 2θ position, crystallinity (% internal, % external and % full) and various stress components. The screening results can be displayed in a color-coded map, 3D surface plot, or pass/fail map with user-defined criteria as is shown in Figure 2.31.

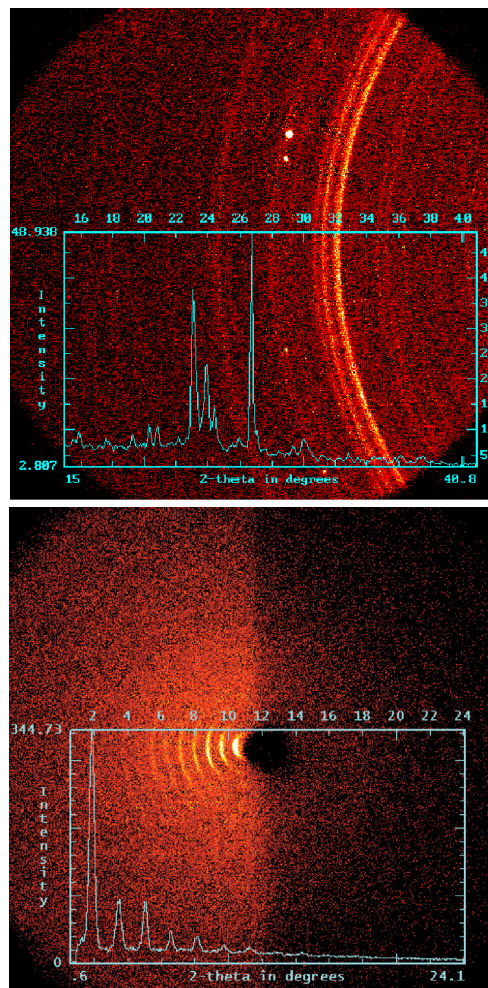


Figure 2.30 - 2D frames and integrated diffraction profiles, each from a single library point

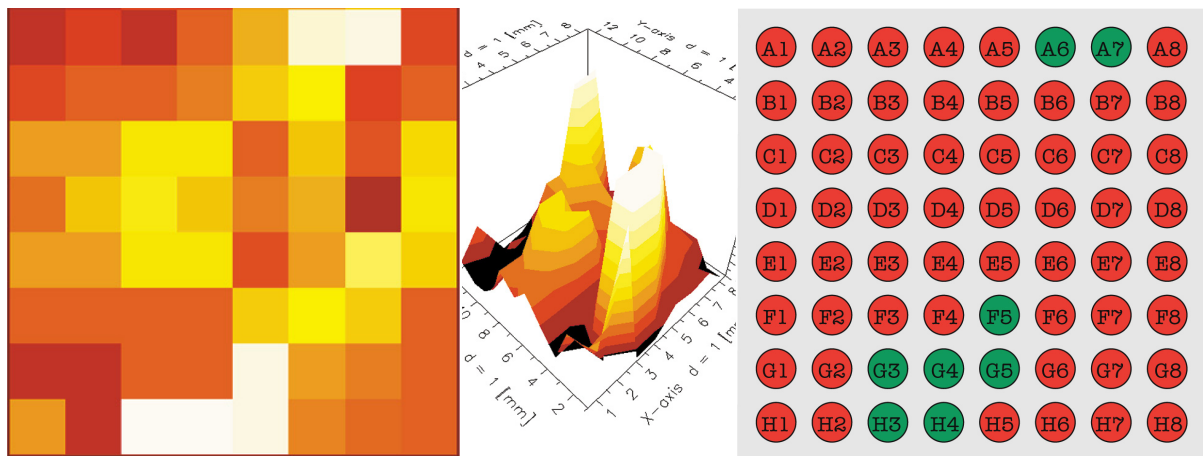


Figure 2.31 - The screening parameters are displayed in color scale, 3D surface plot or pass/fail plot on the material library map

3. Basic System Operation

This section covers the procedures used in basic system operation of the D8 DISCOVER with GADDs, including steps for turning on the system, choosing the detector position, collecting detector correction files, calibrating the system, positioning the sample, and collecting data.

All functions used in this section are described in detail in the GADDs Software Reference Manual or in hardware manuals delivered for hardware components of the diffractometer. It is assumed that the system is installed and aligned according to Bruker AXS standards.

3.1 Starting the System

3.1.1 D8 Series I (K760 Generator)

1. Turn on the generator. (See the generator manual for details on operation and diagnosis.)



CAUTION

Increase high voltage and current in small steps for maximum tube life.

2. Turn on the D8 controller (or GGCS for PLATFORM systems) with the enclosure Power button, and log on to your computer.
3. Turn on the PDC (HI-STAR controller).
4. Start the GADDS software.
5. Start the GADDS software. Wait for the program to establish a connection to the goniometer.
6. Go to Collect > Goniometer > Generator. Ramp up the generator voltage and current to your settings. Give the generator's high voltage a minute to stabilize.

NOTE: The argument provided in the Windows NT shortcut command defines the hardware configuration of the D8 DISCOVER with GADDS (e.g. information about the installed sample stage, the sample alignment tool, etc.). The parameter "/nodiff" disables communication

with the Phoenix/GGCS for this GADDS task. It is often used for data evaluation while a new measurement is running. See the Running GADDS section of M86-Exx008 GADDS Software Reference Manual for further details.

3.1.2 D8 Series II (K780 Generator)

1. Turn on the D8 controller with the green enclosure Power button.
2. Turn on the generator high voltage by turning the switch clockwise. Wait until you hear a click.
3. Turn on the PDC (HI-STAR controller).
4. Start the GADDS software.
5. Start the GADDS software. Wait for the program to establish a connection to the goniometer.
6. Go to Collect > Goniometer > Generator. Ramp up the generator voltage and current to your settings. Give the generator's high voltage a minute to stabilize.

3.2 Selecting Optics

The universal beam path concept (UBC) offers a variety of X-ray optics. For specific applications beam path, brilliance, monochromacy, divergence, and cross-section are optimized with collimators, single or cross-coupled Göbel Mirrors, monochromators, Monocaps, slits, pinholes, etc.

Exchanging these optics is very easy. Different collimators are delivered with standard systems. Replace the collimator in use as follows:

1. Open the collimator clamp.
2. Carefully remove the collimator tube and mount the attached labyrinth to the new collimator.
3. Position the new collimator in the collimator mount.
4. Ensure that any monochromator or Göbel Mirror exit is fully covered by the labyrinth and that the collimator position is fixed by both the setscrew and the spring-loaded clamp of the collimator mount.

NOTE: You can replace the pinholes within collimators with the Bruker AXS pinhole tool. First remove the collimator tip and screw the pinhole tool into the pinhole, and then use the pinhole tool to pull the pinholes.

3.3 Choosing the Detector Position

1. Ensure that the Detector Bias switch on the PDC is turned off.



CAUTION

To avoid damaging the detector, always ensure that the Detector Bias switch is turned off before changing the sample-to-detector distance.

2. Move the detector to the sample-to-detector distance you will use for your specific application, for optimum angular coverage and resolution, per the following criteria:
 - For the HI-STAR area detector, the angular coverage varies linearly from about 70° at 6 cm to 18° at 30 cm.
 - At the same time, the angular detector resolution (defined by: $\tan(\text{angular detector resolution}) = \text{pixel dimension} / \text{sample-to-detector distance}$) changes from .1–.02° in 2-theta for high-resolution mode.
 - In choosing the detector resolution and distance, see also the tables in Section 2.

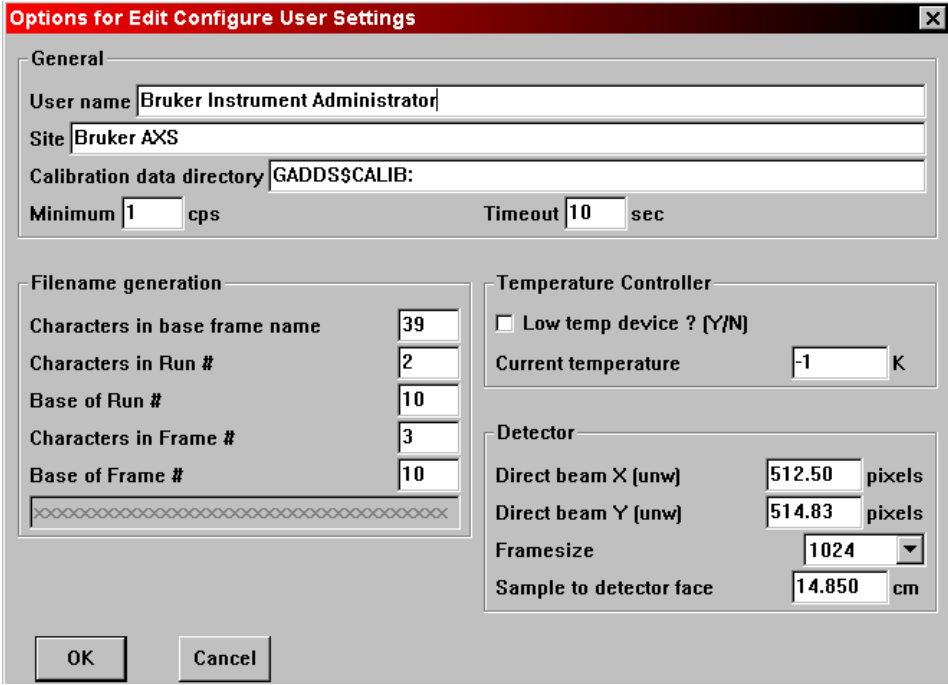
To move the detector on the dovetail, loosen the detector setscrews, grasp and slide the detector at the dovetail mount (for smoothest movement), then tighten the setscrews.

CAUTION

Avoid touching or scratching the detector window, as it contains poisonous beryllium.

Position the detector precisely and with high reproducibility by putting a pin in the dove-tail hole for the desired standard sample-to-detector distance. Note the distance for later entry in the GADDS software.

3. Turn on the PDC and the detector high voltage.
4. In the GADDS software, left-click Edit > Configure > User Settings (see Figure 3.1).
5. Enter the sample-to-detector distance (noted in Figure 3.1) and choose either 1024 or 512 framesize (1024 is recommended).



Options for Edit Configure User Settings

General

User name: Bruker Instrument Administrator

Site: Bruker AXS

Calibration data directory: GADDS\$CALIB:

Minimum: 1 cps Timeout: 10 sec

Filename generation

Characters in base frame name: 39

Characters in Run #: 2

Base of Run #: 10

Characters in Frame #: 3

Base of Frame #: 10

Temperature Controller

☐ Low temp device ? [Y/N]

Current temperature: -1 K

Detector

Direct beam X (unw): 512.50 pixels

Direct beam Y (unw): 514.83 pixels

Framesize: 1024

Sample to detector face: 14.850 cm

OK Cancel

Figure 3.1 - Edit > Configure > User Settings window

3.4 Detector Aberration Analysis

Before routinely collecting data with the D8 DISCOVER with GADDS, you must perform a detector analysis, which involves a flood-field correction and a spatial correction. In performing these corrections, GADDS creates correction tables. The flood-field table is used to correct for inhomogeneities in the wire of the detector grids. The spatial table is used to compensate for parallax effects (caused by the finite distance between detector grids and flatness of the HI-STAR area detector. The parallax effects disappear for long sample distances).

We recommend performing these steps every six to eight weeks and whenever you change the sample-to-detector distance. For high-resolution applications, you might have to perform them more often. You should verify that the correct flood-field and spatial corrections are loaded. If not loaded, see your Administrator and refer to the GADDS Administrator Manual.

NOTE: If you perform this procedure at one distance, then another, and then return to a previous distance, you can avoid performing this procedure again and instead automatically load the correction files and settings for that previous distance using the command Process > Flood > Load and Process > Spatial > Load.

Perform the corrections as follows:

1. Mount the glassy iron foil (for Cu radiation) or the Fe^{55} source (for other radiation) on the sample stage, and ensure that the sample and detector surface are parallel. For exact alignment, see Sample Positioning.

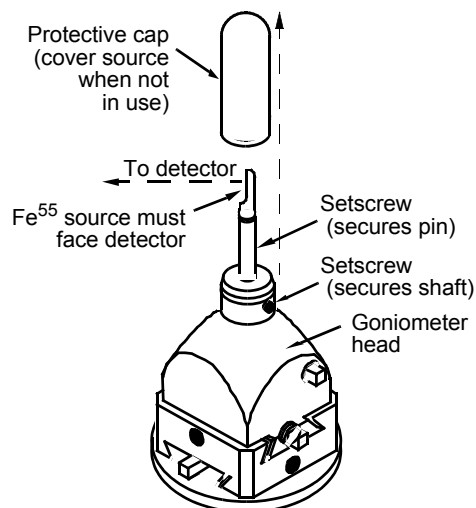
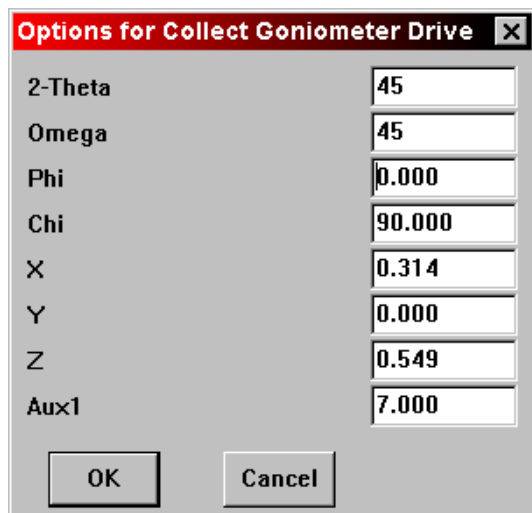


Figure 3.2 - Fe^{55} source mounting detail

2. Set the detector bias switch for the radiation you will use, as follows. When using Cu radiation as the standard radiation, set the bias switch at the PDC to Auto and use the command Collect > Detector > Fe Bias to set the Fe settings. For other radiation, turn the bias switch to Fe settings as marked on

the PDC. Note that the lowest field on the right is set to Fe Bias.

3. Left-click Collect > Goniometer > Drive. The Goniometer/Drive options window will appear (see Figure 3.3).



The image shows a software window titled "Options for Collect Goniometer Drive" with a close button (X) in the top right corner. The window contains a list of parameters on the left and their corresponding numerical values in input fields on the right. The parameters and their values are: 2-Theta (45), Omega (45), Phi (0.000), Chi (90.000), X (0.314), Y (0.000), Z (0.549), and Aux1 (7.000). At the bottom of the window are two buttons: "OK" and "Cancel".

Parameter	Value
2-Theta	45
Omega	45
Phi	0.000
Chi	90.000
X	0.314
Y	0.000
Z	0.549
Aux1	7.000

Figure 3.3 - Options for Collect Goniometer Drive window

4. Enter values in the first and second line to drive the detector out of the primary beam. Consult Table 3.1 for appropriate goniometer and generator settings for 2-theta and omega.

Sample-to-detector distance	Detector and Fe foil assembly rotation angle	Generator power for 0.5 and 0.8 mm collimator
6 cm	50°	40kV/5mA
10 cm	50°	40kV/10mA
15 cm	45°	40kV/10mA
20 cm	40°	40kV/15mA
25 cm	30°	40kV/20mA
30 cm	20°	40kV/20mA
>35 cm	15°	40kV/25mA

Table 3.1 – Recommended angle and generator power for the amorphous Fe foil calibration

NOTE: For theta-theta systems, set theta1 (tube) to the angle in Table 3.1 and theta2 (detector) to zero.

3.4.1 Flood-Field Correction

Begin the flood-field correction.

1. Left-click Process > Flood > Linear to disable any existing flood-field correction. The main window will appear (see Figure 3.4).

The correction filename and additional related information display in the lower right corner of the GADDS window. Note that the field after FloodFld (in the main window) is set to linear.

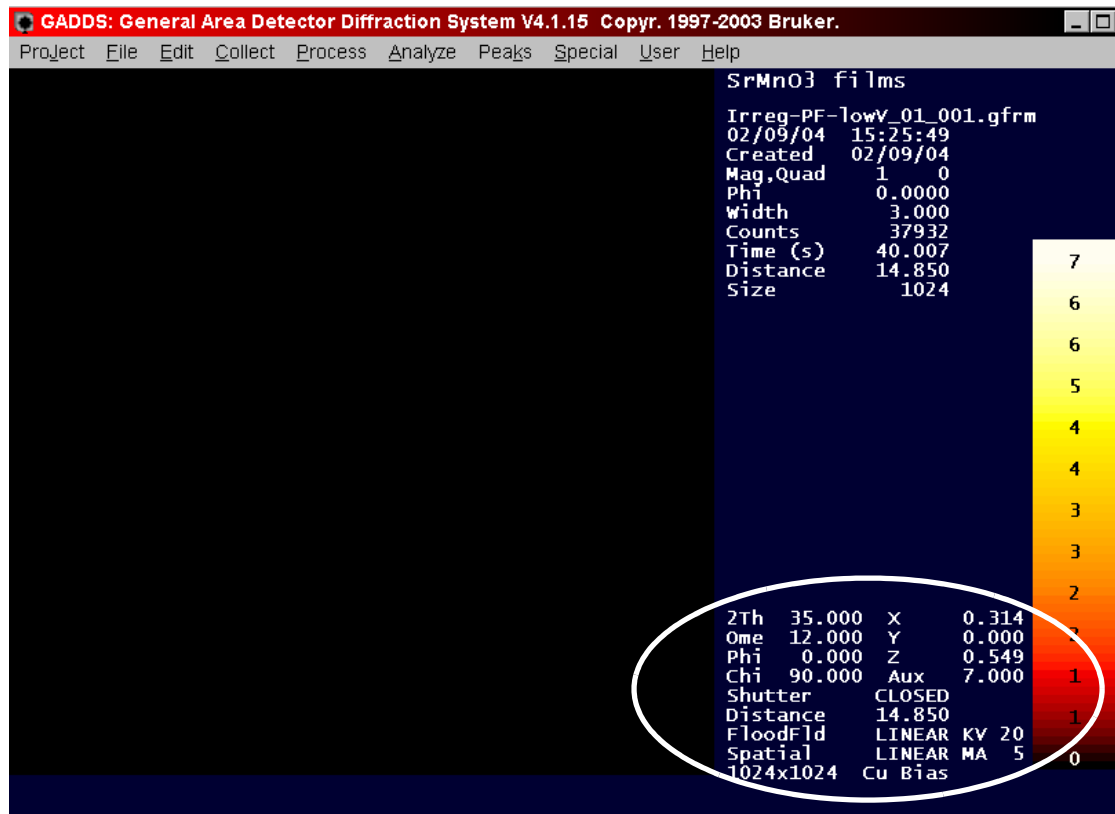


Figure 3.4 - Main window

- Left-click Process > Flood > New. The FLOOD/NEW Options window appears (see (see Figure 3.5).

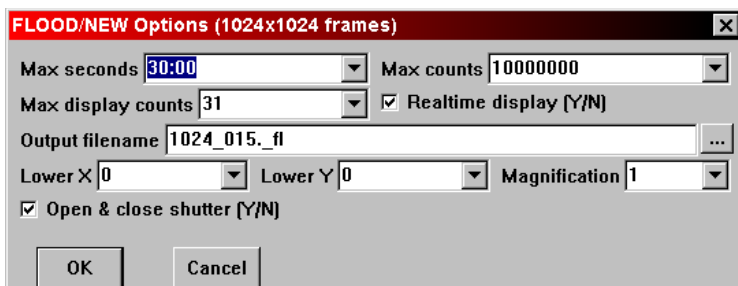


Figure 3.5 - FLOOD/NEW Options window

NOTE: The GADDS software will suggest a default output filename in line 5. Do not change the filename. The first four digits describe the detector resolution as set in the configuration table (accessed with Edit > Configure > Edit). For the HI-STAR, the digits can be either 1024 or 0512. The fifth default digit is an underscore (_). The last three digits stand for the sample-to-detector distance in cm (e.g., 006 stands for the sample-to-detector distance close to 6 cm). Using the filename as is (without pathname), the GADDS software will write the file to the frames default directory, which enables the software to automatically reload the file. If you want the file written to a different directory, include that pathname before the filename.

- If using the glassy iron foil, check (enable) the “Open & close shutter” checkbox. If using the Fe 55 source, uncheck (disable) it.
- Set the appropriate data fields to collect long enough to reach 10000000 counts for the total detector area.
- Press the OK button to start data collection. After the measurement is done, the Flood-Fld entry in the GADDS window displays the new correction table (e.g., 0512_010._fl).
- Mount the brass plate to the detector surface. Ensure that:
 - the two pins on the detector fit the two mid-size holes of the plate;
 - the elongated midsize hole is oriented to the negative 2-theta direction; and
 - the flat brass plate surface faces the detector window.

3.4.2 Spatial Correction

Using the same system setup and bias settings as for the flood-field data collection, perform the following steps:

1. Left-click Process > Spatial > Linear to disable any existing spatial correction. Note that the field after Spatial (in the main window) is set to linear.
2. Left-click Process > Spatial > New. The Options for Process Spatial New window appears.

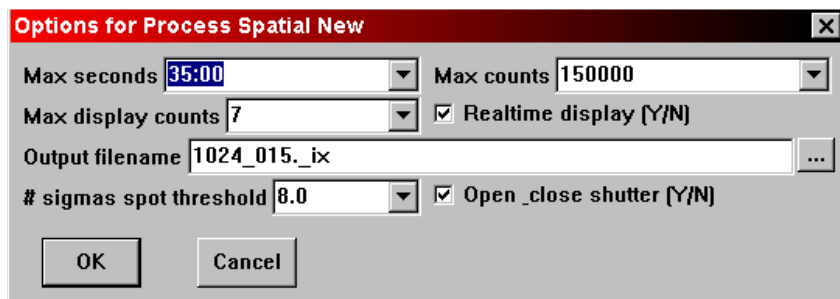


Figure 3.6 - Options for Process Spatial New window

NOTE: The GADDS software will suggest a default output filename, as shown in Figure 3.6. Do not change the filename.

NOTE: The total counts collected at this time will be less than for the flood-field data collection due to the brass plate.

3. Set identical parameters as for the flood-field data collection.

4. Press OK to start data collection and collect one frame. The spots in Figure 3.7 appear on the screen during measurement and represent the rays of light transmitted through the holes in the brass plate. During this time, the software calculates centroid positions for each spot (ray), from which later X,Y calculations will be made for analyzing substances.

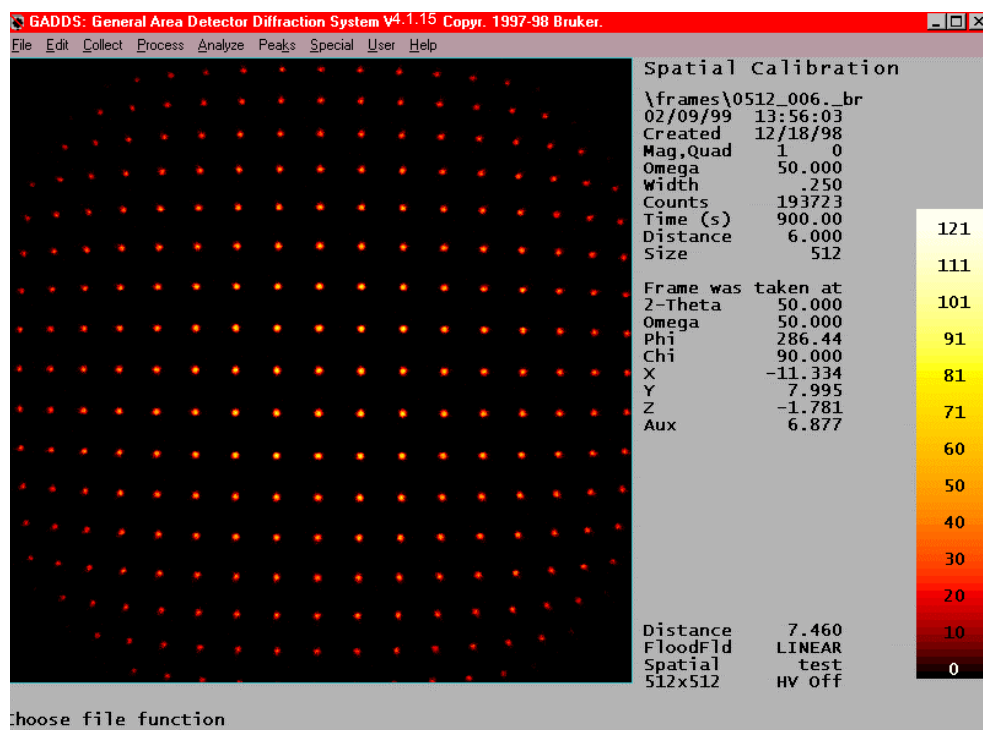


Figure 3.7 - Screen during measurement

GADDS software fits splines to the position of all local intensity maxima above the pre-set threshold. The splines describe a map function that moves the locations of the intensity maxima to the positions of the holes in the brass plate.

After the measurement is done, the Spatial entry in the GADDS window displays the new correction table (e.g., 0512_010._ix).

On the screen appears a blue overlay (see Figure 3.8), indicating that the software has analyzed the collected frame. The overlay

includes an X,Y graph for pinpointing centroids and a spotted grid with up to 19 rows and columns (less for close sample-to-detector distances). Each blue spot represents a centroid calculated from the spots of the transmitted rays. The blue spots should form a regular, complete, and balanced grid (slightly bowed toward the edges. A grid missing spots along an edge (as shown) is acceptable. However, stray spots (within or outside grid lines) and jagged grid lines are not acceptable.

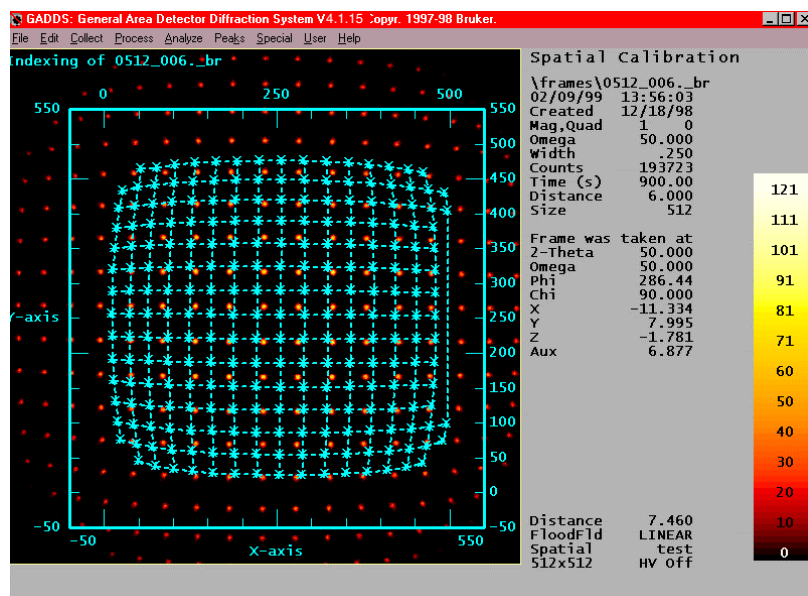


Figure 3.8 - Blue-spotted grid

NOTE: Though the X-ray spots still appear on the screen's background, they are of no concern at this moment. The grid is a scaled-down representation of the X-ray spot pattern to provide space for the X,Y graph.

5. Check that all spots are present (except for those along an edge) and form the grid, and that no stray spots or jagged lines exist. If there are too few or too many spots, left-click Process > Spatial > Reprocess and enter the output filename. Then increase the threshold if too many spots exist, or decrease it if too few spots exist. Press OK. A new grid appears.

NOTE: As a starting point when adjusting the threshold, we recommend a threshold of 4.

NOTE: You might have to repeat the reprocessing (step 4) for threshold optimization.

3.5 System Calibration

Two methods are available for reliable calibration of the sample-to-detector distance and beam center. You can use either method. Use manuals 269-023301 Detector Distance and Beam Center Calibration for GADDS and 269-02200 GADDS Application Test for instructions on one method or use the following:

1. Mount corundum standard plate to the sample stage either as a flat sample (for reflection measurements) or in a capillary (for transmission measurements). (See Sample Positioning for mounting details.)

2. Left-click Collect > Scan > SingleRun and collect one or several frames at detector swing angles within the 2-theta range you need to calibrate. (See Data Collection for details on performing this step.) If using a corundum plate, XY sample oscillations may improve the quality of the scan.

Options for Collect Scan SingleRun

Frames: 1 Seconds/frame: 90

2-Theta: 40 deg Omega: 20 deg Phi: 0.000 deg Chi: 90.000 deg

X: 0.314 mm Y: 0.000 mm Z: 0.549 mm Aux: 7.000 mm

Scan Axis #: None Frame width: 0.0

Mode: STEP ☐ Rotate sample Sample Osc: XY Amplitude: 1 mm

Frame header information

Title: Corundum

Sample name: Corundum

Sample number: 1

Filename generation

Job name: Corundum-500um Run #: 00 Frame #: 001

First filename: Corundum-500um_00_001.gfrm

Max display counts: 7 ☒ Realtime display

☒ Pre-clear ☐ Capture video image ☐ Auto Z Align N

OK Cancel

Figure 3.9 - Options for Collect Scan SingleRun window

NOTE: Get the best results by measuring at detector angles where a diffraction line is expected. At these detector angles, the parameters become independent.

3. Left-click Process > Calibrate. The following window will display.

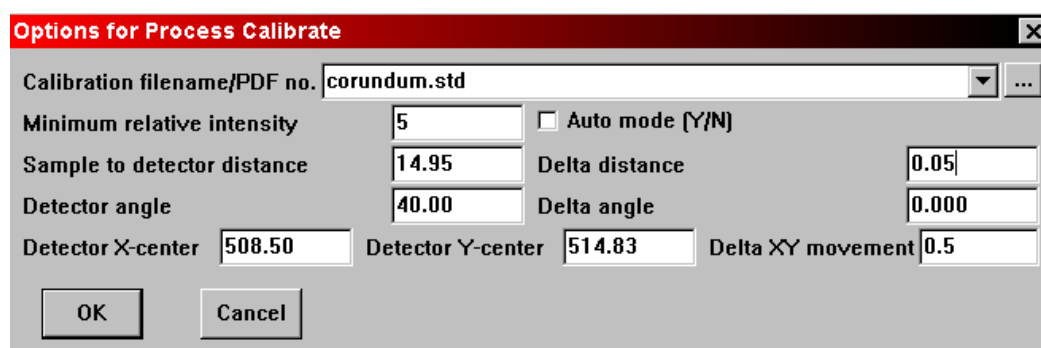


Figure 3.10 - Process > Calibrate

4. Set the window parameters as follows.

- 4.1 Ensure that the first line points to the file "corundum.std". This is an ASCII data file that contains JCPDS powder diffraction file (PDF) information like d-spacings and relative intensities for the corundum standard. For other standard materials, you can create your own *.std file.

- 4.2 Check that the above start value for sample-to-detector distance is close to the value on the scale.

- 4.3 Ensure that the detector center is close to 512 or 256, depending on whether you use low or high resolution.

**CAUTION**

Do not change the delta angle from 0.0. Doing so would destroy the fixed factory calibration.

Blue rings will be overlaid on the frame's diffraction pattern. The rings indicate the theoretical position of the calculated standard pattern.

5. Adjust the sample-to-detector distance and x and y beam center settings so the rings of the calculated pattern coincide with those of the measured one. To adjust the settings, toggle between center mode (changing x and y) and calibrate mode (changing the distance) by pressing C and nudging the rings with the arrow keys until you get the results shown in Figure 3.11.
 - 5.1 Use the y parameter to get symmetry around the horizontal axis (i.e., the deviations between the calculated and measured pattern are identical for the top and bottom of the detector).
 - 5.2 Use the x parameter to locally adjust the ring sections of measured and calculated rings in the detector center.
 - 5.3 Use the distance parameter to get full coincidence.

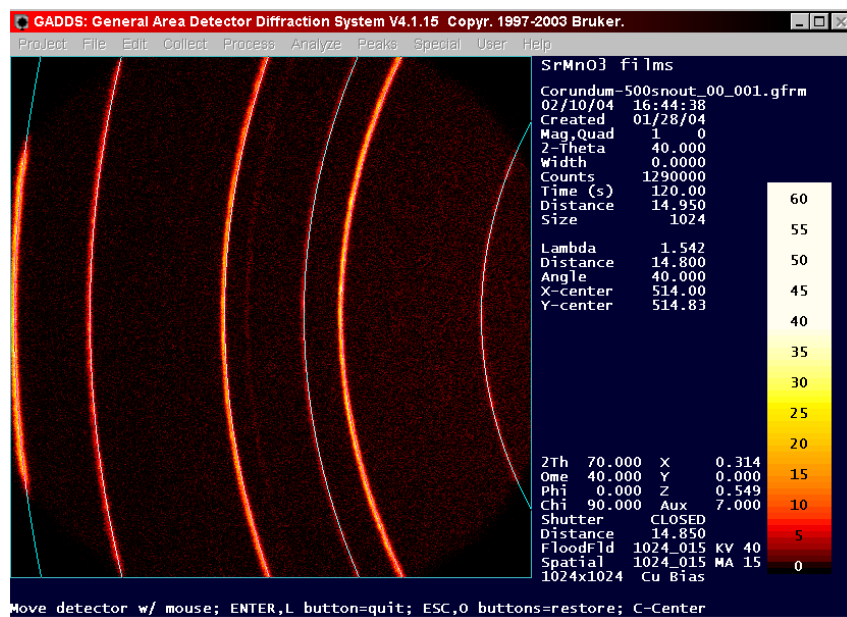


Figure 3.11 - Adjust the rings

6. If you are the Instrument Administrator, press Enter to update the current configuration.

3.6 Sample Positioning

3.6.1 XYZ Stage

The sample positioning procedure makes sure that either the surface of a sample for reflection measurements or the geometrical center of the sample for transmissions mode is in the center of the diffractometer. For this procedure, you need either the video microscope or the laser video alignment system.

1. Mount the sample to the sample stage. Ensure that the major sample axes are parallel to the major axes of the sample mount and to the major axes of the sample stage (e.g., an orthorhombic sample is mounted with its x-, y-, and z-axes parallel to the x-, y-, and z-axes of the xyz-stage or of a standard goniometer head).

NOTE: Ensure that the beam stop is attached to the collimator if you are going to measure in transmission mode or at 2-theta and omega angles below 2° .

2. **Reflection mode—optical microscope:** Drive omega to 0° and adjust the sample height until the focus line of the microscope is in the microscope crosshair.

Reflection mode—laser video sample

alignment system: Drive 2-theta to 55° . Use the video camera crosshair and laser spot to align the sample in x and y.

NOTE: The video camera has a zoom function that is supported in manual mode. Adjust the sample height until the laser spot appears in the crosshair.

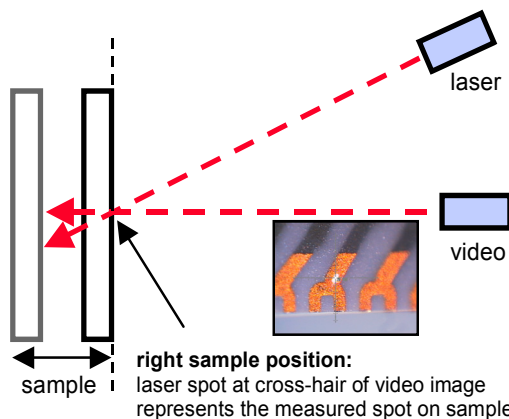


Figure 3.12 - Adjust sample height

Transmission mode: Ensure that the beam stop is attached to the collimator. Drive omega to -30° . Adjust the sample holder x- and y-coordinates so that the sample is centered in the crosshair. Ensure that for the angles $\phi = 0, 90, 180$, and 270 the sample is centered in the crosshair. For flat samples, do not drive ϕ . Align to the surface. Do not rotate.

**WARNING**

For the Huber Centric cradle, do not drive omega to -30° because the collision limit is -20° .

For flat/thin samples (e.g., polymer films, powder, etc.) on a quarter cradle with phi equal to 0° , drive omega to 0° . Mount the sample. In manual mode, turn the camera and laser on. Adjust the position of the sample with y and z. Use x to bring the laser spot into the center of the crosshair.

When using a capillary on a cradle, check the rotation of the sample after performing the steps above.

NOTE: Generally, in transmission mode the plain normal to the optical axis containing the geometrical sample center can be adjusted in focus at $\omega = 55^\circ$. At $\omega = -30^\circ$ the optical axis is parallel to the surface.

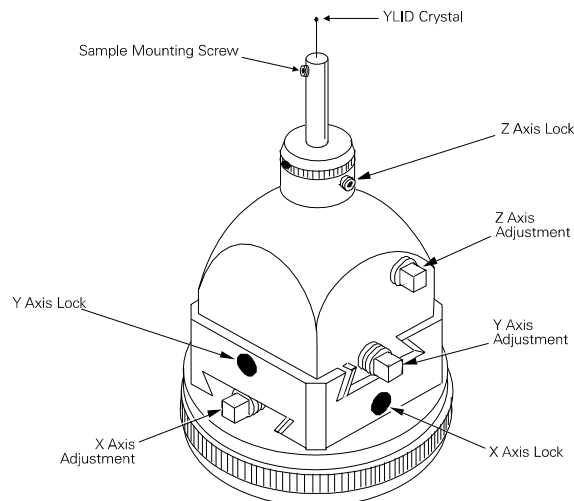
3.6.2 Goniometer Head

Figure 3.13 - Goniometer head showing X, Y, and Z adjustments

Samples mounted on a goniometer head (see Figure 3.13) can be used in either reflection or transmission mode. Transmission samples must be centered to the goniometer center, while reflection samples must have the sample surface touching the goniometer center.

For transmission samples: The procedure for mounting and aligning samples on the goniometer head is:

1. Mount the sample to the goniometer head and then attach the assembly to the goniometer.

2. Start GADDS online version (for your particular stage).
3. Collect > Goniometer > Optical command and verify the base angles are correct.

Base Angles	Values
2-THETA	0° or -60°, or some out-of-the-way position, so that microscope is easily accessed.
OMEGA	D8: variable, usually about -30° (330°), PLATFORM: -30° (330°), Aztalan - 90° (270°), P4: 0° or 330° (345° with LT).
PHI	D8: 0°, PLATFORM: 0°, Aztalan: 0°, P4: 30°.
CHI	D8, PLATFORM: 54.74° (or -54.74°), Aztalan: 45°, P4: 330°. Typically, one uses the fixed chi value on systems with a chi axis.

4. Using the manual control box: Phoenix: Press SHIFT, F1, 1, then ENTER. GGCS: Depress button A, then press AXIS PRINT button. The goniometer will drive to the first optical alignment position, where the goniometer head's X & Z axes are perpendicular to the microscope's view direction (if not, your base angles are wrong).
5. View your sample through the microscope, VIDEO program, or LCD monitor depending on your system. We will refer to these as "microscope" in the remainder of this procedure.
6. For the moment, assume that the microscope's crosshairs are properly aligned. You can rotate the crosshairs (physically on microscope, software controlled on VIDEO, can't on LCD) for easier viewing. Align crosshairs simple axis with phi axis and the division axis (with tick marks) perpendicular to phi axis.
7. Using goniometer head tool, adjust Z (vertical) and X (left/right) until the sample is centered on the crosshairs.
8. While viewing the sample in the microscope, use the manual control box: Phoenix: Press ENTER. GGCS: Press AXIS PRINT. Goniometer will drive phi by 180°. The sample will move away from the crosshairs, then return. It should stop centered on the cross hairs (yes jump to step 9). If not, then your crosshairs are misaligned, which is extremely common.
 - 8.1 Using the goniometer head tool, move the sample half way to the crosshairs (use the tick marks). Repeat this step, adjusting the sample position until the start and end positions coincide. If the Z crosshairs is misaligned, then the rotation center will be above or below the crosshairs. Sometimes it is useful to coarsely adjust the Y position (see steps 9 & 10).
9. Using the manual control box:
 - 9.1 Phoenix: Press 2, then ENTER.
 - 9.2 GGCS: Press B, then AXIS PRINT. Goniometer will drive phi by 90°.

10. Using goniometer head tool, adjust Y (left/right) until sample is centered on the crosshairs (or the true crosshairs center as determined in step 8).
11. While viewing the sample in the microscope perform, use the manual control box. [Phoenix: Press ENTER. GGCS: Press AXIS PRINT.] Goniometer will drive phi by 180°. The sample should remain centered in the true crosshairs center.
12. Optional: Use the other two optical positions (Phoenix: 3 & 4, GGCS: C & D) to double check your sample centering.
3. Collect > Goniometer > Manual command.
4. Using the manual control box, drive omega, phi, and/or chi until the microscope is viewing down the sample's surface plane.
5. Using the goniometer head tool, adjust X, Y, and or Z until the surface plane is center along the crosshairs cursor.
6. If possible, drive 180° in omega and look down the other direction.
7. Exit manual command by pressing ESC on the frame buffer's keyboard.

Axis Button	Position (4-Circle)	Position (3-Circle)
1-2-theta, A- ϕ	Base Position	Base Position
2-omega, B- χ	+ 90 in ϕ	+ 90 in ϕ
3-phi, C-2-theta	+ 180 in χ	+ 180 in ω
4-chi, D- ω	+ 180 in chi + 90 in ϕ	+ 180 in ω + 90 in ϕ

13. Exit optical command by pressing ESC on the frame buffer's keyboard.

For reflection samples: The procedure for mounting and aligning samples on the goniometer head is (assumes no laser attachment):

1. Mount the sample to the goniometer head, then attach assembly to the goniometer.
2. Start GADDS online version (for your particular stage).

3.6.3 Collision Limits for Your Sample

A GADDS system has many moving components, such as the detector, X-ray source, optics, and sample stages. Caution must be taken to prevent collision between moving or stationary components and samples. A collision may cause component damage, sample damage or misalignment. In order to prevent collisions between components and samples, GADDS systems have many hardware limit switches and software controlled limits, depending on the configuration. Due to the complexity of a GADDS system, and variety of sample size and shape, those limit switches and software limits can protect the system only if used with caution. Some good practices for operating a GADDS system are the following:

- Be aware of the locations and set limits of all the hardware limit switches. Consult Bruker Service if you need this information.
- If it is necessary to relocate the hardware limit switches from the manufacturing settings for a particular application, mark the original positions, make a note, and recover the limit switch immediately after finishing the application.
- Check all software limit settings immediately after starting the instrument and software, or after changing components or a sample of different size and shape.
- Manually drive each axis for the range to be used in data collection before starting an automatic data scan, especially for a new sample or goniometer position.
- Update the software limit settings based on data collection strategy and sample size.
- Find a “safe path” from one goniometer position to another position—driving all axes to the new positions randomly or simultaneously may cause a collision. The “safe path” can typically be found by manually driving all axes from the existing position to the new position.
- Add “safe path” positions in a .slm file for automatic data collection.
- Before starting an unattended long-term data collection session, take a test run first with the same data collection strategy, but short collection time and coarse steps.
- Before “homing” an axis, drive other axes to clear space for the “home” position. Then drive that axis to the vicinity of the home position.
- Remember all of the emergency software or hardware measures to stop a run in case of danger of collision.

3.7 Data Collection

This section describes the main procedure for data collection and first data treatment.

NOTE: Ensure that the detector cannot be hit with the primary beam by using a beam stop or suitable goniometer angles.

Use one of the following methods to collect data.

3.7.1 Scan Method

1. Left-click Collect > Scan and:
 - 1.1 > SingleRun to collect one or more frames while rotating one goniometer axis in step, scan (continuous), or oscillation mode.
 - 1.2 > MultiRun to run several SingleRuns.
 - 1.3 > MultiTarget to perform one SingleRun on many sample locations.
 - 1.4 > CoupledScan to collect a raw spectrum in conventional Bragg-Brentano geometry where 2-theta and omega are coupled in a 2:1 ratio.

NOTE: Refer to M86-Exx008 GADDS Software Reference Manual for details on these scan options.

NOTE: All data for these scans are saved, and all of the corrections are applied, automatically. Frames are named using the job name, run number, and frame number with the file extension .gfrm. Frame series get the same job name and run number.

3.7.2 Add or Rotation Method

1. Left-click Collect > Add (to collect data at fixed goniometer angles) or Collect > Scan > Rotation (to collect one frame while rotating the phi-axis with constant rotation speed). Refer to the GADDS Software Reference Manual for details on these scan options.
2. Left-click Process > Spatial > Unwarp to correct for spatial distortion. Enter the number of frames in the second line and the full output file name in the third line.

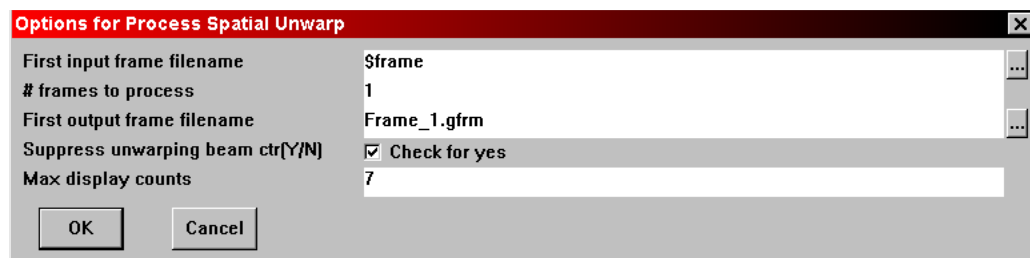


Figure 3.14 - Options for Process Spatial Unwarp window

NOTE: The output file name can be identical to the input file name. Many users add a “u” to the original file name to mark it as unwrapped. Also, if you want to unwarp a series of frames, enter the full name including extension of the first data file in the first line.

3.8 Basic Data Analysis and Preparation

For an initial analysis of the 2D data, use the special GADDS cursors from the Cursors menu. (See M86-Exx008 GADDS Reference Manual for details.)

To determine peak position before an integration, use Conic Cursor (F9).

To create and analyze a 1D diffraction pattern, perform the following:

1. Left-click Peaks > Integrate > Chi to integrate the 2D diffraction data into an intensity-versus-2-theta plot (and to determine peak position before an integration). The Integrate window appears.

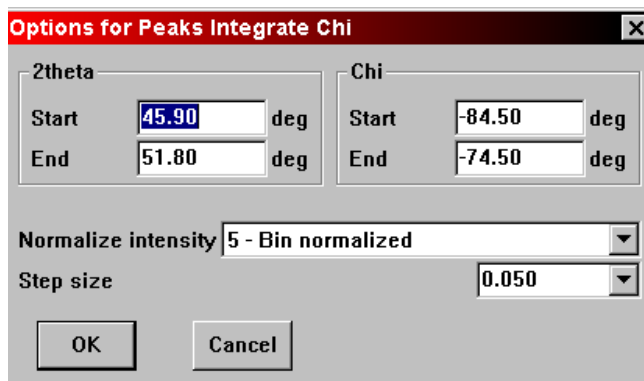


Figure 3.15 - Options for Peaks Integrate Chi window

2. Set the intensity normalization to 5-bin normalization.

3. Select an integration area in one of the following ways:
 - If you know the integration range, enter start and end values for 2-theta and chi in the first four lines. Press OK and hit Enter. The integration result will appear.
 - Press OK to exit the window. A blue frame appears. One at a time, select numbers 1–4 and move the edges of the blue frame (with the arrow keys or by dragging the mouse) to define the start and end values of 2-theta and chi.

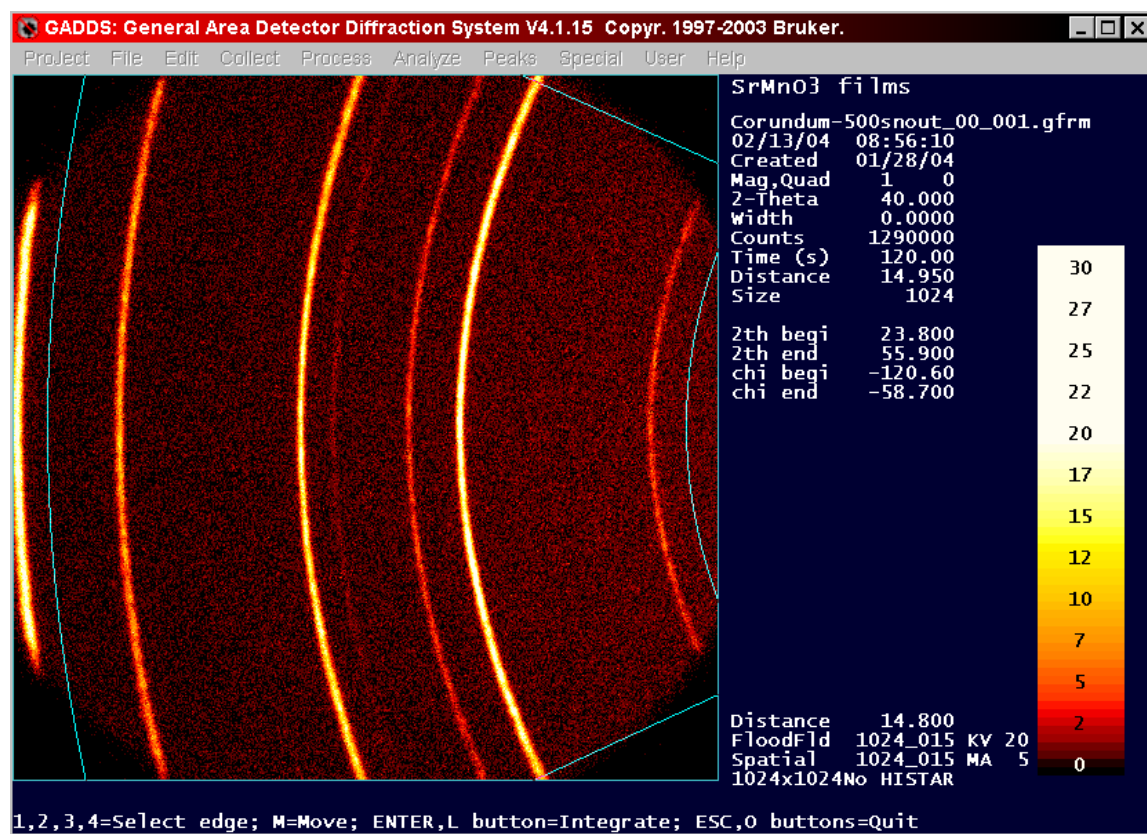


Figure 3.16 - Define the values of 2-theta and chi

4. Press Enter. A typical plot is shown in Figure 3.17.

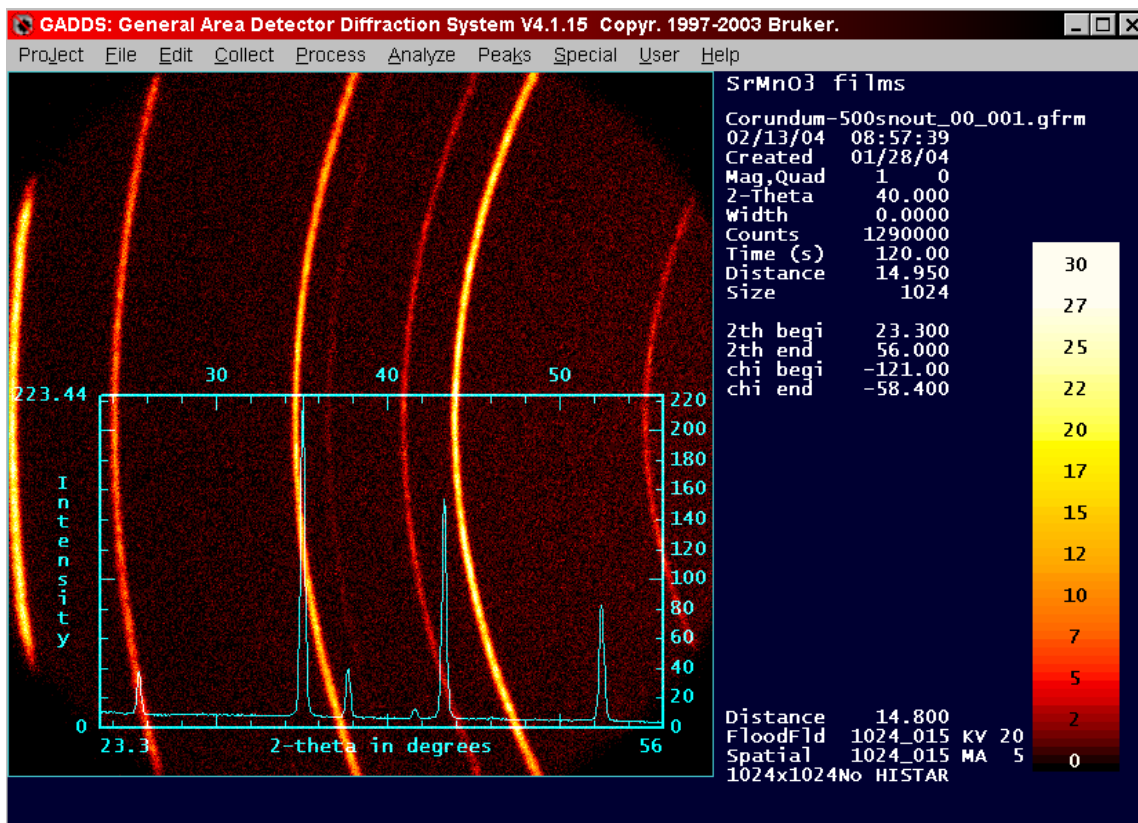


Figure 3.17 - 1D diffraction pattern

5. A pop-up window will appear prompting you to save the integrated data. Enter the file name, title, and set the file format to DIFFRACplus. You can append (add) integration results from several frames into one DIFFRACplus file by checking the Append checkbox.

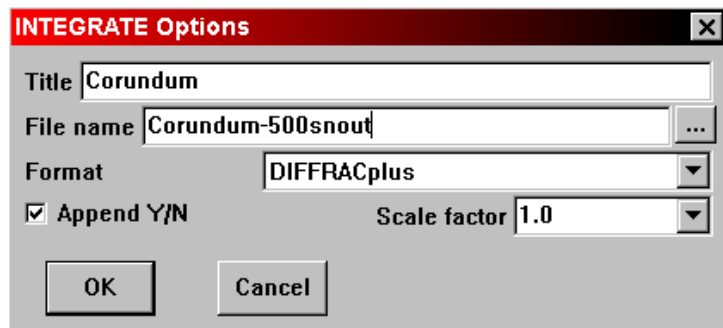


Figure 3.18 - Integrate options window

4. Phase ID

4.1 Overview

GADDS is a very powerful tool for analyzing the chemical composition of powder samples. Because of its capability to collect the diffracted intensity from a large angular range, the area detector has strong advantages compared to a conventional point detector system. The large area of the GADDS detector allows for a large 2θ range to be analyzed without any movement of the sample and detector. This results in a huge speed advantage over conventional systems. (See the comparison between point, position-sensitive, and area detector in Figure 4.1).

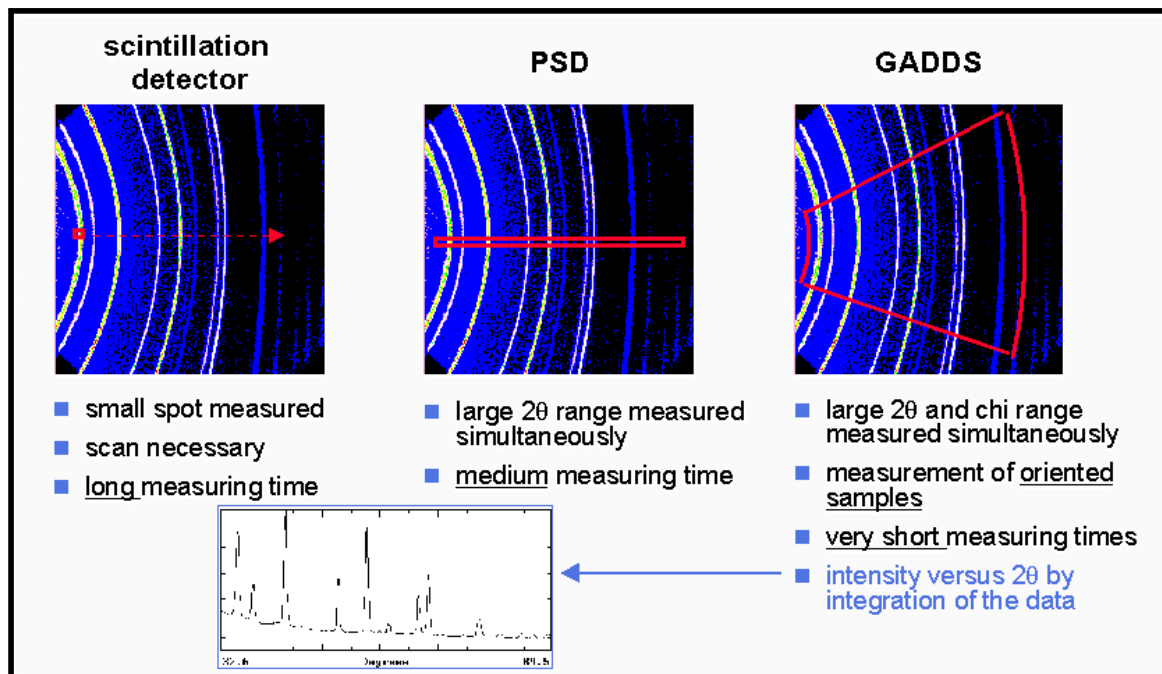


Figure 4.1 - Comparison between a point, position-sensitive and area detector

The GADDS software allows easy integration of the 2D diffraction data into intensity versus 2θ plots. This enables the collection of powder patterns even from large grained and textured samples without losing information. (See Figures 4.2a through 4.2c.)

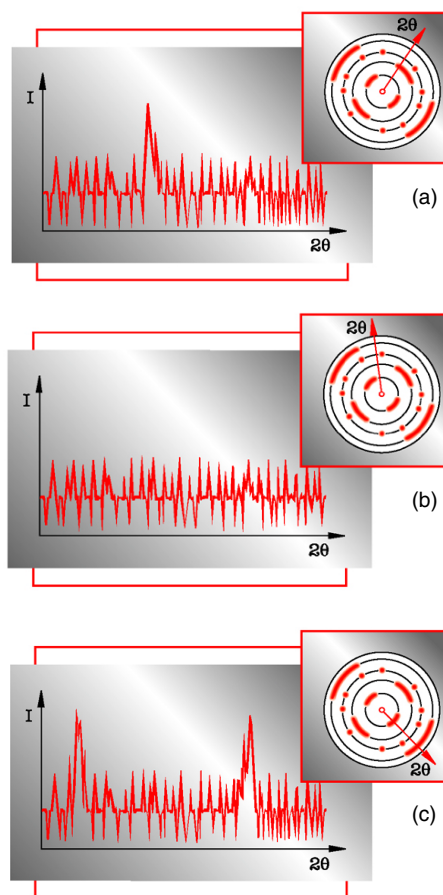


Figure 4.2 - From a large grained and textured sample

The schematic intensity (I) versus 2θ plots show the results of a point detector scan through a diffraction pattern, which is shown in the upper right corner of each plot. The red arrow indicates the scanning direction of the point detector. Due to the non-isotropic sample structure—large grains and texture—the intensity distribution along the Debye rings is inhomogeneous. Consequently, the scans strongly differ as a function of the scanning direction.

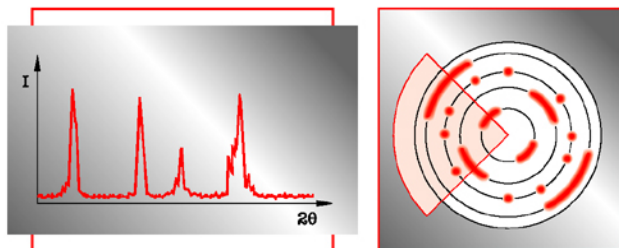


Figure 4.3 - Schematic intensity versus 2θ

The intensity versus 2θ plot shows the χ integration result of the two-dimensional intensity distribution collected with an area detector. The plot clearly shows all lines of the sample. This is not true for the schematic point detector scans in Figure 4.1.

After integration, use DIFFRAC^{plus} Evaluation Search Match software and import the integrated spectra. This package allows you to use the ICDD/PDF database (formerly JCPDS) for final phase identification. See the DIFFRAC^{plus} EVA manual and Figure 4.4.

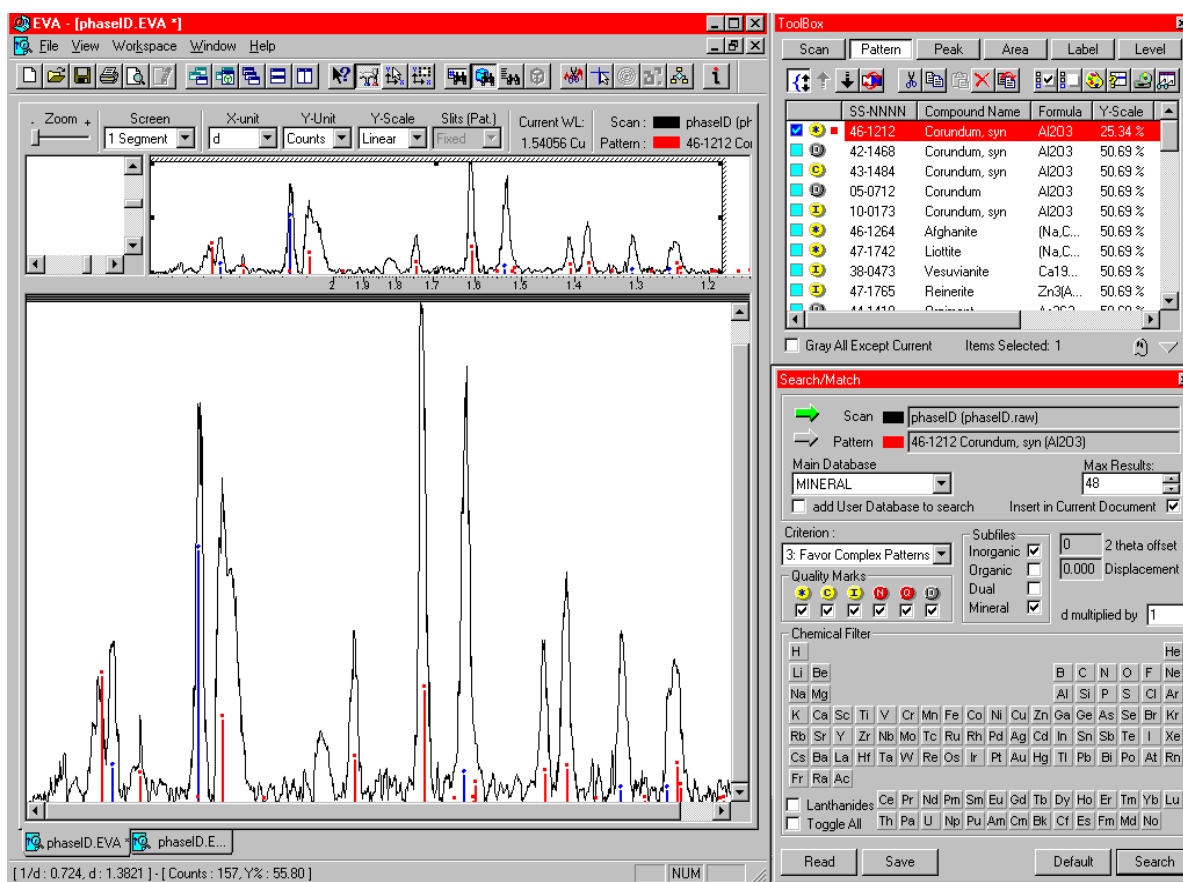


Figure 4.4 - Database search for unknown phases

4.2 Performing a phase ID analysis

The following procedure contains the necessary steps to perform a phase ID analysis:

1. Choose a wavelength that does not cause fluorescence in the sample. If you have to change X-ray tubes, see your GADDS Administrator and refer to the GADDS Administrator's Manual.
2. Mount the sample. See also section 3.
3. Use high resolution (1024x1024) mode.
4. Move the detector to the appropriate detector distance. Make sure you can resolve all lines at that distance. See also section 3 for calibration.
 - Single frame Phase ID for quick, qualitative results.
 - Multiframe Phase ID for better results (especially reflection mode).
5. Make sure you measure the lowest diffraction line available from the sample. Note that in reflection geometry the smallest detectable reflection is at $2\theta = \omega$. (beam stop!)
6. Set up a SingleRun measurement to collect at one or several detector and ω angles. Make sure the 2θ coverage for the different goniometer positions overlaps. Best resolution is obtained close to $2\theta = 2\omega$ because of

focusing effects in reflection and minimum absorption effects in transmission.

7. Choose a collimator with a diameter that matches the sample dimensions.
8. Start the measurement and wait.
9. Load the first frame.
10. Left-click Peaks > Integrate > χ -integration (see Figure 4.5) and select the region to be integrated, the normalization mode 3 and an appropriate step width (typically .05).



Figure 4.5 - Peaks > Integrate > Chi Integration

11. Save the integrated scan in a separate file.
Use the DIFFRAC^{plus} format.
12. Repeat the last step for each frame. Make sure you keep step width and integration mode constant. The 2θ ranges have to overlap in at least one point. The End value of one range has to match one step of the next range.
13. Use the Merge software tool to merge the scans.

14. Use DIFFRAC^{plus} Eva to perform the database search. See the DIFFRAC^{plus} EVA manual.

Figure 4.6 shows a measured diffraction pattern from a textured sample surface. The integrated diffraction spectrum is a function of the selected integration range.

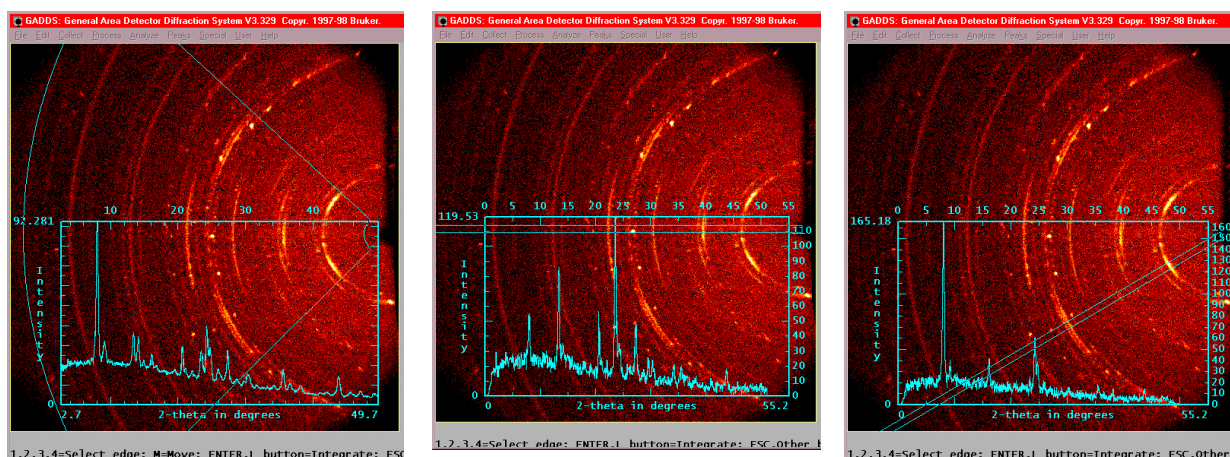


Figure 4.6 - Measured diffraction patterns

Figure 4.7 shows the result from a phase identification measurement on ZrO_2 .

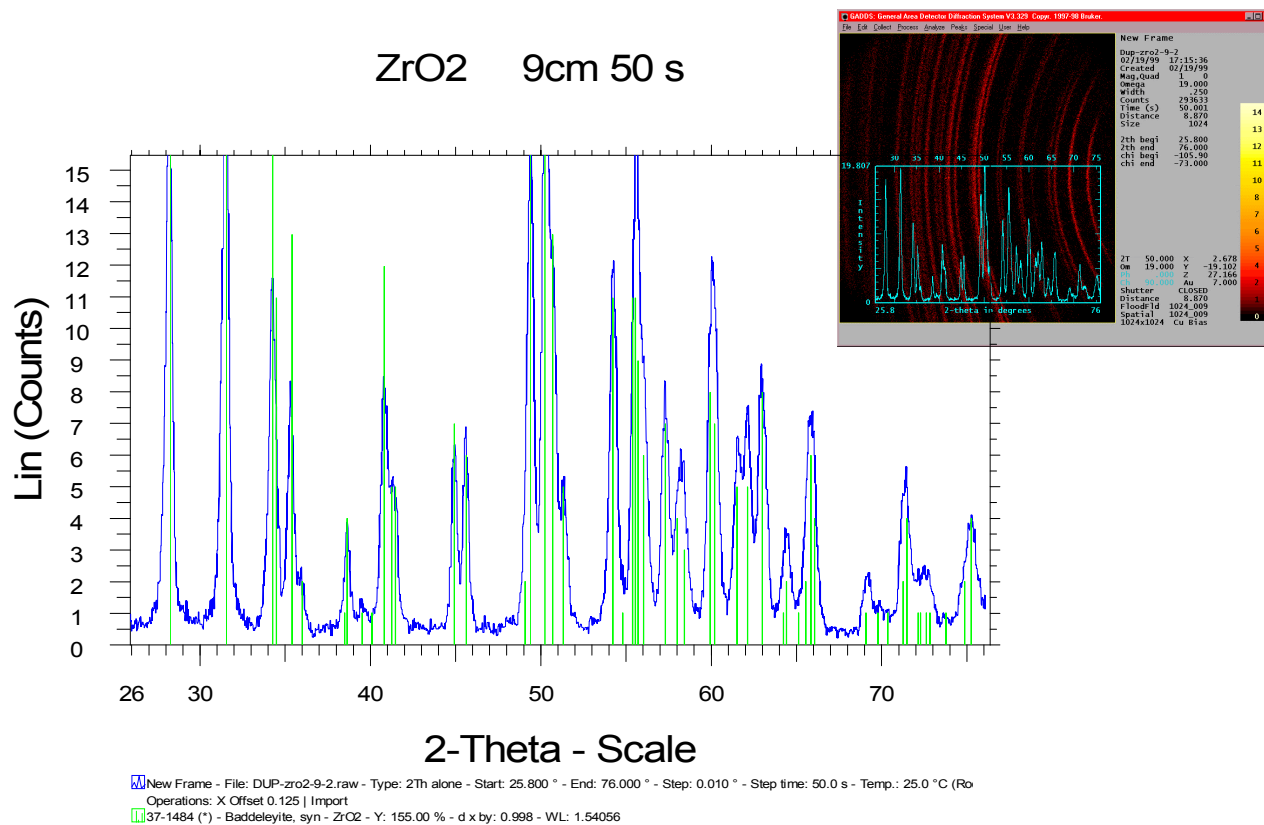
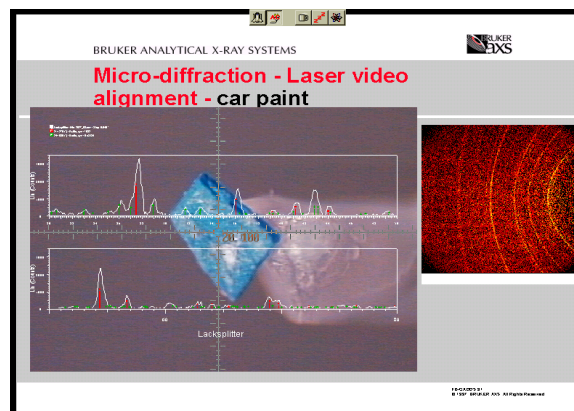


Figure 4.7 - Phase identification measurement

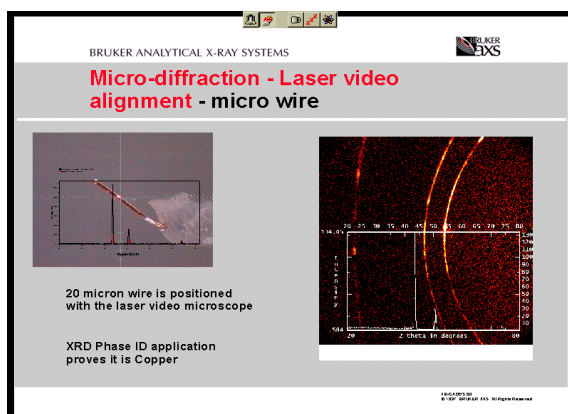
XRD phase identification on very small samples is called Microdiffraction. Due to its high speed and sensitivity, the D8 DISCOVER with GADDS is ideal for these usually extremely time-consuming applications. The system can measure with beam diameters as small as 50 microns.

Figures 4.8a through 4.8c show typical applications for forensic work. The measurements were performed on a 20 micron wire (4.8a), different layers of a car paint (4.8b), and on very small amount of different sands (4.8c).

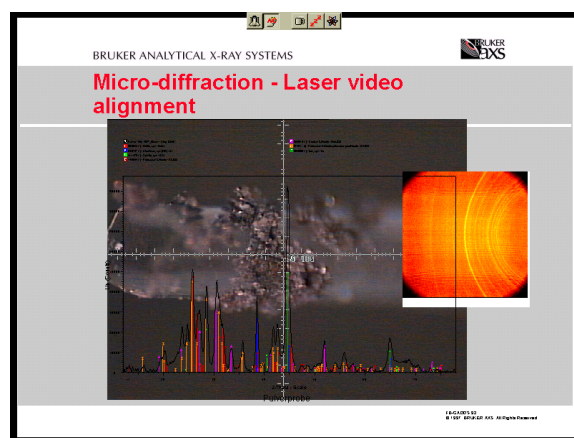
NOTE: See sections 10.3 and 10.5 for examples of creating a Phase ID script and adding it to the menu bar.



(b)



(a)



(c)

Figure 4.8 - Typical applications for forensic work

5. Texture

5.1 Overview

A major part of condensed matter like minerals, rocks, soils, ice (but also artificially-synthesized phases like metals, ceramics, etc.) are found to be polycrystalline [Bunge]. Classic examples of materials that have been examined by texture analysis are geologic samples, rolled metal sheets and polymer fibers. New materials that are examined include thin film layers on silicon and superconductor thin films. The sample morphology is defined by properties like position, crystallite size, grain boundaries, shape, and orientation of the individual crystallites. *Crystallographic texture*, also known as *crystallite orientation (distribution)*, is an important property of materials. The meaning of orientation becomes obvious when looking at macroscopic properties that are anisotropic for single crystals. Misarranged crystallites can cause excessive “earring” in deep draw sheets, breakage in fibers, poor bonding in composites, and high

rejection rates for semiconductors. As more materials are formulated at a molecular level, texture must be specified and controlled to ensure proper product performance. Texture analysis is the key to understanding material properties like:

- Mechanical strength and elasticity
- Electrical resistance and capacitance
- Thermal conductivity
- Magnetic and optical properties
- Scattering of electromagnetic or mechanical waves

An example for a specimen with only one orientation is a single crystal. Ideal polycrystalline material has diffracting domains or *crystallites* that are randomly distributed. Texture is described with respect to a sample coordinate system.

X-ray diffraction allows the direct measurement of the (hkl)-axes' distribution by looking at a fixed 2θ -range while varying the sample orientation in the diffractometer. The intensity distribution could be visualized as "intensity mountains" on the pole sphere, where each unit of the pole sphere represents the diffracted intensity at a sample orientation.

The 3D pole sphere is typically reduced to a 2D pole figure by stereographic projection, which is the primary representation used to describe crystallite orientation (see Figure 5.1 & Cullity, 1978). These projections are relative to sample directions such as sample normal (ND) and machine or rolling direction (RD). For wires and fibers, the sample axis direction is used for RD.

Typically, one to four independent reflections (hkl-values) are measured for a quantification of the major orientations in a material. Using all co-linear reflections, such as 001, 002, and 004, will not suffice. It is necessary to examine reflections along each axis, such as the 100, 110, and 002.

Pole figure data can be used to determine the Orientation Distribution Function (ODF), which quantifies the orientation density of the crystallites and provides the (volume) percent of crystallites oriented in specific directions. In general, the ODF gives the volume part in the investigated volume for a given orientation respectively a given orientation range. While some orientation distributions require a three-dimen-

sional orientation representation (e.g., Eulerian angles), texture in samples such as films and fibers can often be described with a compact description of the orientation since these samples are either one- or two-dimensional in nature. The texture of many films and fibers can be described by a representation known as a Fiber Texture Plot (FTP), while polymer orientation is often characterized with Hermans and White-Spruiell orientation indices.

The pole figure's relative intensity can be normalized such that it represents a fraction of the total diffracted intensity integrated over the pole sphere. Typically, the pole sphere is stereographically projected to the pole figure, but you can also use polar projection for non-standard uses. Three projection directions are supported, depending on how you mount your sample on the goniometer. For fibers and wires, project the pole sphere along X (1). For flat samples, determine the direction of the sample normal (typically either along X (1) or 2 (3)). Additionally, you can tilt, invert, and rotate the projection of the pole sphere until you get the projection required.

In a pole figure displayed with the GADDS software, the angle α , is defined as the angle between the normal to the reflecting plane of interest (that is, the pole of interest) and a physical reference plane in the sample (for projection=3 the sample surface) (see Figure 5.1).

$$\alpha = 90^\circ - \chi$$

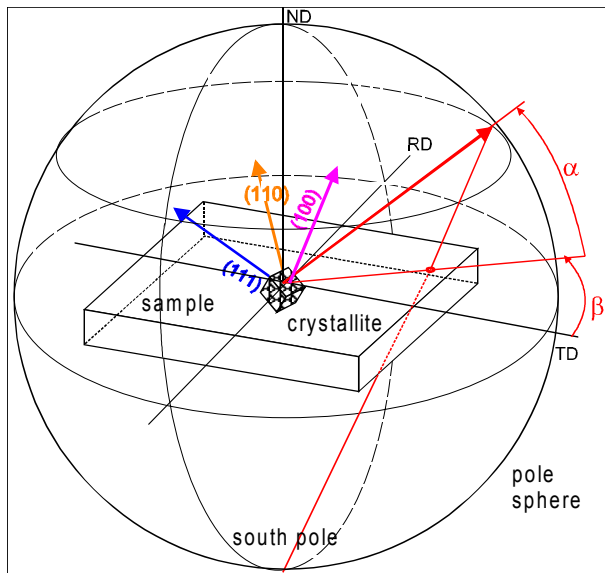


Figure 5.1 - Definition of the angles α and β and stereographic projection

For example, in a cubic system, a (100) pole figure which has intensity at $\alpha = 90^\circ$ implies that the [100] direction is normal to the surface. A (111) pole figure from this sample would have intensity at $\alpha = 54.74^\circ$, which is the angle between the [100] and [111] directions. The angle beta (β) is the angle between the normal to the reflecting plane of interest and a second reference direction orthogonal to the first direction, usually a machine direction (MD), also called rolling direction (RD) or fiber axes for wires/fibers. Keep in mind that the reciprocal and direct (real) space crystallographic directions are only coincident in cubic systems.

Other conventions will be noted here for reference. Metallurgists typically define α either identical to GADDS definition or as the angle from sample normal to diffraction vector (which is $\alpha' = 90^\circ - \alpha$). Beta is defined starting at RD (which is $\beta' = \beta + 90^\circ$). Polymerists define χ (chi) (instead of α) as either $\chi = \alpha$ or $\chi = 90^\circ - \alpha$. Phi is used instead of Beta. As Bruker AXS uses ϕ and χ for diffractometer angles, we will use α and β for pole figures (for less confusion).

In Figure 5.2, the upper left quadrant shows measured reflections of multiple discrete grains in an inorganic thin film. The upper right plot shows the 2θ values for each of the lines. The lower right plot, a 2θ integration proves the existence of texture in the thin film, and the lower left shows the final pole figure for the film. Notice again that several (hkl) lines are collected on the area detector simultaneously. As long as corrections are made for sample absorption and polarization, it is possible to collect data for several (hkl) lines and thus several pole figures simultaneously, which greatly reduces data collection time.

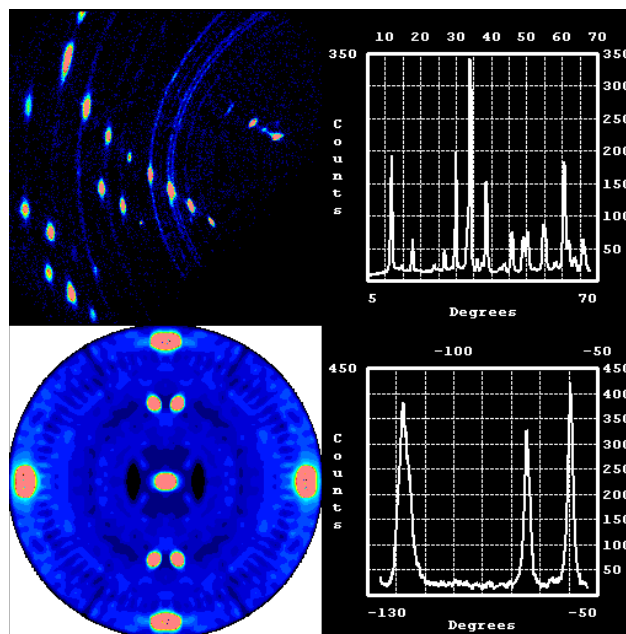


Figure 5.2 - Raw data to pole figure

Figure 5.3 shows a 3D-represented pole figure of a highly oriented thin film. Two distinct orientations are observed (90° and 45°) with a weak third orientation normal to the surface.

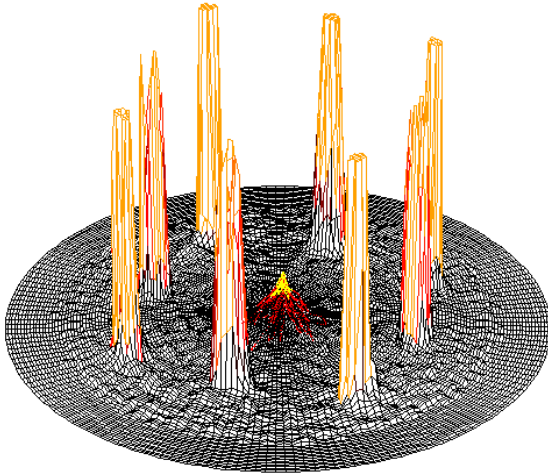


Figure 5.3 - Contours of oriented thin film

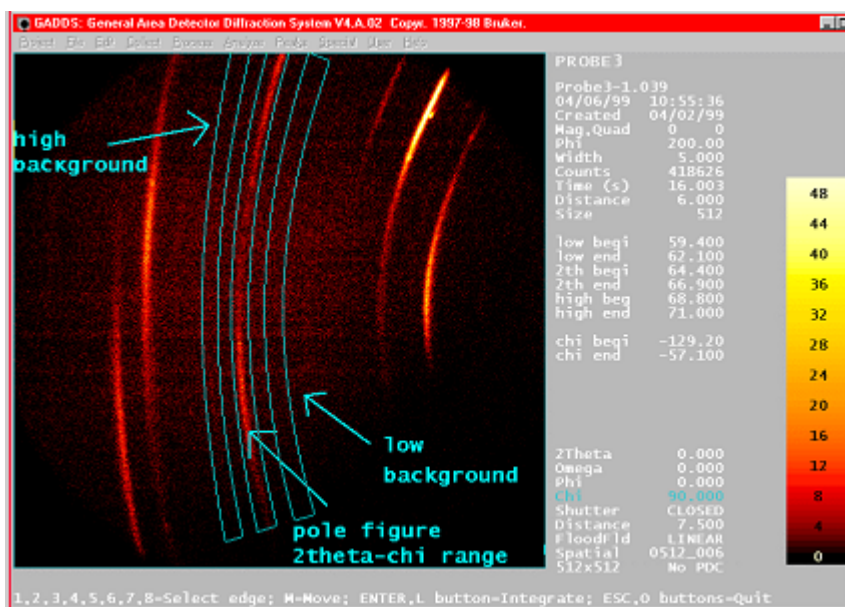


Figure 5.4 - Data processing

5.2 General Data Collection

Considerations for Texture Analysis

With the fixed χ stage (842-050600) and two-position χ stage (842-050800), not all tilt angles, α (the angle between the incident beam and the sample normal) are accessible. With a fixed χ stage, complete pole figures (to $\alpha = 80^\circ$) can only be collected for pole $2\theta < \sim 38^\circ$. With a two-

position χ stage, complete pole figures can only be collected for pole $2\theta < \sim 55^\circ$. The $\frac{1}{4}$ -cradle (810-300500) can reach all tilt angles by adjusting χ appropriately. The XYZ stage (842-050700) lacks ϕ and χ motion, so only the central portion of the pole figure is observable. With the XYZ stage, the maximum $\alpha = \pm\theta$ in reflection mode only.

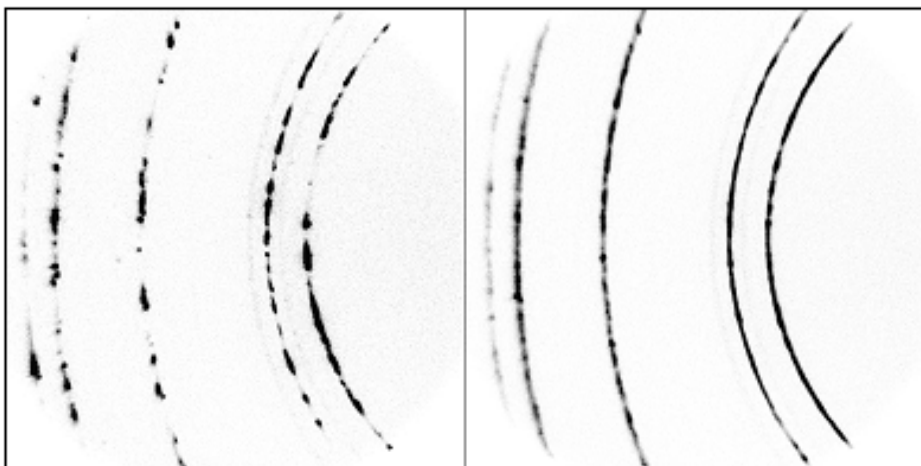


Figure 5.5 - Effect of sample oscillation on a large-grained aluminum specimen. Data on the left is collected without sample oscillation; data on the right is with sample oscillation

The choice of sample-to-detector distance for a texture experiment depends on the resolution required to separate adjacent diffraction lines and the need to collect multiple poles simultaneously. For most metals and polymers, the distance is 6 cm.

To sample a larger number of crystallites, an oscillator can be attached to the two-position χ stage or $\frac{1}{4}$ -cradle. A maximum of 12 mm of stroke is attainable. Two types of oscillators exist: 1) rotation below translation (Rot-Trans) and 2) translation below rotation (Trans-Rot). The Rot-Trans design can be used with the $\frac{1}{4}$ -cradle. Trans-Rot samples different grains as a function of rotation. Rot-Trans samples the same grains as a function of rotation.

The following are other general considerations for texture measurements:

- For disk space considerations, the recommended frame size for complete pole figures is 512x512. For fiber texture plots, 1024x1024 frames can be used.
- For pole figure data collection, a 0.5 mm collimator is recommended. Smaller collimators are only necessary when collecting selected-area (microtexture) data.
- The recommended sample-to-detector distance for texture measurements is 6 cm. Larger distances are only necessary to resolve closely spaced lines.
- For reflection measurements, adjust the machine direction (MD) of the sample to be vertical when $\chi = 90^\circ$, then use GONIOMETER/UPDATE to set $\phi = 0^\circ$ before starting pole figure data collection. If this is not done, the pole figure can be tilted during data processing to orient the MD vertically in the pole figure.
- The collimator tip may be removed to allow more sample clearance.
- Using the manual control box, verify that the SCHEME-recommended measuring parameters do not cause collisions with the current instrument configuration.
- If the two-position χ stage is used, verify that the appropriate χ angle is set both on the stage and in the software. Use collect/goniometer/fixedaxis to update χ . If pole figure data has been collected at any wrong, fixed angle, the value may be corrected with the *FRMFI*X utility. Use filename.* to process an entire series of frames.
- When using an oscillator, make certain the sample is securely fastened to its holder.
- The Trans-Rot oscillator for the two-position χ stage must be secured to the stage with its support rails.
- After repositioning χ on the two-position χ stage, the sample height should be readjusted. After adjusting the sample height with the threaded, knurled specimen mount

for the oscillator, snug down the set screw on that mount. Use GONIOMETER/UPDATE whenever the specimen is physically rotated.

- Verify that the ω angle is not so shallow that closely spaced peaks are overlapped due to broadening. If a $\frac{1}{4}$ -cradle is used, it is recommended to vary χ rather than ω to minimize peak broadening.

5.3 Preparation for the Texture Experiment

Consult the JCPDS-ICDD database, and examine the PDF card for the material. If the card is not in the PDF file, then collect a standard powder diffraction scan rotating the sample in ϕ while scanning in ω . Set $\chi = 54.74^\circ$ to sample a larger unique section of reciprocal space than can be observed with $\chi = 90^\circ$. For alloys and non-stoichiometric materials, PDF cards frequently do not exist, though there may be cards for related materials. For thin films, always determine the line positions because the layer of interest may have infused material causing peak shifts from the phase-pure material.

To determine optimal data collection parameters, it is recommended to collect several frames with the sample in different orientations with respect to the X-ray beam, if possible at different χ settings. In this way, for example, intense single crystal substrate peaks may be avoided. For highly textured materials, such as many electronic thin films, it is important to scan ω over a $5\text{--}15^\circ$ range to observe the textured reflections. In summary, confirm the phases present, and get an overview of the orientation.

5.4 Data Collection Considerations for ODF Analysis

Pole figures collected for ODF analysis using the popLA software must cover at least $70^\circ \alpha$. For other programs, the requirement may be as high as $80^\circ \alpha$. Consult the specific ODF software documentation for detailed requirements before collecting pole figure data. For the material of interest, examine the Bravais lattice type on the PDF card. If the reflections are indexed, select the unique lines for the particular lattice. For cubic, tetragonal, and hexagonal (or rhombohedral), two lines are needed. For monoclinic and orthorhombic, three lines are required. The trigonal case requires five pole figures due to an overlap of the (hkl) and (khl) reflections. More lines may be required for the higher symmetry space groups if there is no sample symmetry. For many sample symmetries, it is unnecessary to collect pole figures covering $360^\circ \beta$ since symmetry can be used to expand the collected data within the GADDs software using POLE_FIGURE/SYMMETRIZE and also within most ODF packages. For an unknown system, collecting the full pole figure is advisable.

The accuracy of an ODF series expansion depends on the number of terms in the series (typically 16). The quality of the coefficients in the series depends on the number of unique pole figures used in the analysis and on the quality of the pole figure measurements. Additional considerations for large-grained materials or complex orientations are the statistical significance of the grain sampling (related to sample oscillation) and the possibility of unobserved grains due to data collection conditions.

5.5 Other Texture Representations

In some cases, only a small section of the pole figure is necessary to represent the necessary sample orientation information. Other widely used partial pole figure representations include rocking curves and fiber texture plots. A rocking curve (ω scan) is the simplest check for orientation. In single crystal work, it is a way to check for crystal quality if only one orientation exists. If more than one orientation exists, then two or more crystals exist with different orientations for that specific reciprocal lattice plane. In general, rocking curves give a good relative comparison of texture strength. The full width at half maximum (FWHM) of the fiber texture plot quantifies the *pole spread*, with a larger FWHM indicating a weaker (more random) texture. Two other methods used to characterize orientation mostly in the polymer field and are related to direction cosines of intensity-weighted pole figures. The functions are described by the Hermans and the White-Spruiell orientation indices.

5.6 Using POLE_FIGURE/SCHEME to Plan Strategy and Coverage

Sample shadowing is one of the difficulties that can be overcome using POLE_FIGURE/SCHEME. For a given set of data collection conditions, the simulated pole figure can have a central hole in reflection mode or the poles missing in transmission mode. To fill in this missing polar data, which is caused by the α , β angles not being in the diffracting condition or the reflections not being on the detector face, additional data must be collected, usually at a second ω value. With a $\frac{1}{4}$ -cradle when planning coverage using POLE_FIGURE/SCHEME, change χ first and ω second. At distances larger than 6 cm, three or more ω values may be necessary. A typical second ω value is $\frac{1}{2} * 2\theta + X^\circ$ (with $X = 5^\circ$). To fill in the center or north/south poles of a pole figure, the value of X increases as the χ value decreases. Adjust the value until the simulated pole figure is complete. The central part of the pole figure in reflection mode is always attainable at $\chi = 90^\circ$ by setting $\omega = \theta$. If rotation is available, a 180° scan in ϕ will give the complete central portion of the pole figure to a given β value.

The *Projection Direction*, PD, indicates the relationship of the sample normal to the X-ray beam. PD = 1 is defined as the sample normal being parallel to the x-ray beam when $\chi = 0^\circ$. This is usually specified when examining polymer sheets in transmission or with fibers. PD = 3

is defined as the sample normal being coincident with the z-axis of the goniometer, which is vertical. In cases where both transmission and reflection pole figure data is collected, the data should be processed as either PD = 1 or PD = 3. If the sample requires remounting, POLE_FIGURE/TILT and POLE_FIGURE/ROTATE may be necessary to orient the pole figure properly with respect to the original sample setting.

In Figure 5.6, the upper diagrams represent the physical sample while the lower represent the corresponding pole figures. FA is the fiber axis. MD is the machine direction. This is usually a processing direction (*e.g.* drawing or rolling direction). TD is the transverse direction. N is the normal direction. MD, TD, and N are orthogonal. The MD in the pole figure is determined by ϕ_0 . Position the sample MD at ϕ_0 for the resulting pole figure to have its MD pointing conventionally vertical.

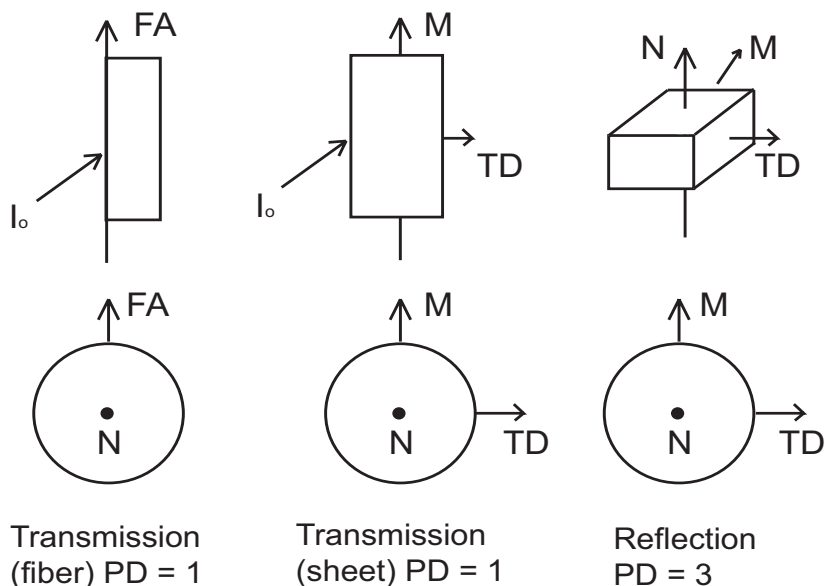


Figure 5.6 - Relationship between the significant directions in texture specimens and their associated pole figure

Once a suitable set of data collection parameters is determined with POLE_FIGURE/SCHEME, change the output filename from \$null to \$scan to update the scan lines in the MULTIRUN list. The data collection parameters may be edited with COLLECT/SCAN/EDITRUNS (e.g., reduce the default data collection time from 120 sec).

5.7 Using POLE_FIGURE/PROCESS

Once the pole figure frames are collected, the following two processing steps are used to create a pole figure:

1. Apply Lorentz and polarization corrections, if desired, using the appropriate CORRECTION command. The Lorentz correction depends on the diffraction geometry and sample properties. It differs for powders, single crystals, and textured materials. For details, see Blake (1933) and the International Tables (1967). Presently, no Lorentz correction is implemented in GADDS. The polarization correction depends on the incident beam optics (e.g. K β filter, monochromator, Göbel Mirrors). If fiber or plate absorption corrections are desired, it is faster to apply them as options of POLE_FIGURE/PROCESS rather than applying the CORRECTION command to the entire series of frames.
2. Use POLE_FIGURE/PROCESS to integrate the reflection of interest in each of the frames. Typically, 72 frames are collected (5° steps in ϕ), and all frames are processed in sequence from *.001 through *.072, unless a frame number is manually changed to break the sequence.

For accurate ODF and percent random analysis, background must be removed (see figure 5.4). For unfamiliar systems, the integration should be monitored to spot potential problems. For example, if a substrate reflection occurs in a background region, the integrated area will be negative. A status line on the bottom of the screen will indicate the number of pixels that were negative and the magnitude of the largest. The remedy is to select a background away from the interfering intensity. The background removal model in GADDS is linear. If the material has amorphous content, background should not be removed near the amorphous region in the frames, unless it is present under the crystalline line position.

The example in Figure 5.7 shows the effect of X-ray absorption on pole figures. The more penetrating Mo radiation samples more grains in the highly absorbing tungsten resulting in a smoother pole figure than obtained with Cu. While the texture is qualitatively similar for each radiation, it is not necessarily the case that the subsurface texture of the material is identical to its surface texture, unless the sample has been prepared according to ASTM standard E81-90 "Standard Test Method for Preparing Quantitative Pole Figures," which applies only to metals. The sample surface texture could be the result of a machining operation, such as cross-sectioning or grinding.

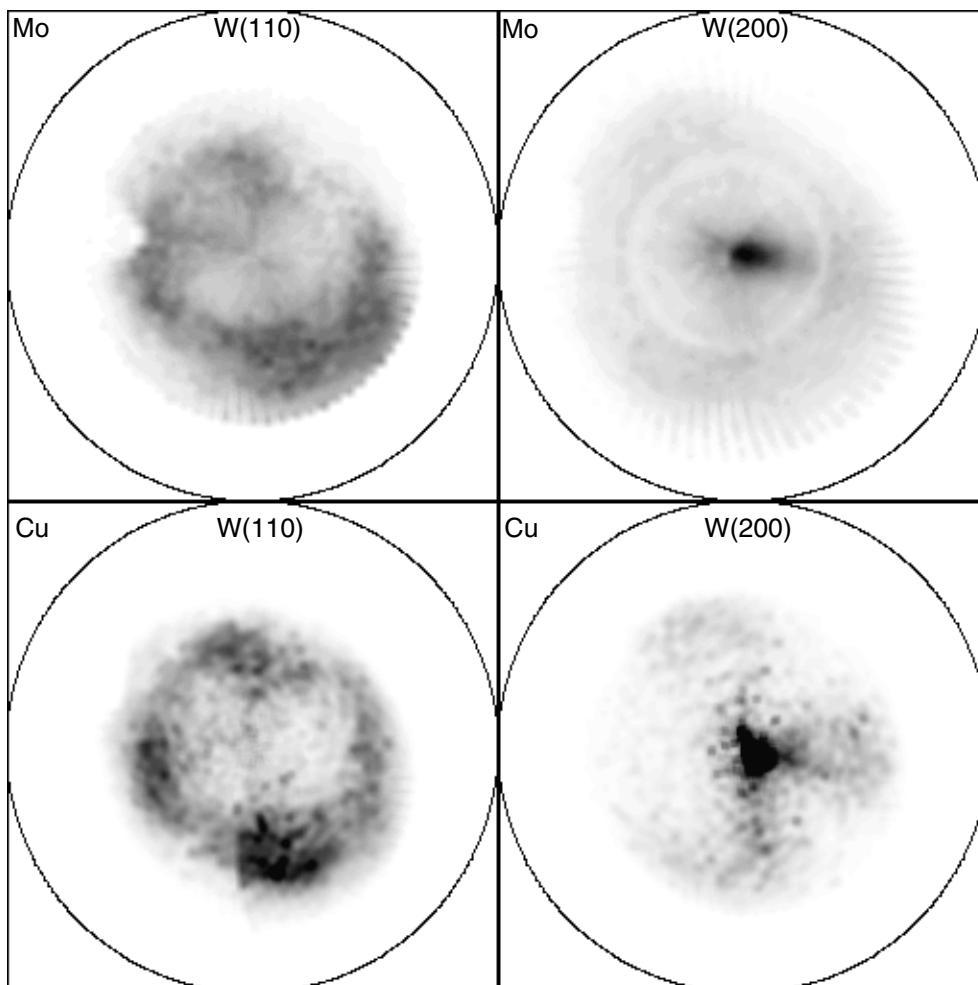


Figure 5.7 - (110) and (200) pole figures from a tungsten (W) cylinder collected with Mo and with Cu radiation. Data was collected from the curved portion of the cylinder

When merging multiple segments for a pole figure, absorption corrections must be applied. An empirical and an analytical method of absorption correction exist. In the empirical method, a reference pole figure is collected from a randomly oriented specimen of the same material as the textured specimen. This method is valid for infinitely thick samples in reflection or fibers and films in transmission. The analytical method is based on the absorption coefficient and the sample thickness. The first method is implemented in many ODF programs, while the second is implemented in GADDS. Keep in mind that the absorption coefficient of a material depends on the wavelength of X-rays in use. Also, the units of the absorption coefficient and the thickness must be consistent (e.g., cm^{-1} and cm). Typically, if the absorption is less than 10%, it can be ignored, except if extremely accurate ODF results are desired.

If the density and chemical composition are unknown, a method of selective integration and intensity scaling can be used, as follows:

1. When collecting data for this method, break the frame sequence by a least one frame number (e.g. 001-072, 075-146). There should be a separate sequence for each ω value used during pole figure data collection (as previously determined using POLE_FIGURE/SCHEME).
2. POLE_FIGURE/PROCESS each series of frames separately with the same 2θ range but different χ ranges. Set the χ ranges based on the fall-off in the integrated intensity observed using PEAKS/INTEGRATE/ 2θ . This intensity fall-off may be due to sample absorption or shadowing. There should be a small (e.g., 0.1°) gap left between the specified χ ranges. They should not overlap. This is done to enable the different segments of the pole figure to be properly scaled before merging.
3. Save the individual segments of the pole figure, then use FILE/LOAD to overlay each adjoining segment. Zoom in on the region of the gap in the data and examine the map of pixel intensities. From those values, estimate an average intensity scale factor.
4. Reload the segment of the pole figure to be scaled using the scale factor.
5. POLE_FIGURE/INTERPOLATE to fill in the gap. The resulting pole figure may then be smoothed using SMOOTH. The recommended option is SMOOTH/CONVOLVE 4.
6. Repeat this procedure for all pole figure segments (typically 2 or 3).
7. Save the final pole figure.

5.8 Polymer Orientation

Data collection from polymers usually differs from that of three-dimensional orientation in that the orientations are usually one- or two-dimensional. Therefore, a complete pole figure is not required to obtain orientation information. The simplest orientation is that of a fiber. Usually, the fiber axis is close to the chain orientation direction in a fiber. This is described as the *meridional* direction in a pole figure. The direction normal to the fiber axis is defined as the *equatorial* direction. Fibers are usually rotationally symmetric. In other words, if a fiber were mounted along the ϕ axis, the same diffraction pattern would be observed regardless of the ϕ rotation. For any given 2θ range, a single sample position is required to obtain orientation information in the equatorial plane. The meridional reflections usually have a maximum intensity at the Bragg angle. This means that several frames (i.e. a rocking curve) describe these reflections. The rocking curve width is related to the distribution of the orientations of the molecular chains about the physical axis. Note that in this discussion a rocking curve is not necessarily an ω scan, but may also be a ϕ or χ scan, depending on the orientation of the fiber. This discussion applies to a single filament or a carefully prepared fiber bundle. Preparation of a multiple fiber bundle should be done so that all of the fibers are oriented in the same direction and under the same tension. Loose filaments are undesirable. Keep in mind that the X-ray beam

is only 0.5 mm or less in diameter, so every fiber contributes to the diffraction pattern.

Polymer orientation measurements are performed in transmission. Remember to use the beam stop. The collimator size should be selected that is as near as possible to the diameter of the sample. This reduces parasitic air scatter. The trade-off here is that for single filaments which are typically under 50 μm in diameter, data collection times may be prohibitively long. The compromise is to use a larger collimator and subtract a background frame collected under the same conditions in the absence of the sample. The length of time the background frame is collected can be less than that of the sample frame, but long enough to ensure that statistically reliable corrections can be made. This frame is subtracted from the original frame using FILE/LOAD with the /SCALE = -n qualifier which scales the background frame to the time of the data frame. If there is significant absorption in the polymer sample, the background frame should be scaled so that the parasitic scattering around the beam stop is reduced to near zero. For 0.3 mm or larger collimators, the 6° beam stop should be used. Otherwise, use the 4° beam stop.

5.9 Fiber Orientation

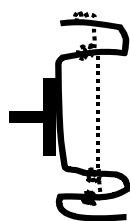


Figure 5.8 - Wire fiber holder attached to an SEM specimen mount. The dashed line is a fiber

For orientation work, the fiber should be mounted on a wire frame. These frames are readily made from paper clips. The length of the fiber should be no longer than 2 cm and the distance from the fiber to the back portion of the frame should be no longer than 1.5 cm. The goniometer head used for mounting fibers should be of the eucentric type. This allows fine adjustment of the physical fiber axis with respect to the goniometer axis. The fiber frame can be affixed with wax or clay to an aluminum SEM specimen holder (available from electron microscopy supply houses) which mounts in the goniometer head. The wax should have good adhesion properties at temperatures up to 40°C and should not undergo elastic relaxation. The physical fiber axis should be aligned vertically, either using the two-position χ stage, or with an adapter mount for the fixed χ stage. With this arrangement, a meridional reflection up to 30° can be observed with either the fixed or two-position χ stages with the detector at 6 cm. For the 1/4-cradle, this restriction is removed by plac-

ing $\chi = 0^\circ$. After setting the fiber axis vertical for both the two-position and fixed χ stage, COLLECT/GONIOMETER/FIXED AXES should be used to set $\chi = 0^\circ$. When this is done, processing the pole figure with PD = 1, the fiber axis will be vertical on the pole figure diagram. If the fiber is instead mounted at 54.74°, the χ value should not be updated. If angles > 30° must be collected on the meridian, the sample must be physically remounted so that the fiber axis is horizontal. For those measurements, χ should be updated to 90°.

For equatorial reflections, pole figure data is collected in a single frame and processed using the POLE_FIGURE/PROCESS/FIBER option. The resulting pole figure will show a rotationally symmetric data pattern. Figure 5.9 shows a data frame and (200) pole figure from a bundle of Kevlar 149 fibers.

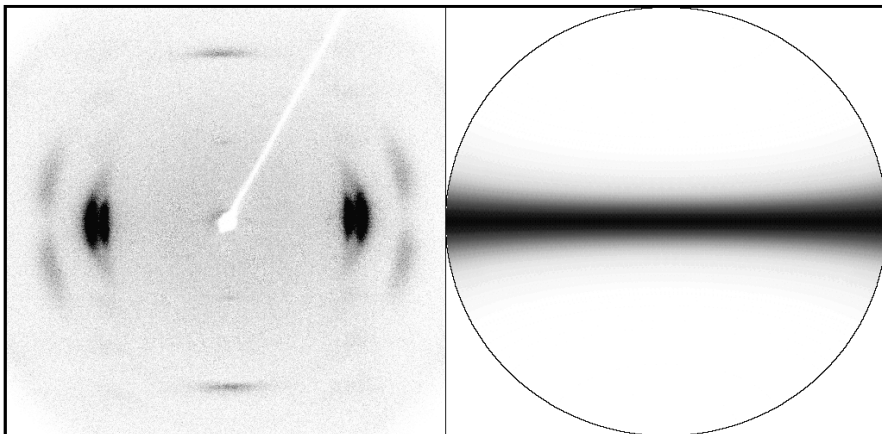


Figure 5.9 - Data frame (left) and (200) pole figure (right) from Kevlar 149 fibers

Meridional reflections are collected as follows:

1. With the physical fiber axis vertical, set $\phi = 0^\circ$ with COLLECT/GONIOMETER/UPDATE, and set $\chi = 90^\circ$ with COLLECT/GONIOMETER/FIXED AXES.
2. In SCAN/SINGLE_RUN, set $\phi = 0^\circ$. If the reflection occurs below $10^\circ 2\theta$, set $\phi = -10^\circ$.
3. Set scan axis equal 3 (the ϕ axis).
4. Set step size for 2° .
5. Collect 16 frames.
6. Process the frames using POLE_FIGURE/PROCESS without the /FIBER option.

5.10 Sheet Orientation

Polymer sheet data collection is similar to that for reflection samples. The difference is that with the detector at 6 cm, the complete Debye rings are on the detector. This reduces the number of required frames for pole figures by at least a factor of two. The preparation of the specimen is very important. For polymer films that are rigid, it is possible to hold them in place using a small alligator clip mounted to a goniometer head. If the film is not rigid, a piece is often trimmed to mount in the same frame as the fiber.

The width of the sheet should be equal to the sheet thickness, if possible; otherwise, the reflections arising from planes parallel to the surface will not be proportional in intensity to those out of plane. The total transmitted intensity is a linear function of the sample thickness, t , multiplied by an attenuation factor:

$$I_{\text{transmitted}}/I_0 = t e^{-\mu t}$$

where μ is the linear absorption coefficient of the material. Differentiating this equation, the optimal thickness of the sheet to obtain the maximum transmitted intensity is found to equal the inverse of the material's linear absorption coefficient.

The polymer sheet should be aligned similar to that of a fiber except that a machine direction should be set along the ϕ axis. Once the sheet is in place, so that the sheet normal is along the microscope axis, update $\phi = 0^\circ$ with COLLECT/GONIOMETER/UPDATE. Use POLE_FIGURE/SCHEME to plan the data collection strategy, and use POLE_FIGURE/PROCESS to obtain the pole figure. If the sheet is supported, make sure the X-ray beam does not hit the frame during rotation, otherwise an intensity of zero will be merged with a positive intensity collected at another orientation.

5.11 Near Single Crystal Thin Film Orientation

Orientation and texture are usually synonymous terms for the distribution of crystallites with respect to a sample direction. For large single crystals or single crystal wafers, orientation refers to the tilt of the crystallographic axis with respect to the sample surface. In some cases, two or more angles are necessary to define the orientation of the crystallographic axis to the sample axes. These measurements are necessary in quartz oscillators and single crystal turbine blades. The determination of these values is typically performed by Laue diffraction where the complete X-ray spectrum from a tungsten X-ray tube is used. Laue was the first X-ray diffraction technique used for characterization. It is fast and is usually used in 100% industrial inspection applications. Using characteristic radiation, several reflection centroids can be determined without a goniometer, and the orientation can be determined based on a known unit cell. Usually the sample must have a specific orientation within set tolerances. The measured diffraction pattern and orientation information obtained is compared to theoretical values or standard patterns. Diffraction analysis software usually interacts with the production line in an accept or reject mode.

For single crystal thin films on single crystal substrates, an area detector can provide a view of reciprocal space in a short period of time. Single-crystal analysis techniques can then be used to determine orientation matrices for both the film(s) and substrate. The resulting orientation matrices provide the information necessary to determine the angle between any sample direction and a crystallographic direction. This type of an analysis is faster and more descriptive than pole figures for single crystal films on single crystal substrates. In addition, if both the orientation matrix of the film and the substrate are determined, the relationship between the two cells can also be determined. This type of single crystal analysis is relatively advanced. A simpler, though less powerful approach, is available using CURSOR commands.

5.12 Semiquantitative Analysis with CURSOR Commands

CURSOR/CIRCLE is useful for examining pole figures displayed in stereographic projection because a circle represents a constant area on a sphere. This is not the case if the pole figure is displayed in polar projection. This cursor provides the total intensity, average intensity, peak-to-background ratio (I/σ) and centroids in screen coordinates and stereographic angles. It can be used to compare the intensity of a line at specific orientations. For example, to determine the intensity ratios of (111) to (200) for planes at $45^\circ \alpha$ in a drawing direction, set the cursor at $45^\circ \alpha$, $0^\circ \beta$, and compare the total intensities normalized by the (111) to (200) intensity ratio from the PDF card to account for structure factor differences. Another application would be to examine an area of 10° solid angle at the center of a pole figure and compare it to the same solid angle at $54.74^\circ \alpha$. This would give the ratio of crystallites (e.g., 1:1, 2:1) in these two directions.

CURSOR/CIRCLE can also be used to determine the tilt and twist of single crystal films. Figure 5.10 shows the (111) pole figure from an epitaxial thin film on a Si substrate. CURSOR/CIRCLE can be used to determine the α and β centroids for the film and substrate reflections. The difference in the α centroids gives the tilt of the film with respect to the substrate. The difference in the β centroids gives the twist of the film with respect to the substrate. This analysis is

valid only for cubic materials. For more general crystal classes, use the orientation matrix approach (using PEAKS/REFL_ARRAY), provided the films are near single crystal.

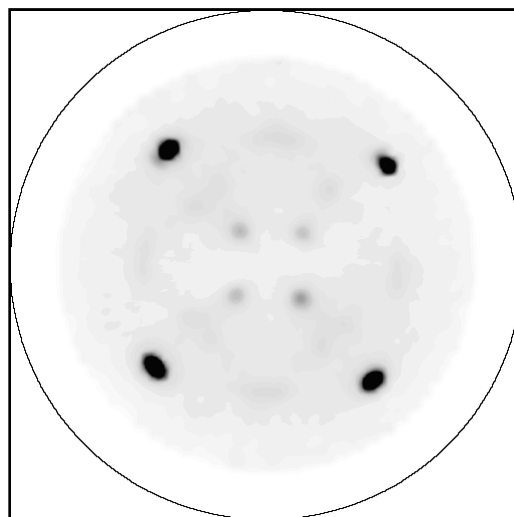


Figure 5.10 - (111) pole figure of an epitaxial thin film of Si_xGe_y deposited on a single crystal Si substrate. The larger, darker spots are from the substrate reflections

CURSOR/PIXEL gives the intensity at the intersection of the crosshairs and the values of α and β . By definition, $\alpha = 0^\circ$ at the outer edge and $\alpha = 90^\circ$ at the center of the pole figure. Conversely, $\chi = 0^\circ$ at the center and $\chi = 90^\circ$ at the outer edge of the pole figure.

CURSOR/BOX, CURSOR/CONIC, and CURSOR/VECTOR are not particularly useful for pole figure evaluation.

5.13 Preparation for ODF Analysis with popLA and ODF AT

Preferred Orientation Package—Los Alamos (popLA) performs an ODF using vector methods. The orientation space is divided up into a number of “cells” within which the ODF is assigned a constant value. A simple initial value of each cell is determined from the experimental data. The resultant pole figures from such an ODF are compared with the observed pole figures and adjustments are made to improve the match. This process is repeated until no further improvement is observed. Vector methods are best suited to ODF's which contain a few sharp features.

The second line of the popLA file contains an RM parameter which is the maximum pole figure α . This must be edited to indicate the edge of the pole figure data. The permutation parameter, IPER, must also be set according to whether the GADDS pole figure data was collected in transmission or reflection. In the transmission cases described in Figure 5.6, the IPER parameter has the value (312). In the reflection case described in Figure 5.6, the IPER parameter has the value (213).

No additional processing is required for GADDS data exported with POLE_FIGURE/TEXTUREAT for use with ODF AT.

5.14 Hermans and White-Spruiell Orientation Indices

Figure 5.11 shows the relationship between the external (physical) coordinate system of the sample and an internal (crystallographic) reference frame. The angles between the axes 1, 2 and 3 of the individual molecular units and the main sample directions x, y and z are denoted φ_{1x} , φ_{2x} , φ_{3x} ; φ_{1y} , φ_{2y} , φ_{3y} ; and φ_{1z} , φ_{2z} , φ_{3z} . In amorphous polymers there are no true crystallites, and one observes rotation around each of the molecular axes. In polymers, discrete crystallites can be observed in which a crystallographic axis coincides with at least one of the molecular axes. In addition, this crystallographic axis is usually aligned with a physical axis. As in other materials, the crystal symmetry can range from cubic to triclinic, and the standard rules concerning the position of rotation axes apply. In any case, the following Pythagorean relation must hold true:

$$\cos^2 \varphi_{1x} + \cos^2 \varphi_{1y} + \cos^2 \varphi_{1z} = 1.$$

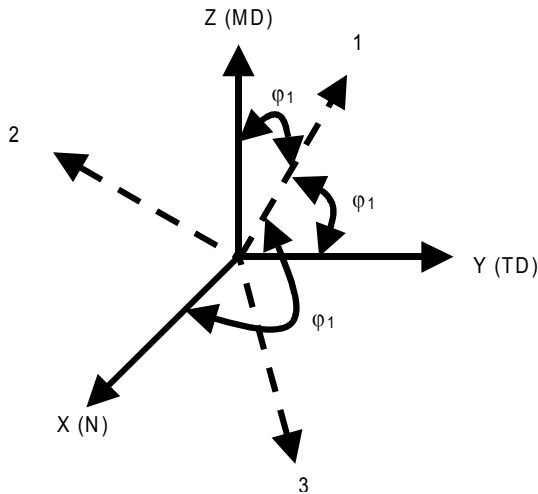


Figure 5.11 - Relationship between the external (physical) coordinate system of the sample and an internal (crystallographic) reference frame

In fibers, uniaxial orientation is the most commonly observed symmetry. If the z-axis is taken as the fiber axis, then $\cos^2 \varphi_{1x} = \cos^2 \varphi_{1y}$. Substitutions simplify the Pythagorean relation and lead to the *Hermans orientation index*:

$$f^H = \frac{1}{2} (3 \cos^2 \varphi_{1z} - 1)$$

which is an analytical representation of orientation of unit cells in a specimen based on the second moment of a specific unit cell axis (e.g., the fiber axis) with respect to a specific direction in the specimen (e.g., the machine direction).

In films and sheets, biaxial orientation is more common. White and Spruiell modified the treat-

ment for uniaxial orientation to obtain *biaxial orientation indices*:

$$f^B_z = 2 \cos^2 \varphi_{1z} + \cos^2 \varphi_{1y} - 1$$

$$f^B_y = 2 \cos^2 \varphi_{1y} + \cos^2 \varphi_{1z} - 1$$

Regardless of whether uniaxial or biaxial orientation is present, the orientation factors are usually displayed as diagrams which show the relationship between the crystallite orientation and the orientation of the sample. For the simultaneous calculation of Hermans and White-Spruiell indices, the pole figure can be submitted to POLE_FIGURE/ORIENT. A graphical representation of the orientation indices known as a *Stein triangle* is obtained using POLE_FIGURE/STEIN.

This method may be used to determine the orientation not only in polymers, but also in other fibrous or sheet-like materials. It has been used on polypropylene sheets and talc, many different types of fibers, and on films comprised of layers of different polymers. In a multilayer, the orientation of each layer can be determined as well as how each layer aligns itself with the layer below it. This experiment is done using the ω angle optimized to observe the specific layer, similar to a glancing angle experiment. Another application is the determination of the orientation of a mineral within a cut block. The machine direction in this case is the direction that the sample was cut and is not related to any observed growth pattern.

5.15 Fiber Texture Plots

X-ray diffraction can provide the orientation of a film with respect to its substrate. The technique involves collecting pole figures (Figure 5.12), which are stereographic representations of the grain orientations in three-dimensional space. The HI-STAR area detector can collect large sections of many diffraction cones simultaneously, which enables a complete range of grain orientations to be observed.

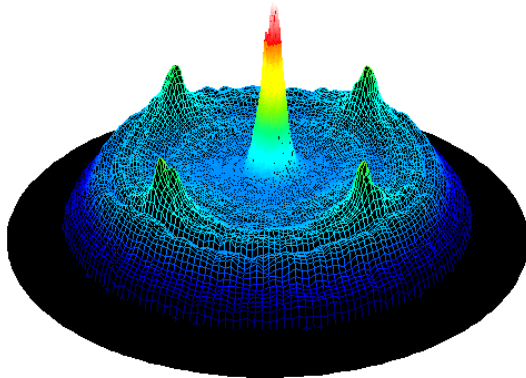


Figure 5.12 - Al (111) on Si (100) substrate

Texture strength can be quantified using Orientation Distribution Function (ODF) software. At least three pole figures are required for ODF analysis, which may lead to undesirably long data collection times. In addition, many ODF programs have difficulty handling sharply textured materials, which is the case with many electronic thin films. Since most thin films have symmetrical fiber or near fiber texture, in which the orientation distribution possesses rational symmetry about the substrate normal, the texture strength can be quantitatively represented from a single pole figure as a Fiber Texture Plot (FTP, Figure 5.13).

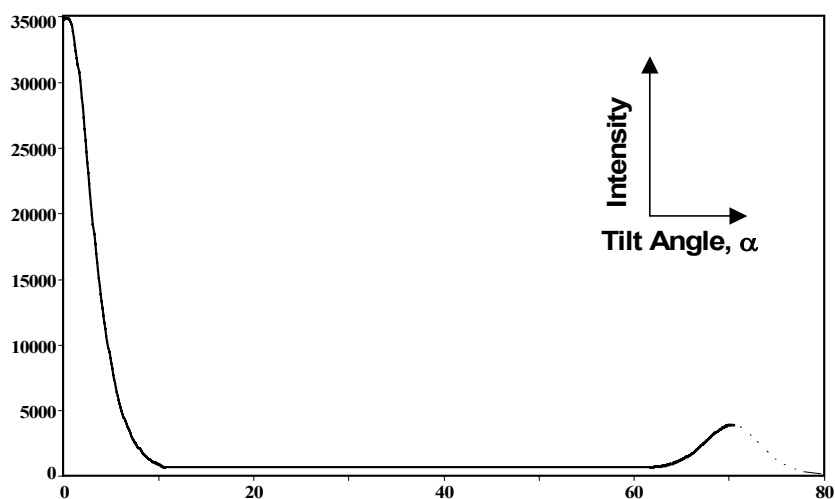


Figure 5.13 - Fiber texture plot of Al

The FTP is essentially a slice integration from the center ($\alpha = 0^\circ$) to the outer edge ($\alpha = 90^\circ$) of the pole figure. An $\alpha = 0^\circ$ represents reciprocal lattice planes oriented parallel to the substrate, while an $\alpha = 90^\circ$ represents reciprocal lattice planes oriented perpendicular to the substrate (see Figure 5.14). In reality, measurement of orientation perpendicular to the substrate requires X-ray diffraction in transmission rather than reflection, so most FTP representations extend from $\alpha = 0^\circ$ to $\alpha = 85^\circ$. The example shows the Al (111) planes parallel to the Si (100) substrate.

Since Al is cubic, the angle between the (111) plane and the other $\langle 111 \rangle$ family members is 70.5° , which is verified in the FTP by the second intensity peak. It is important to remember that the crystallographic system of the film dictates where intensities are expected to be observed in FTPs. The reciprocal and direct (real) space crystallographic directions are only coincident in cubic systems. For example, in Ti (which has a hexagonal lattice), the (100) reciprocal lattice plane is perpendicular to the [210] direction, not to the [100] direction.

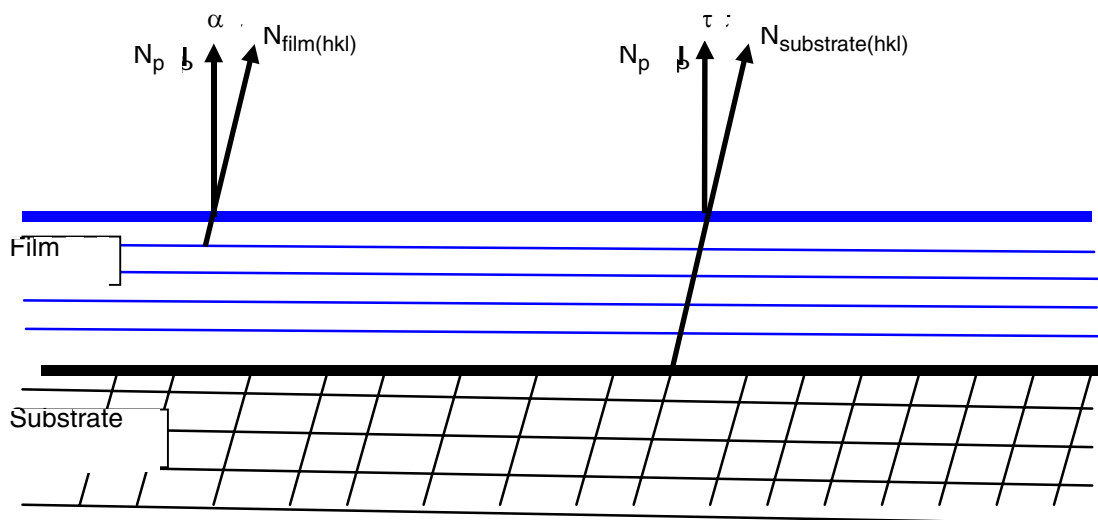


Figure 5.14 - Angle between the substrate normal and the normal to a given diffraction plane

The shape of the FTP curve provides a simple qualitative picture of the fiber or near fiber texture. The area under the FTP can be integrated to obtain a quantitative representation of the texture strength, from which pole spread and/or pole tilt can be quantified. With appropriate background correction of the measured raw data, the linear background under the FTP can be used to quantify the percent random distribution of the grains. Texture quantification is reported as the volume fraction or half width, ω_{90} and ω_{50} , where ω represents the half angle (in degrees) in which a specified fraction of the intensity (90%, 50%) is contained. For example, the half angle containing 50% of the (111) grain orientations is ω_{50} . From this definition, the smaller the value for ω_{50} , the narrower the (111) grain distribution (the smaller the pole spread) and the stronger the texture. For the FTP in Figure 5.13, the reported ω values representing the pole spread and texture strength are $\omega_{90} = 3.2^\circ$ and $\omega_{50} = 0.8^\circ$, with 4% randomness.

The value τ in Figure 5.14 represents the angle between the substrate normal and the normal to a given diffraction plane. It is sometimes called the “off-cut” or “mismatch” angle. Its value is not important for the determination of α , but is required to determine the relationship between the film and substrate orientations.

Because the FTP is essentially a slice of a complete pole figure, some of the information available in a complete set of pole figures is absent.

For example, if the pole is not completely symmetric about the perfect fiber normal, which can occur if the pole is tilted or spread in one direction, the slice selected may misrepresent the true texture. For this reason, it is often useful to create FTPs from both one slice (of about 10°) and from a full 360° pole figure integration. Otherwise, the more general ODF analysis is required.

5.16 References

1. L. E. Alexander, *X-Ray Diffraction Methods in Polymer Science* (Krieger Publishing Company, Malabar, Florida, 1985).
2. C. F. Blake, "On the Factors Affecting the Reflection Intensities by the Several Methods of X-Ray Analysis of Crystal Systems," *Rev. Mod. Phys.* 5(3), 169-202 (1933).
3. H.-J. Bunge, *Texture Analysis in Materials Science* (Butterworths, Boston, 1982).
4. H.-J. Bunge, ed., *Experimental Techniques of Texture Analysis* (DCM Informationsgesellschaft, Germany, 1986).
5. B. D. Cullity, *Elements of X-ray Diffraction* (Addison-Wesley, New York, 1978).
6. C. R. Desper, and R. S. Stein, "Measurement of Pole Figures and Orientation Functions for Polyethylene Films Prepared by Unidirectional and Oriented Crystallization," *J. Appl. Phys.* 37(11), 3990-4002 (1966).
7. *International Tables for X-ray Crystallography*, Vol. II (Kynoch Press, Birmingham, 1967).
8. D. B. Knorr, H. Weiland, and J. A. Szpunar, "Applying Texture Analysis to Materials Engineering Problems," *J. Materials* 46(9), 32-36 (1994).
9. D. B. Knorr, and J. A. Szpunar, "Applications of Texture in Thin Films," *J. Materials* 46(9) 42-47 (1994).
10. M. Lorenz, and K. C. Holmes, "Computer Processing and Analysis of X-ray Fibre Diffraction Data," *J. Appl. Cryst.* 26, 82-91 (1993).
11. D. E. Sands, *Vectors and Tensors in Crystallography* (Addison-Wesley, New York, 1982).
12. J. L. White and J. E. Spruiell, "Specification of Biaxial Orientation in Amorphous and Crystalline Polymers," *Polym. Eng. Sci.* 21(13), 859-868 (1981).
13. Z. W. Wilchinsky, "Recent Developments in the Measurement of Orientation in Polymers by X-ray Diffraction," *Adv. X-ray Anal.* 6, 231-241 (1962).
14. H.J. Bunge, *Cesling, Advances and Applications of Quantitative Texture Analysis*, Clausthal, 1989.

6. Residual Stress

The GADDS system has very strong residual stress measurement capability. The two-dimensional (2D) detector and laser sample alignment system give GADDS advantages over other instruments in dealing with highly textured materials, large grain size, small sample area, weak diffraction, stress mapping, and biaxial stress tensor. This feature along with phase analysis, texture, and other functions will make GADDS more desirable to users in semiconductor, electronics, and auto industries.

GADDS can measure residual stress (strain) using one of two approaches, conventional or two dimensional. These are discussed in detail in the following sections.

6.1 Principle of Stress Measurement

6.1.1 Theory of Conventional Method

In the conventional approach, GADDS data on each frame is reduced by integration to a one-dimensional diffraction profile, so that the area detector measures stress in the same way as a linear position-sensitive detector (PSD). This approach involves collecting data with GADDS and evaluating stress using DIFFRAC^{plus} STRESS software.

The fundamental equation used for conventional stress measurement is given as [1]

$$\varepsilon_{\phi\psi} = \varepsilon_{11} \cos^2 \phi \sin^2 \psi + \varepsilon_{12} \sin 2\phi \sin^2 \psi + \varepsilon_{22} \sin^2 \phi \sin^2 \psi + \varepsilon_{13} \cos \phi \sin^2 \psi + \varepsilon_{23} \sin \phi \sin^2 \psi + \varepsilon_{33} \cos^2 \psi \quad (6-1)$$

where $\varepsilon_{\phi\psi}$ is the measured strain in the orientation defined by ϕ and ψ angles and ε_{11} , ε_{12} , ε_{22} , ε_{13} , ε_{23} , and ε_{33} are strain tensor components in the sample coordinates $S_1S_2S_3$ as shown in Figure 6.1(a).

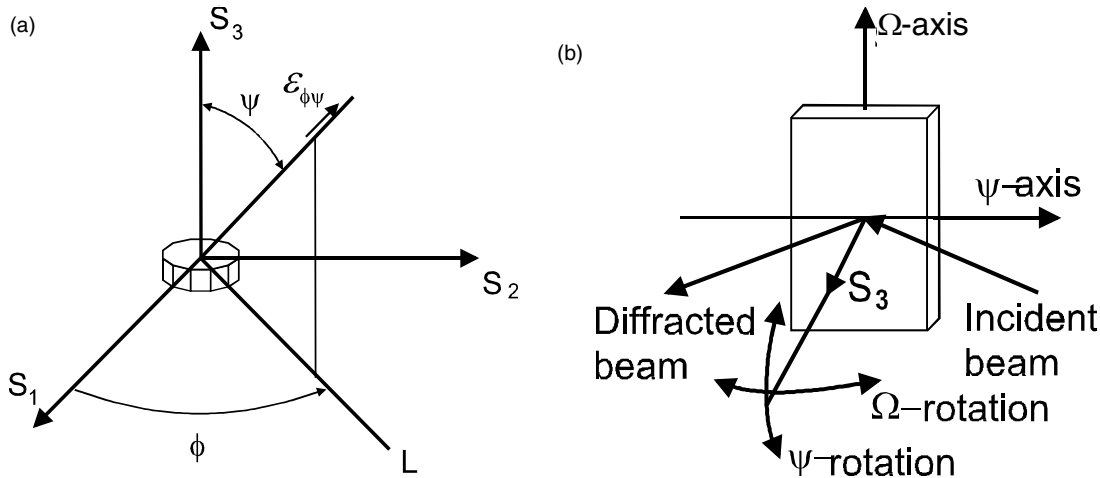


Figure 6.1 - Configurations for conventional stress measurement method. (a) The relation between the measured strain $\varepsilon_{\phi\psi}$ and the sample coordinates $S_1S_2S_3$. (b) Two kinds of ψ -tilt.

In the equation (6-1), one 2θ shift value (d-spacing change) is considered at each sample orientation (ψ , ϕ). This is suitable to the stress measurement with point detectors or one-dimensional position-sensitive detectors. In the conventional stress measurement method, the ψ -tilt is achieved by two kinds of diffractometer configurations, shown in Figure 6.1(b). One is

Ω -diffractometer (also called iso-inclination) configuration, in which the ψ -rotation axis is perpendicular to the diffractometer plane that contains the incident and diffracted beams. The other is ψ -diffractometer (or side-inclination) configuration, in which the ψ -rotation axis is in the diffractometer plane. The $\sin 2\psi$ method derived from equation (6-1) is most often used to calculate residual stress on the sample surface in ϕ direction, σ_ϕ . The details are described in [1,2] and the DIFFRAC^{plus} STRESS software manual.

6.1.2 Theory and Algorithm of 2D Method

The two-dimensional approach has been developed to evaluate stress from 2D diffraction data. The principle of the 2D method is to use all the data points on diffraction rings to calculate stresses, getting better measurement results with less data collection time [3-5].

The diffracted beams from a polycrystalline sample form a series of cones corresponding to each lattice plane, as is shown in Figure 6.2(a). The incident X-ray beam lies along the rotation axis of the cones. The apex angles of the cones are determined by the 2θ values given by the Bragg equation. The apex angles are twice the 2θ values for forward reflection ($2\theta < 90^\circ$) and twice the values of $180^\circ - 2\theta$ for backward reflection ($2\theta > 90^\circ$). The γ angle is the azimuthal angle from origin at the 6 o'clock direction with rotation axis on the incident X-ray beam in the opposite direction. The γ angle defines each diffracted beam on the diffraction cone. The γ angle here is not to be confused with the sample rotation γ angle in 4-circle goniometer convention. The diffraction cones from an unstressed polycrystalline sample are regular cones in which 2θ is independent of γ and $2\theta = 2\theta_0$. Introducing a stress into the sample distorts the diffraction cone shape so that it is no longer a regular cone. The 2θ becomes a function of γ , $2\theta = 2\theta(\gamma)$, this function is uniquely determined by the stress tensor and the sample orientation.

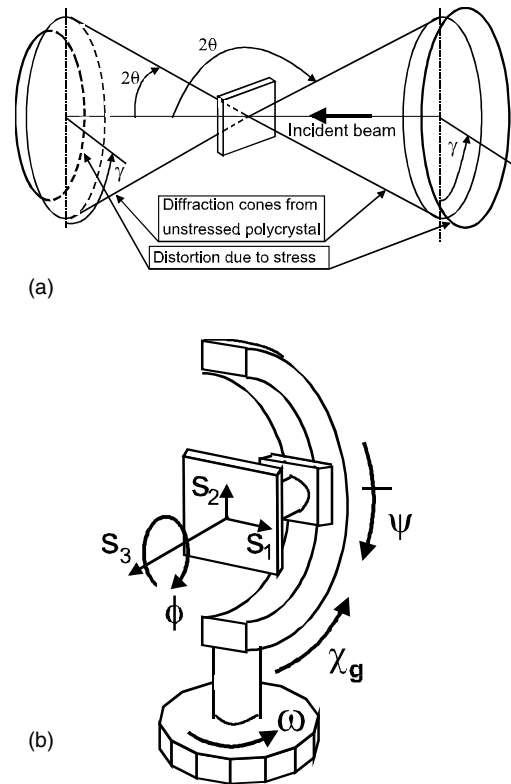


Figure 6.2 - (a) The diffraction cones from an unstressed polycrystalline sample and the diffraction cone distortion due to stresses. (b) Sample orientation in terms of ω , ψ and ϕ angles

Figure 6.2(b) shows the sample orientation angles ω , ψ , and ϕ . $S_1S_2S_3$ are sample coordinates with S_1S_2 on the sample surface plane and S_3 as surface normal. At $\omega = \psi = \phi = 0$, S_1 is in the opposite direction of the incident X-ray beam, and S_2 points up and overlaps with ω -axis. The ω -axis is fixed on the laboratory coordinates. ψ is a rotation above a horizontal axis and ϕ is a left-hand sample rotation about its normal S_3 . ψ -axis varies with ω rotation and ϕ axis varies with ω and ψ rotation. ψ and χ_g have the same axis but different starting position and rotation direction, and $\chi_g = 90^\circ - \psi$.

The surface of the area detector can be considered a plane intersecting with the diffraction cones. Figure 6.3 shows the diffraction data collected on the area detector. α is the detector swing angle. When imaged on-axis ($\alpha = 0^\circ$), the conic sections appear as circles. When the detector is at off-axis position ($\alpha \neq 0^\circ$), the conic section may be an ellipse, parabola, or hyperbola. For convenience, all kinds of conic sections will be referred to as diffraction rings hereafter in this paper. All diffraction rings collected with a single exposure will be referred to as frames. The area detector image (frame) is stored as intensity values on a 1024x1024 pixel grid. The 2θ and γ values on each pixel are also given by GADDS. The diffraction profile on a particular γ line can be calculated from the 2D image by a γ integration within a given χ range. The peak position at each γ angle can be deter-

mined from the diffraction profile by one of the many available peak-fitting methods. The number of data points from one ring depends on the total γ range and γ integration steps. The diffraction cone distortion due to stresses is recorded as a function $2\theta(\gamma)$. All the information about the sample orientation, diffraction cone orientation, and diffraction cone distortion leads to the resolution of the stress or strain:

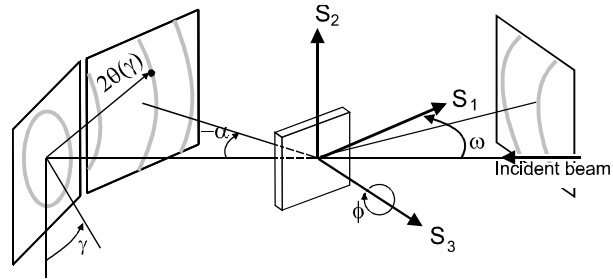


Figure 6.3 - The diffraction rings collected on area detectors at on-axis or off-axis positions

In the sample coordinate system $S_1S_2S_3$, the strain tensor is

$$\begin{bmatrix} \varepsilon_{11} & \varepsilon_{12} & \varepsilon_{13} \\ \varepsilon_{21} & \varepsilon_{22} & \varepsilon_{23} \\ \varepsilon_{31} & \varepsilon_{32} & \varepsilon_{33} \end{bmatrix}$$

where $\varepsilon_{12} = \varepsilon_{21}$, $\varepsilon_{13} = \varepsilon_{31}$, and $\varepsilon_{23} = \varepsilon_{32}$.

The strain tensor in the sample coordinates, the sample orientation (ω , ψ , ϕ), and the diffraction data (γ , 2θ) are related by the following expression.

$$f_{11}\varepsilon_{11} + f_{12}\varepsilon_{12} + f_{22}\varepsilon_{22} + f_{13}\varepsilon_{13} + f_{23}\varepsilon_{23} + f_{33}\varepsilon_{33} = \ln \frac{\sin \theta_0}{\sin \theta} \quad (6-2)$$

where strain coefficients f_{ij} can be calculated from simplified equations listed in Table 6.1. $\ln(\sin \theta_0 / \sin \theta)$ determines the diffraction cone distortion at the particular (γ , 2θ) position.

Table 6.1 – Equations for Calculation of Strain Coefficients f_{ij}

Strain Coefficients:	f_{11}	f_{12}	f_{22}	f_{13}	f_{23}	f_{33}
=	h_1^2	$2h_1h$	h_2^2	$2h_1h$	$2h_2h$	h_3^2
$a = \sin \theta \cos \omega + \sin \chi \cos \theta \sin \omega$ $b = -\cos \gamma \cos \theta$ $c = \sin \theta \sin \omega - \sin \gamma \cos \theta \cos \omega$ $h_1 = a \cos \phi - b \cos \psi \sin \phi + c \sin \psi \sin \phi$ $h_2 = a \sin \phi + b \cos \psi \cos \phi - c \sin \psi \cos \phi$ $h_3 = b \sin \psi + c \cos \psi$						
In GADDs, χ_g is used instead of ψ , so use $\psi = 90^\circ - \chi_g$ in the equation. Use ω , ψ and ϕ angles in the equation even if the rotation is not available. For example: for fixed chi holder, use $\chi_g = 54.74^\circ$ or $\psi = 35.26^\circ$ in the equation; for XYZ stage, ψ or ϕ rotation are not available, use 0 in the equation.						

$\{h_1, h_2, h_3\}$ are components of the unit vector of the diffraction vector \mathbf{H}_{hkl} expressed in the sample coordinates. Equation (6-2) is the fundamental equation for strain and stress measurement by diffraction using 2D detectors, which gives a direct relation between the diffraction cone distortion and strain tensor. Since it is a linear equation with six unknowns, in principle, the strain tensor can be solved with six (γ , 2θ) data points. The least squares method can be used to solve the strain or stress tensor with very high

accuracy and low statistics error. For isotropic materials, there are only two independent elastic constants, Young's modulus E and Poisson's ratio ν or the macroscopic elastic constants $\frac{1}{2}S_2 = (1 + \nu)/E$ and $S_1 = -\nu/E$. Then we have

$$P_{11}\sigma_{11} + P_{12}\sigma_{12} + P_{13}\sigma_{13} + P_{22}\sigma_{22} + P_{23}\sigma_{23} + P_{33}\sigma_{33} = \ln \frac{\sin \theta_0}{\sin \theta} \quad (6-3)$$

where

$$P_{ij} = \begin{cases} \left(\frac{1}{E} \right) ((1 + \nu)f_{ij} - \nu) = \left(\frac{1}{2}S_2 f_{ij} + S_1 \right) & \text{if } i = j \\ \left(\frac{1}{E} \right) ((1 + \nu)f_{ij}) = \frac{1}{2}(S_2 f_{ij}) & \text{if } i \neq j \end{cases}$$

The anisotropy correction can also be included in the X-ray elastic constants $\frac{1}{2}S_2(hkl)$ and $S_1(hkl)$ to replace the macroscopic elastic constants $\frac{1}{2}S_2$ and S_1 . The equations for calculating X-ray elastic constants are:

$$\frac{1}{2}S_2(hkl) = \frac{1}{2}S_2[1 + 3(0.2 - \Gamma(hkl)\Delta)]$$

$$S_1(hkl) = S_1 - \frac{1}{2}S_2[0.2 - \Gamma(hkl)\Delta]$$

$$\Gamma(hkl) = \frac{h^2k^2 + k^2l^2 + l^2h^2}{(h^2 + k^2 + l^2)^2}$$

$$\Delta = \frac{5(A_{RX} - 1)}{3 + 2A_{RX}} \quad (6-4)$$

The factor of anisotropy (A_{RX}) is a measure for the elastic anisotropy of a material. Values of A_{RX} for the most important cubic materials are given in the following table, additional values may be taken from literature.

Materials	A_{RX}
Body-centered cubic (bcc) Fe-base materials	1.49
Face-centered cubic (fcc) Fe-base materials	1.72
Face-centered cubic (fcc) Cu-base materials	1.09
Ni-base materials (fcc)	1.52
Al-base materials (fcc)	1.65

The values of A_{RX} have to be given by the user in the calculation settings dialog. For most commonly measured biaxial stress, an approximate $2\theta_0$ will introduce a pseudo hydrostatic stress component, σ_{ph} . The equation becomes:

$$p_{11}\sigma_{11} + p_{12}\sigma_{12} + p_{22}\sigma_{22} + \frac{1 - 2\nu}{E}\sigma_{ph} = \ln \frac{\sin \theta_0}{\sin \theta} \quad (6-5)$$

Considering the coefficient of σ_{ph} as $(1-2\nu)/E$, σ_{11} , σ_{12} , σ_{22} , and σ_{ph} can be solved by least squares method. When doing ω scan only, σ_{11} is equivalent to the conventional in iso-inclination mode, or when doing ψ (or χ_g) scan only, σ_{22} is equivalent to the conventional in side inclination mode.

For biaxial stress with shear, where $\sigma_{13} \neq 0$ and $\sigma_{23} \neq 0$ we have $P_{11}\sigma_{11} + P_{12}\sigma_{12} + P_{22}\sigma_{22} + P_{13}\sigma_{13} + P_{23}\sigma_{23} + P_{ph}\sigma_{ph} =$
 $\ln \frac{\sin \theta_0}{\sin \theta}$ (6-6)

The biaxial stress state corresponds to the straight line of the $d\text{-}\sin^2\psi$ plot. And the biaxial stress with shear is the case when there is a split between the data points in $+\psi$ side and $-\psi$ side. The general normal stress (σ_ϕ) and shear stress (τ_ϕ) at any arbitrary given ϕ angle are given by

$$\sigma_\phi = \sigma_{11}\cos^2\phi + \sigma_{12}\sin 2\phi + \sigma_{22}\sin^2\phi$$

$$\tau_\phi = \sigma_{13}\cos\phi + \sigma_{23}\sin\phi \quad (6-7)$$

6.1.3 Relationship Between Conventional Theory and 2D Theory

In order to find the relationship between the conventional theory and the new 2D theory, we first compare the configurations used for data collection in both cases. The conventional diffraction profile is collected with a point detector scanning in the diffractometer plane or a position-sensitive detector mounted in the diffractometer plane. The 2D diffraction data consists of diffracted X-ray intensity distribution on the detector plane. The intensity distribution along any line defined by a fixed γ (χ may be used alternatively) is a diffraction profile analogous to the data collected with a conventional diffractometer. Figure 6.4 shows the relation between a 2D detector and a conventional detector. The diffraction profiles at $\gamma=90^\circ$ and $\gamma=-90^\circ(=270^\circ)$ on the 2D detector are equivalent to the diffraction profiles collected in the conventional diffractometer plane. Therefore, you can use diffraction profiles at $\gamma=90^\circ$ and $\gamma=-90^\circ$ on a 2D detector to imitate a conventional diffractometer.

In theory, it has been proved that the conventional fundamental equation is a special case of the 2D fundamental equation. In the same way, a conventional detector can be considered as a limited part of a 2D detector. Depending on the specific condition, you can choose either theory for stress measurement when a 2D detector is used. If the conventional theory is used, you have to get a diffraction profile at $\gamma=90^\circ$ or

$\gamma = -90^\circ$, this is normally done by integrating the data in a limited γ range. The disadvantage is that only part of the diffraction ring is used for stress calculation. When the new 2D theory is used, all parts of the diffraction ring can be used for stress calculation.

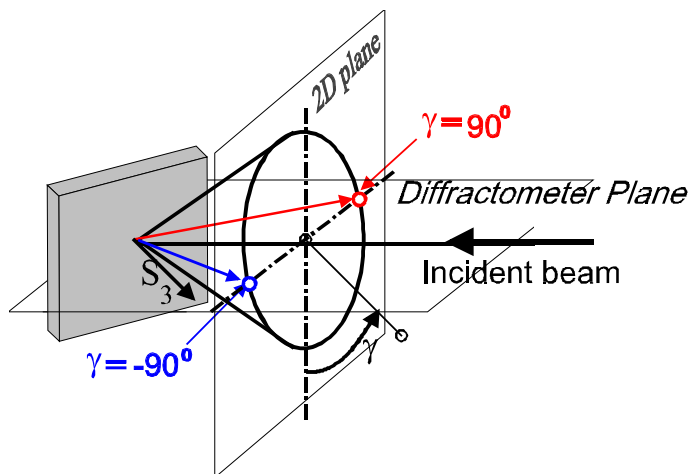


Figure 6.4 - Relationship between diffraction ring on 2D detectors and 1D detector on diffractometer plane

6.1.4 Advantages of Using 2D Detectors

There are many advantages of using 2D detectors for residual stress measurement, no matter if the conventional “ $\sin^2 \psi$ ” theory or the new 2D theory is used. The experiments have shown that advantages to using 2D detectors for stress measurement include, but are not limited to, high sensitivity, high measurement speed, high accuracy, and virtual oscillation for large crystals and textured samples.

In the case of materials with large grain size or microdiffraction with a small X-ray beam size, the diffraction profiles are distorted due to poor counting statistics. To solve this problem with conventional detectors, some kind of sample oscillations, either translation oscillations or angular oscillations, are used to bring more crystallites into diffraction condition. In another words, the purpose of oscillations is to bring more crystallites in the condition such that the normal of the diffracting crystal plane coincides with the instrument diffraction vector. For 2D detectors, when the γ -integration is used to generate the diffraction profile, we actually integrate the data collected in a range of various diffraction vectors. The angle between two extreme diffraction vectors is equivalent to the oscillation angle in a so-called ψ -oscillation. Therefore, we may call this effect “virtual oscillation.” Figure 6.5 shows the relation between the γ -integration range, $\Delta\gamma$, and the virtual oscillation angle, $\Delta\psi$. The 2θ value of the γ -integrated profile is an

average over the Debye ring defined by the γ -range. The average effect is over a region of orientation distribution, rather than a volume distribution.

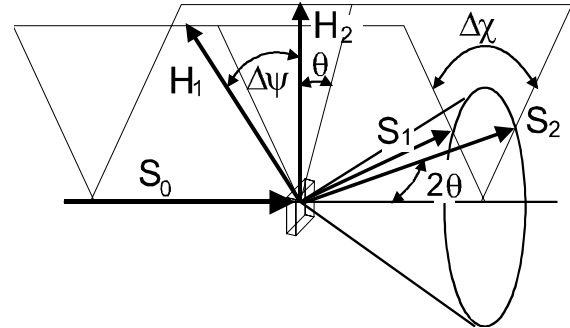
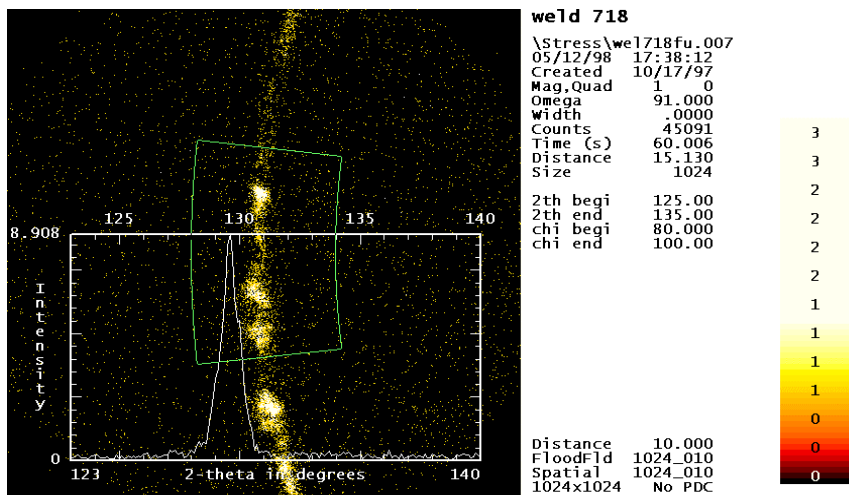


Figure 6.5 - The relationship between the γ -integration range, $\Delta\gamma$, and the virtual oscillation angle $\Delta\psi$

The virtual oscillation angle $\Delta\psi$ can be calculated from the integration range $\Delta\chi$ and Bragg angle θ ,

$$\Delta\psi = 2 \arcsin[\cos\theta \sin((\Delta\gamma)/2)] \quad (6-7)$$

For example, Figure 6.6 is a frame taken from a stainless steel with large grain size. If we integrate from $\chi=80^\circ$ to 100° , $\Delta\chi=20^\circ$, $\theta \approx 64^\circ$, the virtual oscillation angle $\Delta\psi = 8.7^\circ$. In the conventional oscillation, mechanical movement may results in some sample position error. Since there is no actual physical movement of the sample stage during data collection, the virtual oscillation has no such problem.



1,2,3,4=Select edge; M=Move; ENTER,L button=Integrate; ESC,O buttons=Quit

Figure 6.6 - A diffraction frame taken from a stainless steel. The virtual oscillation by γ -integration over $\Delta\gamma = 20^\circ$ gives a smooth diffraction profile

When the 2D method is used for stress measurement, the virtual oscillation effect is further enhanced due to the larger γ range. It is more important that the smearing effect, caused by γ -

integration in the conventional method, can be minimized by using the 2D method. In the conventional method, the γ -integrated profiles are treated as if the data were collected within the diffractometer plane ($\gamma=90^\circ$). While in the 2D method, the data points along the diffraction ring are treated at their exact γ values.

The diffraction frames collected with a 2D detector contain both stress and texture information. Two functions can be derived from the diffraction ring. One is the peak position as a function of γ , $2\theta = 2\theta(\gamma)$, which is uniquely determined by the stress tensor and the sample orientation. Another is the integrated intensity as a function of γ , $I = I(\gamma)$, which is determined by the sample texture. Figure 6.7 shows four frames collected from samples with no texture, weak texture, strong texture, and very strong texture. For the case with very strong texture, the conventional diffractometer using a scanning point detector or PSD will miss the diffraction ring, so as not to be

able to measure the diffraction peak. For mild texture, the virtual oscillation can be used for the stress calculation. For strong texture, the diffraction profiles integrated over a large $\Delta\gamma$ may not accurately represent the angular position of measurement. In this case, the new 2D method should be used for stress calculation from the diffraction profiles generated at various γ angles with a relatively small $\Delta\gamma$. Since the diffraction data includes both stress and texture information, 2D detectors also make it possible to measure stress and texture simultaneously. This is necessary for corrections on the elastic anisotropy caused by texture.

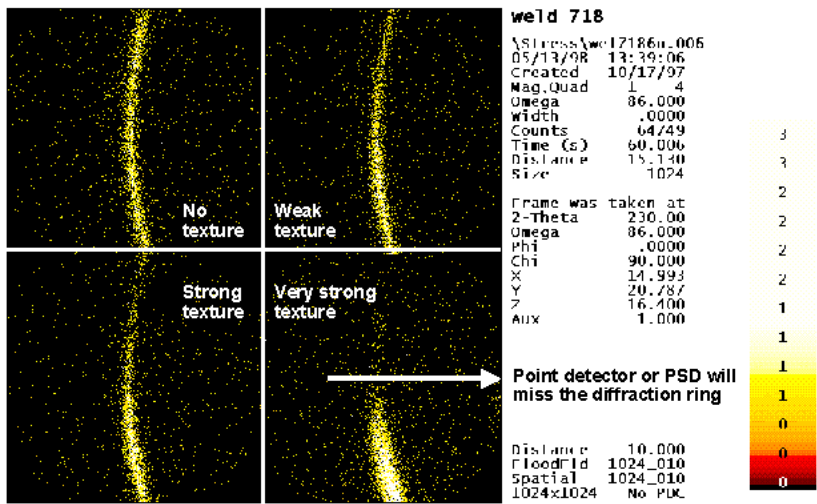


Figure 6.7 - Frames collected from samples with various degrees of texture, from random powder to very strong texture. With the very strong textured sample, a conventional diffractometer may miss the diffraction ring

6.1.5 Parameters

The parameters required for X-ray stress determination are crystal lattice parameter, d-spacing, Miller index, X-ray wavelength (target material), non-stress two-theta $2\theta_0$, Young's modulus E , Poisson's ratio ν and anisotropic factor A_{RX} . Among these parameters, the most important parameters are Young's modulus E and Poisson's ratio ν . In principle, stress and strain values can be determined from any measured diffraction rings in either transmission mode or reflection mode using the 2D method with given E and ν . In order to have a higher angular resolution and enough sample rotation range, diffraction rings with $2\theta_0$ in the range of 110° to 160° are preferred. Table 6.2 lists the parameters for most commonly used materials. These parameters are supplied only for your convenience. Since the parameters, especially E and ν , are different with different material conditions, different experimental methods, or even different theoretical assumptions, you are encouraged to determine the parameters based on your experience and sources.

Table 6.2 – The parameters of commonly used materials for stress measurement

Materials	a (/c)	$\langle d_{hkl} \rangle$	(HKL)	Target	$2\theta_0$	E	n	A_{RX}
Parameter	Å	Å			degree	MPa		
Ferritic and martensitic steel (bcc)	2.866	1.170	211	Cr	156.0	210000	0.280	1.49
		1.013	220	Co	124.1			
Austenitic Steel (fcc)	3.571	1.263	220	Cr	130.2	180000	0.3	1.72
		1.031	222	Co	120.5			
		0.798	420	Cu	149.8			
Aluminum (fcc)	4.049	1.221	311	Cr	139.5	70600	0.345	1.65
		0.929	331	Co	148.7			
		0.826	422	Cu	137.7			
Copper (fcc)	3.615	1.278	220	Cr	127.3	129800	0.343	1.09
		1.044	222	Co	118.1			
		0.829	331	Cu	136.7			
α-Brass (fcc)	3.680	1.301	220	Cr	123.4	100600	0.350	
		0.920	400	Co	153.2			
		0.823	420	Cu	139.1			
β-Brass (bcc)	2.945	1.202	211	Cr	144.6	74000	0.290	
		0.930	310	Co	146.4			
		0.850	222	Cu	130.1			
Chromium (bcc)	2.884	1.177	211	Cr	153.0	279000	0.210	
		1.020	220	Co	122.7			
		0.912	310	Cu	115.3			
Nickel (fcc)	3.529	1.248	220	Cr	133.7	199500	0.312	1.52
		1.019	222	Co	122.9			
		0.810	331	Cu	145.0			

Materials	a (/c)	<d _{hkl} >	(HKL)	Target	2 θ_0	E	n	A _{RX}
Parameter	Å	Å			degree	MPa		
Titanium (α -hcp)	2.951 /4.686	1.247	112	Cr	133.3	120200	0.361	
		0.918	114	Co	154.6			
		0.821	213	Cu	139.5			
Manganese (hcp)	3.210 /5.210	1.366	112	Cr	113.9	44700	0.291	
		0.976	105	Co	133.1			
		0.899	213	Cu	118.0			
Molybdenum (bcc)	3.147	1.285	211	Cr	126.0	324800	0.293	
		0.995	310	Co	128.0			
		0.841	321	Cu	132.6			
Niobium (bcc)	3.307	1.348	211	Cr	116.3	104900	0.397	
		1.045	310	Co	117.7			
		0.884	321	Cu	121.2			
Silver (fcc)	4.086	1.231	311	Cr	136.9	82700	0.367	
		0.938	331	Co	145.2			
		0.834	422	Cu	134.9			
Gold (fcc)	4.079	1.230	311	Cr	137.1	78000	0.440	
		0.936	331	Co	145.8			
		0.833	422	Cu	135.4			
Tungsten (bcc)	3.165	1.292	211	Cr	124.9	411000	0.28	
		0.914	222	Co	156.8			
		0.791	400	Cu	155.0			

6.1.6 GADDS System Requirements

The conventional method requires that the sample surface normally stay within the diffractometer plane during data collection scanning. A two-position chi stage at $\psi=0^\circ$ ($\chi_g=90^\circ$) position, or an XYZ stage or a 1/4-cradle at $\psi=0^\circ$ ($\chi_g=90^\circ$) position can satisfy this requirement. The new 2D stress method will work for any of the current sample stages: fixed-chi, two-position chi, 1/4-circle cradle, and XYZ stage. The laser sample alignment system is highly recommended for residual stress measurement. XYZ stage is necessary for stress mapping function. The 1/4-circle Eulerian Cradle or similar kind stages with all rotations (ω , ψ , ϕ) and translation (X,Y,Z), can dramatically increase GADDS stress tensor capability.

One example is to measure residual stress of a steel sample using the GADDS Microdiffraction system with Cr-K α radiation. The configuration is shown in Figure 6.8. The XYZ stage can be replaced by a two-position stage if stress tensor measurement is desired. The detector position can be set to an appropriate value depending on the diffraction peak position. For most ferrous alloys (steels), (211) peak at approximately 156° $2\theta_0$ is used. The detector is set at $D=15$ cm and highest swing angle (-143°). The ψ -tilt is achieved by ω rotation. The relation between ω and ψ -tilt is given by

$$\omega = 180^\circ - \psi - \theta_0 \quad (6-9)$$

For example, for most steel with bcc (bct) crystal structure, $2\theta_0 \cong 156^\circ$, the neutral ω position is 102° . If you want to set a stress data collection from $\psi = 45^\circ$ to -45° with 15° steps, you would have to set ω step scan from 57° to 147° with 15° steps.

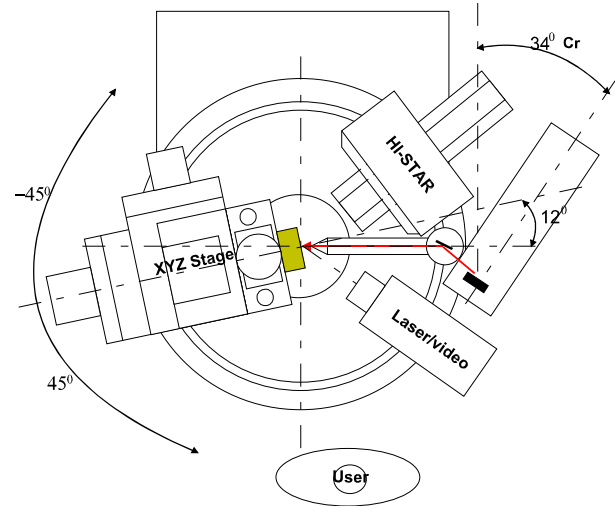


Figure 6.8 - The stress measurement configuration of GADDS Microdiffraction System

6.1.7 Data Collection Strategy

X-ray diffraction measures stress by measuring the d-spacing change caused by the stress. The diffraction vector is in the normal direction of the measured crystalline planes. It is not always possible to have the diffraction vector on the desired measurement direction. In the reflection mode X-ray diffraction, it is easy to have the diffraction vector normal to the sample surface, but impossible to have the vector on the surface plane. The stress on the surface plane, or biaxial stress, is calculated by elasticity theory. The final stress result can be considered as an extrapolation from the measured values. So that, in the conventional $\sin^2\psi$ method, several ψ -tilt angles are required, typically from -45° to $+45^\circ$. The same is true with an XRD² system. The diffraction vectors corresponding to the data scan can be projected in a 2D plot in the

same way as the pole density distribution in a pole figure.

The GADDS software has a '2D Scheme' function, which simulates the diffraction vectors distribution relative to the sample orientation S_1 and S_2 . The data scan strategy can be simulated to estimate the outcome from the stress calculation. Figure 6.9 shows the input parameters for 2D scheme. 'Stress Peak' is the approximate value of the stress-free 2θ , '2-theta' is the detector position, 'Omega', 'Phi' and 'Chi' are the goniometer angles, 'Distance' is the sample-to-detector distance, '#frames' is the total number of frames collected in the data scan, 'Scan axis' can be set to '2-Omega', '3-Phi' and '4-Chi', and 'Frame width' is the scan step. The parameters in Figure 6.9 are for a (211) peak of steel sample using Cr radiation.

Options for Analyze Stress Scheme 2D

Output file: \$null

☒ Pre-clear [Y/N] Stress Peak: 156.0 deg

Scan Parameters

2-theta: -143.0 deg Omega: 57 deg Phi: 0.0 deg Chi: 90.0 deg

Distance: 15.0 cm # frames: 7 Scan axis #: 2 Omega Frame width: 15

OK Cancel

Figure 6.9 - The input menu of the 2D scheme function used to plan the stress data collection strategy

The 2D scheme plot from the parameters in Figure 6.9 is shown in Figure 6.10. The diffraction vectors are clustered along the sample axis S_1 . So that the data collected with the above setting will yield the best stress result for σ_{11} . If we collect the data with the same ω scan at $\phi=0^\circ$, 45° and 90° , the 2D scheme in Figure 6.11 shows that the data is good for biaxial stress tensor including the components: σ_{11} , σ_{12} and σ_{22} . The scheme function can be used for a more complicated data collection strategy to reduce the data collection time and still achieve the best result.

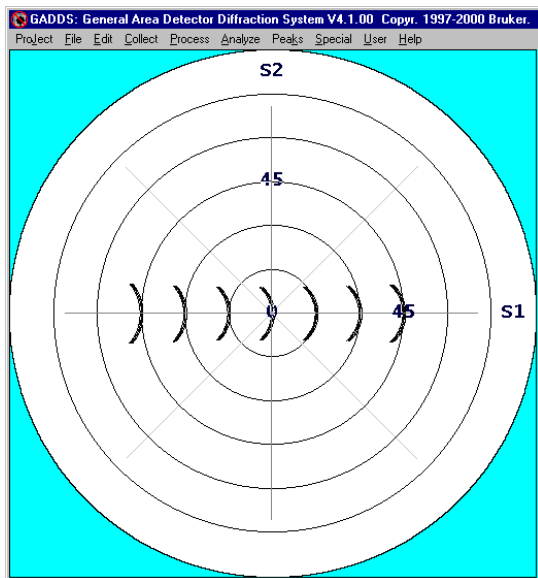


Figure 6.10 - The 2D scheme plot simulated from the parameters in Figure 6.9. The diffraction vectors are clustered along S_1 direction

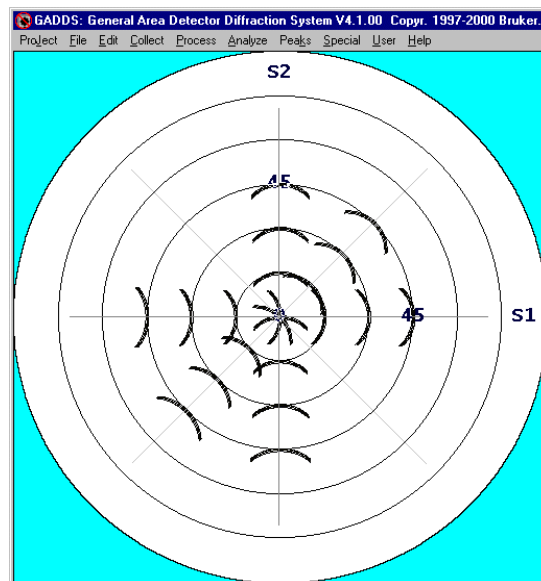


Figure 6.11 - The 2D scheme plot simulated from the same ω scan at $\phi=0^\circ$, 45° and 90° . The diffraction vectors are distributed in S_1 , S_2 and 45° directions. The data is good for biaxial stress tensor

6.1.8 Data Collection Procedures

(1) Load sample

Load the sample in a way that, when ω is in 90° position, the incident beam hits the sample surface in the perpendicular direction. The sample coordinates are so defined that when ω is set at 0° position, S_1 is opposite to the incident beam direction, S_2 is on the ω rotation axis, and S_3 is the normal of the sample surface. If the laser/video sample alignment system is available, the sample surface Z position should be aligned by bringing the laser spot to the center of the reticule (see Figure 6.22).

(2) Check collision limit

Manually drive ω position of the sample stage to the minimum and maximum ω angles for all the samples on the stage to ensure no collision between the sample stage and the detector, and the laser/video microscope. All selected measurement positions should be tested if XYZ stage is used for multiple sample or stress mapping. The ϕ and ψ rotations should also be checked if the fixed-chi stage, the two-position stage, or the $\frac{1}{4}$ circle stage is used for ϕ and ψ scans during data collection.

(3) Data collection

Data collection functions, such as SingleRun, MultiRun, and MultiTarget are all suitable for stress data collection.

(4) Unwarp frames

Unwarp the data frame before stress evaluation if this step is not performed automatically.

(5) LPA correction and absorption correction (optional)

The LPA (Lorentz, polarization, air/faceplate absorption) and sample absorption correction can also be performed before stress evaluation. It is, however, not necessary for most cases. Experiments shows that the correction contributes less than 1% variation in the final stress values.

6.2 Stress Evaluation Using One-Dimensional Data (Conventional Method)

For GADDS software version 3.323 or later, the conventional stress function is added under the Analyze menu. First, follow these steps to process the data in GADDS:

1. Load (or open) the first frame. For example, if a set of 7 data frames “strsnom.000-006” is used for stress evaluation, open the first frame “strsnorm.000” (Figure 6.12). Input an appropriate “High counts” value so the diffraction ring and background region are visible.

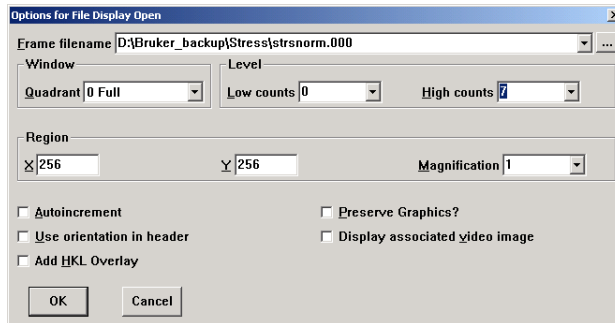


Figure 6.12 - Open file menu of GADDS

2. Select Analyze > Stress > Conventional to activate the parameter menu for stress data processing (Figure 6.13) and input the parameters shown.

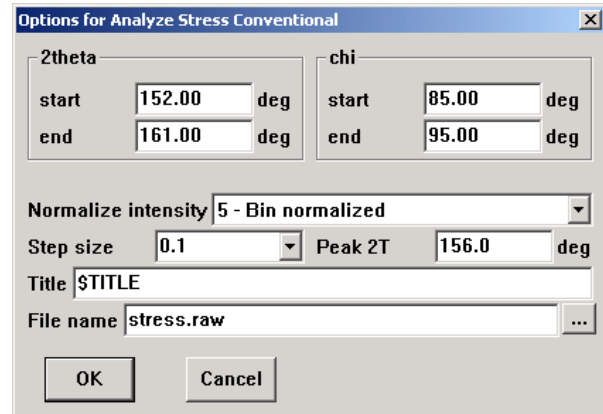


Figure 6.13 - Parameter input menu for Conventional Stress Analysis

2theta start—lower 2θ of conic region, $2\theta_1$;

2theta end—upper 2θ of conic region, $2\theta_2$;

Chi start—lower χ (γ) of conic region, $\chi_1 = 90 - \Delta\chi$;

Chi end—upper χ (γ) of conic region, $\chi_2 = 90 + \Delta\chi$;

Normalize intensity—3 for solid angle;

Step size— 2θ step size in the integrated profile data, default 0.1, choose smaller value for sharper peak;

Peak 2T—Input the estimated or pre-determined $2\theta_0$, use 156 for most steels. This value is used to calculate ψ tilt;

Title—'\$Title' to use the frame title or input other title;

File name—The processed data will be saved in DIFFRAC^{plus} format into this filename (*.raw) for all ψ angles.

$2\theta_1$, $2\theta_2$, χ_1 , χ_2 defines the integrated region. $2\theta_1$ and $2\theta_2$ determine the background of the profiles. χ_1 and χ_2 determine the integrated region along the diffraction ring. Normally, use

$\Delta\chi=5$ to 10 degrees, i.e. integrate over the χ range of 85-95 or 80-100.

3. Click OK to start processing. You can redefine $2\theta_1$, $2\theta_2$, χ_1 , χ_2 using the mouse for each frame. After you have defined the integrated region, click the mouse on the region to process the data (see Figure 6.14).

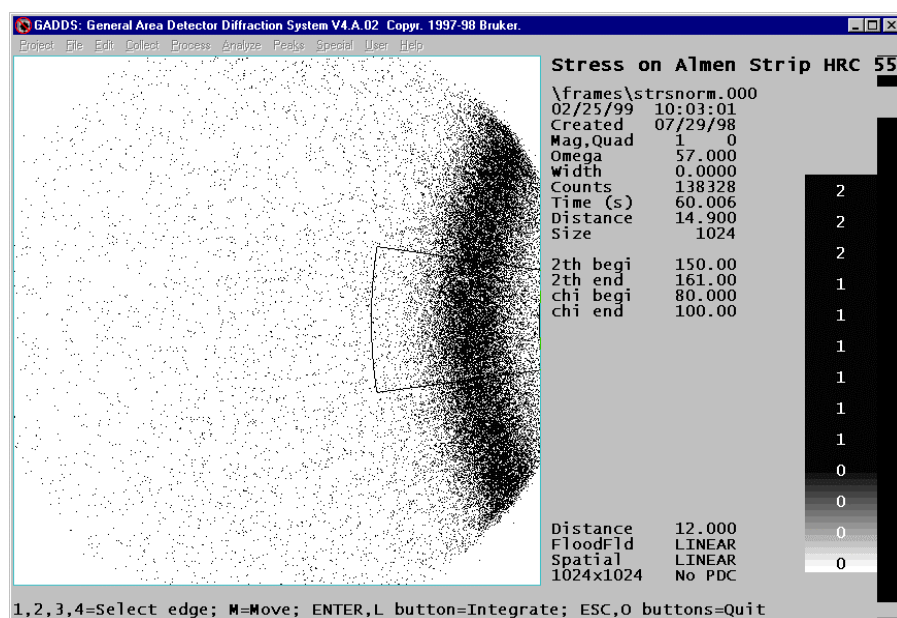


Figure 6.14 - The χ -integration region on data frame

After the above steps, GADDS saves the processed data in DIFFRAC^{plus} format (*.raw). For the above example, the filename is “strs-norm.raw.”

The next step is to calculate stress using DIFFRAC^{plus} STRESS software. DIFFRAC^{plus} STRESS can open the data saved in the last step. For data format compatibility reasons, the ψ -tilt of GADDS data is saved as the χ value for DIFFRAC^{plus} STRESS. As such, DIFFRAC^{plus} STRESS will process GADDS data as if it were collected in side-inclination mode, although the GADDS data was collected in iso-inclination mode. This will not change the stress result as long as the absorption and polarization corrections are not performed in DIFFRAC^{plus} STRESS. These corrections can be made in GADDS before data processing with DIFFRAC^{plus} STRESS. Verify that those correction functions are disabled when analyzing GADDS data with DIFFRAC^{plus} STRESS. Refer to the DIFFRAC^{plus} STRESS manual for details.

6.3 Stress Evaluation Using Two-Dimensional Data (2D Method)

For GADDS software version 4.0 or above, the new two-dimensional approach is added to the Analyze menu. All data processes and stress evaluations are performed within GADDS software, so the DIFFRAC^{plus} STRESS software is not necessary. Follow these steps to process and evaluate the stress data in GADDS:

1. Load (or open) the first frame. For example, if a set of 7 data frames “strsnom.000-006” is used for stress evaluation, open the first frame “strsnom.000” (Figure 6.15). Input an appropriate “High counts” value so the diffraction ring and background region are visible.

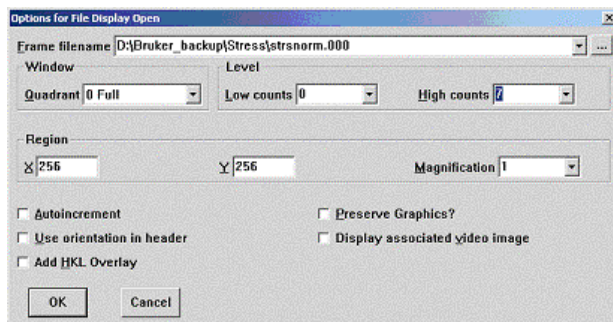


Figure 6.15 - Open file menu of GADDS

2. Select Analyze > Stress > Biaxial 2D to activate a parameter input menu for stress data processing (Figure 6.16). Input the following parameters:

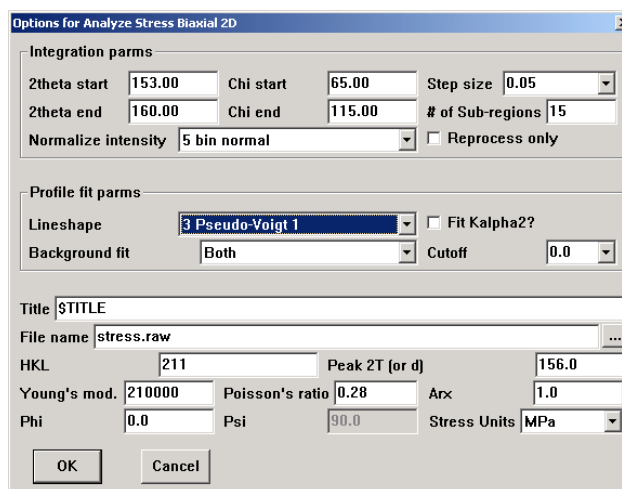


Figure 6.16 - Parameter input menu for stress analysis using 2D method

2theta start—lower 2θ of conic region, $2\theta_1$;

2theta end—upper 2θ of conic region, $2\theta_2$;

Chi start—lower χ of conic region;

Chi end—upper χ of conic region;

Normalize intensity—3 for solid angle;

Step size— 2θ step size in the integrated profile data, default 0.1, choose smaller value for sharper peak;

of Sub-regions (n)—Choose the number (3 to 64) of data points in the selected diffraction ring.

Peak 2T (or d)—Input the estimated or pre-determined $2\theta_0$ (d_0), use 156 for most steels. This value is also used as initial peak 2θ value in profile fitting so: $2\theta_1 < 2\theta_0 < 2\theta_2$;

Title—'\$Title' to use the frame title or input other title;

File name—The processed raw data will be saved in this filename.

HKL—The diffraction plane index;

Young's modulus, Poisson's ratio and anisotropic factor A_{RX} can be found in previous sections or literature;

Lineshape—select one of the four peak-fitting functions.

- Click OK to display the selected data region. You can redefine $2\theta_1$, $2\theta_2$, χ_1 , χ_2 by using the mouse or keyboard (see Figure 6.17).

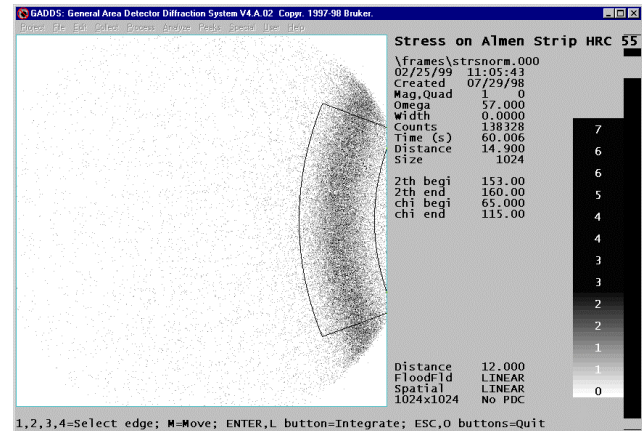


Figure 6.17 - Selected data region on frame

$2\theta_1$, $2\theta_2$, χ_1 , χ_2 define the selected diffraction ring. $2\theta_1$ and $2\theta_2$ determine the background of the profiles. χ_1 and χ_2 determine the angular range of the diffraction ring. The χ -integration range ($\Delta\chi$) of each profile is determined by $\Delta\chi = (\chi_2 - \chi_1)/n$.

It is very important to keep the parameters and settings consistent through all the measurements. You should select a set of parameters and settings for a particular material and use the same parameter and settings for all the same materials. It is deceptive to compare stress values calculated with different parameters or settings.

4. Click the mouse on the frame to process the data. Calculated stress is reported as shown in Figure 6.18.

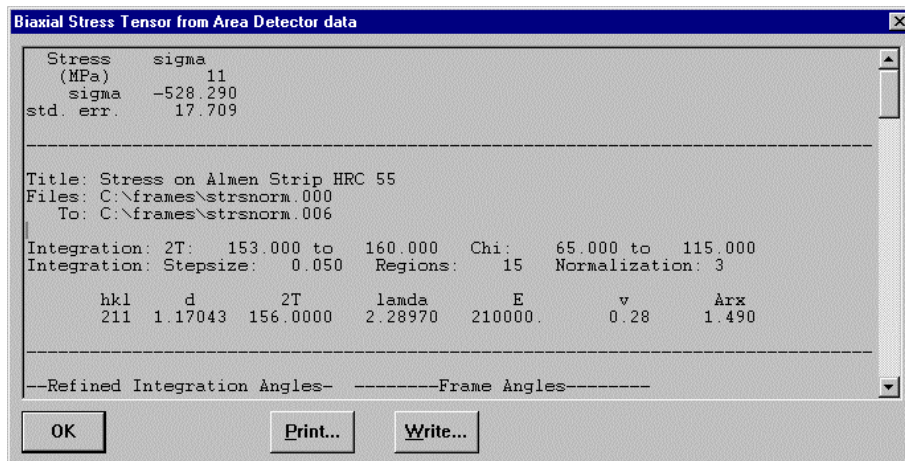


Figure 6.18 - Stress result menu showing normal stress

In the above example, all the seven frames were collected with ω scan only, $\phi=0^\circ$, $\psi=0^\circ$ ($\chi_g=90^\circ$), and $\omega=57^\circ, 72^\circ, 87^\circ, 102^\circ, 117^\circ, 132^\circ$, and 147° respectively. For stress tensor measurement, the data frames should be collected with two or more scanning angles. For example, for a set of seven frames collected at

Frame	1	2	3	4	5	6	7
w=	57x	72x	87x	102x	117x	132x	147x
f=	0x	45x	90x	0x	45x	90x	0x

Following the same steps, the stress result is given as shown in Figure 6.19.

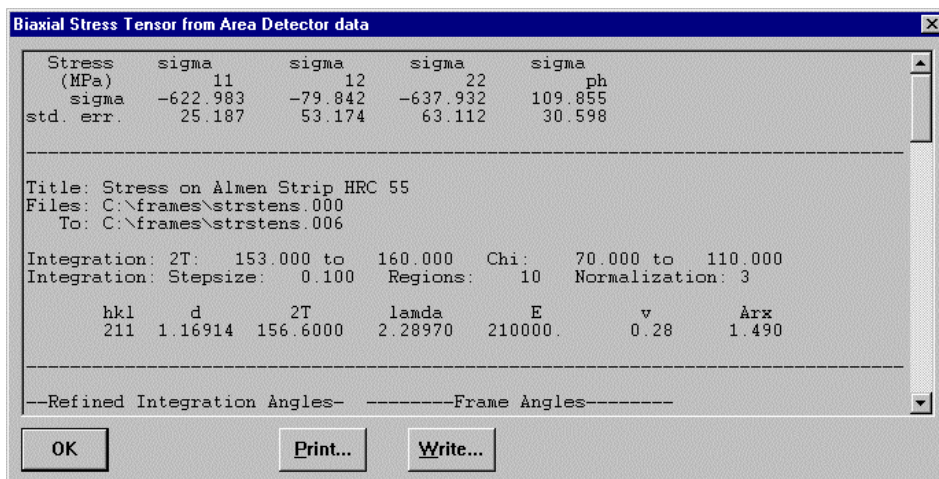


Figure 6.19 - Stress result menu showing biaxial stress tensor

The quality of the stress measurement can be evaluated by viewing the peak-fitting data points (peak 2 θ values) and a diffraction ring calculated from the stress result. Follow these steps:

1. After the stress value is calculated, open the first frame in GADDS or move back to the first frame by pressing the Ctrl+← keys a few times.

2. Select Analyze > Stress > View 2D to activate the data display menu (Figure 6.20). Input the following parameters by following the instructions at the bottom of the GADDS window.

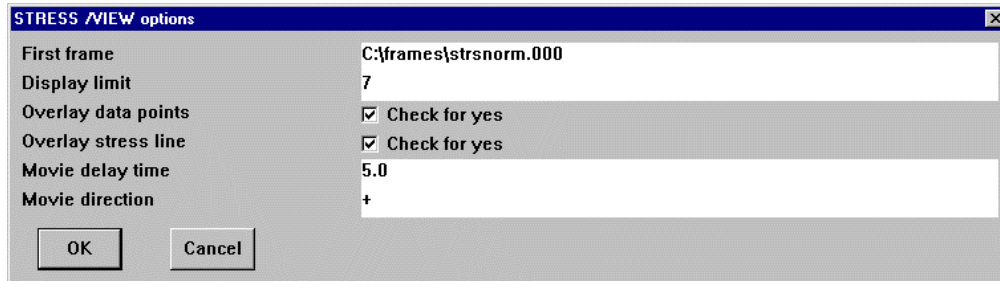


Figure 6.20 - Stress result display menu

- Click on OK to display the data one by one with the defined movie delay time (see Figure 6.21).

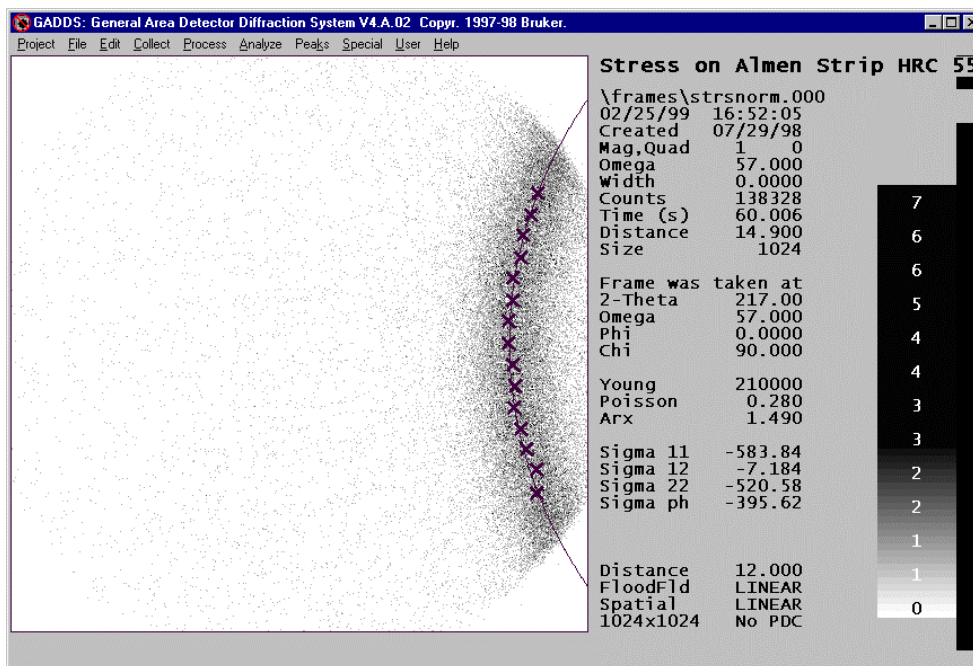


Figure 6.21 - The stress data points and the simulated diffraction ring corresponding to the measured stresses are displayed on the frame

6.4 Application Examples

6.4.1 Example 1. (Conventional Method) Residual Stress Measurement with GADDs Microdiffraction System

This is an example of residual stress measurement with the GADDs Microdiffraction System. The residual stress on the inside surface of a spring was measured with Cr tube and 0.3mm collimator. Since the size of the spring is relatively small (coil diameter -10mm, wire diameter 1mm, and coil pitch 4mm) the Laser Video Sample Alignment System was used to position the inside surface of the spring. The spring was made of precipitation-hardenable stainless steel 17-7PH. The (211) diffraction ring of the alpha phase was used for stress measurement.

Figure 6.22 shows the laser spot on the inside surface of the spring wire. When the laser spot is in the center of the crosshair, the sample surface is aligned to the goniometer center.

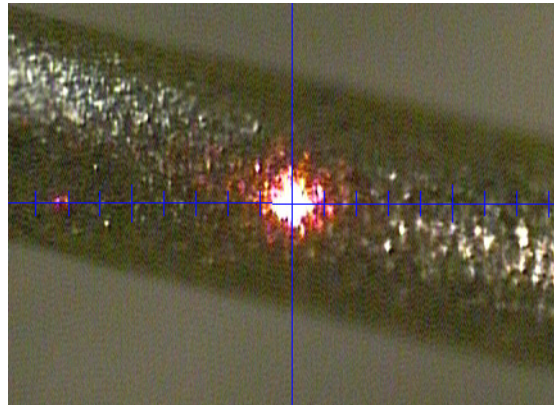


Figure 6.22 - The image from the laser video sample alignment system

Figure 6.23 shows a part of the spring. The incident X-ray beam and diffracted beams can pass through the gap between spring wires so the residual stress can be measured nondestructively.

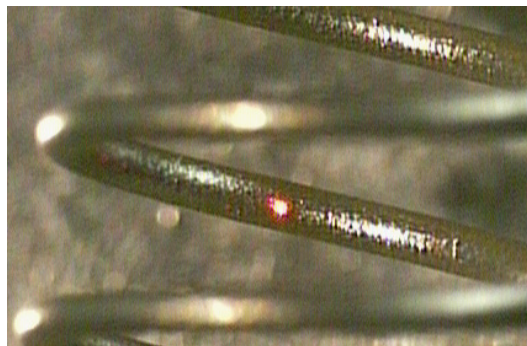


Figure 6.23 - The video image showing a section of the spring. The diffracted beams can pass through the gap between the wires

Figure 6.24 shows one of the measured frames with chi-integrated profile. The broken blue lines indicate the shadow of the wires. For data evaluation, the frames were first processed with the GADDS stress function and then imported to DIFFRAC^{plus} STRESS software for stress analysis.

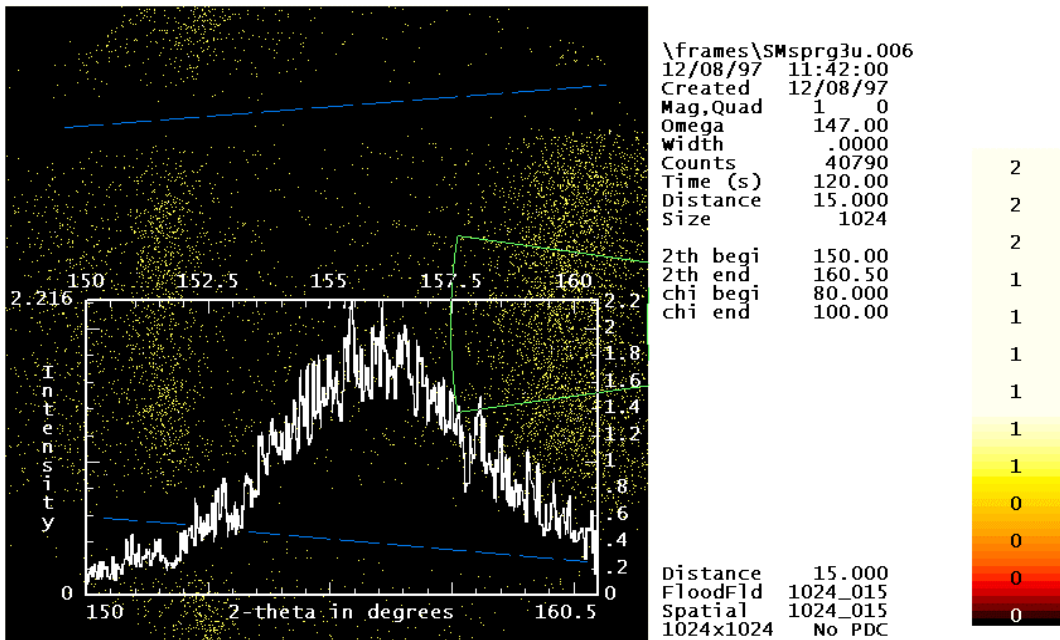
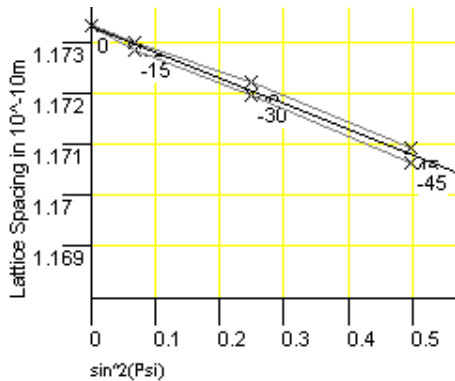
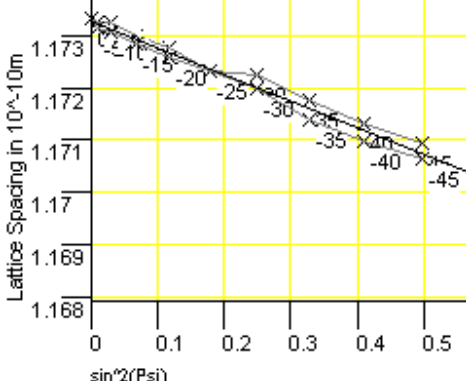


Figure 6.24 - A measured frame with chi-integrated profile.
The green broken line box defines the chi integration region.
The blue broken lines indicate the shadow of the wires

The results are listed in Table 6.3. The ψ tilt is achieved by iso-inclination (Ω scan). The residual stress values determined in scans of 7 and 19 steps agree very well. The 19 points measurement has a lower standard deviation, about 3.5%.

Table 6.3 – Residual stress measurement results of the inside surface of a stainless-steel spring

Number of frames	7	19
ψ angles and steps	-45° to 45°, 15° steps	-45° to 45°, 5° steps
Data collection time	14 minutes	38 minutes
Measured stress	-864 (\pm 48) MPa	-875 (\pm 31) MPa
d vs. $\sin^2\psi$ plot		

6.4.2 Example 2. (2D Method) Comparison Between 2D Method and Conventional Method

The residual stresses in the end surface of a carbon steel roller were measured by the conventional method and the new 2D method. The roller is a cylinder, 1" long and 6/8" in diameter. The stress data was taken from the center of the roller end. The sample was loaded on the XYZ stage of the GADDs microdiffraction system. A total of 7 frames were taken with ω angles at 33, 48, 63, 78, 93, 108, 123° (corresponding to ψ tilts of 69, 54, 39, 24, 9, 6 and -21° for a negative detector swing angle) with Cr-K α radiation.

Figure 6.25 shows the frame collected at $\omega=123^\circ$. The (211) ring covers the χ range from 60° to 120°. In order to have sufficient background for each profile, the χ range of 67.5° to 112.5° was used for stress analysis. First, the frame data was integrated along the χ angle in the interval of $\Delta\chi=5^\circ$. A total of 9 diffraction profiles were obtained from the χ integration. The diffraction profile at each χ value is an integration in the range from $\chi-1/2\Delta\chi$ to $\chi+1/2\Delta\chi$. For example, the profile at $\chi=70^\circ$ is the χ -integration from 67.5° to 72.5°. The peak position 2θ for each χ angle was then obtained by fitting the profile with Pearson VII function. A total of 63 data points in the form of $2\theta(\chi)$ can be obtained from the 7 frames.

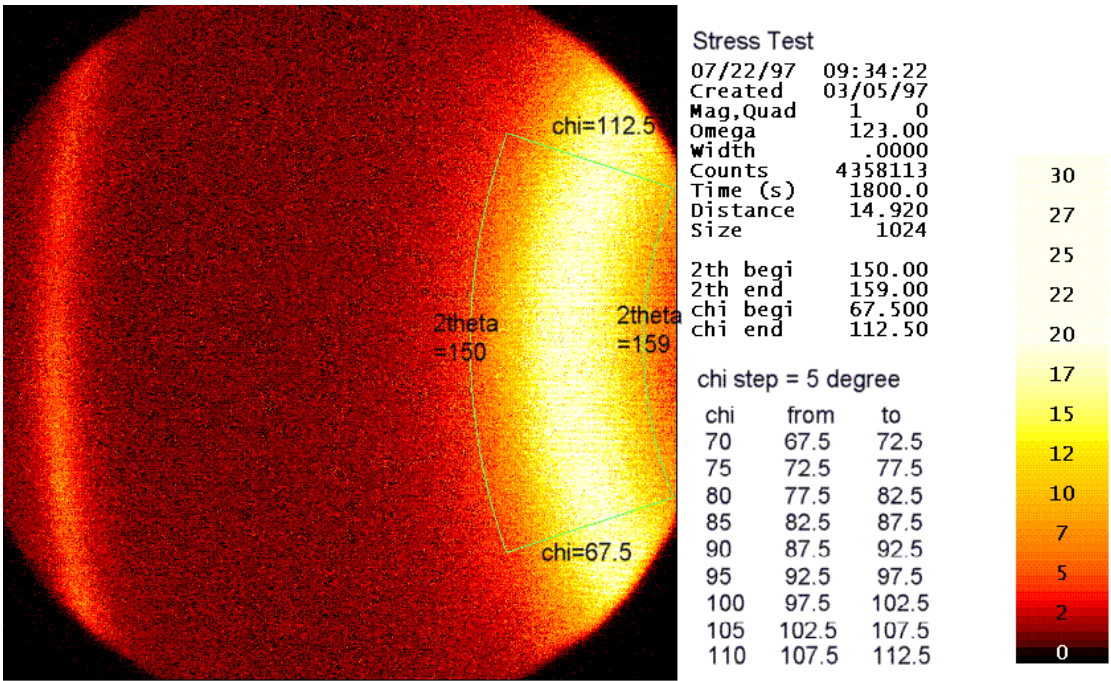


Figure 6.25 - The diffraction data collected with the HI-STAR area detector. The frame is collected on a steel roller at $\omega=123^\circ$. A total of 7 frames were collected at ω angles from 33° to 123° . A total of 9 profiles can be obtained from each frame by χ integration over $\Delta\chi$ intervals of 5°

The data points at $\chi=90^\circ$ from 7 frames, a typical data set for an Ω -diffractometer, are used to calculate stress with the conventional $\sin^2\Psi$ method. For the 2D method, in order to compare the statistical error between different numbers of data points, the stress is calculated 3, 5, 7, and 9 data points on each frame. The results from

the conventional method and the new 2D method are summarized in Table 6.4 and compared in Figure 6.26. The measured residual stress is compressive and the stress values from different methods agree very well. With the data taken from the same measurement (7 frames), the new method gives lower statistical error and the error decreases with increasing number of data points from the diffraction ring.

Table 6.4 – The measured stress with the conventional method and the new 2D method

Conventional method	The new method with different numbers of data points			
	3 points	5 points	7 points	9 points
-776 ±62 MPa	-769 ±38	-775 ±33	-777 ±26	-769 ±23

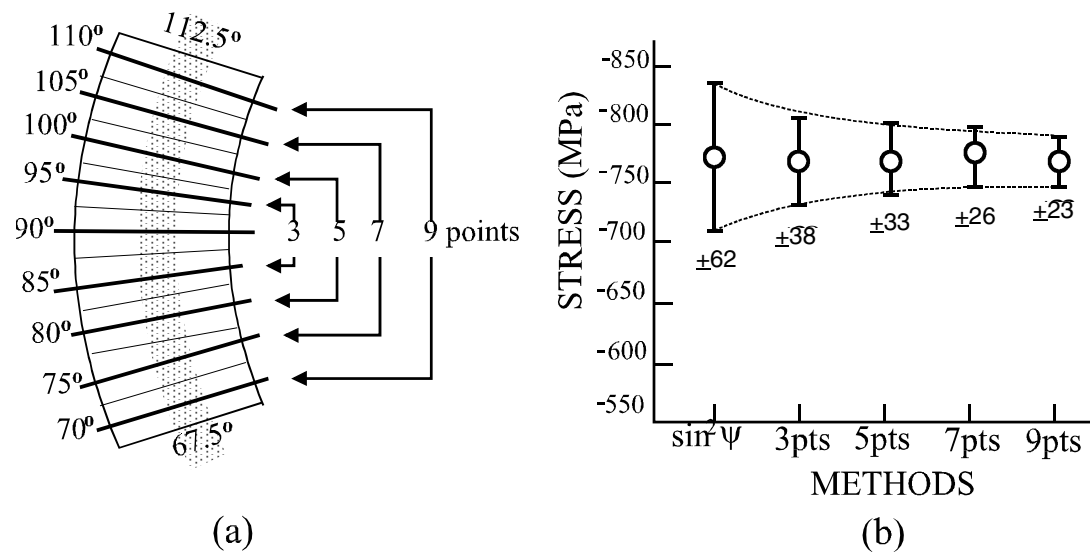


Figure 6.26 - Comparison of the conventional method and the new method with different numbers of data points. (a) Data points taken from the diffraction ring, total of 9 points from the diffraction ring in the χ range of 67.5° to 112.5° with $\Delta\chi=5^\circ$; (b) Measured stress and standard deviation by different methods and from various numbers of data points

6.4.3 Example 3. Stress Mapping with 2D Method

Residual stress mappings on friction stir welded samples are measured on a GADDS with Huber 1/4-circle Eulerian cradle using the 2D method [6]. The system with XYZ stage allows users to select the mapping area and steps. The stress results are processed and mapped to the grid based on the user-selected stress component.

The stress is measured on the aluminum (311) planes with $\text{Cr-K}\alpha$ radiation. The X-ray beam size is 0.8 mm in diameter. Each diffraction frame is collected in 30 seconds and 5 frames per stress data point at various ψ and ϕ angles. Two specimens were made by friction stir welding with rotation speed of 580 rpm and welding speed of 113 mm/min and 195 mm/min respectively. The specimens will be denoted as 113 and 195 thereafter. The stress mapping takes 1 mm stepwise scan for 0–40 mm from the center line and 5 mm stepwise scan from 40 mm to the edges.

The specimen is loaded on the XYZ stage of the Eulerian cradle (Figure 6.27) and each mapping spot is aligned to the instrument center with the laser-video alignment system.

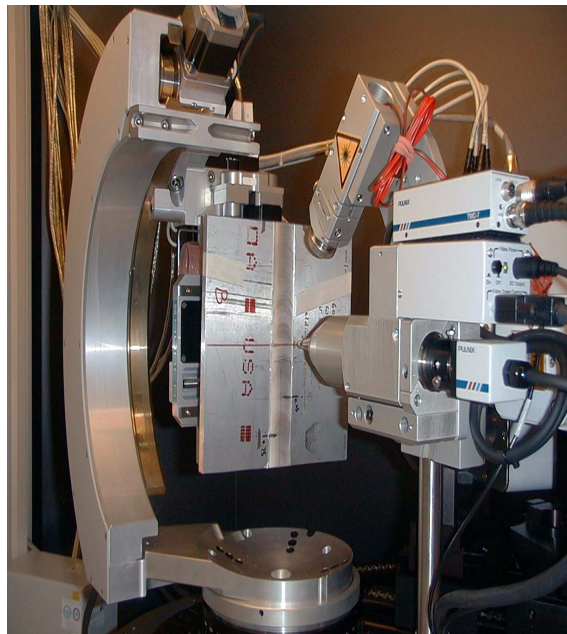


Figure 6.27 - Specimen loaded on the XYZ stage of the Eulerian cradle and the mapping spot is aligned with the laser-video system

The residual stress mapping results on the top surface with 40 mm from the center line are shown in Figure 6.28. The stresses in the longitudinal direction (σ_{22}) form a double-peak profile symmetric to the weld center line. A similar profile was observed with neutron diffraction. The relative small X-ray beam size may be the cause of severe scattering data.

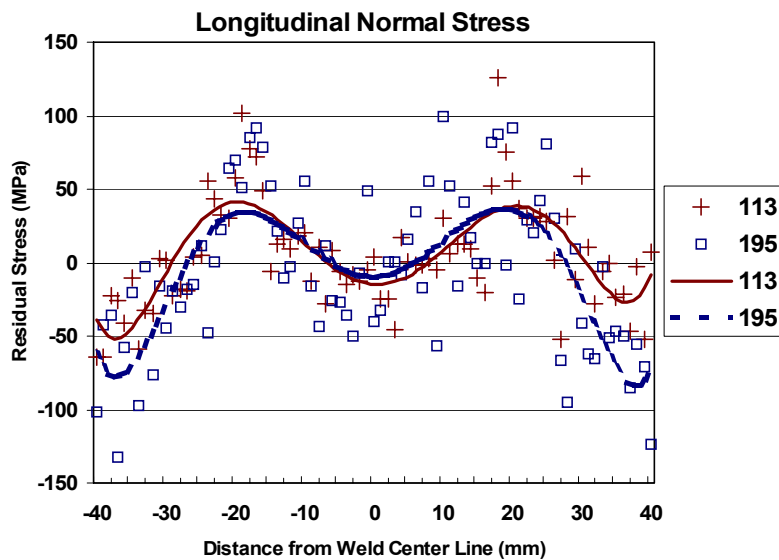


Figure 6.28 - Residual stresses in longitudinal direction (σ_{22}) on the top surface within 40 mm from the weld center line

6.5 References

1. I. C. Noyan and J. B. Cohen, *Residual Stress*, Springer-Verlag, New York, 1987.
2. Jian Lu, *Handbook of Measurement of Residual Stress*, The Fairmont Press, Lilburn, GA, 1996.
3. Baoping B. He and Kingsley L. Smith, A New Method for Residual Stress Measurement Using An Area Detector, Proceedings of The Fifth International Conference on Residual Stresses (ICRS-5), Linkoping, Sweden, 1997.
4. Bob B. He, Uwe Preckwinkel and Kingsley L. Smith, Advantages of Using 2D Detectors for Residual Stress Measurement, *Advances in X-ray Analysis, Vol. 42, Proceedings of the 47th Annual Denver X-ray Conference*, Colorado Springs, Colorado, USA, 1998.
5. Bob B. He, Residual stress measurement with two-dimensional diffraction (invited), *The 20th ASM Heat Treating Society Conference Proceedings, Vol. 1*, pp 408-417, St. Louis, Missouri, 2000.
6. Bob B. He, et. al., Stress mapping using a two-dimensional diffraction system, Proceedings of 2001 SEM Spring Conference on Experimental and Applied Mechanics, Portland, Oregon, USA, 2001.

7. Crystal Size

A *crystallite* is the smallest diffracting domain in a material. *Crystallite size*, sometimes called *grain size*, is not to be confused with particle size. A particle may be comprised of many crystallites. Crystallite size can be correlated with various thermal, mechanical, electrical, and magnetic properties and with other effects such as catalytic activity.

7.1 Line Broadening Principles for Crystallite Size

The traditional measure of crystallite size is based on the Scherrer equation:

$$t = \frac{C\lambda}{B\cos\theta}$$

where λ is the X-ray wavelength (Å), B is the full width at half maximum (FWHM) of the peak (radians) corrected for instrumental broadening, θ is Bragg angle, C is a factor (typically from 0.9 to 1.0) depending on crystallite shape (see Klug and Alexander, 1974), and t is the crystallite size (Å). The FWHM values are those of unresolved $K\alpha$ peaks, not those of resolved $K\alpha_1$ peaks. This equation shows an inverse relationship between crystallite size and peak profile width: the wider the peak, the smaller the crystallites.

Not all peak broadening is due to crystallite size, however. Both instrumental broadening and microstrain can contribute to peak broadening and influence peak profile shape.

7.2 Instrumental Broadening

Determination of all peak broadening due to instrumental parameters (e.g. collimator size, detector resolution, beam divergence) is critical. Only peak broadening due to crystallite size should be considered in the crystallite size calculation. To correct for instrument broadening, a standard such as NIST SRM 660 LaB₆ (lanthanum hexaboride) should be measured. With this standard, all broadening is due to instrumental parameters, which include beam size, sample-to-detector distance, and air scatter. A suitable standard should have no strain, particles larger than 1 μm (no size broadening), a similar lattice type as the material to be characterized, and similar X-ray absorption properties. With a two-dimensional detector, data from a standard and an unknown must be collected at the same incident angle (ω angle), since the peak width varies as a function of this angle. Also, as a general rule, the ω value should be selected as $\frac{1}{2}$ the 2θ value of the sample reflection to be characterized. For reflections below $\sim 25^\circ$ 2θ , the ω value may be selected larger than $\frac{1}{2}$ the 2θ value to avoid unnecessarily large instrumental broadening caused by the large projected area of the X-ray beam at low incident angles. If the material is suspected to possess microstrain (e.g., the specimen is a thin film), the Warren-Averbach or Single Line methods should instead be used.

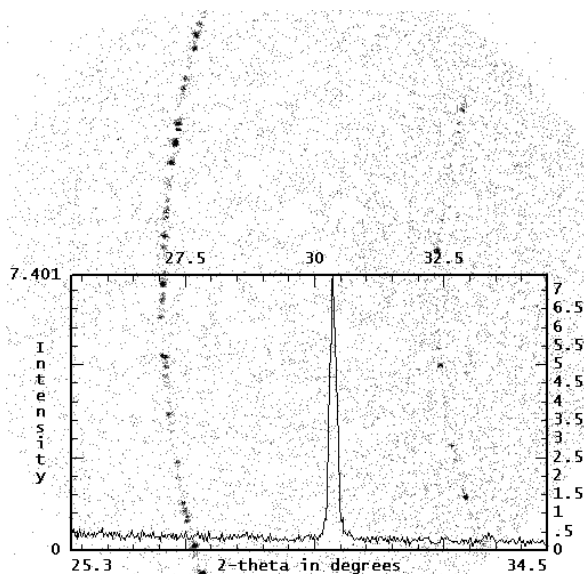


Figure 7.1 - NIST Standard Reference Material 660, lanthanum hexaboride, LaB_6 . Profile fitting of the peak shown gives a FWHM of 0.162° with a Gaussian profile and 0.133° with a Cauchy

The subtraction of the standard peak from the unknown peak has two limits, depending on whether the peaks have been fit with Gaussian or Cauchy (Lorentzian) functions. These two functions have different mathematical properties concerning the addition properties of their FWHMs. Gaussian profiles subtract in quadrature as

$$B^2 = U^2 - S^2$$

while Cauchy profiles subtract linearly

$$B = U - S,$$

where B is the corrected FWHM for use in the Scherrer equation, and U and S are the FWHMs of the unknown and standard peaks, respectively. The above results can be derived using the Fourier convolution theorem with the different function types. Bear in mind that other profile shape functions do not have the same additive properties of their FWHMs. Usually Cauchy profiles are used for two-dimensional detector work, but the beam profile is Gaussian. The smaller the crystallite size, the closer the values obtained from the Scherrer equation for the Cauchy and Gaussian profile shapes will agree. For example, assume a sample has a diffraction line at $30^\circ 2\theta$ and a line width of 2.83° and that a standard LaB_6 pattern has been measured with a line width of 0.09° . This would yield crystallite sizes of 29 \AA with a Gaussian fit and 30 \AA with a Cauchy fit. Now, assume the same unknown has a line width of 0.26° . This would produce crystallite sizes of 348 \AA with a Gaussian fit and 545 \AA with a Cauchy fit. Figure 7.2 shows the corrected full width at half maximum, B , computed from the Scherrer equation as a function of crystallite size, t , and 2θ value.

Table 7.1 – Size broadening [°] calculated from the Scherrer equations for a given crystallite size, t [Å], and 2θ [°] value with $C = 0.9$ and $\lambda = 1.54184$ Å

t [Å]	2θ [°]									
	5	10	15	20	30	40	50	60	70	80
20	3.98	3.99	4.01	4.04	4.12	4.23	4.39	4.59	4.85	5.19
30	2.65	2.66	2.67	2.69	2.74	2.82	2.92	3.06	3.24	3.46
40	1.99	2.00	2.00	2.02	2.06	2.12	2.19	2.30	2.43	2.59
50	1.59	1.60	1.60	1.61	1.65	1.69	1.75	1.84	1.94	2.08
100	0.80	0.80	0.80	0.81	0.82	0.85	0.88	0.92	0.97	1.04
200	0.40	0.40	0.40	0.40	0.41	0.42	0.44	0.46	0.49	0.52
300	0.27	0.27	0.27	0.27	0.27	0.28	0.29	0.31	0.32	0.35
400	0.20	0.20	0.20	0.20	0.21	0.21	0.22	0.23	0.24	0.26
500	0.16	0.16	0.16	0.16	0.16	0.17	0.18	0.18	0.19	0.21
1000	0.08	0.08	0.08	0.08	0.08	0.08	0.09	0.09	0.10	0.10
2000	0.04	0.04	0.04	0.04	0.04	0.04	0.04	0.05	0.05	0.05
4000	0.02	0.02	0.02	0.02	0.02	0.02	0.02	0.02	0.02	0.03

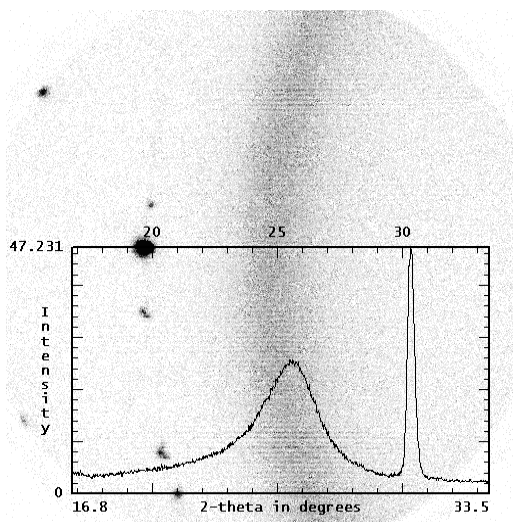


Figure 7.2 - u (111) peak from a semiconductor tab tape. Profile fitting with a Cauchy function gives a peak location of $43.455^\circ 2\theta$ and a FWHM of 0.300° . Using LaB_6 as an instrumental broadening standard with a Cauchy FWHM of 0.133° , the corrected FWHM is 0.167° , and the Scherrer equation gives a crystallite size of 512 \AA

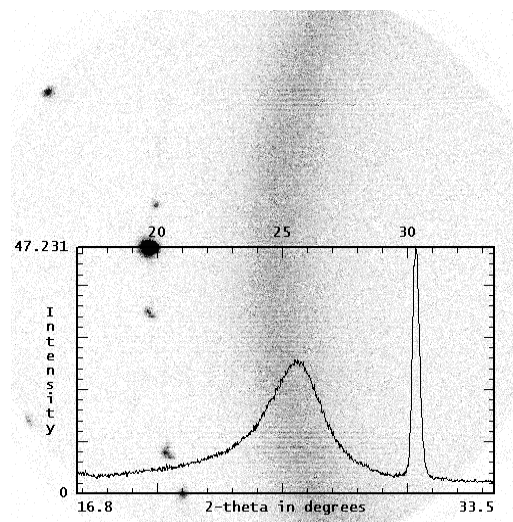


Figure 7.3 - Graphite-coated beads. Profile fitting the graphite peak with a (split) Cauchy gives a peak location of $25.705^\circ 2\theta$ and a FWHM of 2.748° . Using LaB_6 as an instrumental broadening standard with a Cauchy FWHM of 0.133° , the corrected FWHM is 2.615° , and the Scherrer equation gives a crystallite size of 32 \AA . Note that to ensure proper fitting of the graphite peak, the substrate peak was also fit (with a Gaussian profile)

7.3 Microstrain Broadening

Peak broadening due to microstrain can also be determined. This technique usually involves analysis of the peak profile shape, from which contributions due to crystallite size and microstrain are separated. Microstrain in materials increases the line width as a function of 2θ . The deconvolution of the width from crystallite size and lattice distortion is based on the Warren-Averbach method. This method involves the measurement of the complete profile of multiple orders of the same reflection (e.g., (100), (200), (300)). In summary, the peak profiles of the standard and unknown are deconvolved into Fourier coefficients that are corrected for instrumental broadening. Plotting the Fourier coefficients as a function of the (hkl) values of the measured reflections, a crystallite size distribution and a microstrain distribution are obtained, which yield an average crystallite size and root mean squared microstrain. The Single Line method is based on the Warren-Averbach method with additional assumptions (i.e. crystallite size broadening has a Cauchy profile, while microstrain broadening has a Gaussian profile). It can be used when only one diffraction peak is available for analysis, provided that both crystallite size and microstrain effects are present in the sample of interest. The Single Line method also provides a crystallite size distribution, but one of the assumptions is that the microstrain is constant.

DIFFRAC^{plus} Profile (an optional package) calculates crystallite size using an implementation of the Scherrer equation. *DIFFRAC^{plus}* Cysize (an optional package) implements the Warren-Averbach and Single Line methods. Refer to the software manuals and online help files of those packages for details. Since the derivations and assumptions behind the Scherrer method and the Warren-Averbach method differ (see Klug and Alexander, 1974 for details), the average crystallite size values obtained from each method will not necessarily be comparable. For many applications, precision (reproducibility) is more important than absolute accuracy. These methods (and variations thereof) are frequently used for quality-control comparisons.

7.4 Data Collection for the Warren-Averbach and Scherrer Methods

Determination of all peak broadening due to instrumental parameters (e.g., collimator size, detector resolution, beam divergence) is critical. Only peak broadening due to crystallite size can be considered in the crystallite size calculation.

The detector distance of 30 cm is chosen to maximize resolution and minimize peak FWHM due to detector resolution. In this way, peak broadening due to crystallite size is not obscured by instrumental peak broadening. Data was collected with both a 0.1 mm collimator and a 0.2 mm collimator with the same 2θ and ω angles using LaB_6 . Data collection times were adjusted to obtain comparable signal to noise. No additional peak broadening of LaB_6 was observed with a 0.2 mm collimator (above that observed with the 0.1 mm collimator). It was observed that the 0.3 mm collimator did contribute additional peak broadening.

In crystallite size measurements on randomly oriented materials (e.g., fine powders), there is no reason to rotate or oscillate the sample. If sample characteristics warrant sample rotation or oscillation (e.g., the sample has preferred orientation), then the standard should be collected under identical measurement conditions.

NIST standard LaB_6 (SRM 660) is used to determine instrument broadening. With this standard, all broadening is due to instrumental parameters. With 99% of its particles larger than $1\ \mu\text{m}$, LaB_6 contributes less than 0.01° FWHM due to size broadening. This sample should be measured on the GADDS system with the following instrument parameters:

Radiation	Cu
Sample-to-detector distance	30 cm
Collimator	0.2 mm
kV, Ma	40, 40
Data collection time	At least 1 hr
Sample rotation	As necessary
Sample oscillation	As necessary

As previously discussed, the ω and 2θ values should be selected appropriately. Measurement conditions for the standard and unknown must be identical. If crystallite size measurements are made in transmission, it is important to match the thickness of the sample and the standard.

7.5 References

1. G. Allegra and S. Brückner, "Crystallite-Size Distributions and Diffraction Line Profiles Near the Peak Maximum," *Powder Diffr.* *8*(2), 102-106 (1993).
2. R. Delhez, Th. H. de Keijser, and E. J. Mittemeijer, "Determination of Crystallite Size and Lattice Distortions through X-ray Diffraction Analysis: Recipes, Methods and Comments," *Fresenius Z. Anal. Chem.* *312*, 1-16 (1982).
3. L. Dengfa and W. Yuming, "The 'Hook Effect' of X-ray Diffraction Peak Broadening of Multilayer Thin Films," *Powder Diffr.* *2*(3), 180-182 (1987).
4. H. Ebel, "Crystallite Size Distributions from Intensities of Diffraction Spots," *Powder Diffr.* *3*(3), 168-171 (1988).
5. H. P. Klug and L. E. Alexander, *X-ray Diffraction Procedures for Polycrystalline and Amorphous Materials*, 2nd ed. (John Wiley, New York, 1974).
6. R. C. Reynolds, "Diffraction by Small and Disordered Crystals," In *Reviews in Mineralogy*, Vol. 20, (Mineralogical Society of America, Washington, DC, 1989).

8. Percent Crystallinity

8.1 Principle of Percent Crystallinity

The crystallinity of a material influences many of its characteristics, including mechanical strength, opacity, and thermal properties. In practice, crystallinity measurements are made both for research and development and for quality control. X-ray scattering occurs from both the crystalline and non-crystalline material illuminated with X-rays. The difference between the two types of scattering is in the ordering of the material. Materials, especially polymers, have some amorphous contributions. The ability to deconvolute the amorphous from the crystalline scattering is the key to obtaining a reliable number that is consistent with other techniques such as NMR and calorimetry.

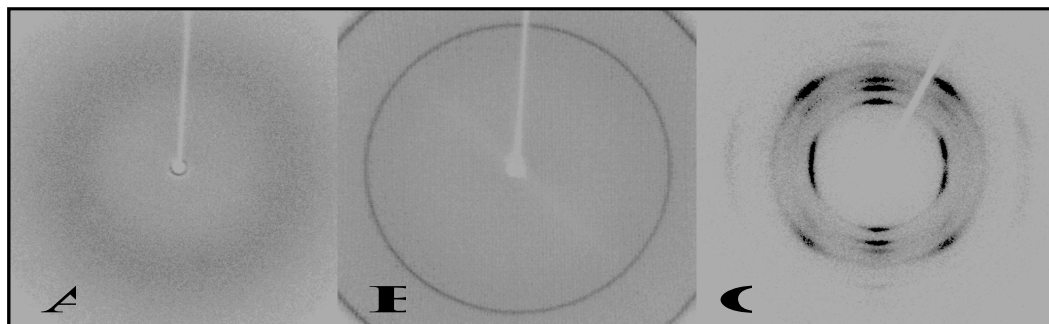


Figure 8.1 - A) amorphous scattering, B) unoriented polycrystalline scattering, C) oriented polycrystalline and amorphous scattering

As shown in Figure 8.1, X-ray scattering from amorphous material produces a “halo” of intensity which, when integrated, obtains a broad, low-intensity “hump.” X-ray scattering from a crystalline material produces well-defined spots or rings, which integrate to sharp, higher-intensity peaks. *Percent crystallinity*, as obtained by X-ray measurements, is defined as the ratio of intensity from the crystalline peaks to the sum of the crystalline and amorphous intensities:

$$\text{percent crystallinity} = I_{\text{crystalline}} / (I_{\text{crystalline}} + I_{\text{amorphous}}).$$

The measured total intensity may have significant contributions other than crystalline and amorphous scattering from the sample. Air scatter, specimen holder scatter (e.g., capillary glass scatter), and Compton (or incoherent) scatter must be taken into account.

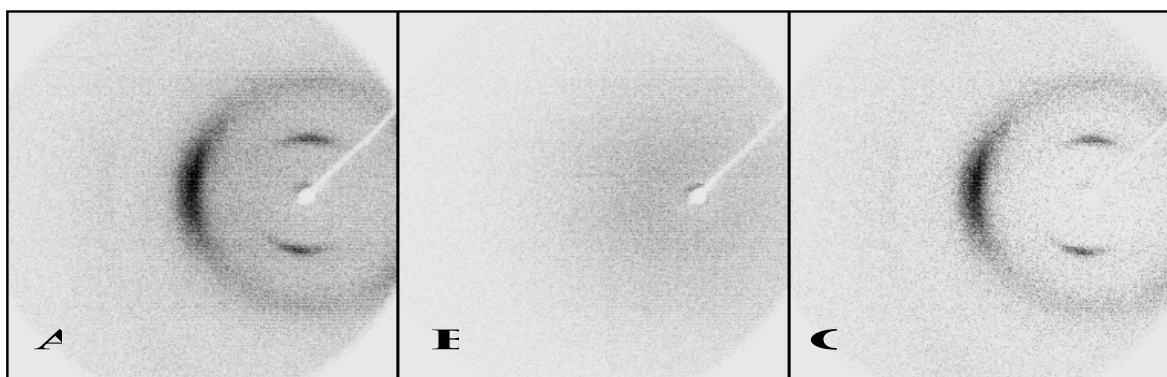


Figure 8.2 - A) Nylon frame with air scatter, B) air scatter frame, C) Nylon frame with air scatter subtracted

You can correct air scatter occurring after the specimen and specimen holder scatter by measuring “blank” frames under identical conditions as the sample (with the exception of the measurement time). You subtract these frames from the data frames using FILE/LOAD with the /SCALE = -n qualifier, which scales the background frame to the time of the data frame. Note that the beam stop must not be repositioned between the measurement of the blank and data frames for measurements in transmission mode.

- The beam stop will also cause considerable scattering if it is not properly aligned (to block the primary beam). A pair of screws is present on the beam stop for this alignment.
- Another air scatter effect arises from incident-beam scattering, which is a function of

the sample geometry. The best approach is to reduce this effect by putting the sample as close to the incident beam as possible and use a beam that is smaller than the sample. This practice eliminates the shadow on the detector, which is absorption of the air scatter before the sample.

Compton (incoherent) scattering contributes to the diffuse background in an X-ray diffraction pattern in a way that can be modeled.

8.2 Data Evaluation for Two-Dimensional Data

8.2.1 Methods Supporting Percent Crystallinity

Four methods that support percent crystallinity calculation are available with GADDS. These are Compton, Internal, External, and Full. External and internal methods employ user-specified areas of frame data for a relative measurement of percent crystallinity. Thus, the value obtained is not absolute. The same is true of the PERCENT_CRYSTAL/FULL method.

Compton Method (PERCENT_CRYSTAL/COMPTON)

Compton scattering can make a substantial contribution to the background intensity. If it is not corrected for, the percent crystallinity value can be artificially low, especially for polymeric materials. For further discussion, see Alexander (1985). Compton scattering can be modeled and removed in both the internal and external methods. This correction is unnecessary if the same material is examined and its density varies no more than ~20%.

The Compton scattering table used by GADDS is SAXI/GADDS32/COMPTON.TBL, which you can view using a text editor such as NOTEPAD. Examples of the empirical formula syntax follow:

- AL+3 2 O 3 for aluminum oxide Al_2O_3 . If O-2 were instead used, a warning would be issued that no such entry exists in the scattering table.
- C 12 H 22 O 2 N 2 for Nylon 66. For polymers, input the repeat unit.

Note that the default values in the table for C and O are not for covalently bonded systems. Two new entries should be made in this table (see Table 3.4.4.2B in the International Tables, Vol. III., 1968):

$\sin\theta/\lambda$	0.0	0.1	0.2	0.3	0.4	0.5	0.6	0.7	0.8	1.1
CV	0.000	1.203	2.914	3.826	4.238	4.486	4.686	4.871	5.044	5.462
OV	0.000	0.966	2.777	4.275	5.243	5.818	6.170	6.408	6.593	7.025

To correct for Compton scattering:

1. Compute the scattering function using PERCENT_CRYSTAL/COMPTON.
2. Specify the /COMPTON qualifier with PERCENT_CRYSTAL/INTERNAL or PERCENT_CRYSTAL/EXTERNAL. (Presently, PERCENT_CRYSTAL/FULL does not allow for the Compton correction).

Internal Method (PERCENT_CRYSTAL/INTERNAL)

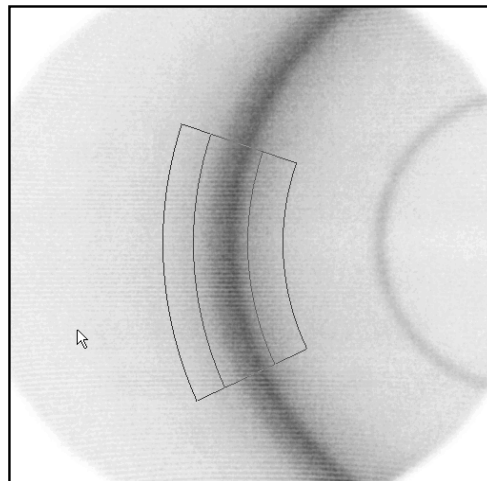


Figure 8.3 - γ -Nylon powder

You'll want to use the internal method when you see overlap of the crystalline and amorphous regions (i.e., in frames containing a continuous Debye ring) and only for materials with a single crystalline peak or unresolvable peaks in the crystalline region. While this method can be used for oriented peaks, the external method is better suited for such materials. For unoriented materials, the start and end χ values for the background must equal those of the peak. Otherwise, the region bounded by the difference in the χ values is also considered amorphous.

1. Before using the internal method, you'll need to determine the boundaries. To determine the boundaries of the crystalline and amorphous regions, integrate the areas using PEAKS or DIFFRAC^{plus} Profile (an optional package), and use profile fitting to deconvolve the crystalline and amorphous peaks. If you use PEAKS, do not use the default peak function (which is too sharp). Instead, model the peak with PEAKS/SIMULATE with an appropriate FWHM.

The final fitting will show the extent (2 θ limits) of both peaks.

2. Enter these values for the lower and upper limits of this function.
3. Set the crystalline peak 2 θ limits but not so far out that the polynomial option for the amorphous background would be modeled as a straight line. One approach to determine if you've met this condition is to first compute the crystallinity based on a linear background, then compare the results computed under the same conditions with a polynomial background. The linear background should provide an upper limit to the crystallinity value. The extent in χ is arbitrarily chosen.
4. To be confident in your results, repeat the measurements on the same system, and obtain identical values of all angles (as these are necessary).

External Method (PERCENT_CRYSTAL/EXTERNAL)

The external method is used for oriented polymers.

1. To determine the boundaries of the amorphous region, integrate this area using PEAKS or DIFFRAC^{plus} Profile (an optional package). If you use PEAKS, do not use the default peak function, which is too sharp. Instead, model the peak with PEAKS/SIMULATE with an appropriate FWHM.

The final fitting will show the extent (2 θ limits) of the amorphous region. The amorphous region, rather than the region containing both crystalline and amorphous scatter, will give the best information on the extent of the amorphous scatter.

2. Enter these values for the lower and upper limits on the amorphous external function. The same 2 θ limits can also be used for the crystalline region.
3. Examine the crystalline region with a 2 θ integration to determine the boundary in χ to set for the crystalline scattering.

Note that the "crystalline region" must also contain amorphous scatter. However, this region must not overlap with the previously selected "amorphous region." The amorphous χ range does not have to match the crystalline χ range. The area of the amorphous region is scaled to the area of the

crystalline region. There can be multiple, oriented crystalline peaks in the crystalline region, unlike the internal method. The amorphous region must have no crystalline scatter within its boundaries. If the sample has unoriented crystallites, the external method will include this scatter in the amorphous component. This will lead to a lower crystallinity. If the amount of material that is randomly oriented is constant, this method is still valid as a relative measure of crystallinity.

4. Set the boundary for the crystalline scattering.

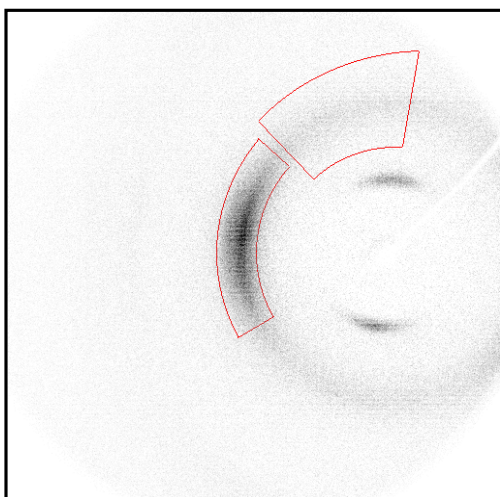


Figure 8.4 - γ -Nylon fiber

Full Method (PERCENT_CRYSTAL/FULL)

The full method is best to use when amorphous scattering has texture.

1. Before using PERCENT_CRYSTAL/FULL, collect data so that the background is well determined (that is, so that the pixel-to-pixel variation is within 3σ).

To ensure an acceptable variation, use the box cursor (11 x 11 in 1024 mode) to examine the counting statistics. The background and the mean must be within 0.4 counts, and with $1/\sigma(I) = 0 \pm 1$ as you move the cursor around the background regions of the frame (i.e. non-crystalline, low amorphous content regions). Also, use the pixel cursor with the right mouse button to examine the actual pixel values at higher 2θ values. You should see little variation ($\leq 3\sigma$) between pixels. If these conditions are not met, add to the collected frame. After collecting a satisfactory frame, unwarp the frame and smooth it using CONVOLVE=2. Save this processed frame.

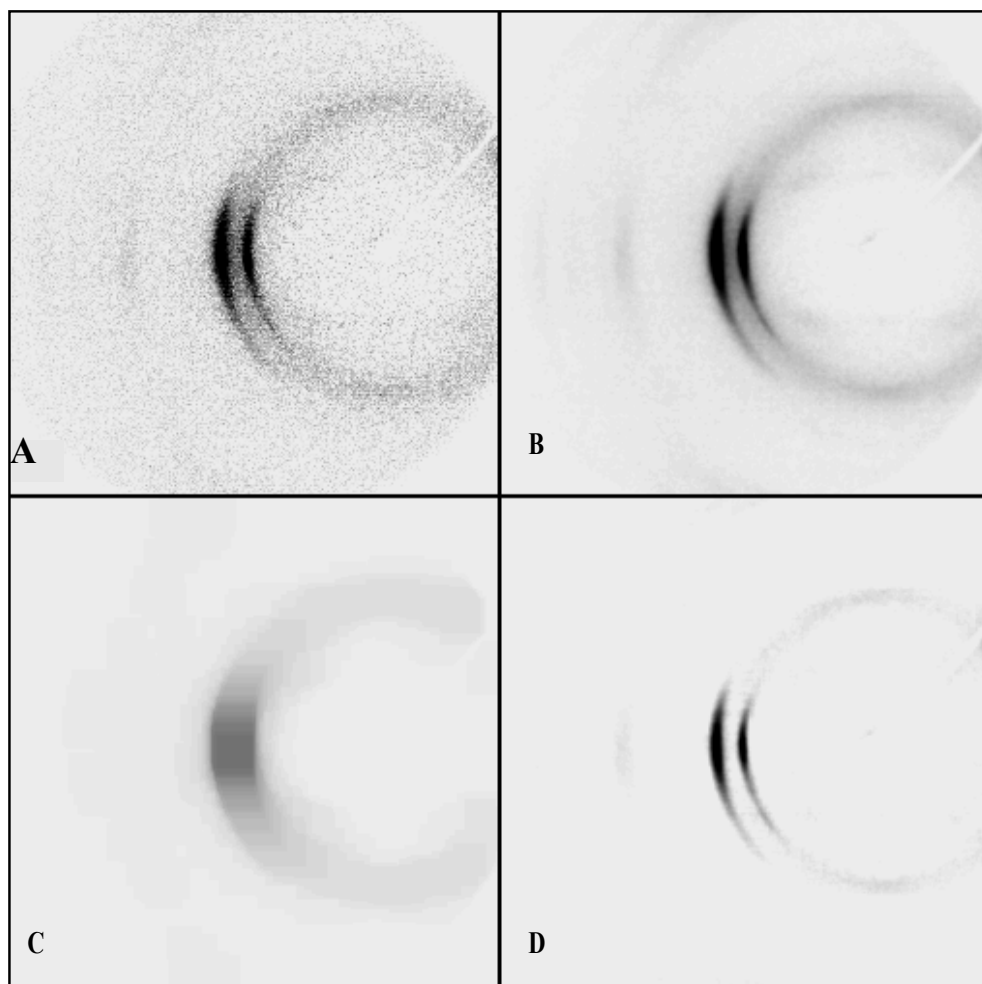


Figure 8.5 - A) Nylon fiber frame with air scatter removed, B) smoothed Nylon fiber frame with air scatter removed, C) amorphous scatter from PERCENT_CRYSTAL/FULL, D) crystalline scatter (difference frame of A and C)

2. Enter PERCENT_CRYSTAL/FULL, and start with the defaults to see what part of the crystalline pattern appears.

The radius and height parameters affect the shape of the “sliding ellipsoid” used to characterize the non-crystalline scatter. The smaller the radius parameter, the closer the background surface follows the frame image. The height parameter affects the shape of the “sliding” ellipsoid. A height of zero obtains a disk. A height equal to the radius parameter produces a sphere.

3. Adjust the pattern as appropriate:
 - If the crystalline peaks are sharp, increase the height parameter.
 - If no crystalline features appear on the frame with the default values, decrease the radius parameter until a crystalline pattern is observed. Then, increase the radius until the resultant pattern is free of the crystalline scatter. The initial radius can be determined with the vector cursor. Set the cursor normal to a diffraction feature.
4. Record the length of the cursor (D-pixel) from the statistics at the end of the screen. Half the D-pixel value gives the radius needed for the PERCENT_CRYSTAL/FULL input screen.

The resulting frame from PERCENT_CRYSTAL/FULL is an unwarped amorphous scattering frame.

5. Save the final frame under a new name. To obtain the crystalline scattering frame, use FILE/LOAD with the original, smoothed frame as the input file and the amorphous scattering frame as the background file using the argument /SCALE = -1.

8.2.2 Application Examples

Depth-Dependent Percent Crystallinity

The GADDs system has high spatial resolution by virtue of its finely engineered point source and optics of fine magnification. This magnification enables sample properties to be characterized as a function of depth. For example, skin-core effects in polymer sheets can be studied in transmission through thin sections. The most convenient stage for such an operation is the XYZ stage, though any stage can be used.

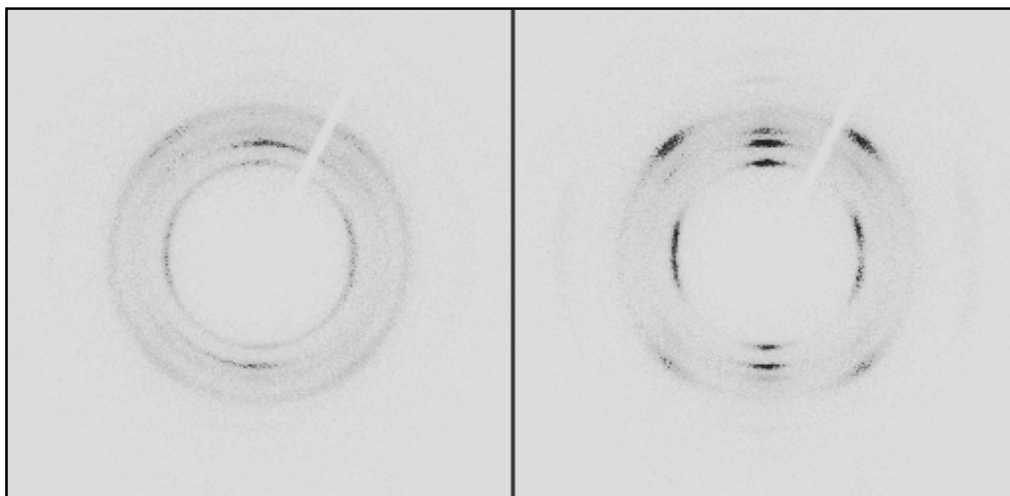


Figure 8.6 - Depth-dependent crystallinity measurements on polypropylene-based material 200 μm apart

Percent Crystallinity of a Fiber

Fibers are the most challenging samples for data collection (and, therefore, determination of percent crystallinity). Usually, the fiber axis is close to the chain orientation direction in a fiber. This is described as the *meridional* direction. The direction normal to the fiber axis is defined as the *equatorial* direction. Fibers are usually rotationally symmetric. In other words, if a fiber were mounted vertically, the same diffraction pattern would be observed regardless of the ϕ setting. For any given 2θ range, a single sample position is required to obtain orientation information in an equatorial plane. The meridional reflections usually have a maximum intensity at the Bragg angle. This means that for an arbitrary sample position with respect to the incident beam, different percent crystallinities would be determined based on the amount of the meridional reflection in the scan. To determine the percent crystallinity, all reflections that are not on the equator must be scanned. The scanning of the sample introduces a pseudo-randomization of the pattern. The equatorial, amorphous, and random components have one Lorentz correction, and the meridional reflections have another. In order to weight these classes of reflections appropriately:

1. Determine the angle of rotation about ϕ or ω that includes the meridional reflections for the same time as the equatorial reflections.

(This is equivalent to having a powdered specimen.)

2. Determine the breadth of the rocking curve of the meridional reflections.
3. Set the scan range in COLLECT/SCAN to start at $-\frac{1}{2}$ the reflection breadth from the peak maximum, and set the scan width to the reflection breadth. If multiple frames are necessary to collect data out to $68^\circ 2\theta$ (with Cu radiation), take great care when integrating χ in overlapping 2θ regions. Try to obtain all of the meridional and equatorial reflections in one frame at low angles. Usually, the meridional reflections on most fibers become very weak above $30^\circ 2\theta$.

In merging the integrations from the frames for profile analysis with DIFFRAC^{plus}Profile, use the following scheme:

1. Subtract a background scattering frame from each frame using FILE/LOAD with the /SCALE = -n qualifier which scales the background frame to the time of the data frame. If the sample is broader than the beam, use an attenuation factor. GADDS obtains the scale factor from the absorption formula

$$I_t/I_0 = e^{-\mu t}$$

where μ is the linear absorption coefficient of the material and t is its average thickness. For C, H compounds, the absorption is usually less than 3%. Therefore, if the

background frame and the data frame were collected for the same time, the scale factor would be -0.97, instead of -1.00.

2. Integrate each frame, setting χ to a unique part of reciprocal space, usually a quadrant.
 3. If two or more frames are required in χ to obtain all the scattering, check the χ limits so the regions integrated over do not overlap.
 4. Use the MERGE utility with the /S switch to merge adjacent frames in 2θ and the same range in χ .
 5. Use the "Add./Subt." feature in the (optional) DIFFRAC^{plus}EVA toolbox to merge the adjacent frames in χ and overlapping in 2θ . Alternatively, use a profile fitting technique to obtain the integrated area for both the crystalline and amorphous peaks. Remember to subtract the intensity contribution caused by Compton scattering before obtaining the integrated area for the amorphous and crystalline peaks.
1. Polymer percent crystallinity measurements are performed in transmission. Remember to use the beam stop.
 2. The collimator size should be selected that is as near as possible to the diameter of the sample. This reduces parasitic air scatter. The trade-off here is that for single filaments, which are typically under 50 μm in diameter, data collection times may be prohibitively long. As a compromise, use a larger collimator and subtract a background frame collected under the same conditions in the absence of the sample.
 3. Collect a background frame using a length of time long enough to ensure that statistically reliable corrections can be made.
 4. Subtract this frame from the original frame using FILE/LOAD with the /SCALE = -n qualifier which scales the background frame to the time of the data frame. If you observe significant absorption in the polymer sample, scale the background frame so that the parasitic scattering around the beam stop is reduced to near zero. For 0.3 mm or larger collimators, use the 6° beam stop. Otherwise, use the 4° beam stop.

The following discussion applies to a single filament or a carefully prepared fiber bundle. Preparation of a multiple fiber bundle should be done so that all of the fibers are oriented in the same direction and under the same tension. Loose filaments are undesirable. Keep in mind that the X-ray beam is only 0.5 mm or less in diameter, so every fiber contributes to the diffraction pattern.

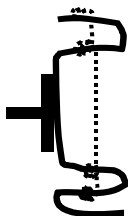


Figure 8.7 - Wire fiber holder attached to an SEM specimen mount. The dashed line is a fiber

5. Tie a fiber (no longer than 2 cm) on a wire frame such as a paper clip fashioned as shown in Figure 8.7. The distance from the fiber to the back portion of the frame should be no longer than 1.5 cm.
6. Affix the fiber frame with wax or clay to an aluminum SEM specimen holder (available from electron microscopy supply houses). Then mount the holder in the goniometer head. The goniometer head used for mounting fibers should be of the eucentric type. This allows fine adjustment of the physical fiber axis with respect to the goniometer axis.

The wax should have good adhesion properties at temperatures up to 40°C and should not undergo elastic relaxation.

7. Align the physical fiber axis vertically, using the two-position χ stage (or the fixed χ stage with an adapter mount). With this arrangement, you can observe a meridional reflection up to 30° with the detector at 6 cm. For

the ¼-cradle, this restriction is removed by placing $\chi = 0^\circ$.

8. Use COLLECT/GONIOMETER/FIXED AXES to set $\chi = 0^\circ$. If the fiber is instead mounted at 54.74°, do not update the χ value. If you must collect angles >30° on the meridian, physically remount the sample so that the fiber axis is horizontal. For those measurements, update χ to 90°.

Percent Crystallinity of a Sheet

Polymer sheet data collection is similar to that for reflection samples. The difference is that in transmission with the detector at 6 cm, the complete Debye rings are on the detector. The preparation of the specimen is very important. To mount polymer films that are rigid, you can clip and hold them in place using a small alligator clip and mount the clip to a goniometer head. If the film is not rigid, you may be able to trim the piece and mount it in the fiber (paper clip) frame.

The width of the sheet should be equal to the sheet thickness, if possible. Otherwise, the reflections arising from planes parallel to the surface will not be proportional in intensity to those out of plane. The total transmitted intensity is a linear function of the sample thickness (t) multiplied by an attenuation factor:

$$I_{\text{transmitted}}/I_0 = t e^{-\mu t}$$

where μ is the linear absorption coefficient of the material. Differentiating this equation, the optimal thickness of the sheet to obtain the maximum transmitted intensity is found to equal the inverse of the material's linear absorption coefficient.

You should align the polymer sheet similar to that of a fiber, except that you should set a machine direction along the ϕ axis. Once the sheet is in place, so that the sheet normal is along the microscope axis, update $\phi = 0^\circ$ with COLLECT/GONIOMETER/FIXED AXES. If the

sheet is supported, make sure the X-ray beam does not hit the frame during rotation. If hit, an intensity of zero will be merged with a positive intensity collected at another orientation.

Reflection Data Collection

Reflection mode data collection for percent crystallinity measurements is performed in a similar manner as transmission work, except that only 45% of the diffraction sphere is available. This low percentage is not a problem for powdered samples, because the sample is rotated and ω is scanned over 2° during data collection. The low percentage does become a problem for plate and needle samples, however. For these samples, prepare or mount the sample such that the unique axis or plate normal is not along a rotation direction. This holds true for other samples with preferred orientation as well.

A check to see if most or all of the preferred orientation was eliminated is to overlay a PDF card with the intensities corrected for "variable slits." These patterns are from randomly-oriented specimens. If the measured intensities show the same trend, then the data can be used for percent crystallinity determination.

8.3 References

1. L. E. Alexander, *X-Ray Diffraction Methods in Polymer Science* (Krieger Publishing Company, Malabar, Florida, 1985).
2. International Tables for X-ray Crystallography, Vol. III (Kynoch Press, Birmingham, 1968).
3. N. S. Murthy and H. Minor, "General procedure for evaluating amorphous scattering and crystallinity from X-ray diffraction scans of semicrystalline polymers," *Polymer* **31**, 996-1002 (1990).
4. N. S. Murthy, H. Minor, M. K. Akkapeddi, and B. Van Buskirk, "Characterization of Polymer Blends and Alloys by Constrained Profile-Analysis of X-Ray Diffraction Scans," *J. Appl. Polym. Sci.* **41**, 2265-2272 (1990).
5. K. B. Schwartz, J. Cheng, V. N. Reddy, M. Fone, and H. P. Fisher, "Crystallinity and Unit Cell Variations in Linear High-Density Polyethylene," *Adv. in X-Ray Anal.* **38**, 495-502 (1995).

9. Small-Angle X-ray Scattering

9.1 Principle of Small-Angle Scattering

The physical principle of small-angle X-ray scattering (SAXS) is the same as for wide-angle X-ray scattering (WAXS). Both techniques observe the coherent scattering from a sample as a function of the electron distribution in the sample. A simple difference between the two is that WAXS has a diffraction 2θ angle range of 0.5° to 180° , while SAXS is in the range from 0° up to roughly 2 or 3° . WAXS normally deals with long range periodicity in all three dimensions with the d-spacing range from a fraction of 1\AA to 10\AA ($< 1\text{ nm}$). The crystal structures of most inorganic and organic materials fall into this category. The SAXS covers the size range between 10\AA and 1000\AA ($1\text{--}10^2\text{ nm}$), depending on the collimation system, and not necessarily with long range order within each particle. The size, shape, and distribution of the particles are normally observed with SAXS.

With the HI-STAR area detector, the SAXS data can be collected at high speed. Anisotropic features from specimens, such as polymers, fibrous materials, single crystals, and bio-materials, can be analyzed and displayed in two-dimension. De-smearing correction is not necessary due to the collimated point X-ray beam. Since one exposure takes all the SAXS information, you can easily scan over the sample to map the structure information from the small-angle diffraction.

9.1.1 General Equation and Parameters in SAXS

SAXS pattern represents the scattering variation due to the point-to-point variations in electron density. The variation can be expressed by the scattering amplitude of the X-ray illuminated volume V by the following transformation,

$$A(\vec{q}) = A_e(\vec{q}) \int_V p(\vec{r}) \exp(-i\vec{q} \cdot \vec{r}) d^3r \quad (9-1)$$

\vec{q} is the scattering vector with modulus

$$q = \vec{q} = \frac{4\pi}{\lambda} \sin\theta, A_e(\vec{q}) \text{ is the scattering ampli-}$$

tude of a single electron, \vec{r} is the vector that defines the position of a point relative to an arbitrary origin, and $p(\vec{r})$ is the spatial distribution of electron density. SAXS deals with the size range well above the interatomic distance, so

that $p(\vec{r})$ can be approximated as a continuous variable of the position \vec{r} in the specimen. The actual measured intensity is given by the product amplitude $A(\vec{q})$ and its complex conjugate $A^*(\vec{q})$.

$$I(\vec{q}) = A(\vec{q}) \cdot A^*(\vec{q}) = I_0 \left| \int_V p(\vec{r}) \exp(i\vec{q} \cdot \vec{r}) d^3r \right|^2 \quad (9-2)$$

where I_0 is a constant defined by the conditions of the SAXS instrument. The intensity distribution (SAXS pattern) as a function of \vec{q} is uniquely determined by the structure in terms of its electron density distribution. In principle, the structure can be uniquely determined from the SAXS pattern. For instance, if the scattering is spherically symmetric (i.e., $I(\vec{q})$ depends only on q), then we have

$$I(q) = 4\pi \int_0^\infty p(r) \frac{\sin qr}{qr} dr \quad (9-3)$$

where $p(r)$ is the so-called pair-distance distribution function (PDDF) which gives the number of difference electron pairs with a mutual distance between r and $r+dr$ within the particle. We can see that, like the electron spatial distribution

function $p(\vec{r})$, $p(r)$ is a function of the structure. $p(r)$ is given by the inverse transformation from the scattering intensity

$$p(r) = \frac{1}{2\pi^2} \int_0^\infty I(q) qr \sin(qr) dq \quad (9-4)$$

The equation gives the direct relationship between the measured scattering intensity $I(q)$ and the PDDF $p(r)$. More basic equations for the SAXS can be found in a number of textbooks and literature listed at the end of this section.

9.1.2 X-ray Beam Collimation

The collimation system defines the size, shape, and divergency of the X-ray beam. The collimation also determines the resolution of a SAXS system. When GADDS is used for SAXS, either the supplied pinhole collimators or custom made collimators are used for the system, depending on the required achievable resolution. Figure 9.1 shows the collimation of the SAXS system with pinhole collimator, sample, beam stop, and detector. The primary beam, consisting of parallel and divergent components, is blocked by the beam stop. The maximum angular resolution α_{\max} is given as

$$\alpha_{\max} = \alpha_1 + \alpha_2 \quad (9-5)$$

where α_1 is the maximum angular divergence of the incident beam, which is given in Table 2.7 of section 2 denoted as β . And α_2 is the maximum angular deviation of the X rays recorded in the detector, defined by the beam spot on the sample (D) and the resolution element of the detector (d). D is listed in the same table as above, and the spatial resolution $d=0.2$ mm for HI-STAR detector.

$$\alpha_2 = \frac{D+d}{L} \quad (9-6)$$

The resolution R , defined as the theoretically largest Bragg spacing, is given as

$$R = \lambda / \alpha_{\max} \quad (9-7)$$

where λ is the wavelength of the X-ray radiation. R is so chosen, that for a lattice spacing smaller than R , the angle between two consecutive orders of Bragg-reflections is larger than α_{\max} . The actual achievable resolution is also limited by the beam stop size (B_s), and the resolution limit of beam stop (R_{BS}) is given as

$$R_{BS} = \lambda \cdot \frac{2L}{B_s} \quad (9-8)$$

The typical beam stop size is 4 mm in diameter for the GADDS He-beam path and vacuum beam path. The pinhole scattering is defined as the scattering from the pinhole materials (second pinhole in Figure 9.1).

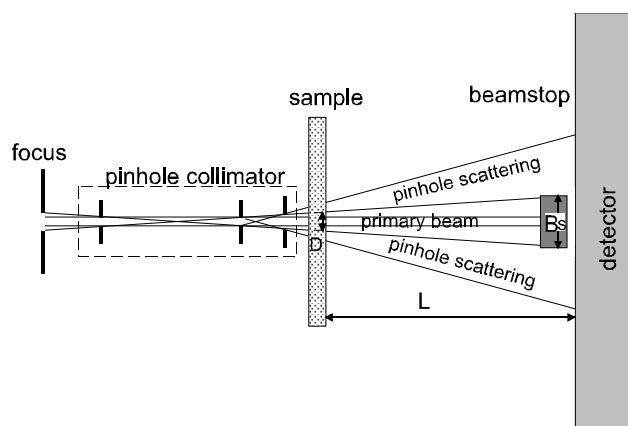


Figure 9.1 - Pinhole collimation for SAXS

The region of the pinhole scattering is limited by the anti-scattering pinhole (third pinhole). The size of the anti-scattering pinhole should be small enough to block as much pinhole scattering as possible, but not so small as to 'touch' the primary beam. The pinhole scattering, observed as a halo around the shadow of the beam stop, is also called parasitic scattering. If the scattering signal from the sample is much stronger than the parasitic scattering, or if the halo is evenly distributed around the beam stop, the parasitic scattering will not limit the achievable resolution. Some efforts are necessary to reduce the parasitic scattering, such as using high parallel beam (Göbel mirrors), smaller pinhole size and appropriate pinhole combination. Table 9.1 lists the beam divergence (α_1), the primary beam stop on the sample (D), the maximum angular resolution (α_{\max}), the resolution (R), and the resolution limit of beam stop (R_{bs}) for various collimator sizes (0.05 mm to 0.5 mm) at a sample-to-detector distance of 300 mm. It can be seen that the beam stop determines the achievable resolution for most cases.

Table 9.1 – The resolution power of various SAXS configurations

Sample-Detector Distance: L=300 mm					
Collimator	α_1 (°)	D (mm)	α_{\max} (°)	R (Å)	R_{bs} (Å)
Graphite Monochromator					
0.05	0.04	0.071	0.09	951	231
0.10	0.08	0.143	0.15	599	231
0.20	0.16	0.286	0.26	344	231
0.30	0.23	0.418	0.34	257	231
0.50	0.27	0.639	0.43	207	231
Göbel Mirrors					
0.05	0.04	0.071	0.09	951	231
0.10	0.06	0.131	0.12	716	231
0.20	0.06	0.231	0.14	620	231
0.30	0.06	0.331	0.16	546	231
0.50	0.06	0.531	0.20	442	231

9.2 Data Collection and Analysis

9.2.1 SAXS Attachments Installation

Figure 9.2 shows the beam stop assembly attached to the HI-STAR detector.

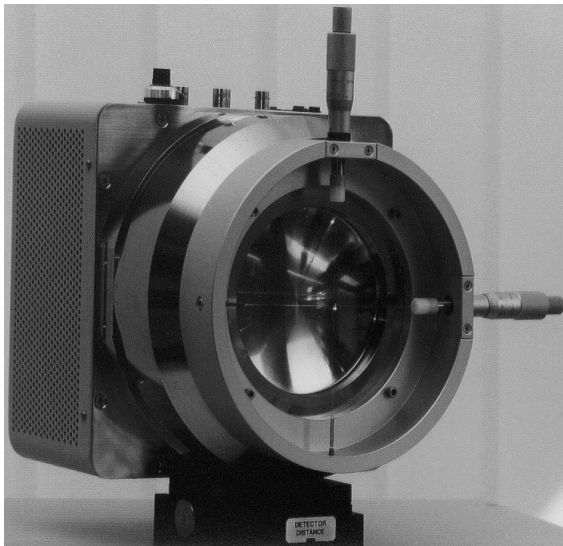


Figure 9.2 - Small-angle scattering beam stop attached to HI-STAR detector

Figure 9.3 shows the Helium beam path attached on the beam stop assembly.

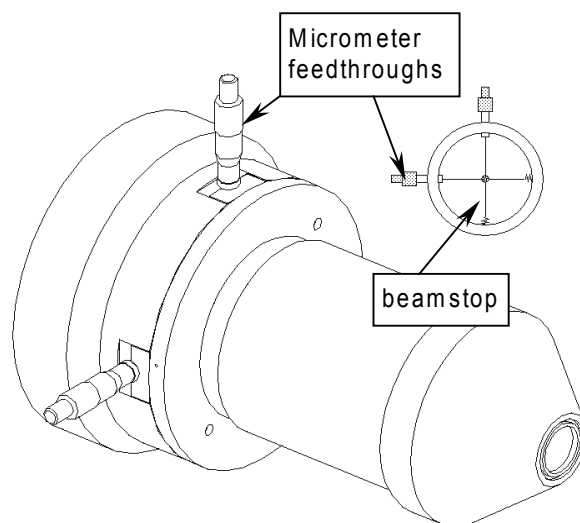


Figure 9.3 - Helium beam path for small-angle X-ray scattering measurement. The cross section shows the beam stop and adjustment micrometer feedthroughs

The beam stop is attached through nylon wires to two linear motion feedthroughs. The beam stop can be positioned accurately to the X-ray beam center. In order to reduce the air scattering, a He-beam path is normally attached to the beam stop assembly as follows.

1. Attach the beam stop to the detector first, ensuring that the beam stop flange mounts flush against the gasket on the detector face.
2. Apply a small amount of vacuum grease to the gasket surface before attaching the Plexiglas cones. This ensures a gas-tight seal.
3. If the gasket does not have precut holes through which the alignment pins for the fiducial plate extend, then remove the alignment pins. And use the threaded standoffs to secure the beam stop assembly to the detector.
4. Attach the Plexiglas cone to one of the Plexiglas rings before inserting the ring in the Plexiglas base. Grease the large O-ring, then insert it in the groove on the Plexiglas base.
5. Attach the Plexiglas assembly to the beam stop using four long screws. The orientation should be such that the gas inlet and outlet tubes are vertical. The range of the sample-to-detector distance for use with the helium beam path is approximately 15–30 cm.
6. Before attaching the helium line, you may mount a user-supplied bubbler (a water-filled, U-shaped glass tube) to the bottom gas port with 1/16th inch rubber tubing. This device helps regulate the gas pressure and gives a visual indication of the flow rate.
7. Attach the helium line to the top port. Use the lowest pressure setting on the gas cylinder's regulator. Failure to do so may cause the front cone to be propelled into the collimator support.
8. Though not a critical parameter, increase the helium's flowrate slowly, watching for bulging of the front Mylar window. Significant bulging indicates too high a pressure (and too high a flowrate). Typical purge rates are in the range of 100–500 cc/min. Once the cone has been initially purged of air (elapsed time typically 30–60 min), a lower flowrate may be maintained. You may experimentally determine the required purge time (as a function of the specific flow conditions) by collecting frames at intervals and observing the decrease in background scatter with time.

If the SAXS beam stop attachment is to be used with our high-temperature attachment, we recommend operating the heater without its shroud. Otherwise, the plastic shroud material will contribute undesirable scatter.

9.2.2 SAXS System Adjustment and Calibration

Selecting a Collimator

The most critical part of the operation is to find a suitable pinhole collimator to reduce parasitic scattering but not sacrifice too much of the beam intensity. Ideally, you should use the smallest available collimator, 50 μm or 100 μm . The limiting factors are data collection time and desired resolution. While the pinholes cannot be repositioned within the standard collimator tube, you may try different combinations of pinholes to reduce parasitic scatter. The beam stop diameter (4 mm) and the available collimator sizes limit the achievable resolution. This resolution is 200–250 Å (at the edge of the beam stop) for a He-beam path (with the detector positioned at 30 cm), using 1024x1024 frames and copper radiation.

Performing a Flood-Field Correction

Initial flood-field and spatial corrections were done before installation of the beam stop and the beam path, and these corrections may be adequate depending on your needs. For instance, some users collect flood-field data with the beam stop in place, while others contend that a linear flood-field is adequate with the detector at 30 cm and beyond. The same holds true for the spatial correction with the fiducial plate. However, if the scattered image occupies only the center part of the detector and you wish it to cover more, you can use an alternate correction method to refine the flood-field and obtain smoother images. You initiate that method with the FLOOD/REPROCESS \$1 \$2 /XMIN /YMIN /MAG command (see the SAXS Software Reference Manual, 269-0204xx, section 5.1.4). With this command, you can increase the number of pixels per degree using a selected area of the detector. This is an electronic interpolation technique, which produces smoother images. For example, the command:

```
FLOOD/REPROCESS NORMAL._PJ  
ZOOM._FL /XMIN=4096/YMIN=4096/  
MAG=2
```

will use a quarter of the detector about the beam center. The number of pixels will remain 1024x1024 starting from the origin XMIN, YMIN, but each pixel is now 50 μm , instead of the usual 100 μm . The maximum recommended magnification is 4.

Adjusting the Beam Stop

1. Adjust the X and Y micrometers to visually position the beam stop in the center of the detector.
2. Position the glassy iron foil in the X-ray beam path. At low generator power, open the shutter. Alternatively, the Fe^{55} source may be used.
3. Perform a 30-second ADD. Display the frame with a maximum display count of 1. The position of the beam stop should be evident on the frame by the image of a dark circle.



CAUTION

Avoid exposing the detector to the direct beam. To avoid detector damage, never let the intensity exceed 200 CPS/pixel.

Three situations can occur:

1. No direct beam is observed. In this case, if a rotating anode generator is used, open the shutter and allow the beam to warm the beam stop at the power level to be used during the measurement for approximately 30 minutes prior to final beam stop adjustment.
2. Part of the direct beam is observed. In this case, move the beam stop to block the direct beam.

3. The direct beam is not obscured by the beam stop. In this case, follow correction in 2) above.

For 1024x1024 frames with $\text{MAG} = 1$, each pixel is approximately $100\text{ }\mu\text{m}$. Use the vector cursor to determine the number of pixels from the beam center to the beam stop center, and adjust the micrometers accordingly.

4. To finely align the beam stop, set the generator power to the level to be used for data collection and make any necessary adjustments as follows. Assuming perfectly aligned pinholes, the scattering about the X-ray axis is symmetrical. Therefore, remaining scatter around the beam stop, if any, should also be symmetrical. If the pinholes are not perfectly aligned (or positioned), the asymmetrical, parasitic scattering will be evident. With an Anton Paar HR-PHK, you can eliminate this parasitic scatter by adjusting the guard pinhole whose micrometer adjustments are located inside the sample chamber. For Göbel Mirrors and pinhole collimator systems, adjust the beam stop to eliminate as much of this scattering as possible.

Calibrating the Beam Center and Detector Distance

1. For accurate determination of the beam center and sample-to-detector distance, calibrate the beam center and detector distance using a calibration standard and materials, such as silver behenate (Figure 9.4). At 30 cm, you can observe five orders of silver behenate (00 l) reflections. Standard files (*.std) for calibration are located in either the SAXSSYSDATA: directory or the SAXISYSDATA directory. You can create additional calibration files with a text editor, such as NOTEPAD.
2. Collect a calibration frame using silver behenate powder sample as shown in Figure 9.4.

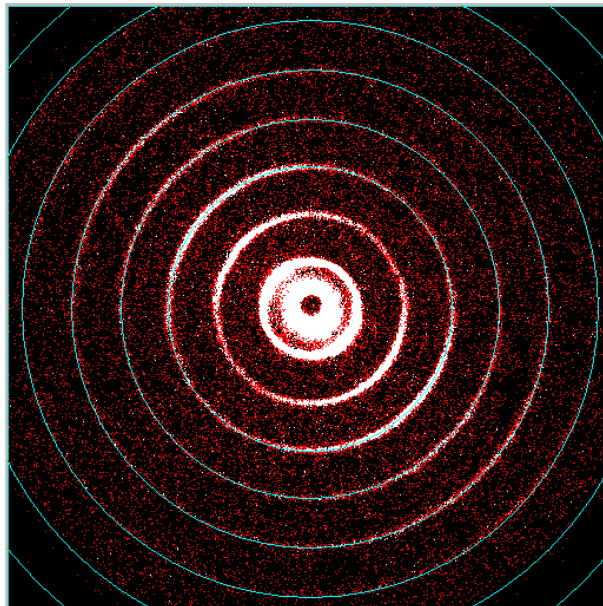


Figure 9.4 - Scattering pattern from silver behenate, a low-angle calibration material

3. Readjust the beam stop to the center of the beam by checking the shadow of the beam stop with the conic cursor (F9). The above calibration frame then redisplay with 4x magnification in Figure 9.5. The conic cursor shows that the beam stop position is higher than the true beam center.
4. In this case, you should readjust the beam stop until the calibrated conic cursor is concentric with the shadow of the beam stop.

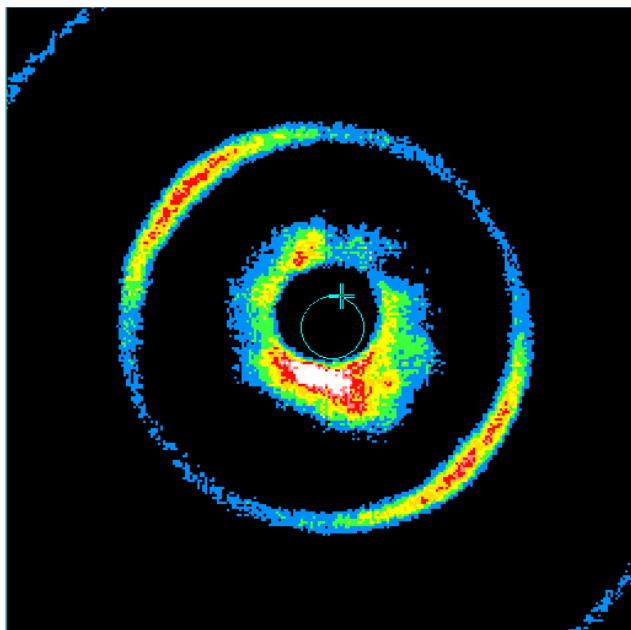


Figure 9.5 - The center of the beam stop is above the center of conic circle

9.2.3 Data Collection

A rat-tail tendon sample is used as an example of data collection and to test the SAXS performance. The SAXS result measured with NanoSTAR (a high-end system dedicated to SAXS) is shown as a reference in Figure 9.6. The frame is in the magnification of 2x. The chi-integration profile (in the chi range of 75–105°

and two-theta range of 0.2–2°) shows the second to above ninth order peaks of SAXS pattern from the rat-tail tendon sample. The scattering vector length q (nm^{-1}) is also marked above the profile plot. For Cu-K α radiation, the relation between q and $2\theta(^{\circ})$ is

$$q (\text{nm}^{-1}) = 0.71 \times 2\theta(^{\circ}) \quad (9-9)$$

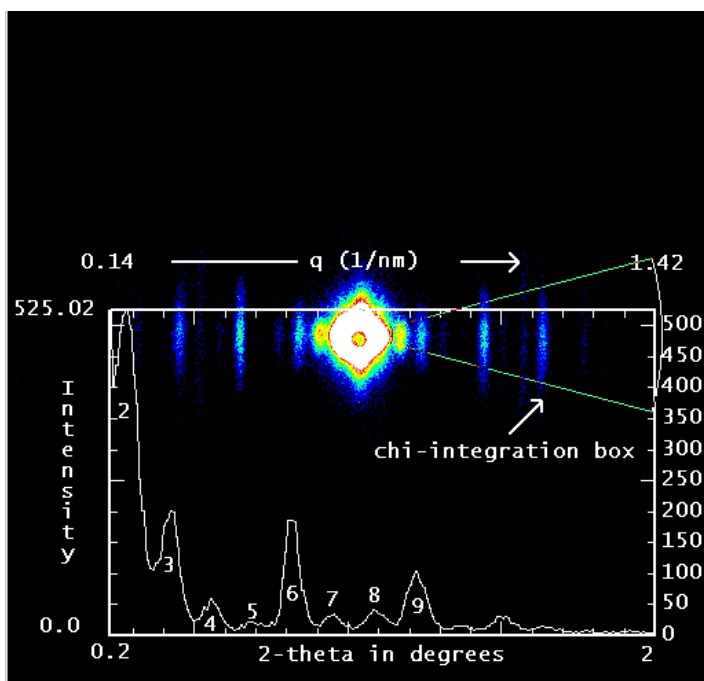


Figure 9.6 - The SAXS frame collected with NanoStar magnified by 2x on rat-tail tendon. The chi-integrated profile in the chi range of 75–105° and two-theta range of 0.2–2° shows the second to above ninth order peaks

The data frame collected with He-beam path (Figure 9.7) shows some parasitic scattering in the left of the beam stop, but most regions around the pinhole are free from parasitic scattering. Figure 9.8 shows the same frame in 8x magnification. The conic cursor marked the most achievable resolution, which is about 250\AA , equivalent to 0.35° in two-theta and $0.25\text{ (nm}^{-1}\text{)}$ in scattering vector length (q). This is

maximum resolution with 30 cm He-beam path, 0.1 mm pinhole collimator, 4 mm beam stop, and Cu tube. Figure 9.9 shows the data frame magnified by 4x. The chi-integrated profile in the chi range of $75\text{--}105^\circ$ and two-theta range of $0.3\text{--}2^\circ$ shows the third, sixth, and ninth order peaks of SAXS pattern from the rat-tail tendon sample.

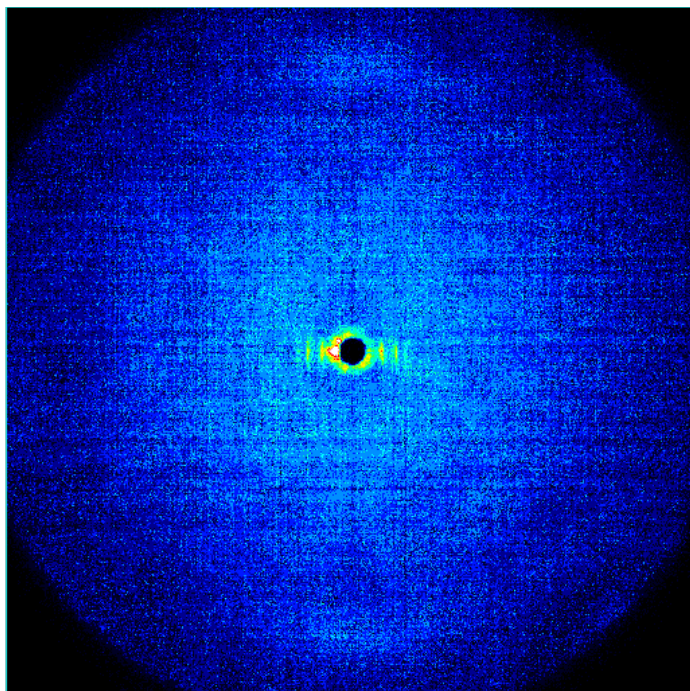


Figure 9.7 - Data frame collected from rat-tail tendon with He-beam path

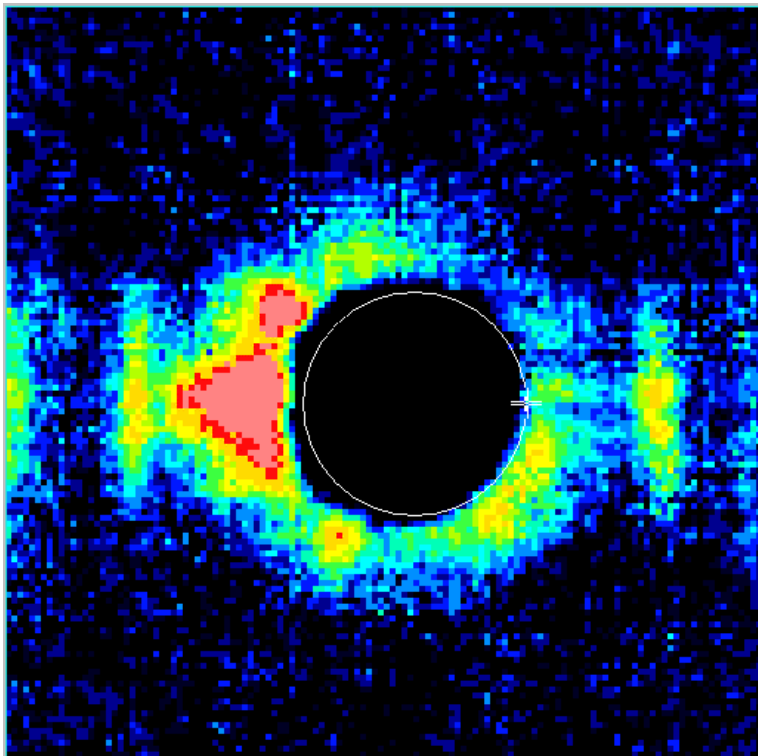


Figure 9.8 - Conic cursor shows the maximum resolution by the beam stop edge at $\chi=90^\circ$ is 248 Å

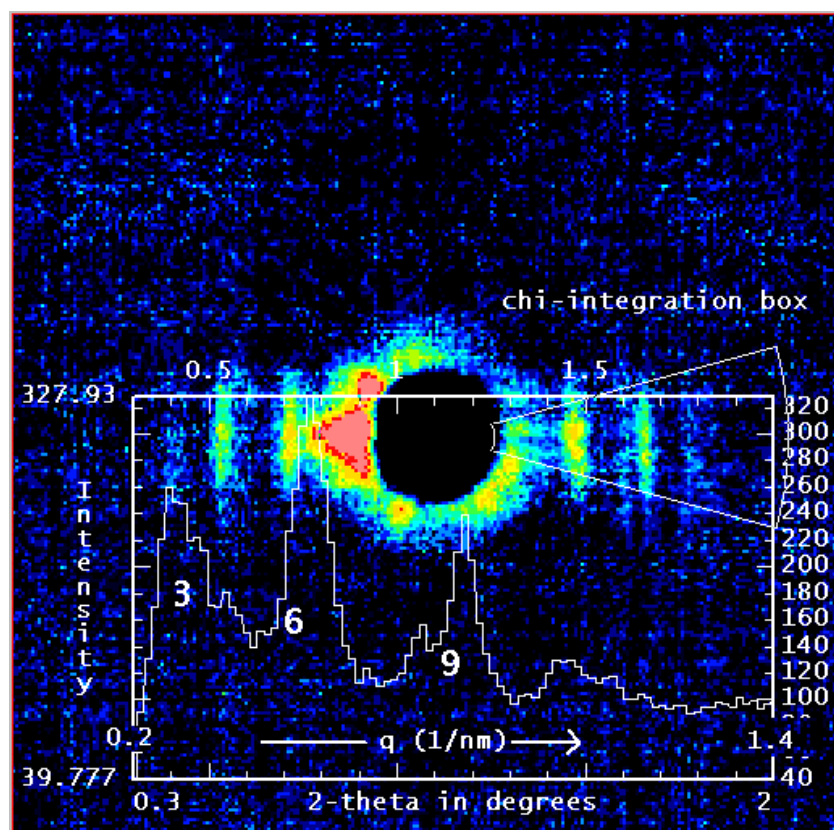


Figure 9.9 - The chi-integrated profile in the chi range of 75° to 105° and two-theta range of 0.3° to 2° shows the third, sixth and ninth order peaks of SAXS pattern from the rat-tail tendon sample

9.3 Applications Examples

Types of information obtainable from small-angle X-ray scattering include:

- Lamellar repeat distance (the distance from the center of one bi-layer to the center of its neighbor, which includes the thickness of associated water layers).
- Radius of gyration (the first moment of the scattering center distribution function).
- Large-scale structure (25 Å–5,000 Å with pinhole optics) and long-range order (distances between similar structures).
- For example, the pattern in Figure 9.10 can yield the arrangement of a column structure, its diameter, and the distances between columns.

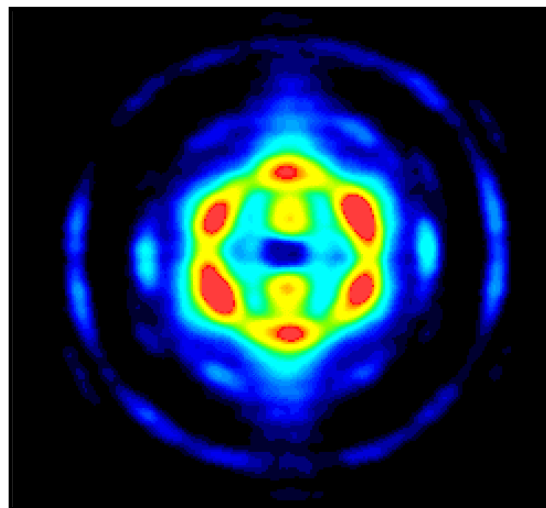


Figure 9.10 - Small-angle scattering pattern of a polymer sheet cross section showing a hexagonal columnar structure

Types of samples for small-angle X-ray scattering include:

- Polymers/fibers
- Wood products
- Detergents/surfactants
- Lipids/membranes.
- Liquid crystals
- Catalysts/ceramics
- Glasses

9.4 References

1. O. Glatter, *Small-angle techniques, International Tables for Crystallography, Volume C*, edited by A. J. C. Wilson, pp 89-112, (Kluwer Academic Publishers, Dordrecht, The Netherlands, 1995).
2. L. E. Alexander, *X-Ray Diffraction Methods in Polymer Science* (Krieger Publishing Company, Malabar, Florida, 1985).
3. F. J. Baltá-Calleja and C. G. Vonk, *X-ray Scattering of Synthetic Polymers* (Elsevier Science Publishing Company, New York, 1989).
4. S. Fakirov, Z. Denchev, A. A. Apostolov, M. Stamm, and C. Fakirov, "Morphological characterization during deformation of a poly(ether ester) thermoplastic elastomer by small-angle X-ray scattering," *Colloid Polym. Sci.* 272, 1363-1372 (1994).
5. P. Fratzl and A. Daxer, "Structural Transformation of Collagen Fibrils in Corneal Stroma During Drying: An X-ray Scattering Study," *Biophys. J.* 64, 1210-1214 (1993).
6. P. Fratzl, F. Langmayr, and O. Paris, "Evaluation of 3D Small-Angle Scattering from Non-Spherical Particles in Single Crystals," *J. Appl. Cryst.* 26, 820-826 (1993).
7. O. Glatter and O. Kratky, eds. *Small Angle X-ray Scattering* (Academic Press, New York, 1982).
8. A. Guinier, G. Fournet, C. B. Walker, and K. L. Yudowitch, *Small-Angle Scattering of X-Rays* (John Wiley, New York, 1955).
9. R. W. Hendricks, "The ORNL 10-Meter Small-Angle X-ray Scattering Camera. *J. Appl. Cryst.* 11, 15-30 (1978).
10. T. C. Huang, H. Toraya, T. N. Blanton, and Y. Wu, "X-ray Powder Diffraction Analysis of Silver Behenate, a Possible Low-Angle Diffraction Standard," *J. Appl. Cryst.* 26, 180-184 (1993).
11. H. P. Klug and L. E. Alexander, *X-ray Diffraction Procedures for Polycrystalline and Amorphous Materials*, 1st ed. (John Wiley, New York, 1954).
12. O. Paris, P. Fratzl, F. Langmayr, G. Vogl, and H. G. Haubold, "Internal Oxidation of Cu-Fe. I. Small-Angle X-Ray Scattering Study of Oxide Precipitation," *Acta Metall. Mater.* 42, 2019-2026 (1994).
13. "Proceedings of the VIIth International Conference on Small-Angle Scattering, Leuven," *J. Appl. Cryst.* 24, 413-877 (1991).

10. Script Files

Scripts (sometimes called macros) are a very powerful feature of the GADDS software. A script is a series of GADDS commands that you group together as a single command to accomplish a task automatically. That is, instead of manually performing a series of time-consuming, repetitive actions in GADDS, you can create and run a single script—in effect a custom command—that accomplishes the task for you. Thus, it is convenient (and accurate) to think of a script as a means for automating operation of the diffractometer or frame processing from a higher level.

Some typical uses of scripts are to:

- Automate repetitive tasks (commands) via a single command.
- Process samples in “batch” mode (without user intervention).
- Simplify menu input by hiding unneeded entries.

- Customize the menu-bar with “user-task” commands.
- Create demo loops for presentations.

Scripts are comprised of one or more script files, which are simply ASCII files that contain a list of commands, where each command is executed in sequential order. That is, GADDS simply starts at the beginning of the script file and proceeds one line at a time until it reaches the end, at which point it stops. You can create script files in two ways, using the auto-script recorder or a text editor. The auto-script recorder can help you get started creating scripts. After you've assigned a script to a user-task, running the script is as simple as clicking the menu item.

Bruker AXS script files are sometimes called SLAM files (for Scripting Lexical Analyzer and Monitor). By convention, Bruker AXS script files have the extension .slm. Wherever GADDs asks for the name of a script file, the .slm extension is assumed unless you specifically give a different extension.

For examples of script files, see the demo loop script files located in the %GADDs\$TEST:% directory (default is "C:\saxi\gadds32") or see the examples later in this section.

10.1 SLAM Command Conventions

Each command within a script is entered in the SLAM command line syntax, which is similar to the DOS command line syntax (and to DCL under VMS). You use this syntax to enter commands in either a script file or on the command line (at the GADDs> prompt). You do not use any special words (for example, "begin" or "end") in the script. Branching, logical, and conditional statements (Flow Control) was not allowed prior to release 4.0.14. Flow control is discussed later in Section 10.7.

To understand a SLAM command, you must become familiar with each component of a command. Either a space or a required slash delimits each component. For readability, we recommend always using spaces to delimit SLAM components.

Command verb:

Appearing first, the command verb (also called "name") identifies the command or group of commands and has the form <name>. You may abbreviate the verb, but the verb must have enough characters to be distinguished from all other legal command verbs.

Subcommand:

Whenever the verb designates a group of commands, it is immediately followed by a subcommand, which must begin with a slash character and has the form /<name>.

Commands will either always take a sub-command or never take a sub-command. The combination of command and sub-command directly relates to an entire dialog box in menu mode. A few commands are only available in command mode and do not have corresponding dialog boxes, such as the comment and the execute-script commands. You may abbreviate the subcommand, but it must have enough characters to be distinguished it from all other subcommands and qualifiers used for this verb.

Arguments:

The remaining components, parameters and both types of qualifiers, are collectively referred to as arguments. Each argument consists of an argument name, an argument value, or both. All argument names must begin with the slash character and have the form /<name>. All argument values consist of either a text string or a number. Any argument value that contains slashes or embedded spaces must be enclosed within double quotations (for example, /TITLE="My title has slashes and/or spaces"). Some arguments are required and if missing, the program will display that command's dialog box and wait for user input. Missing non-required arguments are defaulted to either the current default value or to "N" (for Yes/No input arguments).

Parameters:

Parameters consists of only an argument value and are recognized by the order in which they appear in the argument list. In the command syntax descriptions in this manual, "\$N" is used to refer to the Nth parameter in the list (for example, \$1 refers to the first parameter, \$2 refers to the second parameter). Up to ten parameters are allowed in a command, the tenth being \$0. Most parameter arguments are required.

Qualifiers:

Valued qualifiers and non-valued qualifiers are collectively referred to as qualifiers. Because they are identified by name, qualifiers may occur in any order after the command name and may be intermixed with parameters. Most qualifier arguments are not required. You may abbreviate the qualifier's name, but it must have enough characters to be distinguished it from all other subcommands and qualifiers used for this verb.

Valued Qualifiers:

Valued-qualifiers have the syntax /<name>=<value>, where <name> represents the name of the qualifier, and <value> is a text string (<S>) or numeric value (<N>). The value you specify for such a qualifier is related directly to the value you

specify for the corresponding input panel item in menu mode.

Non-valued Qualifiers:

Non-valued qualifiers have the syntax /<name>, and represents a corresponding menu-mode input-panel item which takes Y or N (for yes or no) as its value, which includes all check box entries. If the qualifier is present on the command line, the effect is the same as if Y (yes or checked) was specified for the corresponding input-panel item; if absent, the effect is an N (no or unchecked) entry.

Some parameters and valued qualifiers may use special variables as their value. These are: @1 which refers to the current value of the 2 θ axis, @2 for ω , @3 for ϕ , @4 for χ , @5 for X, @6 for Y, @7 for Z, and @8 for zoom. Release 4.0.14 added @9 for delta axis. Also, all parameter and valued qualifiers can take replaceable parameters (%1 to %0) for their value or partial value, as will be discussed later in section 10.3. Release 4.0.14 adds both replaceable variables (%A to %Z, see section 10.7) and new special variables (@P for project name, @Q for folder, @F for filename, @J for jobname, @R for frame run, and @N for frame number) which refer to the currently loaded frame. Release 4.1.13 adds additional special variables (@A for anode "Cu", @C for total counts, @D for description [project name], @S for seconds, @T for title [1st line], @W for wavelength [Kavg]) which refer to the

currently loaded frame. While special variables cannot be used in flow control statements, all variables and replaceable parameters may be used in any SLAM command. In release 4.1.13, all special variables can now be used in flow control statements.

Each SLAM command consists of one or more SLAM lines in the script file. SLAM lines are limited to 512 characters and SLAM commands are limited to 1024 characters. You can continue a long SLAM command on the next line by placing an ampersand at the end of the line, for example:

```
DISPLAY /NEW SAXI$TEST:cor30u.001 &  
/QUADRANT=0 /LO=0 /HI=100 &  
/X=255 /Y=255 /MAG=1
```

Because one purpose of script files is to operate the GADDS system in batch mode, you do not wish to suspend the execution of a script whenever a warning condition exists. Thus within script files, warnings are displayed for only a few seconds before they time-out and default to either OK or Yes. You may override the time-out by entering OK, Yes, or No at any time. You can also control the command mode time-out interval by using the Edit > Configure > User Settings (GADDS 4.x) or Edit > Configure > Edit (GADDS 3.x) command.

Finally, do not confuse SLAM syntax with startup qualifier syntax. While startup qualifiers, which are used when starting GADDS from icon

or command prompt window, allow either “:” or “=” between qualifier name and value, SLAM only recognizes the “=” convention. Also, SAXISWCHAR can be used to override the default switch character for startup qualifiers, but has no effect on SLAM qualifiers.

10.2 Executing Script Files

When the program is in command mode, you can execute a script file by using the @ command, which instructs the program to start accepting the SLAM commands within the script file as if each command was typed, one at a time, directly on the command line. You must specify the name of the script file immediately after the @ symbol. You may follow the filename with the optional replaceable parameters, as will be explained later in section 10.4.

The methods, for entering into command mode and starting a script file, are as follows:

- If you are already working in GADDS, you can execute the Special > Command Mode command, which will change GADDS operation from menu mode to command mode. The menu-bar becomes gray (disabled) and the command prompt (GADDS>) appears at the bottom of the window, where you enter the @ script command.
- You can start GADDS with the startup qualifier (/COMMAND) to immediately enter into command mode when starting GADDS. Then you enter the @ script command at the command prompt (GADDS>).
- You can start GADDS into command mode and immediately start executing the script by using the startup qualifier with the script command attached (for example, GADDS / COMMAND=@PhaseID).

- You can setup and use the script as a user task, as explained in section 10.5.

To interrupt a script while it is executing, press the control key combination <CTRL/C> or <CTRL/BREAK>. This will stop the script execution and exit from the script, returning the user to the program's command line prompt.

To exit command mode and return to menu-mode, simply type "menumode" and Enter on the command line by the GADDS> prompt. You may wish to add this Menumode command as the last command of the script, particularly for scripts called as user tasks.

Several example scripts are provided in your system. The scripts are stored in the GADDS\$TEST: directory and are used as part of the demo loop. To execute this demo routine on the frame buffer PC:

```
@GADDS$TEST:gadds
```

You can also start a script execution that uses replaceable parameter (see section 10.4). For example, to start a script that takes four replaceable parameters, the first is the filename, the second is the sample title, the third is the sample name, and the fourth is the scan time would look something like:

```
@PhaseID cor "My sample" Corundum 60.00
```

10.3 Creating Script Files

You can create and edit script files with any ASCII text editor such as NotePad (under NT). Word processors (Write, WordPad, Word or WordPerfect) do not work for creating script files! GADDS also contains an automatic script generating function, which logs each interactively executed command as the equivalent SLAM command into a script file (see the File > ScriptFile command for more details). To create your script file(s), you may either use the auto-script generating facility, an editor, or both. The example below uses both.

Problem

Suppose you simply wish to identify the phases of a sample, which is often called qualitative phase identification. You need to collect several frames so that the diffraction pattern will extend from 5 to 110 degrees in 2θ . Next you need to integrate the frame files into raw files. Finally, you need to merge the raw pattern into a single range for inputting into the search/match routine. Such mundane repetitiveness is ideally suited to using script files. So let's create a script for this purpose.

1. Decide which functions you wish to automate. By writing down the sequence of commands, you are less likely to omit a crucial step or invert the required order of commands. In our case, we need to use:
 - Scan > SingleRun to collect all the frames, one each at 20, 45, 70, and 95 degrees in 2θ .
 - Spatial > Unwarp to unwarp the frames prior to integration. Under GADDS 4.0, this step is automatically done during the scan command, but GADDS 3.X users must include this step.
 - File > Load & Peaks > Integrate > Chi (for each frame) to convert each frame into a raw range.
 - The external MERGE utility to convert the multi-range RAW file into a single-range RAW file.
 - The external EVA program in batch mode to perform the search/match operation.
2. Place your sample on the instrument or use the corundum sample. Optically align the sample. Because there is no automated way of mounting and aligning your sample, we will create the script procedure to begin after the GADDS user manually did this step.
3. Place GADDS menu's into level 2 using the Special > Level 2 command.

- Place GADDS into auto-script mode using the File > ScriptFile command. Give a file-name of "PhaseID" and an Append value of N (unchecked). GADDS will automatically add the .slm extension to the filename.

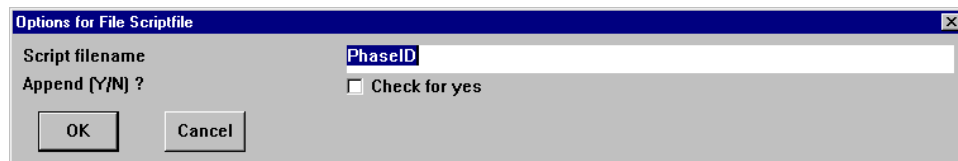


Figure 10.1 - Options for File Scriptfile

- For GADDS 3.X users, skip to step 6. For GADDS 4.0 users, each sample should reside in a separate project. (Alternatively, you may consider the project to be "qualitative phase identification" and thus all samples would belong to that project). Use the Project > New command. Give a new values for Project information and Directory information parameters. You may set Crystal information parameters to "?".

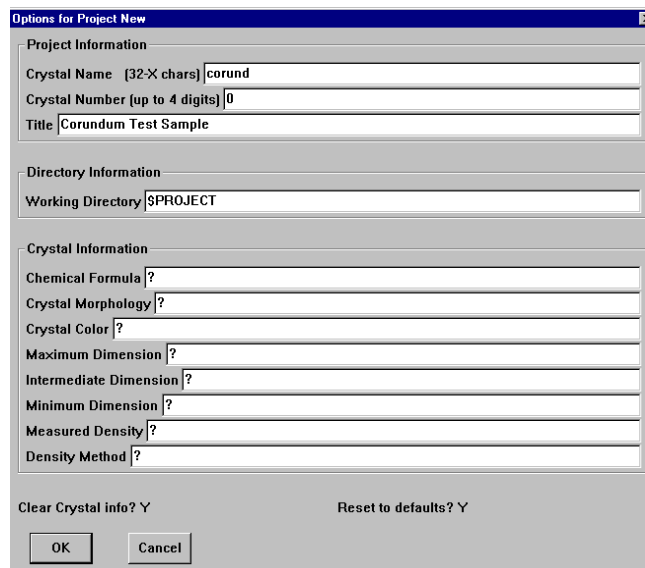
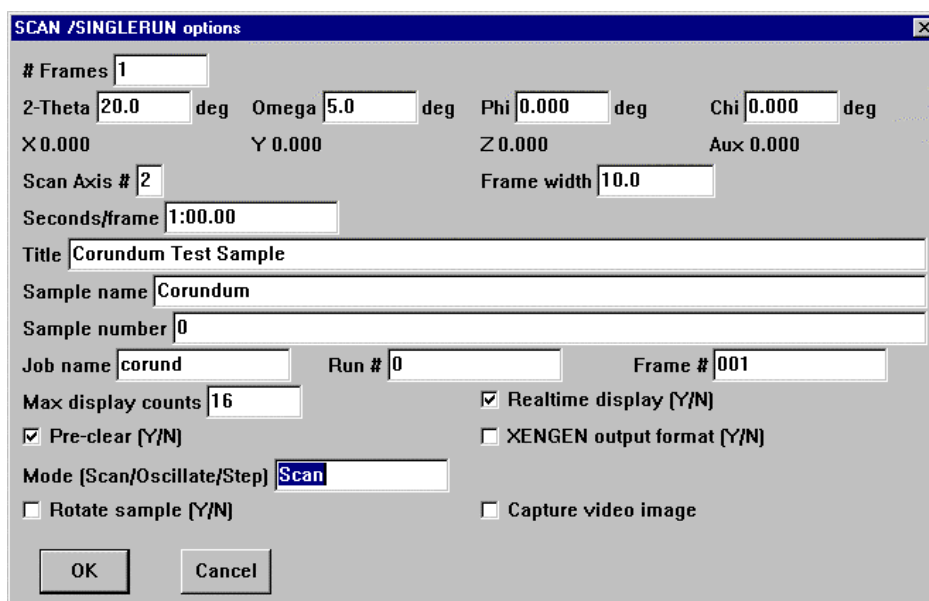


Figure 10.2 - Options for Project New

6. Collect first frame using the Collect > Scan > SingleRun command. Start at 20 degrees in 2θ and scan in ω from 5 to 15 degrees. Collect the second frame using another Collect > Scan > SingleRun command using 45 for 2θ , 17.5 (to 27.5) for ω , and 002 for frame number. Collect the third frame using another Collect > Scan > SingleRun command using 70 for 2θ , 30 (to 40) for ω , and 003 for frame number. Collect the last frame using another Collect > Scan > SingleRun command using 95 for 2θ , 42.5 (to 52.5) for ω , and 004 for frame number.



The image shows a dialog box titled "SCAN /SINGLERUN options". It contains various input fields and checkboxes for configuring a scan. The fields are as follows:

- # Frames: 1
- 2-Theta: 20.0 deg
- Omega: 5.0 deg
- Phi: 0.000 deg
- Chi: 0.000 deg
- X: 0.000
- Y: 0.000
- Z: 0.000
- Aux: 0.000
- Scan Axis #: 2
- Frame width: 10.0
- Seconds/frame: 1:00.00
- Title: Corundum Test Sample
- Sample name: Corundum
- Sample number: 0
- Job name: corund
- Run #: 0
- Frame #: 001
- Max display counts: 16
- ☒ Pre-clear [Y/N]
- ☒ Realtime display [Y/N]
- ☐ XGEN output format [Y/N]
- Mode [Scan/Oscillate/Step]: Scan
- ☐ Rotate sample [Y/N]
- ☐ Capture video image

At the bottom of the dialog box are two buttons: "OK" and "Cancel".

Figure 10.3 - SCAN /SINGLERUN options

7. For GADDS 4.0 users, skip to step 8. For GADDS 3.X users only, you will need to unwarp the frames next. Use the Spatial > Unwarp command, specifying the first file-name, corund0.001 and the number of frames as 4. We will assume GADDS 4.0 and skip this command.
 8. Integrate each frame into a multi-range raw file. This requires a File > Load and Peaks > Integrate > Chi commands for each frame.
 - Use File > Load to load the first frame, corund0.001.
 - Use Peaks > Integrate > Chi to integrate from 5 to 35 degrees (-120 to -60 in chi). Save as file corund and no append.
 - Use File > Load to load the second frame, corund0.002.
 - Use Peaks > Integrate > Chi to integrate from 30 to 60 degrees (-110 to -70 in chi).
 - Save as file corund and yes to append.
 - Use File > Load to load the third frame, corund0.003.
 - Use Peaks > Integrate > Chi to integrate from 55 to 85 degrees (-105 to -75 in chi). Save as file corund and yes to append.
 - Use File > Load to load the fourth frame, corund0.004.
 - Use Peaks > Integrate > Chi to integrate from 80 to 110 degrees (-105 to -75 in chi). Save as file corund and yes to append.
 9. Merge the multi-range raw file into a single range. Use the Special > System command to spawn the merge command.
 10. Use the File > Script Enabled command to toggle status, which will stop the auto-scripting feature. Then close the GADDS program.
- Now we will edit the auto-created script file using NotePad. We need to add comments and to correct any mistakes and omissions.
11. Start NotePad and load the PhaseID.slm file from the project's working directory. Make sure "word-wrap" is off.

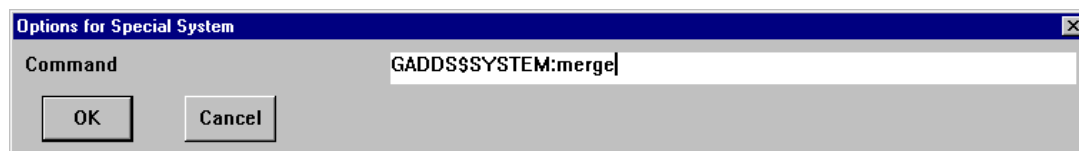


Figure 10.4 - Options for Special System

12. Print the script file so you have a reference to refer to. The file should look like:

```
PROJECT /NEW /CNAME=Corundum 0 /TITLE="Corundum Test Sample" &
/WORKDIR=D:\frames\Corundum0\ /FORMULA=? /MORPH=? /CCOL=? /DENSITY=? &
/DENSMETH=? /CLEAR /RESET
SCAN /SINGLERUN 1 /2THETA=20.0 /OMEGA=5.0 /PHI=0.0 /CHI=54.74 /AXIS=2 &
/WIDTH=10.0 /SCANTIME=1:00.00 /TITLE="Corundum Test Sample" &
/SAMPLE=Corundum /NUMSAMPLE=0 /NAME=corund /RUN=0 /FRAMENO=001 &
/DISPLAY=16 /REALTIME /CLEAR /MODE=Scan
SCAN /SINGLERUN 1 /2THETA=45.0 /OMEGA=17.5.0 /PHI=0.0 /CHI=54.74 /AXIS=2 &
/WIDTH=10.0 /SCANTIME=1:00.00 /TITLE="Corundum Test Sample" &
/SAMPLE=Corundum /NUMSAMPLE=0 /NAME=corund /RUN=0 /FRAMENO=002 &
/DISPLAY=16 /REALTIME /CLEAR /MODE=Scan
SCAN /SINGLERUN 1 /2THETA=70.0 /OMEGA=30.0 /PHI=0.0 /CHI=54.74 /AXIS=2 &
/WIDTH=10.0 /SCANTIME=1:00.00 /TITLE="Corundum Test Sample" &
/SAMPLE=Corundum /NUMSAMPLE=0 /NAME=corund /RUN=0 /FRAMENO=003 &
/DISPLAY=16 /REALTIME /CLEAR /MODE=Scan
SCAN /SINGLERUN 1 /2THETA=95.0 /OMEGA=42.5 /PHI=0.0 /CHI=54.74 /AXIS=2 &
/WIDTH=10.0 /SCANTIME=1:00.00 /TITLE="Corundum Test Sample" &
/SAMPLE=Corundum /NUMSAMPLE=0 /NAME=corund /RUN=0 /FRAMENO=004 &
/DISPLAY=16 /REALTIME /CLEAR /MODE=Scan
LOAD corund0.001 /DISPLAY=63 /SCALE=-n /OFFSET=0.0
INTEGRATE /CHI 5.000 35.000 -120.000 -60.000 /NORMAL=3. /STEPsize=0.1
INTEGRATE /WRITE $TITLE /FILENAME=corund /FORMAT=DIFFRACplus /SCALE=1.0
LOAD corund0.002 /DISPLAY=63 /SCALE=-n /OFFSET=0.0
INTEGRATE /CHI 30.000 60.000 -115.000 -75.000 /NORMAL=3. /STEPsize=0.1
INTEGRATE /WRITE $TITLE /FILENAME=corund /FORMAT=DIFFRACplus /APPEND &
/SCALE=1.0
LOAD corund0.003 /DISPLAY=63 /SCALE=-n /OFFSET=0.0
INTEGRATE /CHI 55.000 85.000 -115.000 -75.000 /NORMAL=3. /STEPsize=0.1
INTEGRATE /WRITE $TITLE /FILENAME=corund /FORMAT=DIFFRACplus /APPEND &
/SCALE=1.0
LOAD corund0.004 /DISPLAY=63 /SCALE=-n /OFFSET=0.0
INTEGRATE /CHI 80.000 110.000 -115.000 -75.000 /NORMAL=3. /STEPsize=0.1
INTEGRATE /WRITE $TITLE /FILENAME=corund /FORMAT=DIFFRACplus /APPEND &
/SCALE=1.0
SYSTEM GADDS$SYSTEM:merge
```

13. Add comments to the script file. Comments start with a exclamation, !, as the first character of a line. Use comments to identify the script file's purpose, history, parameters (if any), and major steps.

```
! PhaseID.slm: Qualitative Phase Identification Script File: Version 1.0
! Created by: KLS 06Jan98  Last modified by: no one
! -----
! This script will collect 4 frames (at 20,45,70,95 deg), integrate, and
! merge results into a single range RAW file for input into EVA's search
! match routine.
!
! Step 1: define a new project (GADDS 4 users only)
... Place the PROJECT command here
!
! Step 2: collect the frames (and unwarp)
... Place all SCAN commands here
!
! Step 3: integrate each frame into a raw range
... Place all LOAD & INTEGRATE commands here
!
! Step 4: merge multi-range raw file into single range raw file
... Place the SYSTEM command here
!
! Step 5: spawn EVA and perform a search match operation
! n.y.i.: see your EVA manual on how to do this.
```

14. Check for omissions within the script file and enter the appropriate syntax for any missing commands. Only the last command to spawn EVA is missing from our script. As there are many version of EVA, I will leave this command to the user to determine (see your DIFFRAC^{plus} EVA manual).

15. Check for errors or unwanted features in the script file, such as expanded logical names or non-echoed information.

For instance, in the PROJECT /NEW command, the working directory's value was expanded from the logical name of \$PROJECT. Change it back to read:

```
PROJECT /NEW /CNAME=Corundum 0 /TITLE="Corundum Test Sample" &
/WORKDIR=$PROJECT /FORMULA=? /MORPH=? /CCOL=? /DENSITY=? &
/DENSMETH=? /CLEAR /RESET
```

In the MERGE utility, the inputs were not echoed to the script file. This is typical of spawned utilities or programs. Refer to the Merge section of the GADDS Software Reference Manual or the SLAM Appendix for the complete command line syntax for the MERGE utility. Then modify the line to read:

```
SYSTEM GADDS$SYSTEM:merge corund.raw corundMerged.raw
```

16. Now we could simplify the script file somewhat by deleting duplicate qualifiers from subsequent re-issuance of the same command. For example, the second SCAN /SINGLERUN command does not need to contain the qualifiers: /PHI=0.0 /CHI=0.0 /WIDTH=10.0 /SCANTIME=1:00.00 /RUN=0 /DISPLAY=16 /REALTIME /CLEAR. These arguments are not required and can be omitted. The program will, thus, default to the settings used in the first SCAN /SINGLERUN command. However, we will leave the script as is.
17. Print the script file again.

18. Save the file and close NotePad.

The script should now look like:

```
! PhaseID.slm: Qualitative Phase Identification Script File: Version 1.0
! Created by: KLS 06Jan98   Last modified by: no one
! -----
! This script will collect 4 frames (at 20,45,70,95 deg), integrate, and
! merge results into a single range RAW file for input into EVA's search
! match routine.
!
! Step 1: define a new project (GADDS 4 users only)
PROJECT /NEW /CNAME=Corundum 0 /TITLE="Corundum Test Sample" &
  /WORKDIR=$PROJECT /FORMULA=? /MORPH=? /CCOL=? /DENSITY=? &
  /DENSMETH=? /CLEAR /RESET
!
! Step 2: collect the frames (and unwarp)
SCAN /SINGLERUN 1 /2THETA=20.0 /OMEGA=5.0 /PHI=0.0 /CHI=54.74 /AXIS=2 &
  /WIDTH=10.0 /SCANTIME=1:00.00 /TITLE="Corundum Test Sample" &
  /SAMPLE=Corundum /NUMSAMPLE=0 /NAME=corund /RUN=0 /FRAMENO=001 &
  /DISPLAY=16 /REALTIME /CLEAR /MODE=Scan
SCAN /SINGLERUN 1 /2THETA=45.0 /OMEGA=17.5.0 /PHI=0.0 /CHI=54.74 /AXIS=2 &
  /WIDTH=10.0 /SCANTIME=1:00.00 /TITLE="Corundum Test Sample" &
  /SAMPLE=Corundum /NUMSAMPLE=0 /NAME=corund /RUN=0 /FRAMENO=002 &
  /DISPLAY=16 /REALTIME /CLEAR /MODE=Scan
SCAN /SINGLERUN 1 /2THETA=70.0 /OMEGA=30.0 /PHI=0.0 /CHI=54.74 /AXIS=2 &
  /WIDTH=10.0 /SCANTIME=1:00.00 /TITLE="Corundum Test Sample" &
  /SAMPLE=Corundum /NUMSAMPLE=0 /NAME=corund /RUN=0 /FRAMENO=003 &
  /DISPLAY=16 /REALTIME /CLEAR /MODE=Scan
SCAN /SINGLERUN 1 /2THETA=95.0 /OMEGA=42.5 /PHI=0.0 /CHI=54.74 /AXIS=2 &
  /WIDTH=10.0 /SCANTIME=1:00.00 /TITLE="Corundum Test Sample" &
  /SAMPLE=Corundum /NUMSAMPLE=0 /NAME=corund /RUN=0 /FRAMENO=004 &
  /DISPLAY=16 /REALTIME /CLEAR /MODE=Scan
!
! Step 3: integrate each frame into a raw range
LOAD corund0.001 /DISPLAY=63 /SCALE=-n /OFFSET=0.0
INTEGRATE /CHI 5.000 35.000 -120.000 -60.000 /NORMAL=3. /STEPSIZE=0.1
INTEGRATE /WRITE $TITLE /FILENAME=corund /FORMAT=DIFFRACplus /SCALE=1.0
LOAD corund0.002 /DISPLAY=63 /SCALE=-n /OFFSET=0.0
```

```
INTEGRATE /CHI 30.000 60.000 -115.000 -75.000 /NORMAL=3. /STEPSIZE=0.1
INTEGRATE /WRITE $TITLE /FILENAME=corund /FORMAT=DIFFRACplus /APPEND &
/SCALE=1.0
LOAD corund0.003 /DISPLAY=63 /SCALE=-n /OFFSET=0.0
INTEGRATE /CHI 55.000 85.000 -115.000 -75.000 /NORMAL=3. /STEPSIZE=0.1
INTEGRATE /WRITE $TITLE /FILENAME=corund /FORMAT=DIFFRACplus /APPEND &
/SCALE=1.0
LOAD corund0.004 /DISPLAY=63 /SCALE=-n /OFFSET=0.0
INTEGRATE /CHI 80.000 110.000 -115.000 -75.000 /NORMAL=3. /STEPSIZE=0.1
INTEGRATE /WRITE $TITLE /FILENAME=corund /FORMAT=DIFFRACplus /APPEND &
/SCALE=1.0
!
! Step 4: merge multi-range raw file into single range raw file
SYSTEM GADDS$SYSTEM:merge corund.raw corundMerged.raw
!
! Step 5: spawn EVA and perform a search match operation
! n.y.i.: see your EVA manual on how to do this.
```


10.4 Using Replaceable Parameters within Script Files

A replaceable parameter is an “information” placeholder that you add to a script file to permit automatic replacement of a different value for that parameter each time you run the script. For instance, you may want to insert a replaceable parameter for the script’s title, sample name, or data files (common uses of replaceable parameters) so that the script may be used for more than one sample.

Ten replaceable parameters are available (%1 through %0), with %1 representing the first parameter, %2 representing the second parameter, and so forth. You pass the information (text for the replaceable parameter) on the @ command used to invoke the script. SLAM will replace all occurrences of %1 with the first text string, %2 with the second text string, and so forth.

Typically, one modifies an existing script to use replaceable parameters. When inserting replaceable parameters into a script file, keep these rules in mind:

- You must delimit replaceable parameters with either spaces or single quotes within the argument value.
- If you wish to concatenate text and replaceable parameters into a single argument value, then you must use single quotes (see last two rules).

- You may use a replaceable parameter to represent the entire argument value as in: / TITLE=%1.
- You may use a replaceable parameter to represent part of the entire argument as in: / FILENAME='%1'.001
- You may use more than one replaceable parameters in the argument value as in: / FILENAME='%1"%2'.%3'

To execute a replaceable parameter script, you would enter a command in the following format at the command mode prompt:

```
@filename parm1 parm2 ... parm0
```

where filename is the script file's filename (.slm is assumed)

parm1 is the text for %1

parm2 is the text for %2

...

parm0 is the text for %0

For example, if one enters:

```
@PhaseID "Unknown sample XYZ" 1:00.00
```

SLAM replaces all occurrences of %1 with “Unknown sample XYZ” and %2 with 1:00.00 within the file PhaseID.slm.

When using a script with replaceable parameters, keep these rules in mind:

- You must specify parameters where one is required. Unspecified parameters are replaced by blanks, which typically will create problems executing the script file.
- You must enclose inside double quotes any parameter that contains slashes or embedded spaces.
- You cannot use double quotes on any parameter that is used to represent part of an entire argument.

If your script file command is:

```
... /TITLE='%1"%2'
```

And you invoke the script command:

```
@MyScript "This is my sample" XYZ
```

The program will stop on the illegal command:

```
... /TITLE="This is my sample"XYZ
```

(The second double quote is in an invalid position).

Example

Say you wish to identify the phases of numerous samples. Rather than create a separate script file for each sample, you can modify the script you created in previous section (which identifies the phases of the specific corundum sample) to use replaceable parameters as follows:

1. Create and test the script without replaceable parameters. You have already done this in section 10.3.
2. Determine which parameters should be replaceable. Any parameter that is unique to the sample must be replaceable. For this script use:
 - %1 for filenames.
 - %2 for the sample title.
 - %3 for sample name.
 - %4 for the scan time.
3. Using NotePad edit the script file to use the replaceable parameters you have chosen. For example, in line 13, you would replace /SCANTIME=1:00.00 with /SCANTIME=%4 and /TITLE="Corundum Test Sample" with /TITLE=%2. Do not forget to add comments to explain arguments.
4. Print the script file.
5. Save script.

The final script should look like:

```
! PhaseID.slm: Qualitative Phase Identification Script File: Version 1.0
! Created by: KLS 06Jan98  Last modified by: no one
! -----
! This script will collect 4 frames (at 20,45,70,95 deg), integrate, and
! merge results into a single range RAW file for input into EVA's search
! match routine.
!
! %1 Filename, actually jobname part of filename.
! %2 Sample title, often in double quotes.
! %3 Sample number, often in double quotes.
! %4 Scan time, may be time string HH:MM::SS.S.
!
! Step 1: define a new project (GADDS 4 users only)
PROJECT /NEW /CNAME=Corundum 0 /TITLE="Corundum Test Sample" &
/WORKDIR=$PROJECT /FORMULA=? /MORPH=? /CCOL=? /DENSITY=? &
/DENSMETH=? /CLEAR /RESET
!
! Step 2: collect the frames (and unwarp)
SCAN /SINGLERUN 1 /2THETA=20.0 /OMEGA=5.0 /PHI=0.0 /CHI=54.74 /AXIS=2 &
/WIDTH=10.0 /SCANTIME=%4 /TITLE=%2 &
/SAMPLE=%3 /NUMSAMPLE=0 /NAME=%1 /RUN=0 /FRAMENO=001 &
/DISPLAY=16 /REALTIME /CLEAR /MODE=Scan
SCAN /SINGLERUN 1 /2THETA=45.0 /OMEGA=17.5.0 /PHI=0.0 /CHI=54.74 /AXIS=2 &
/WIDTH=10.0 /SCANTIME=%4 /TITLE=%2 &
/SAMPLE=%3 /NUMSAMPLE=0 /NAME=%1 /RUN=0 /FRAMENO=002 &
/DISPLAY=16 /REALTIME /CLEAR /MODE=Scan
SCAN /SINGLERUN 1 /2THETA=70.0 /OMEGA=30.0 /PHI=0.0 /CHI=54.74 /AXIS=2 &
/WIDTH=10.0 /SCANTIME=%4 /TITLE=%2 &
/SAMPLE=%3 /NUMSAMPLE=0 /NAME=%1 /RUN=0 /FRAMENO=003 &
/DISPLAY=16 /REALTIME /CLEAR /MODE=Scan
SCAN /SINGLERUN 1 /2THETA=95.0 /OMEGA=42.5 /PHI=0.0 /CHI=54.74 /AXIS=2 &
/WIDTH=10.0 /SCANTIME=%4 /TITLE=%2 &
/SAMPLE=%3 /NUMSAMPLE=0 /NAME=%1 /RUN=0 /FRAMENO=004 &
/DISPLAY=16 /REALTIME /CLEAR /MODE=Scan
!

! Step 3: integrate each frame into a raw range
```

```

LOAD '%1'0.001 /DISPLAY=63 /SCALE=-n /OFFSET=0.0
INTEGRATE /CHI 5.000 35.000 -120.000 -60.000 /NORMAL=3. /STEPSIZE=0.1
INTEGRATE /WRITE $TITLE /FILENAME=%1 /FORMAT=DIFFRACplus /SCALE=1.0
LOAD '%1'0.002 /DISPLAY=63 /SCALE=-n /OFFSET=0.0
INTEGRATE /CHI 30.000 60.000 -115.000 -75.000 /NORMAL=3. /STEPSIZE=0.1
INTEGRATE /WRITE $TITLE /FILENAME=%1 /FORMAT=DIFFRACplus /APPEND &
/SCALE=1.0
LOAD '%1'0.003 /DISPLAY=63 /SCALE=-n /OFFSET=0.0
INTEGRATE /CHI 55.000 85.000 -115.000 -75.000 /NORMAL=3. /STEPSIZE=0.1
INTEGRATE /WRITE $TITLE /FILENAME=%1 /FORMAT=DIFFRACplus /APPEND &
/SCALE=1.0
LOAD '%1'0.004 /DISPLAY=63 /SCALE=-n /OFFSET=0.0
INTEGRATE /CHI 80.000 110.000 -115.000 -75.000 /NORMAL=3. /STEPSIZE=0.1
INTEGRATE /WRITE $TITLE /FILENAME=%1 /FORMAT=DIFFRACplus /APPEND &
/SCALE=1.0
!
! Step 4: merge multi-range raw file into single range raw file
SYSTEM GADDS$SYSTEM:merge '%1'.raw '%1'Merged.raw
!
! Step 5: spawn EVA and perform a search match operation
! n.y.i.: see your EVA manual on how to do this.

```

6. Test the script file by placing GADDS into command mode using Special > Command Mode. Then type:

```
@PhaseID corund "Corundum Test Sample" Corundum 1:00.00
```

Within the script file, PhaseID.slm, %1 is replaced by corund, %2 is replaced by "Corundum Test Sample", %3 is replaced by Corundum, and %4 is replaced by 1:00.00.

You can now process numerous samples using this script. For example, you could enter these commands at the command line prompt (GADDS>):

```
@PhaseID SampleXYZ "Unknown geologic sample XYZ from stone quarry" XYZ 2:00.00
```

```
@PhaseID A1234 "Unknown whitish powder: Sample A1234" A1234 5:00.00
```

10.5 Adding Script Files to the Menu Bar as User Tasks

Scripts that are run frequently should be added to the menu-bar as a user task, which permits easy execution of the script file by a click of the mouse. Up to 12 user tasks may be added to the menu-bar by editing the GADDS\$SYS-DATA:usertask.ini file and then restarting GADDS. You can create user tasks used by all GADDS users or you can create different user tasks for different GADDS users.

Example

You wish to add the PhaseID script (created in the previous section) to the menu-bar so all your users can easily access the script. The steps are:

1. Using NotePad, open the file usertask.ini which is located in the GADDS\$SYSDATA: directory (default is C:\saxi\gadds32)
2. Edit the file to add a new section for the PhaseID script. See header of usertask.ini for format.

```
[1]
menu="&Phase ID"
help="Collect, integrate, and merge data into 5 to 110 degree range"
slam="@D:\frames\PhaseID"
parm=0,"Baseline","Enter the baseline (jobname) for all filenames"
parm=0,"Title","Enter sample title"
parm=0,"Sample","Enter sample name"
parm=0,"Scan Time","Enter scan time in seconds or as time string"
```

3. Save the file. The final usertask.ini file should look like:

```
; User Task Initialization File for GADDS-NT
;
; Format:
; [#]   Starts section for user task number #
; menu="xxx"   ; menubar text inside quotes
; help="xxx"   ; menubar help text inside quotes (optional)
; slam="xxx"   ; slam command inside quotes, without replaceable parms
; parm=type,"xxx","xxx"
;   ...
; parm=type,"xxx","xxx"
;           ; upto ten replaceable parameters with three values
;           ;   type is currently unused, use 0
;           ;   prompt text inside quotes
;           ;   prompt help text inside quotes (optional)

[1]
menu="&Phase ID"
help="Collect, integrate, and merge data into 5 to 110 degree range"
slam="@D:\frames\PhaseID"
parm=0,"Baseline","Enter the baseline (jobname) for all filenames"
parm=0,"Title","Enter sample title"
parm=0,"Sample","Enter sample name"
parm=0,"Scan Time","Enter scan time in seconds or as time string"
```

4. Re-start GADDS.

Example

You wish to add the PhaseID script (created in the previous section) to the menu-bar so only yourself can easily access the script. The steps are:

1. Create a directory for GADDs customization files for your exclusive use.
C:\saxi\GADDSSmith.
2. Copy, do not move, the GADDs customization files to the new directory. These files are *.lut, *.std, and usertask.ini.
3. Use Start > Settings > Control Panel > System to add (or modify) the GADDs\$SYSDATA: environment variable in user space to point to the new directory.
4. Modify the GADDs\$SYSDATA:usertask.ini file as in the previous example.

10.6 Nesting Script Files

You may create and execute nested script files, which are a script file within another script file. Some typical uses of nesting script files are to:

- Simplify the script file by replacing repeated sections with a nested script file.
- Simplify the script file by replacing similar sections with a nested script file that uses replaceable parameters.
- Create a subroutine procedure that may be called from several different script files.
- Reorder replaceable parameters.
- Modify (concatenate) passed replaceable parameters and pass new replaceable parameters to a nested script.

You start script files using the @ command. By inserting an @ command within a script file, you are calling a nested script file. The primary script file is a first level script and it may call second level nested script files. Script files may be nested up to three levels deep. Re-entry into an already opened script file is not allowed—that is a sub-level script file cannot call an upper level script file.

Example

For three different samples, you collected an entire frame series of 72 frames and then noticed that the configuration settings were incorrectly set. The wavelength, distance, and beam centers were erroneous. You need to correct the frame headers for each frame in the frame series. This task is ideally suited to using a 3 level nested script file.

The first script, UpdateSamples.slm, would look like:

```
@UpdateFrames Corund0
@UpdateFrames Corund1
@UpdateFrames Corund2
```

The second script, UpdateFrames.slm, would look like:

```
@UpdateHeader '%1'.000
@UpdateHeader '%1'.001
...
@UpdateHeader '%1'.071
```

The third script, UpdateHeader.slm, would look like:

```
LOAD %1 /USE_CONFIG
SAVE %1
```

To execute, you would enter

```
@UpdateSamples
```

GADDs executes scripts one line at a time. If the line is a nested script command, the entire nested script file must be executed and completed before GADDs continues with the next line of the original script file.

The first script, UpdateSamples, calls the second script, UpdateFrames, with the replaceable parameter, Corund0. The second script, UpdateFrames, calls the third script, UpdateHeader, with the replaceable parameter, Corund0.000. The third script, UpdateHeaders, executes the commands:

```
LOAD Corund0.000 /USER_CONFIG
SAVE Corund0.000
```

Once the third script, UpdateHeaders, terminates, flow returns to the next line of the second script, which calls the third script with the replaceable parameter, Corund0.001. Flow continues, stepping through the entire frame series of files: Corund0.000 to Corund0.071. Now the second script, UpdateFrames, terminates and flow returns to the next line of the first script, which calls the second script, with the replaceable parameter, Corund1. And so on.

10.7 Flow Control Inside Script Files

GADDs executes script commands sequentially, from first to last. You can modify this sequence by using blocks of executable commands and by transferring control to other commands. (Requires release 4.0.14). Note: Program variables (such as @1, @F, etc.) are not translated inside any flow control statement.

#LET %A = “string value”:

Define the value for a string variable. A blank value is valid. Any value that contains slashes or embedded spaces must be enclosed within double quotations. When nesting script files, the variable value is inherited from the parent script for program. New variable values are not propagated back to the parent script or program.

#LET %C = A + B:

#LET %C = A - B:

#LET %C = A * B:

#LET %C = A / B:

Define the value for a string variable using simple math. Only a single operator, +, -, *, or /, is allowed. A and B can be variables or constants.

#INC %A:

#INC[base] %A:

#INC16 %A:

#INC36 %A:

Increment a string variable using the specified base. Base must be between 2 and 36. If missing, the base defaults to 10.

#ON ERROR THEN CONTINUE:

#ON ERROR THEN NEXT:

#ON ERROR THEN BREAK:

#ON ERROR THEN STOP:

#ON ERROR THEN EXIT:

Define how to handle error conditions. After an error occurs, you may:

- continue to process the next line in the script file.
- next iteration of a #WHILE block.
- break out of a #WHILE block, then continue.
- stop processing the current script.
- exit all scripting.

When nesting script files, the “on error” value is inherited from the parent script or program. New “on error” value is not propagated back to the parent script or program. Default is EXIT. Outside of a #WHILE block,

BREAK is equivalent to STOP. Errors in any flow control statement, always generate at least a STOP (CONTINUE and BREAK are treated as STOP).

#IF (conditional) THEN:

#ELSEIF (conditional) THEN: (optional)

Multiple #ELSEIF's are allowed.

#ELSE: (optional)

#ENDIF:

Define blocks of commands that are conditionally executed. When the conditional expression evaluates to true, the block of commands after the #IF statement is executed and all #ELSEIF and #ELSE command blocks are ignored. When conditional is false, the next #ELSEIF statement is treated as an #IF statement. When all conditionals are false, the block of commands after the #ELSE statement is executed. Nesting of multiple #IF statements is not allowed.

#WHILE (conditional) DO:

#NEXT:

#WEND:

Define a block of commands to be executed, possibly repeatedly, whenever the conditional evaluates to true. When #WEND is reached, control returns to the #WHILE statement and the conditional is re-evalu-

ated. When conditional is false, control continues after the #WEND statement. Thus the #WHILE block of commands is repeatedly executed until either the conditional becomes false or an error occurs. In version 4.1.16, #NEXT forces a jump back to the #WHILE statement.

Use #LET, #WHILE, and #INC statements to emulate a "for" loop as in:

```
#LET %N = 1
```

```
#WHILE ('%N' <= 12) DO
```

```
command block (executed 12 times)
```

```
#INC $N
```

```
#WEND
```

Use #NEXT to skip subsequent commands inside a #WHILE block as in:

```
#LET %N = 1
```

```
#WHILE ('%N' <= 12) DO
```

```
  #INC $N
```

```
  command block (executed 12 times)
```

```
  #IF (clause) THEN
```

```
    #NEXT
```

```
  #ENDIF
```

```
  more commands (may or may not get executed)
```

```
#WEND
```

(conditional):

Conditional expressions must be in the form (TRUE), (FALSE), or (A operator B). A and B are strings which may include replaceable parameters and replaceable variables, but not program variables. (Use single quotes around replaceables). If both A and B are integers, they are converted to integers before performing the operation. Likewise if both are reals (or one real, one integer), they are converted to reals. The operator must be either "==" or "=" for equal, "<>" or "!=" for not equal, ">=" for greater than or equal, "<=" for less than or equal, ">" for greater than, or "<" for less than. Multiple operators (A < B < C) are not allowed.

Example (similar to example in 10.6)

For 3 different samples, you collected an entire frame series with various numbers of frames and then noticed that the configuration settings were incorrectly set. The wavelength, distance, and beam centers were erroneous. You need to correct the frame headers for each frame in the frame series. This task is ideally suited to using a 2 level nested script file and flow control.

The first script, UpdateSamples.slm, would look like:

```
#ON ERROR THEN CONTINUE
@UpdateFrames Corund_0_001
@UpdateFrames Corund_1_001
@UpdateFrames Corund_2_001
```

The second script, UpdateFrames.slm, would look like:

```
! Exit this script file on any error
#ON ERROR THEN STOP
#LET %F = '%1'
! Loop until Display /Next gives error
#WHILE (TRUE) DO
    LOAD '%F'.gfrm /USE_CONFIG
    SAVE '%F'.gfrm
    DISPLAY /NEXT
    #INC %F
#WEND
```

To execute, you would enter

```
@UpdateSamples
```

Example

For a sample, you wish to add with the scan time dependant on the current 2T angle.

The first script, MyAdd.slm, would look like:

```
#IF ('@1' < 0.0) THEN
    #LET %T = 10:00.00
#ELSEIF ('@1' == 0.0) THEN
    #LET %T = 1:00.00
#ELSEIF ('@1' > 0.0) THEN
    #LET %T = 10:00.00
#END
ADD '%T'
```

11. Automation

Automation involves instrument operation with minimal or no user interaction to perform sample control, 24/7 operation, quality control, or an audit trail.

To minimize user interaction, you must first determine how each sample is handled on the instrument. What varies between samples and what stays the same? For sample control, how are multiple samples mounted on the instrument? For 24/7 operation, samples must be removed and replaced with the next samples, usually by robotics. Also, the information for the new samples must be fed to the instrument.

Quality control and audit trail are side effects of automation. By automating procedures and recording changes and steps (i.e., an audit trail), you can achieve consistent results and prove that you followed standard operating procedures (SOP).

Automation is best implemented in phases:

Phase 1: Primitive automation

Phase 2: Optimize automation

Phase 3: Sample handling

Phase 4: Remote control

Phase 5: Audit trails

Phase 5: Audit trails

11.1 Primitive Automation

Let us examine automation with a practical example. Assume we have a typical GADDs-CS configuration (i.e., theta-theta geometry, XYZ stage, and laser alignment option), which is ideal for high sample throughput. Our samples are prepared in batches on sample libraries or plates. Libraries can come in 24-, 48-, or 96-well sizes. Our libraries are 96-well. Each well is labeled, starting at A01 and ending at H12. Each plate has identification and possibly a bar code. When a library of samples is produced, plate information, sample information and the bar code is entered into a database. Our task is to perform Phase Identification on each sample.

First, we will automate the handling of a single library. Assume we have a guide on our XYZ stage, so the library loading can be reproduced. Map the well centers (for wells A01 and H12) using the Scan > GridTargets command and input the distance between each target in the grid (increment). The run (target) numbers are changed to the well id, (i.e., A01 to H12). Set run chars to three and run base to 36 in Edit > Configure > User Settings to properly record the well id.

In the following example, a 96-well plate will be measured using a coupled scan mode, two frames per sample with a 2-theta deviation of 20°. The measurement angles, frame width and scan type can be easily modified depending on

the user application and system configuration (i.e., detector distance).

Example 11.1 - Automatic handling of a library

File: 96wells.slm

```
! Collect targets in a 96 well library
! -----
! Assumes: GADDs-CS system
! Assumes: distance = ?? cm, runbase=36,
!   runchar=3 (or this will fail!)
! Assumes: Target list already defined by
!   the grid targets command with run
!   numbers A01 to H12
!
! List of variables that are inserted into
! the script file before every measurement
! %1 = jobname (base of filename)
! %2 = scan time (1:00) minutes or seconds
! %3 = title ($FILE:filename)
! %4 = sample name (plate id)
! %5 = sample number (barcode)
! -----
! first collect all frames on all targets
#on error then continue
scan /multitargets 2 /thetal=10 &
  /theta2=10 %1 /scantime=%2 /axis=C &
  /width=20 /title=%3 /sample=%4 &
  /numsample=%5 /clear /startrun=1 &
  /endrun=9999 /mode=step
! -----
! Integrate all frames
#on error then continue
! Targets A01 to A12
#let %R = "A01"
#while ('%R' <= "A12") do
```

```

@gadds$scripts:96WellsSub %1 %R
#inc %R
#wend

! Targets B01 to B12
#let %R = "B01"
#while ('%R' <= "B12") do
    @gadds$scripts:96WellsSub %1 %R
    #inc %R
#wend

! Targets C01 to C12
#let %R = "C01"
#while ('%R' <= "C12") do
    @gadds$scripts:96WellsSub %1 %R
    #inc %R
#wend

! Targets D01 to D12
#let %R = "D01"
#while ('%R' <= "D12") do
    @gadds$scripts:96WellsSub %1 %R
    #inc %R
#wend

! Targets E01 to E12
#let %R = "E01"
#while ('%R' <= "E12") do
    @gadds$scripts:96WellsSub %1 %R
    #inc %R
#wend

! Targets F01 to F12
#let %R = "F01"
#while ('%R' <= "F12") do
    @gadds$scripts:96WellsSub %1 %R
    #inc %R
#wend

```

```

! Targets G01 to G12
#let %R = "G01"
#while ('%R' <= "G12") do
    @gadds$scripts:96WellsSub %1 %R
    #inc %R
#wend

! Targets H01 to H12
#let %R = "H01"
#while ('%R' <= "H12") do
    @gadds$scripts:96WellsSub %1 %R
    #inc %R
#wend

```

File: 96wellssub.slm

```

! Nested script file used by 96wells.slm
!
! %1 = jobname
! %2 = run (A01, A02, B01, etc)

! If frame doesn't exist, we exit
! processing this frame
#on error then stop

! load and integrate 1st frame
display /new '%1'_%2'_001.gfrm
INTEGRATE /CHI 10.600 31.500 -122.600 &
    -58.800 /NORMAL=5 /STEPSize=0.050
INTEGRATE /WRITE $TITLE &
    /FILENAME=$BASENAME &
    /FORMAT=DIFFRACplus /SCALE=1.0

! load and integrate 2nd frame
DISPLAY /NEXT
INTEGRATE /CHI 26.000 54.400 -109.200 &
    -71.300 /NORMAL=5 /STEPSize=0.050
INTEGRATE /WRITE $TITLE &

```



```
/FILENAME=$BASENAME &
/FORMAT=DIFFRACplus /SCALE=1.0 /APPEND

! Now merge the two ranges into a single
! range
system "c:\saxi\gaddsnew\merge /b
'%1'_%2'.raw '%1'_%2' merge.raw"
! Note: If the scan parameters are
! changed, the integration range (2theta
! start-end, Chi start-end) also needs to
! be changed to the correct values.
```

11.2 Optimize Automation

In section 11.1 we automated our phase identification on a single library of wells. In this section our goal is to handle many plates as quickly as possible. To do this, we need to identify bottlenecks and minimize efforts.

Bottlenecks to this process are the manual loading of plates and sample information, data acquisition (i.e., two frames on each sample) and data processing. Data processing is faster than data acquisition, so we can process the last library while we're collecting the next library.

Each well has different amounts of samples. Some samples are amorphous and do not diffract. By identifying non-diffracting samples early and then skipping those samples, we minimize effort. For diffracting samples, we identify the minimum data acquisition time. The result is the most time-efficient means of collecting data. Let us say from experimentation with our samples, we've determined that frames below 1000 cps are too weakly diffracting for our purposes, but frames with 250,000 total counts will process and produce acceptable results. We modify our previous script to perform a one second "pre-" scan at the low 2-theta detector position and use frame header variables with flow control to minimize effort. For data consistency, all frames on the same well must have the same acquisition time.

Example 11.2 - Pre-scan

File: 96WellsCollect.slm

```

! Collect targets in a 96 well library
! -----
! Assumes: GADDS-CST system (T2)
! Assumes: distance = 25 cm, runbase=36,
! runchar=3 (or this will fail!)
! Assumes: Target list already defined
! with run numbers A01 to H12
!
! %1 = jobname (base of filename)
! %2 = scan time (1:00) in minutes or
!       seconds (60)
! %3 = title ($FILE:filename)
! %4 = sample name (plate id)
! %5 = sample number (barcode)
!
! -----
! first collect all frames on all targets
#on error then continue

! Targets A01 to H12
#let %N = "01"
#while ('%N' <= "96") do

    ! Drive to next target and quick screen
    ! (pre-scan) for diffraction statistics
    scan /multitargets 1 /thetal=-2.5 &
      /theta2=-2.5 %1 /scantime=1 /axis=2 &
      /width=10 /title=%3 /sample=%4 &
      /numsample=%5 /clear /startrun=%N &
      /endrun=%N /mode=scan &
      /oscillate=XY /amplitude=1

    ! Skip weak diffractor (25 cps is
    ! background?) Also prevents divide by
    ! zero.

```

```

#IF (@C < 1000) THEN
    echo "Skipping WELL -> diffraction is
    too weak"

    ! Collect for 500,000 counts on first
    ! frame (low 2T frame)
    #ELSE

        ! Calculate count time needed for
        ! 500,000 counts
        #LET %T = 500000 / @C

        ! Collect 1st frame: 2T=0, Omega=-5 to
        ! +5 (for T2 systems)
        scan /singlerun 1 /thetal=5.0 &
          /theta2=-5.0 /axis=2 /width=-10 &
          /scantime=%T /title=%3 /sample=%4 &
          /numsample=%5 /name=%4 /run=@R &
          /framen=001 /display=15 /realtime &
          /clear /mode=scan /oscillate=XY &
          /amplitude=1

        ! Collect 2nd frame: 2T=20, OM=-5 to 5
        scan /singlerun 1 /thetal=5.0 &
          /theta2=15 /axis=2 /width=-10 &
          /scantime=%T /title=%3 /sample=%4 &
          /numsample=%5 /name=%4 /run=@R &
          /framen=002 /display=15 /realtime &
          /clear /mode=scan /oscillate=XY &
          /amplitude=1

        ! Collect 3rd frame: 2T=40, OM=-5 to 5
        scan /singlerun 1 /thetal=5.0 &
          /theta2=35 /axis=2 /width=-10 &
          /scantime=%T /title=%3 /sample=%4 &
          /numsample=%5 /name=%4 /run=@R &
          /framen=003 /display=15 /realtime &
          /clear /mode=scan /oscillate=XY &

```

```

    /amplitude=1

#ENDIF

! To next target in EditTargets list
#inc %N
#wend

```

The frame processing is extracted into a separate script file.

Example 11.3 - Frame processing

File: 96WellsProcess.slm

```

! Process frames in a 96 well library
! -----
! Assumes: Frames collected using
! 96WellsCollect.slm
! Assumes: Used run numbers A01 to H12
!
! %1 = jobname (base of filename)

! -----
! Integrate all frames
#on error then continue

! Targets A01 to A12
#let %R = "A01"
#while ('%R' <= "A12") do
    @gadds$scripts:96WellsSub %1 %R
    #inc %R
#wend

etc. (as in Phase 1 Primitive Automation
example)

```

11.3 Sample Handling

In this section, we automate loading the library, sample information entry, and the start of data acquisition. Automating the loading and unloading of libraries involves robotics, which is beyond the scope of this document. We will use remote control of the GADDS program to send the new library information, sample information, and then start the data acquisition script. The project information lines may store library information. The title information lines store individual well information. The amount of information stored in frame headers is limited. Raw headers are even more restrictive.

11.4 Remote Control

Remote control of GADDS is performed by sending individual SLAM commands via win-sockets from your master control program (MCP). Between GADDS and MCP resides the SMARTservice software layer on the frame buffer computer. MCP talks to SMARTservice and SMARTservice talks to GADDS. Unfortunately, the SMARTservice program is no longer supported by Bruker, but it is supplied "as is."

Install and run SMARTservice before starting GADDS. SMARTservice can start GADDS online and GADDS off-line, but won't connect to the off-line GADDS. Only GADDS online will connect to SMARTservice. Use the latest version of GADDS. Instrument status from SMARTservice is not yet implemented.

Our MCP generates several script files and sends them to the frame buffer computer. To send library information, we create a script file called "LibraryABC.slm." We'll use the Project > Edit command to send the library information, but you could also use the Project > New command which will use different folders for each library.

First, create the script file with the library information, such as sample library information (e.g., plate ID, barcode, technician's name). You are limited to five lines of 72 characters each.

Example 11.4 - Script file of library information

File: LibraryABC.slm

```
! MCP created script: 05-Nov-2002
! Operator: K. Smith
!-----
Project /Edit &
  /Title="Default well title 2" &
  /Formula="Library title 1" &
  /Morph="Library title 2" &
  /CCOL="Library title 3" &
  /Density="Library title 4" &
  /Densmeth="Library title 5"
```

Then, execute this script by sending the win-socket command "M @LibraryABC."

Next, create the title information file containing sample information for each well. Without this file, the default well title is used for all wells. You are limited to eight lines of 72 characters each.

Example 11.5 - Title information file

```
! MCP created script: 05-Nov-2002
! Operator: K. Smith
!-----
A01:Title 1 for well A01
A01:Title 2 for well A01 (etc. up to 8
lines)
A02:Title 1 for well A02
etc.
H12:Title 1 for well H12
H12:Title 2 for well H12 (etc. up to 8
lines)
```

When GADDS moves to the next target (i.e., well), the sample information for that target gets loaded using the \$FILE feature of the Scan command by passing "\$FILE:filename" for the title parameter.

Start data acquisition by sending the winsocket command "M @96WellsCollect <jobname> <scantime> <\$FILE:filename> <platenname> <barcode>." MCP monitors the GADDS log stream. When the data acquisition finishes, start data processing in a separate process by sending the commands "w c:\saxi\gaddsnew\gadds /thetatheta /nodif /com=@96WellsProcess <plateid>". You do not have to wait for processing to terminate, just load and start the next library.

11.5 Audit Trails

GADDS produces audit trails for instrument configuration, alignment, and calibration changes. Your MCP must create audit trails for sample tracking.

12. Mapping

Mapping involves the comparison of multiple samples to each other using a predefined feature or characteristic of the data set. The most common examples of these features include but are not limited to peak area, peak 2θ and peak FWHM. By defining one such criterion the GADDs software is then able to extract that information from each frame of a data set. In order for the software to function correctly the scans are required to be consecutive in run number (as they would be in a grid targets array). However, each sample spot measured can be unique and not part of a grid with equal spacing between targets.

12.1 Procedure—Demo Data

The GADDS software (either offline or online versions) must have loaded the project in which the data frames are located (Project > Load). Once you have the project loaded go to Analyze > Mapping.

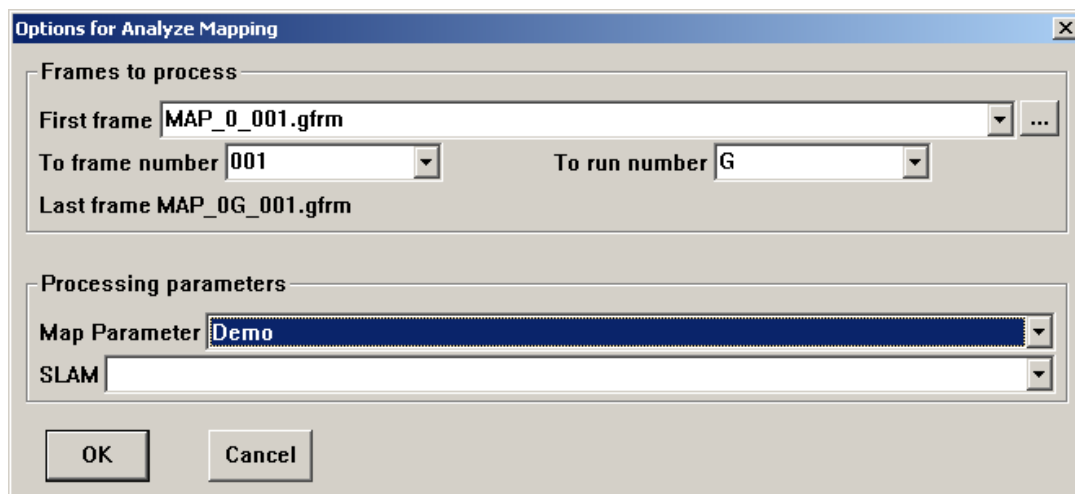


Figure 12.1 - Analyze > Mapping

Using the input information from above, you will see a demonstration of how the mapping software works. Once started, the GADDSmap software automatically starts, importing in computer generated data into a multiple spot array. What you will see from the GADDSmap software is shown in Figure 12.2.

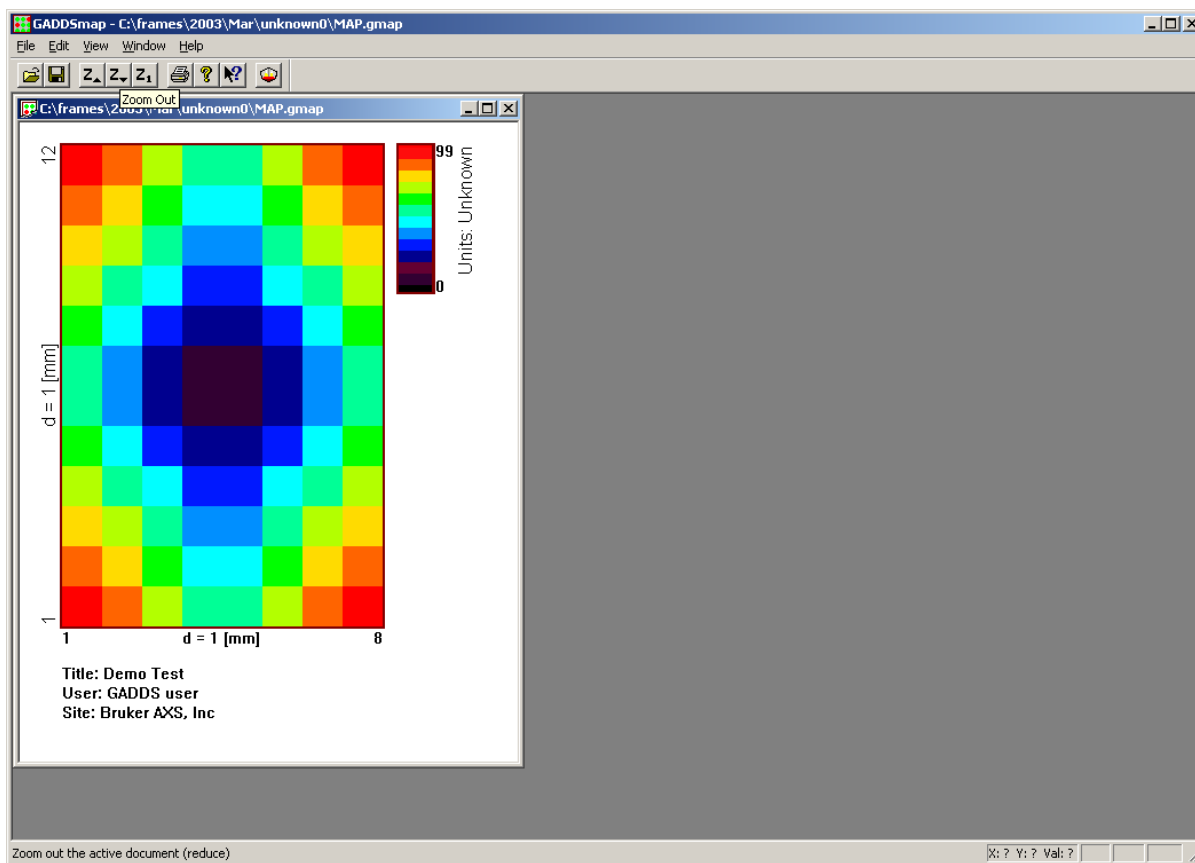


Figure 12.2 - GADDSmap

12.2 Procedure—Real Data

In the evaluation of actual data, however, you will have to change the input parameters to fit the specific functionality that you are looking for. In the following description you will change the mapping parameters to fit the FWHM of a selected peak throughout a data set.

12.2.1 Frames to Process

First frame = first frame of the data set you want to analyze.

To frame number = frame number of each frame from the data set (typically 000).

To run number = run number of the last frame from the data set (the software defaults to the last run in the series).

NOTE: If the default run number is not true for this series of frames, then the number of characters in Run # needs to be changed to the appropriate value under Edit > Configure > User Settings.

12.2.2 Processing Parameters

Map Parameter

Peak FWHM

Mapping Options

1. Type in Start and End values of both 2-theta and Chi for the peak you want to get FWHM information from or say OK.
2. Select them by choosing 1, 2, 3, or 4 and moving the mouse.

3. Choose 5-Bin Normalized and an appropriate Step Size for the detector position.

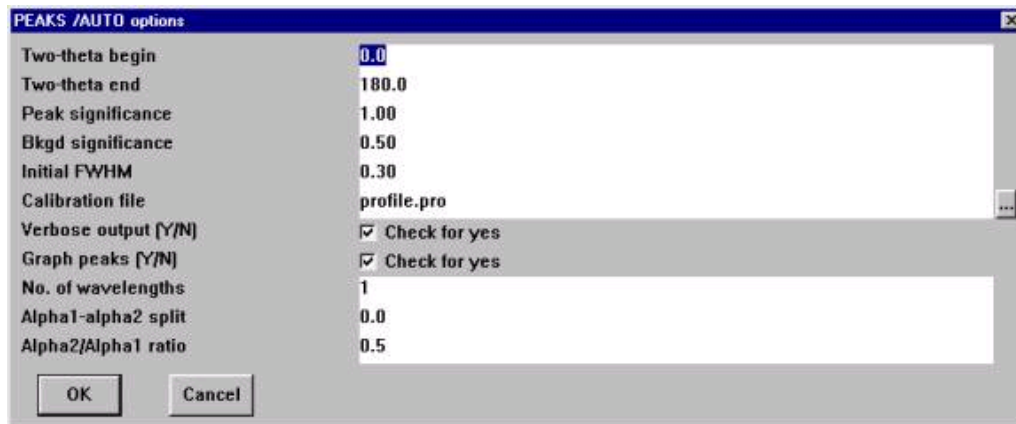


Figure 12.3 - PEAKS /AUTO options

4. Hit OK within the PEAKS/AUTO options window to perform the operation. If you receive an error message, then there is most likely no profile.pro calibration file to profile fit the peak.

5. To set up a Calibration file go to Special > Command mode in the GADDS software.

5.1 Type PEAKS into the command line.

5.2 Hit enter and the following window will appear.

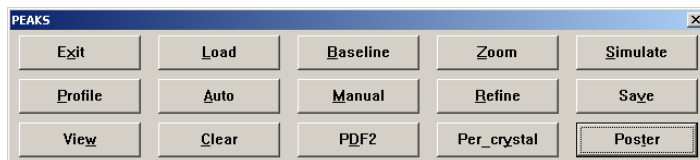


Figure 12.4 - Peaks window

6. Select Profile and then select Add.

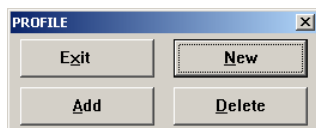


Figure 12.5 - Profile window

7. Select OK.
8. Change values using 1, 2, 3, and 4 while moving the mouse. Values 1 and 2 correspond to the background region at low 2θ while 3 and 4 represent the background region at high 2θ .
9. Select Exit.
10. In the command line type MENU and hit return (GADDS>MENU).
11. Repeat the procedure for mapping from the beginning to achieve the mapping result.

12.3 Mapping Software Features

Once you have an active mapping array displayed there are several features within the program that allow you to customize the display. The first of these is in the drop down menus of the program itself. Select the view menu to change the display of the map to see circular samples, label values and even utilize a pass/fail functionality for each data point. Double-click

on the intensity scale to change the color display and scale, as well as the brightness and contrast. In addition to these display changes, right-click on the map and select 3D plot to get a 3D image of the map. Right-clicking on the 3D map opens a separate window that allows you to customize the 3D display to your liking. An example from the demo data is shown in the following figures.

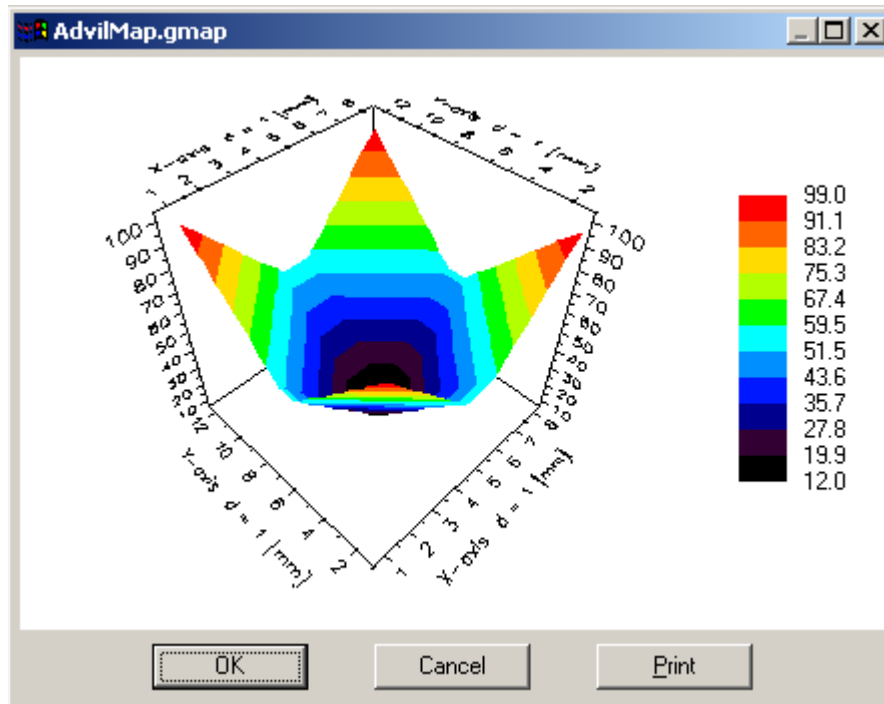


Figure 12.6 - Default Settings

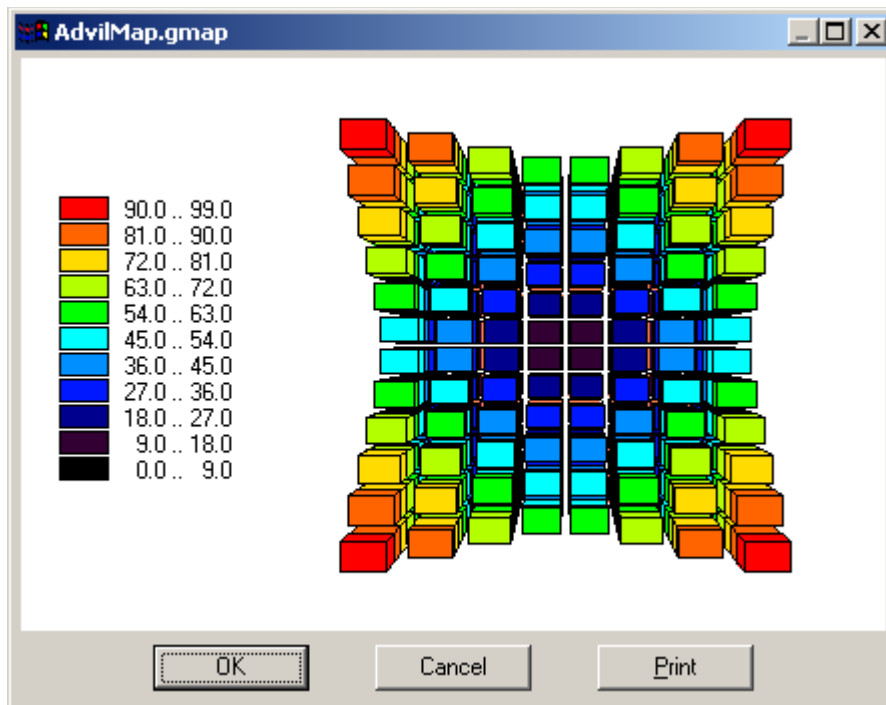


Figure 12.7 - Customized Settings

13. Nomenclature and Glossary

The nomenclature and glossary used in this manual are frequently referred by textbooks and literature and commonly accepted in the X-ray diffraction field. To avoid confusing you with a variety of different definitions of symbols and technical terms, some of the symbols, technical terms, and abbreviations used in this manual are listed in the following sections. The symbols and terms having no ambiguity may not be included in the list.

13.1 Nomenclature

- | | |
|-----------------|--|
| α | The detector swing angle to define the angle between detector center to the laboratory axis X_L , alternatively $2\theta_D$. (<u>2-Theta</u> in GADDs software). |
| α | The maximum angle of convergence. |
| α | The takeoff angle-the angle between exit beam and anode surface in the X-ray tube. |
| α | The angle defining the pole direction of a reflecting plane relative to a sample plane. The stereographic projection of this angle on the 2D pole figure is the radial distance from the outer circle of the pole figure. (<u>Alpha</u> in GADDs software). |
| α_{\max} | The maximum angular resolution of a SAXS system. |

β	The azimuthal angle between the pole direction and a reference direction. The stereographic projection of the angle on the 2D pole figure is the angle from 3 o'clock position in the counterclockwise direction. (<u>Beta</u> in GADDs software).	$2\theta_2$	The higher 2θ boundary of (2θ - or χ -) integration range. (<u>2th end</u> in GADDs software).
β	The maximum divergency angle of the X-ray collimation.	$2\theta_D$	The detector swing angle to define the angle between detector center to the laboratory axis X_L , alternatively α . (<u>2-Theta</u> in GADDs software)
γ	The angle symbol reserved to replace χ in the future document except χ_g . The nomenclature χ , $\Delta\chi$, χ_1 , and χ_2 may appear as γ , $\Delta\gamma$, γ_1 , and γ_2 , in some future documents.	$2\theta_M$	=The Bragg angle of the monochromator crystal.
		λ	The X-ray wavelength
		σ_{ij}	The stress tensor with six components: σ_{11} , σ_{12} , σ_{22} , σ_{13} , σ_{23} , σ_{33} .
$\Delta\psi$	Virtual oscillation angle for stress measurement using the 2D detector.	ϕ	The left-handed sample rotation angle about its surface normal or axis. The ϕ axis is always perpendicular to χ_g (or ψ) axis and the angle between the ϕ axis and ω axis is χ_g .
$\Delta\chi$	χ integration range.		
ε_{ij}	The strain tensor with six components: ε_{11} , ε_{12} , ε_{22} , ε_{13} , ε_{23} , ε_{33} .		
θ	The Bragg angle. The angle between incident X-ray beam (or reflected beam) and the reflecting crystal plane. Commonly denoted as 2θ . (<u>2-Theta</u> in GADDs software)	χ	The azimuthal angle about X_L defining the direction of the diffracted beams on the diffraction cone. χ starts at 6 o'clock direction with right handed rotation axis in the opposite direction of X_L . It is also called the diffraction cone χ angle to distinguish from the instrument χ_g . (<u>Chi</u> in GADDs software).
$2\theta_0$	The unstressed Bragg angle, normally used for stress measurement to represent 2θ value without stress.		
$2\theta_1$	The lower 2θ boundary of (2θ - or χ -) integration range. (<u>2th begi</u> in GADDs software).	χ_1	The lower χ boundary of (2θ - or χ -) integration range. (<u>chi begi</u> in GADDs software).

χ_2	The higher χ boundary of (2θ - or χ -) integration range. (<u>chi_end</u> in GADDS software).	d	The distance between two adjacent crystal planes, also called d-spacing.
χ_g	The sample rotation angle about a rotation axis within the X_L - Y_L plane. When $\omega=0$, The χ_g is a left-handed rotation with the axis on X_L and sample surface normal on Z_L at $\chi_g=0$. (The symbol χ may be used to refer to this angle some times.) (<u>Chi</u> in GADDS software).	d_{hkl}	The d-spacing of a specific crystalline plane with index (hkl).
ψ	The sample rotation with the same rotation axis as χ_g except different starting point. $\chi_g = 90^\circ - \psi$.	d	The pinhole diameter in the collimator.
ψ	The tilt angle between the sample surface normal and the diffraction vector. ψ -tilt is used for stress measurement in the conventional diffractometer.	d_0	The unstressed d-spacing, normally used for stress measurement to represent d value without stress.
ω	The right handed rotation of the sample about Z_L . When $\chi_g = 90^\circ$ and $\omega=0$, the sample surface normal is on Y_L . ω is also the angle between X_L and χ_g axis. (Omega in GADDS software)	f_{ij}	The strain coefficient used for strain measurement with six components: f_{11} , f_{12} , f_{22} , f_{13} , f_{23} , f_{33} .
A_{RX}	The anisotropic factor used in stress calculation.	p_{ij}	The stress coefficient used for stress measurement with six components: p_{11} , p_{12} , p_{22} , p_{13} , p_{23} , p_{33} .
D	The detector distance from the instrument center, also called sample-to-detector distance.	q	The modulus of the scattering vector, most frequently used in the small angle scattering.
		R	The resolution of a SAXS system defined as the theoretically largest resolvable Bragg spacing.
		R_{BS}	The resolution of limit of the beam stop of a SAXS system.
		S_1	One of the macroscopic elastic constants used for stress measurement, also expressed as $S_1(hkl)$ if the anisotropic correction for a specific crystal-line plane is considered.

$\frac{1}{2}S_2$	One of the macroscopic elastic constants used for stress measurement, also expressed as $\frac{1}{2}S_2(hkl)$ if the anisotropic correction for a specific crystal-line plane is considered.			center. Z is normally in the direction of the sample surface normal.
S_1	One of the sample coordinates. It is in the same direction as the sample translation axis X except the origin is fixed on sample.	X_L		One of the laboratory coordinates. X_L is in the direction of the incident X-ray beam.
S_2	One of the sample coordinates. It is in the same direction as the sample translation axis Y except the origin is fixed on sample.	Y_L		One of the laboratory coordinates. Y_L lies in the diffractometer plane and makes up a right handed rectangular coordinate system with X_L and Z_L .
S_3	One of the sample coordinates. It is in the same direction as the sample translation axis Z except the origin is fixed on sample.	Z_L		One of the laboratory coordinates. Z_L is up from the center of instrument and perpendicular to the diffractometer plane.
X	One of the sample translation coordinates with the origin on the instrument center. X is in the opposite direction of the incident X-ray beam when $\omega=\phi=0$. X normally lies on the sample surface.			
Y	One of the sample translation coordinates with the origin on the instrument center. Y normally lies on the sample surface angle and makes a 90° right-handed angle from X.			
Z	One of the sample translation coordinates with the origin on the instrument			

13.2 Glossary

2D Detector

Two-dimensional detectors, such as multi-wire area detector, CCD detector, and image plate.

2DXRD

Two-dimensional X-ray diffraction (system), alternatively XRD².

Absorption

As an X-ray beam passes through a sample, in addition to the scattered beam and transmitted beam, its intensity is also reduced by absorption. The extent of absorption depends on the path length of the beam through the sample, the nature of the material, and the wavelength of the incident X-ray beam.

Anisotropic Factor

A factor that represents the different physical properties in different crystal direction. In this manual, the anisotropic factor A_{RX} is used for stress calculation.

Anode (X-ray)

The electrode in an X-ray generator which emits X-rays when bombarded by fast electrons. Also called target.

Area Detector

A device for measuring 2D (two-dimensional) diffraction pattern at one time. It can be a CCD detector, image plate or multiwire detector. In this manual, it specifically refers to the Hi-Star multiwire area detector.

Attenuation

The intensity reduction of an X-ray beam after passing through a material or a device (attenuator).

Backward Diffraction

The diffraction condition when $2\theta > 90^\circ$.

Beam Center

The pixel position of the direct beam on a 2D detector sitting at on-axis position.

Beam Stop

A device used in a diffraction system to block the direct beam from hitting the detector, commonly in transmission mode diffraction.

Body-Centered Cubic

A crystal structure found in some metals. Within the cubic unit cell, atoms are located at all corners and cell-center positions.

Bragg Law

An equation that defines the diffraction condition based on the relationship among the X-ray incident angle to a crystal plane, reflection angle from the crystal plane, crystalline plane d-spacing, and the X-ray wavelength.

Characteristic Line

X-rays of definite wavelengths, characteristic of a pure substance (generally a metal) and produced when that substance is bombarded by fast electrons. The typical characteristic lines from an X-ray generator are $K\alpha$ ($K\alpha_1$ and $K\alpha_2$) and $K\beta$ lines.

Collimator

A device for producing a parallel beam of radiation.

Crystal

A solid having a regularly repeating three-dimensional array of atoms, ions, or molecules.

Crystal Plane

The repeating two-dimensional atomic arrangement within a crystal. Also called lattice plane.

Crystallinity

For polymers, the state wherein a periodic and repeating atomic arrangement is

achieved by molecular chain alignment. See also percent crystallinity.

Detection Circle

The scanning circle of a point detector within the diffractometer plane.

Detector Angle

The detector (swing) angle is a right-handed rotation angle about the laboratory axis Z_L . When the center of the detector plane is right on the axis X_L , the detector angle is zero. In the manual and software, this angle is denoted by α , $2\theta_D$ or 2-theta.

Detector Distance

The distance between the detection plane and the instrument center (D), also called sample-to-detector distance or crystal-to-detector distance.

Detector Plane

The reference plane that the 2D diffraction pattern is measured. A 2D detector is considered as such a plane in the diffraction geometry.

Detector Position

Detector position consists of detector-to-sample distance (D) and detector swing angle (α or 2-theta).

Diffraction (X-ray)

Constructive interference of X-ray beams that are scattered by atoms of crystals.

Diffraction Cone

The diffracted beams from a powder (polycrystalline) sample form a series of cones corresponding to each lattice index. The rotation axis of the cone lies on the incident X-ray beam. Each cone shape is determined by the Bragg angle 2θ and the azimuthal angle χ .

Diffraction Pattern

The experimentally measured values of intensities, diffraction angles (direction), and order of diffraction for each diffracted beam obtained when a sample is placed in a narrow beam of X-rays or neutrons.

Diffraction Rings

The conic section of the detector plane on the diffraction cones. Also called Debye ring.

Diffractometer

An instrument for measuring diffraction effects, specifically for measuring the directions and intensities of diffracted beams from crystals.

Diffractometer Plane

A plane defined by the laboratory axes X_L and Y_L . In the conventional diffractometer with a point detector or linear PSD, the diffraction data is collected by scanning within the plane. In a two-dimensional diffraction system, the detector center moves within this plane.

Divergence

The angle between two extreme rays in an divergent (X-ray) beam.

Face-Centered Cubic

A crystal structure found in some metals. Within the cubic unit cell, atoms are located at all corners and face-centered positions.

Fiber

Any polymer, metal, or ceramic that has been drawn into a long and thin filament.

Flood-Field Correction

A procedure to create a spatial mapping for the multiwire detector from exposure to a uniform, spherically radiating point source. The flood-field correction does not alter the number of photons counted and reported. It simply applies a spatial "rubber-sheet" stretching and shrinking of reported positions so that the frame collected from a uniform source appears uniform.

Focal Spot (On Target)

In a sealed tube or a rotating anode generator, the area on the anode bombarded by electrons is called focal spot on target.

Depending on the size of filament, the focal spot is categorized as normal focus, fine focus, long fine focus, or micro focus.

Forward Diffraction

The diffraction condition when $2\theta < 90^\circ$.

Four Circle (Geometry)

Sample can be rotated about three axes (omega, phi, and chi) independently, and detector can be rotated about a fourth angle, two theta, concentric with omega.

GADDS

General Area Detector Diffraction System, also refers to General Area Detector Diffraction Software.

Goniometer

An instrument for measuring and moving angles.

Goniometer Head

A device for aligning a sample by means of translation motion and, in some models, moveable arcs.

Integrated Intensity

The total intensity measured at a given angular range, such as chi-integration, 2theta-integration, and area integration.

Laboratory Coordinates

The rectangular coordinate system in a diffraction system with three axes: X_L , Y_L , and Z_L . X_L is the direction of the incident X-ray beam, X_L - Y_L plane defines the diffractometer plane, and Z_L defines the omega and two-theta axes.

Lattice Plane

The repeating two-dimensional atomic arrangement within a crystal. Also called crystal plane.

Least-Squares Fitting (Method)

A statistical method of obtaining the best fit of a large number of observations to a given equation. This is done by minimizing the sum of the squares of the deviations of the experimentally observed values from their respective calculated ones.

Line Focus

The projection of the focal spot perpendicular to the focal spot length with a takeoff angle is line focus. The line focus is commonly used for conventional diffractometer with point detector or PSD.

Line Geometry

The geometry, configuration or X-ray optics for an X-ray diffraction system using line focus X-ray beam, commonly associated with a point detector or PSD.

Microdiffraction

Diffraction applications with small sample or small (micro-) area on a sample. The X-ray beam size used for microdiffraction is in the range from a few hundred microns down to microns or sub-microns.

Monocapillary

A glass tube used for collimating X-ray beam by total external reflection.

Monochromatic

Consisting of radiation of a single wavelength or of a very small range of wavelengths.

Monochromator

A device used to select radiation of a single wavelength by use of diffraction from an appropriate crystal, such as a graphite crystal.

Parallel Beam

All rays of an X-ray beam travel in the same direction within a limited cross-section size. The cross-section size of the X-ray beam does not change with distance.

Parallel Optics

An X-ray optical device which delivers a parallel X-ray beam, such as collimator and Göbel mirror.

Parasitic Scattering

The scattering picked up by the detector from the region around the direct beam caused by pinhole scattering.

Percent Crystallinity

The ratio of integrated (X-ray diffraction) intensity from the crystalline peaks to the sum of the crystalline and amorphous intensity.

Point Detector

A detector used to measure the diffracted X-ray intensity one specific angle at one time. The data collected at one time is treated as one point in the diffraction pattern. The typical point detectors are scintillation counters, proportional counters, and semiconductor detectors. It can also be called 0D (zero-dimensional) detector.

Point Geometry

The geometry, configuration or X-ray optics for an X-ray diffraction system using point focus X-ray beam, commonly associated with a 2D detector.

Pole Figure

The stereographic projection of pole density space distribution of a polycrystalline sample.

Pole Image

Similar or identical to pole figure but not necessarily a stereographic projection.

Pole Sphere

Spherical representation of pole density space distribution.

Powder Diffraction

Diffraction by a crystalline powder (or a polycrystalline sample). The diffraction pattern consists of lines or rings rather than separate diffraction spots.

PSD

Position Sensitive Detector. Commonly 1D linear PSD.

RAG

Rotating anode generator.

Reflection

Since diffraction by a crystal may be considered as reflection from a lattice plane, this term is also used to denote a diffracted beam.

Reflection (Mode)

The diffraction condition that the diffracted beam exits from the same surface that the incident beam strikes on.

Sample Coordinates

A rectangular coordinates fixed on the sample (S_1 , S_2 and S_3). In a typical setup, S_1 and S_2 lie on the sample surface and S_3 is the normal of the sample surface.

Sample Orientation

Sample orientation is determined by the three rotation angles (ω , χ_g and ϕ)

Sample Position

Sample position is determined by the three rotation angles (ω , χ_g and ϕ) and the three translation coordinates (X , Y and Z).

Sample Stage

A device in a diffractometer to hold sample(s) and maneuver the sample orientation and translation. The typical sample stages used in GADDS are fix-chi, 2-position chi, XYZ stages and $\frac{1}{4}$ -circle cradle.

Sample Translation

Sample translation is achieved by moving sample along the three translation coordinates (X , Y and Z).

Small Angle X-ray Scattering (SAXS)

The study of matter by analysis of the diffraction of X-rays with diffraction angles smaller than a few degrees—that is, less than 1 degree for copper radiation.

Spatial Correction

A procedure to build and maintain a position table which corrects raw X, Y positions of detector events. The spatial correction is done by collecting a brass fiducial plate image at a specific detector distance and automatically computing and installing a spatial correction for data subsequently collected at the same distance.

Spot Focus

The projection of the focal spot along the focal spot length with a takeoff angle is spot focus, also called square focus or point focus. The spot focus is commonly used with a 2D detector.

Synchrotron Radiation

Radiation emitted by very high-energy electrons, such as those in an electron storage ring, when their path is bent by a magnetic field. The radiation is characterized by a continuous spectral distribution, a very high intensity, a pulsed-time structure, and a high degree of polarization.

Takeoff Angle

The angle between the anode and the exit X-ray beam in a sealed X-ray tube or RAG.

Target (X-ray)

The electrode in an X-ray generator which emits X-rays when bombarded by fast electrons. Also called anode.

Transmission (mode)

The diffraction condition that occurs when the incident beam strikes the sample in one surface and the diffracted beam exits from the opposite surface. The transmission mode diffraction commonly applies to thin plate samples.

White Radiation

Any radiation, such as sunlight, with a continuum of wavelengths. The term used here denotes the X-ray radiation with such a continuum of wavelengths. It is also called Bremsstrahlung.

X-rays

Electromagnetic radiation of wavelength 0.1-100Å, produced by bombarding a target (generally a metal such as copper or molybdenum) with fast electrons. The spectrum of the emitted radiation has a maximum intensity at a few wavelengths characteristic of the target material.

XRD²

Two-dimensional X-ray diffraction (system),
alternatively 2DXRD

13.3 Glossary of Software Terms**Arguments**

Within script files, arguments are parameters, valued qualifiers, or non-valued qualifiers.

ASCII

A file that consists of pure text characters, no formatting codes.

Batch-mode

Non-interactive processing of data, typically done using scripts.

Command

Within script files, a command consists of a verb, sub-command, and arguments.

Command-mode

Program mode where commands are type on the command prompt line.

Macro

See script.

Menu-Mode

Program mode where commands are invoked from the menu bar and dialog boxes.

Nesting

Calling one script file from within another script file is called nesting.

Parameters

Within script files, parameters are arguments for the command. Typically, these are required arguments.

Qualifier

Within script files, qualifiers are arguments for the command. Typically, these are non-required arguments and can be either valued or non-valued qualifiers.

Replaceable Parameters

Within script files, the variables %1 to %0 are used as placeholders for text strings passed on the @ command line.

Script

The ability to execute a series of commands as a single task is called scripting.

SLAM

Scripting Lexical Analyzer Monitor, which is the syntax for commands within script files.

Spawn

Starting another program from within your current program. Both programs are executing independently.

Spawn and Wait

Starting another program from within your current program, but only the new program is executing. The original program is sus-

pended until the spawned program terminates.

Subcommand

Within script files, the subcommand of the major grouping of commands, such as DISPLAY /NEW.

Subroutine

See nesting.

User-task

A script added to the menu bar is called a user-task.

Variables

Within script files, the variables @1 to @8 can be used to denote the current value of the axes 2θ to zoom.

Verb

Within script files, the verb is the command or major grouping of commands, such as DISPLAY.

